FILE COPY

GEOLOGICAL and DRILLING REPORT

MAL, BAR, WOP, TENAS, BELL and T Claim Groups

"TENAS OPTION"

Watson Lake Mining District
Whitehorse Mining District

By

J.W. Mustard, P.Eng.

CYPRUS ANVIL MINING CORPORATION

April 1982

Field work completed from
August 12 - October 19, 1982

CYPRUS ANVIL

013537

GEOLOGICAL and DRILLING REPORT

MAL, BAR, WOP, TENAS, BELL and T Claim Groups

"TENAS OPTION"

Watson Lake Mining District
Whitehorse-Mining District

By

J.W. Mustard, P.Eng.

CYPRUS ANVIL MINING CORPORATION

April 1982

Field work completed from
August 12 - October 19, 1982

TABLE OF CONTENTS

		PAGE No.
1.0	SUMMARY	1
2.0	INTRODUCTION	2
3.0	LOCATION, ACCESS AND TOPOGRAPHY	4
4.0	OPTION AGREEMENTS AND LAND STATUS	6
5.0	PREVIOUS WORK	12
6.0	GEOLOGY	16
7.0	GEOCHEMICAL SOIL SAMPLING SURVEY	19
	7.1 Copper Contours and Geochemical Values	22
	7.2 Lead Contours and Geochemical Values	22
	7.3 Zinc Contours and Geochemical Values	23
8.0	GEOPHYSICAL SURVEY	25
9.0	1981 DRILL RESULTS	27
10.0	CONCLUSIONS	29
11.0	RECOMMENDATIONS	30

LIST OF FIGURES

Figure 1	Tenas Option - Area of Interest & Geology
Figure 2	Cumulative Frequency Plot - Cu, Pb, Zn

LIST OF TABLES

Table 1	1981 Cost Summary
Table 2	List of Claims
Table 3	Summary of Option Agreements
Table 4	List of Data Obtained from Dupont
Table 5	List of data Obtained from Welcome North

LIST OF MAPS

Map 1	Claim Map and Grid Location - in pocket
Map 2	Geology - in pocket
Map 3	Copper Geochemical Values and Contours - in pocket
Map 4	Lead Geochemical Values and Contours - in pocket
Map 5	Zinc Geochemical Values and Contours - in pocket

APPENDICES

Appendix I	Geophysical Report
Appendix II	1981 Drill Logs

1.0 SUMMARY

During 1981 a combined exploration program totalling some $310,000 was carried out on the Tenas Option. Work consisted of mapping, line cutting, geochemical and geophysical surveys and 1400 m of diamond drilling in three holes. Some encouraging sphalerite mineralization was discovered along with significant alteration assemblages similar to that around the Anvil deposits. A gravity anomaly in association with massive sulfide mineralization remains untested. Further work, leading to diamond drilling, is recommended.

2.0 INTRODUCTION

An exploration program totalling $311,022.50 was carried out by Cyprus Anvil Exploration on the Tenas Option following signed letters of intent from the various optionors involved. These costs are summarized (Table I). Work consisted of line cutting, geochemical and geophysical surveys, diamond drilling, and production of a 1:5,000 scale line map with orthophoto mosaics. The 1981 work including diamond drilling was primarily centered on the Tenas claims.

The drilling consisted of 1417.6 m of NQ core in three holes. The first hole, ET81-01 was to evaluate the reported sulfide bearing graphitic quartzite occuring in the previously drilled DDH 75-02. The two subsequent holes were a follow up of sphalerite mineralization encountered in the first hole.

A geochemical program was carried out to further evaluate the lead and zinc anomalies on the Tenas claims. A reconnaissance geophysical program, using the Phoenix Spectral IP system, was carried out over portions of the grid proximal to the geochemical anomalies. Grid mapping was continued to the immediate vicinity of the drilling.

TABLE 1

SUMMARY OF 1981 TENAS OPTION EXPENSES

	MAL/BAR	WOP	TENAS/BELL	T	TOTAL
SALARIES & WAGES	-	4,000.00	16,733.78	2,000.00	22,733.78
CONSULTING FEES	-	176.20	176.19	-	352.39
LINECUTTING	-	3,936.94	2,109.07	984.24	7,030.25
SURVEYS - GEOCHEMICAL	-	3,089.16	3,590.11	1,669.82	8,349.09
SURVEYS - GEOPHYSICAL	-	11,097.13	8,885.70	4,685.46	24,668.29
SURVEYS - OTHER	1,046.77	1,151.45	732.74	7,536.76	10,467.72
DRILLING	-	-	166,318.90	-	166,318.90
ROADS & AIRSTRIPS	-	-	2,111.00	-	2,111.00
ASSAY & GEOCHEM ANA	-	1,085.66	1,261.71	586.85	2,934.22
FIELD EQUIP & SUPPL	-	-	464.82	-	464.82
CAMP MAINTENANCE	500.00	2,500.00	5,064.90	2,000.00	10,064.90
FUEL	-	631.22	1,472.86	-	2,104.08
ROTARY WING	1,000.00	1,000.00	2,310.38	5,390.88	9,701.26
MISC TRANSPORTATION	-	2,923.59	2,338.87	1,234.41	6,496.87
PROP ACQ & OPTION P	-	5,000.00 *	20,081.93	-	25,081.93
PROPERTY MTCE	205.00	1,230.00	1,450.00	8,860.00	11,745.00
DISTRICT EXPENSE	-	-	398.00	-	398.00
TOTAL EXPENDITURES	2,751.77	37,821.35	235,500.96	34,948.42	311,022.50

* Anvil Range Range Syndicate

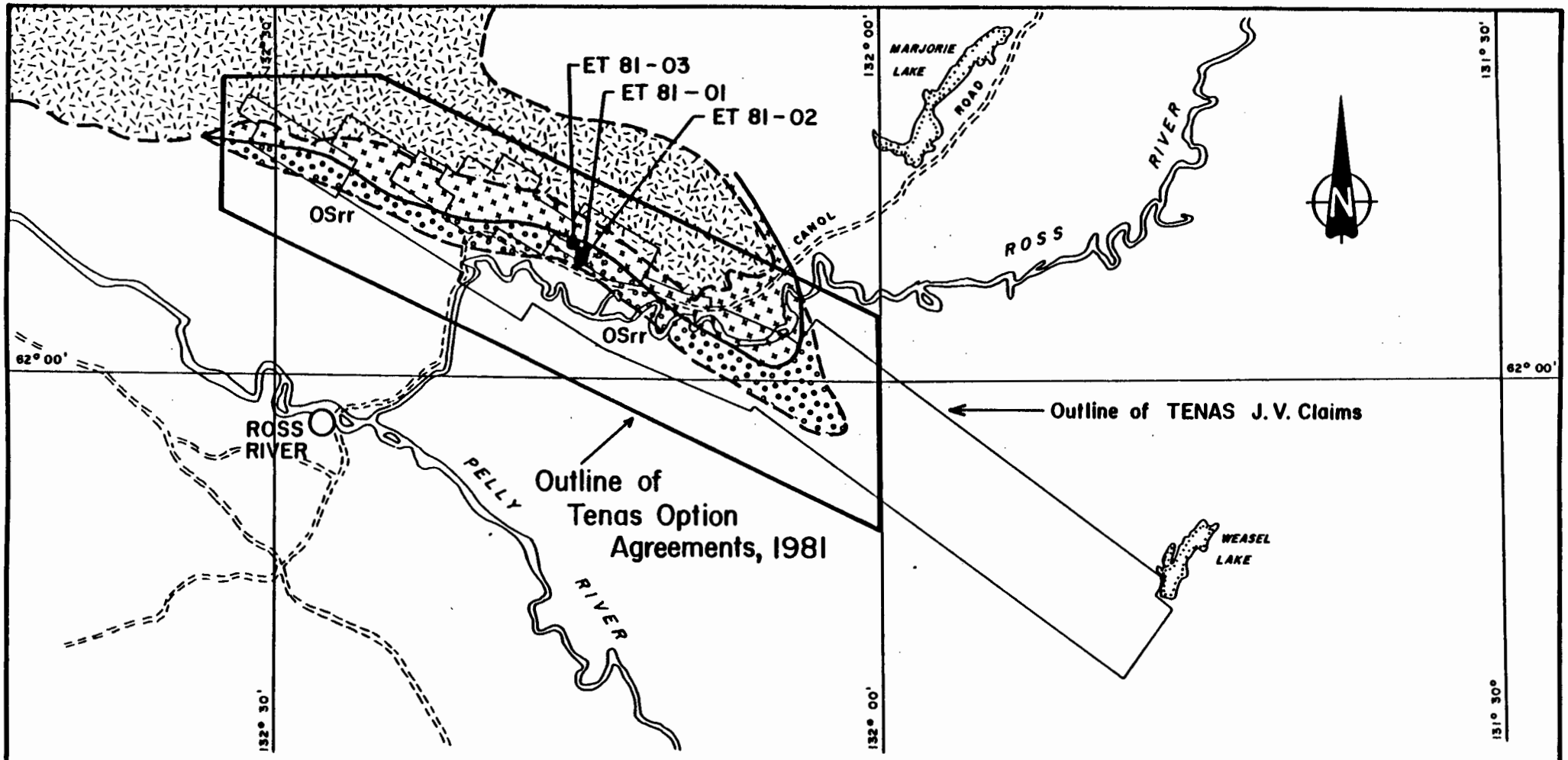
3.0 LOCATION, ACCESS AND TOPOGRAPHY

The claim groups form a linear belt 20 km in length ranging from 3.5 to 5.0 km in width. The mouth of Tenas Creek, a centrally located point, is at 62°03' north latitude and 132°20' west longitude, 10 km N.E. of the community of Ross River (Figure 1).

Access during 1981 was via the Canol Road which traverses the central portion of the claims. Access to those claims south of the Ross River is either by boat or helicopter. There is a helicopter at Ross River for casual hire.

Eighty per cent of the claims lie within the Ross River and Tenas Creek valleys. Outside of the flat sandy terraced, valley floors, the land slopes upward reaching 500 m above river elevation. The lower slopes are very moderate, while those approaching the height of land are steep. The main valley is very swampy with numerous meanders and oxbow lakes.

Thick glacial till blankets the lower elevations, producing sinuous sandy slopes topped by flat benches representing paleo floodplains. This material partially masks bedrock as well as soil geochemical response.



Legend

Kgd		Granodiorite
OSrr		Metabasite, phyllite
€Ov		Calcareous phyllite – Vangorda Formation
HCmm		Non – calcareous phyllite – Mt. Mye Formation
	———	Claim Boundary
	– – –	Contact
	●	Diamond Drill Hole Location

1 : 250,000

7800 5000 2500 0 7500 METRES

4 3 2 1 0 4 MILES

1 INCH = 4 MILES (approx.)

CYPRUS ANVIL MINING CORPORATION

TENAS OPTION AREA OF INTEREST

FIGURE 1

N.T.S. 105 K DRAWN BY: C. L. CORY	DATE: MARCH 19, 1982 FIGURE

4.0 OPTION AGREEMENTS AND LAND STATUS

Current status of all claims is listed in Table 2. Map 1 shows the location of all claims. Table 3 summarizes the critical features of the various option agreements covering the four claim groupings, but does not attempt to include the various choices available to the optioners after total expenditures have been met.

The current agreements consist of the following: MAL/BAR (62 full claims), Welcome North; WOP (66 full claims, 2 fractions), Anvil Range Syndicate - consisting of Dupont 49%, Teck 41%, and R.E. Chaplin 10%; TENAS/BELL (41 full claims and 4 fractions), Welcome North 20%, Westmin 40% and Dupont 40% - from a previous option from Welcome North; T (431 full claims and 16 fractions), Westmin 50% and Dupont 50%.

The Canol Road splits the claims into two groups as it defines the boundary between the Whitehorse and Watson Lake Mining Districts. For purposes of recording assessment work, claims cannot be grouped across district boundaries, thus work done in one district cannot be applied to claims in another district. During 1981 a payment of $8,100 was required to maintain claims within Watson Lake Mining District.

5800
290
$6000

TABLE 2

TENAS OPTION LAND STATUS

CLAIM NO.	GRANT NO.	NO. OF CLAIMS	MINING DISTRICT	RECORDING DATE	DUE DATE
BAR CLAIMS	105K-1				
1-4	Y80328-Y80331	4	Whitehorse	Aug. 22, 1974	Jan. 22, 1986
5-18	Y80332-Y80345	14	Whitehorse	Aug. 22, 1974	Jan. 22, 1984 (14)
MAL CLAIMS	105K-1, 2				
1	Y80379	1	Whitehorse	Aug. 22, 1974	Aug. 22, 1984
2-44	Y80380-Y80422	43	Whitehorse	Aug. 22, 1974	Aug. 22, 1984 (44)
WOP CLAIMS	105K-1				
1-4	Y79660-Y79663	4	Whitehorse	July 22, 1974	Jan. 22, 1987
5-10	Y79664-Y79669	6	"	July 22, 1974	Jan. 27, 1987
11-16	Y79670-Y79675	6	"	July 22, 1974	Jan. 22, 1987
17	Y79696	1	"	July 22, 1974	Jan. 27, 1987
18	Y79697	1	"	July 22, 1974	Jan. 22, 1987
19-20	Y79698-Y79699	2	"	July 22, 1974	Jan. 27, 1987
21-28	Y79676-Y79683	8	"	July 22, 1974	Jan. 27, 1987
29-38	Y80208-Y80217	10	"	Aug. 16, 1974	Jan. 22, 1987
39-56	Y80218-Y80235	18	"	Aug. 16, 1974	Jan. 27, 1987
57-63	Y80236-Y80242	7	"	Aug. 16, 1974	Jan. 22, 1987
64-66	Y80243-Y80245	3	"	Aug. 16, 1974	Jan. 27, 1987
500-501	YA20199-YA20200	2	Watson Lake	June 13, 1977	Jan. 28, 1983
TENAS CLAIMS	105K-1				
1-33	Y80346-Y80378	33	Whitehorse	Aug. 22, 1974	Jan. 27, 1986
34-41	YA3416-YA3423	8	Whitehorse	Aug. 25, 1975	Jan. 27, 1986
100-101 Fr	YA20197-YA20198	2	Watson Lake	June 13, 1977	Jan. 28, 1983
BELL CLAIMS	105K-1				
15-16 Fr	YA4124-YA4125	2	Whitehorse		Jan. 27, 1986

TENAS OPTION CLAIM LIST

CLAIM NO.	GRANT NO.	NO. OF CLAIMS	MINING DISTRICT	RECORDING DATE	DUE DATE
T CLAIMS					
1-17	YA11548-YA11564	17	Watson Lake	Oct. 28, 1976	Jan. 28, 1985
18	YA11565	1	"	"	Jan. 28, 1987
19-24	YA11566-YA11571	6	"	"	Jan. 28, 1985
25	YA11572	1	"	"	Jan. 28, 1983
26	YA11573	1	"	"	Jan. 28, 1985
27	YA11574	1	"	"	Jan. 28, 1983
28	YA11575	1	"	"	Jan. 28, 1985
29	YA11576	1	"	"	Jan. 28, 1983
30-34	YA11577-YA11581	5	"	"	Jan. 28, 1985
35	YA11582	1	"	"	Jan. 28, 1983
36-59	YA11583-YA11606	24	"	"	Jan. 28, 1985
60	YA11607	1	"	"	Jan. 28, 1983
61-68	YA11608-YA11615	8	"	"	Jan. 28, 1985
69-70	YA11616-YA11617	2	"	"	Jan. 28, 1983
71-78	YA11618-YA11625	8	"	"	Jan. 28, 1985
79-80	YA11626-YA11627	2	"	"	Jan. 28, 1983
81-88	YA11628-YA11635	8	"	"	Jan. 28, 1985
89-90	YA11636-YA11637	2	"	"	Jan. 28, 1983
91-98	YA11638-YA11645	8	"	"	Jan. 28, 1985
99	YA11646	1	"	"	Jan. 28, 1983
100	YA11647	1	"	"	Jan. 28, 1985
101 Fr	YA11648	1	"	"	Jan. 28, 1986
102-104 Fr	YA11649-YA11651	3	"	"	Jan. 28, 1985
105 Fr	YA11652	1	"	"	Jan. 28, 1983
106-107	YA11653-YA11654	2	"	"	Jan. 28, 1985
108-111	YA8313-YA8316	4	Whitehorse	Oct. 27, 1976	Jan. 27, 1986
112-121	YA11655-YA11664	10	Watson Lake	Oct. 28, 1976	Jan. 28, 1985
122-123	YA11665-YA11666	2	"	"	Jan. 28, 1983
124-127	YA11667-YA11670	4	"	"	Jan. 28, 1983
128-135	YA11671-YA11678	8	"	"	Jan. 28, 1985
136	YA11679	1	"	"	Jan. 28, 1983
137	YA11680	1	"	"	Jan. 28, 1983
138	YA11681	1	"	"	Jan. 28, 1983
139-144	YA11682-YA11687	6	"	"	Jan. 28, 1983
145	YA11688	1	"	"	Jan. 28, 1983
146	YA11689	1	"	"	Jan. 28, 1983
147	YA11690	1	"	"	Jan. 28, 1985
148	YA11691	1	"	"	Jan. 28, 1983
149	YA11692	1	"	"	Jan. 28, 1985
150	YA11693	1	"	"	Jan. 28, 1983
151	YA11694	1	"	Oct. 28, 1976	Jan. 28, 1985
152	YA8317	1	Whitehorse	Oct. 27, 1976	Jan. 27, 1986
153-158	YA11695-YA11700	6	Watson Lake	Oct. 27, 1976	Jan. 28, 1983
159-160	YA8318-YA8319	2	Whitehorse	Oct. 27, 1976	Jan. 27, 1989
161-180	YA11701-YA11720	20	Watson Lake	Oct. 28, 1976	Jan. 28, 1983
181-190	YA11721-YA11730	10	Watson Lake	Oct. 28, 1976	Jan. 28, 1983

TENAS OPTION CLAIM LIST

CLAIM NO.	GRANT NO.	NO. OF CLAIMS	MINING DISTRICT	RECORDING DATE	DUE DATE
T CLAIMS	(cont'd)				
191-200	YA8320-YA8329	10	Whitehorse	Oct. 27, 1976	Jan. 27, 1989
201-216	YA8330-YA8345	16	Whitehorse	Oct. 27, 1976	Jan. 27, 1985
217-218	YA11731-YA11732	2	Watson Lake	Oct. 28, 1976	Jan. 28, 1983
219-220	YA8346-YA8347	2	Whitehorse	Oct. 27, 1976	Jan. 27, 1989
221	YA8348	1	Whitehorse	Oct. 27, 1976	Jan. 27, 1989
222-226	YA8349-YA8353	5	"	"	Jan. 27, 1989
227-239	YA8354-YA8366	13	"	"	Jan. 27, 1985
240	YA8367	1	"	"	Jan. 27, 1986
241-248	YA8368-YA8375	8	"	"	Jan. 27, 1985
249	YA8376	1	"	"	Jan. 27, 1984
250-272	YA8377-YA8399	23	"	"	Jan. 27, 1985
275-281	YA8779-YA8785	7	"	March 29, 1977	Jan. 27, 1986
282-289	YA12636-YA12643	8	Watson Lake	March 30, 1977	Jan. 28, 1983
290	YA8786	1	Whitehorse	March 29, 1977	Jan. 27, 1986
300-301 Fr.	YA20201-YA20202	2	Watson Lake	June 13, 1977	Jan. 28, 1983
302-303 Fr	YA18061-YA18062	2	Whitehorse	June 9, 1977	Jan. 27, 1989
304 Fr	YA20203	1	Watson Lake	June 13, 1977	Jan. 28, 1983
305 Fr	YA18063	1	Whitehorse	June 9, 1977	Jan. 27, 1986
306 Fr	YA20204	1	Watson Lake	June 13, 1977	Jan. 28, 1983
307 Fr	YA18064	1	Whitehorse	June 9, 1977	Jan. 27, 1986
308 Fr	YA20205	1	Watson Lake	June 13, 1977	Jan. 28, 1983
309 Fr	YA18065	1	Whitehorse	June 9 1977	Jan. 27, 1986
310 Fr	YA20206	1	Watson Lake	June 13, 1977	Jan. 28, 1983
311 Fr	YA18066	1	Whitehorse	June 9, 1977	Jan. 27, 1986
312 Fr	YA20207	1	Watson Lake	June 13, 1977	Jan. 28, 1983
313 Fr	YA18067	1	Whitehorse	June 9, 1977	Jan. 27, 1986
314 Fr	YA20208	1	Watson Lake	June 13, 1977	Jan. 28, 1983
315-316 Fr	YA20209-YA20210	2	"	June 13, 1977	Jan. 28, 1985
317 Fr	YA20211	1	"	June 13, 1977	Jan. 28, 1983
318 Fr	YA18068			June 9, 1977	LAPSED
319 Fr	YA18069	1	Whitehorse	June 9, 1977	Jan. 27, 1986
320 Fr	YA20212	1	Watson Lake	June 13, 1977	Jan. 28, 1985
321-327 Fr	YA18070-YA18076	7	Whitehorse	June 9, 1977	Jan. 27, 1986
350-351 Fr	YA18077-YA18078	2	"	June 9, 1977	Jan. 27, 1989
352 Fr	YA20213	1	Watson Lake	June 13, 1977	Jan. 28, 1983
353-354 Fr	YA18079-YA18080	2	Whitehorse	June 9, 1977	Jan. 27, 1986
355-356 Fr	YA20214-YA20215	2	Watson Lake	June 13, 1977	Jan. 28, 1983
357 Fr	YA18081	1	Whitehorse	June 9, 1977	Jan. 27, 1986
694	YA22103	1	Watson Lake	Aug. 26, 1977	Jan. 28, 1985
699	YA22108	1	"	"	Jan. 28, 1985

TENAS OPTION CLAIM LIST

CLAIM NO.	GRANT NO.	NO. OF CLAIMS	MINING DISTRICT	RECORDING DATE	DUE DATE
T CLAIMS	(cont'd)				
701-707	YA22110-YA22116	7	Watson Lake	Aug. 26, 1977	Jan. 28, 1985
709-720	YA22118-YA22129	12	"	"	Jan. 28, 1985
730-732	YA22139-YA22141	3	"	"	Jan. 28, 1985
735-739	YA22144-YA22148	5	"	"	Jan. 28, 1985
745-759	YA22154-YA22168	15	"	"	Jan. 28, 1985
761-776	YA22170-YA22185	16	"	"	Jan. 28, 1985
778-791	YA22187-YA22200	14	"	"	Jan. 28, 1985
792-818	YA25401-YA25427	27	"	"	Jan. 28, 1985
820-826	YA25429-YA25435	7	"	"	Jan. 28, 1985

TABLE 3

SUMMARY OF TENAS OPTION AGREEMENTS

TERMS	MAL/BAR	WOP	TENAS/BELL	T
CURRENT INTEREST	Welcome NORTH - 100%	Anvil Range Syndicate - Dupont 49% - Teck 41% - R.E. Chaplin 10% (carried)	Welcome North 20% Westmin 40% Dupont 40%	Westmin 50% Dupont 50%
CASH PAYMENT	Initial payment of $10,000.00	---	---	---
CONTINUING OPTION PAYMENTS	$10,000.00/year for a total of $100,000.00 over a 10 year period	---	---	---
WORK COMMITMENTS TO MAINTAIN OPTION	Perform work so that all claims remain in good standing	Total expenditure of $400,000 over a 5 year period, of which $25,000 was committed in 1981	Expenditure of $1.1 million to Dec. 31, 1985 by C.A.M.C. on any or all claims. This expenditure not to be pro-rated	
CAMC EARNED INTEREST	100% after option payments total $100,000	60% net interest by an additional expenditure of $1.0 million over a second five year period	70% if Welcome North elects to convert its 20% interest to 10% N.P.I. 56% otherwise. Based on total expend.	70% after total expenditure of $1.1 million
MINORITY INTERESTS	10% N.P.I. until capital recouped, thence 20% N.P.I.			
Welcome North	---	---	20% with option to convert to 10% N.P.I.	
Dupont	---	14.7%	12%	15%
Teck	---	12.3%	---	---
Chaplin	---	10.0% N.P.I.	---	---
Westmin	---	---	12%	15%
DILUTION OF INTEREST FOR NONCONTRIBUTION	---	Pro-rata to 5% of total expenditure when interest falls to below 5%	Pro-rata to 5% of total expenditure when interest falls to below 5%	Pro-rata to 5% of total expenditure when interest falls below 5%
TERMINATION OF OPTION	Returned in good standing for minimum of two years from termination of option	Leave property in good standing for 1 year from termination of option	Leave property in good standing for 1 year from anniversary date	Leave property in good standing for 1 year from anniversary date

5.0 PREVIOUS WORK

A summary of recent exploration history was given by Jennings, 1980 and is not repeated here. A comprehensive set of data (Table 4 & 5) was acquired from the optionors just prior to the 1981 field season. This data, while of value, was incoherent from a district point of view because of the various scales used for presentation. Data was not integrated onto a common base for the purpose of planning an effective program. Of particular interest is the coincidence of a 2.0 m gal gravity anomaly and the presence of massive sulfide float in a deep gorge on the western flank of the anomaly. This is the "Pelly Anomaly" and is situated on T Claims 51 and 52. Density measurements on samples collected over the anomaly do not show sufficient contrast to explain the feature. The massive sulfide float consists of pyrite, pyrrhotite, galena, sphalerite, chalcopyrite and arsenopyrite. None of the observed float appeared to be stratiform in nature.

Locally, the geology consists of calc-silicates of the Vangorda Formation with metabasites. The calc-silicates are well exposed in the steep gorge, along with some graphitic horizons. Three diamond drill holes have been collared in the area (tesing the gravity high) and did not drill the Vangorda/Mt. Mye contact, host to mineralization in Anvil District. Essentially this anomaly remains untested and thus would require some additional followup work.

Prior to 1981, some 5,000 m of diamond drilling was done on the various claim groups. All of this drilling was based on either geochemical or geophysical targets with the bulk (3,600 m) done on a combination of magnetic and EM anomalies. Only three holes traversed the favourable Mt Mye - Vangorda contact (75-01, T79-01, T79-04). Thus for 20 km of strike length of favourable stratigraphy only 3 holes have tested the contact, host to mineralization within the Anvil camp.

TABLE 4

WELCOME NORTH MINES LTD.

DATA LIST

1. Report on Turam Electromagnetic Surveys
   By Peter E. Walcott & Associates Ltd.---July 1975

2. Helicopter Magnetic & Electromagnetic Survey Ross River area, Y.T. on behalf of Dupont of Canada Exploration Ltd.
   By Aerodat Ltd. November 10, 1978

3. Report on the 1975 work program on the Tenas Claims for Boliden-Preussag Exploration
   By J.B. Paul Sawyer - September 5, 1975

4. Map showing DDH #3 on Monroe Vendor Property (Recorded at Whitehorse August 7, 1974).

5. Geological, Geophysical and Geochemical Report on the Snowcap Claims (Olgie L.)
   By T.W. Muraro March 20, 1967

6. Report on the 1975 work program on the Bar Claims for Boliden Preussag Exploration
   By J.B. Sawyer - September 5, 1975

7. Report on the 1975 work program on the Mal Claim Group for Boliden-Preussag Exploration
   By J.B. Sawyer September 5, 1975

8. Tenas Correlation Program - Pearson, Spearman and Kendall
   By M. Smith December 21, 1976

9. Tenas Project - Report of 1977 activities and results on the Mal, Bar, Tenas and Bell Claims for Welcome North Mines
   By K.A. MacLean January 31, 1978

10. Gravity Survey Report - Mal Claims area
    By C.A. Ager August 10, 1978

11. Report on the Tenas Project for Boliden-Preussag Exploration
    By R. Wares December, 1975

TABLE 5

DUPONT OF CANADA EXPLORATION LTD.

DATA LIST

1. Copy of 1977 and 1979 drill logs

2. Tenas Project Gravity Survey
   By C.A. Ager August 2, 1977

3. Report on the Geology of the T, Tenas, Wop, Bar and Mal Claims
   By F.M. Smith et al November, 1977

4. Report on the geochemical soil survey of the T, Tenas, Wop, Bar and Mal Claims
   By F.M. Smith October, 1977

5. Helicopter magnetic and electromagnetic survey on behalf of Dupont of Canada Exploration Ltd.
   By Aerodat Ltd. November 10, 1978

6. Gravity Survey: T401-T826 Claims
   By C.A. Ager August 10, 1978

7. Geological, Geophysical, Geochemical Surveys and Diamond Drill Results Wop Mineral Claims (Anvil Range syndicate)
   By R.E. Chaplin July 14, 1975

8. Gravity Survey - Wop Claims Grid Addendum: Second Vertical Derivative
   By .A. Ager December 16, 1974

9. Wop Claims - Report on 1977 work programme for Teck Mining Group Ltd. and R.E. Chaplin
   By K.A. MacLean January 31, 1978

10. Report on the Anvil Project Exploration Programme 1974
    Project No. 303
    By R.E. Chaplin no date

6.0 GEOLOGY

Geological mapping in 1981 was confined to the newly established grid at a scale of 1:10,000 since the orthophoto maps were not available during the field season. Data obtained from previous 1:50,000 was combined with the 1981 data and results are shown in Map 2.

The lower Paleozoic stratigraphic section consists of the Mt Mye, Vangorda and Menzie Creek formations. Hadrynian - Cambrian Mt. Mye Formation consists of two principle units - non-calcareous, grey-brown, biotite-muscovite (andalusite) schist/phyllite (H$\mathcal{C}$mmp) and a dark green, variably calcareous massive to foliated metabasite (H$\mathcal{C}$mmb). Andalusite bearing schist is present on line 585E at 162N and is thought to be related to the higher metamorphic gradient in this area. These andalusite schists are typically very similar to the andalusite bearing schists of the Faro deposit. Frequently the Mt. Mye phyllites contain quartzite rich intervals which may reflect the regional correlation of this unit with the upper grit within the Selwyn Basin. The Mt. Mye metabasites are commonly more siliceous than the flows higher in the section and carried 1-2% disseminated pyrhotite.

The overlying Cambro-Ordovician Vangorda Formation consists of the following: variably calcareous, graphitic phyllite ($\mathcal{C}$Ovgp), calcareous muscovitechlorite $\pm$ biotite phyllite ($\mathcal{C}$Ovp), phyllitic marble and silicated marble ($\mathcal{C}$Ovpm), calc-silicate phyllite/schist ($\mathcal{C}$Ovcs), dark green, variably

calcareous massive metabasite (ЄOvb) and laminarly banded, variably calcareous chlorite phyllite (ЄOvcp). In addition, a non-calcareous muscovite-chlorite-biotite phyllite (ЄOvn) was mapped between the Mt. Mye and Vangorda formations.

There is apparently at least two mappable horizons of graphitic phyllite which may not be continuous. The marble and silicated marble horizons are commonly very carbonaceous and it was often very difficult to distinguish it from graphitic phyllite. The calc-silicates appear to be very restricted and are related to the higher metamorphic gradient mentioned previously. The laminarly banded chloritic phyllite is often very siliceous and is garnet bearing.

Overlying the Vangorda Fromation are Ordovician - Silurian chloritic phyllites and chlorite mottled metabasalt and metabasite of the Menzie Creek Formation (OSmc).

A steep fault of the Finlayson Lake Suture Zone justaposes middle to upper Paleozoic rocks to the south against the lower Paleozoic section. This fault zone is based on regional mapping and, in the Tenas area, occurs in the topographically low Ross river and Tenas Creek Valleys. Devono-Mississippian, rocks (DMet), possibly equivalent to Earn Group, are beige, phyllitic chert, carbonaceous phyllite and slate including pebble conglomerate. The Pennsylvanian-Permian Anvil Range Group (PPav) consists of medium to dark green, massive to fragmental finely crystalline alkali basalt. When viewed from the north east, these basalts are clearly visible as flows.

Middle to Upper Cretaceous biotite granodiorite and quartz monzonites (Kgd) of the Orchay Batholith bounds the lower Paleozoic stratigraphic section to the north. The contact is characterized by aplitic, porphyritic and pegmatitic dykes. Quartz veining and lenses become prominent as the contact is approached. Disseminated pyrite and traces of malachite were observed close to the contact.

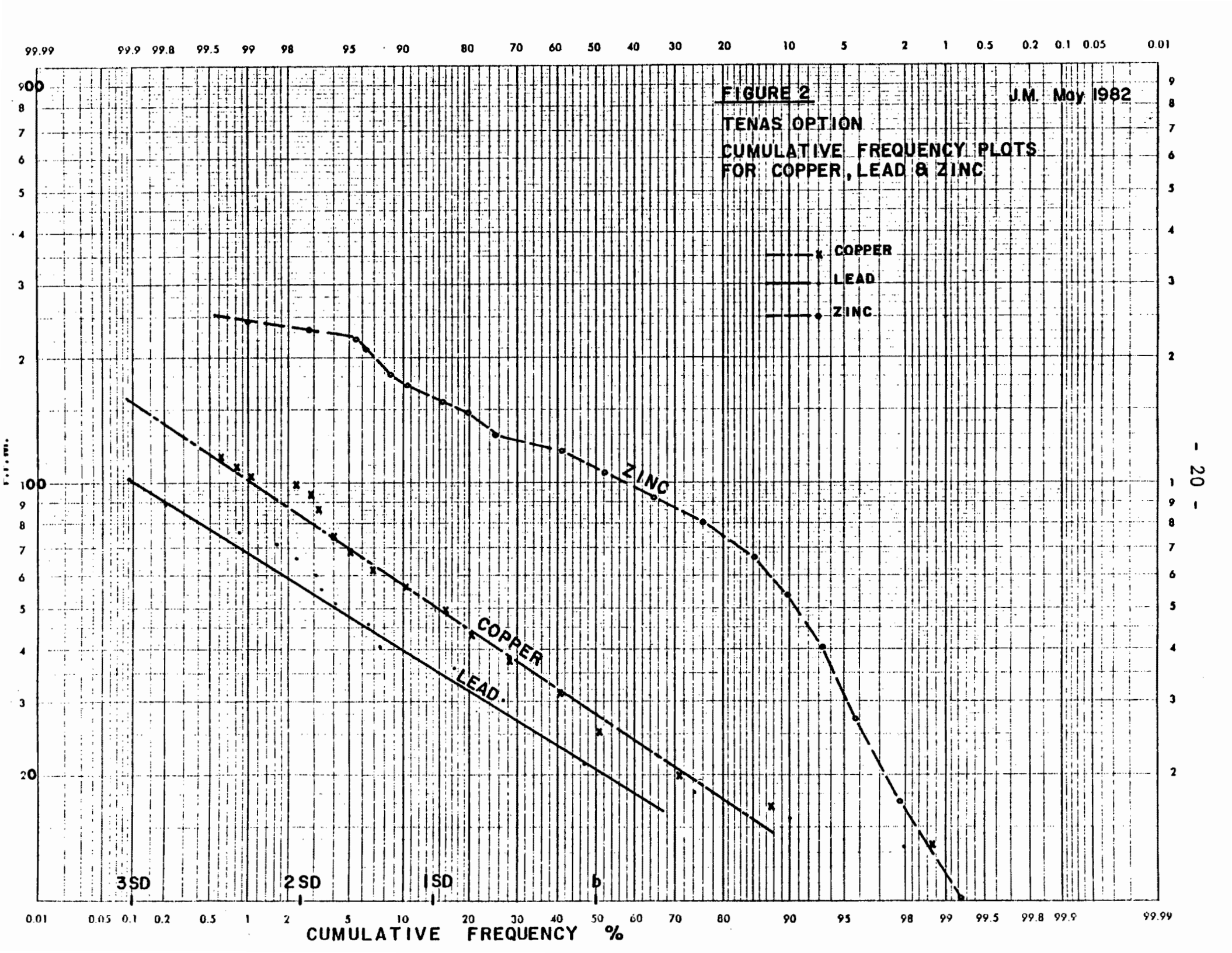
S_2 is the dominant structural fabric observed within the map area and it has a mean strike of 207° with a dip of 57 to 70 degrees to the west. S_1 is assumed to strike in the same direction with a dip that may be somewhat less than that of S_2. The folds shown on Map 2 are thought to be F_3 as outlined by the graphitic phyllite. Numerous small scale F_3 and F_4 folds were observed in outcrop - particularly within €Ovcp towards the west central portion of the map area.

7.0 GEOCHEMICAL SOIL SAMPLING SURVEY

During the 1981 field season, some 1,050 soil samples were taken from the Tenas grid as a follow up survey for potential areas of near surface sulfide mineralization. Samples were taken from either the "B" or "C" horizon at 200 foot intervals along cut lines and compass and topofil lines.

All samples were packaged in Kraft sample bags and sent to the Acme Analytical Laboratory at 852 East Hastings Street, Vancouver, British Columbia. The samples were then dried at 60° centigrade, sieved to -80 mesh and weighed to half a gram. They were then digested in hot dilute aqua reagent in boiling water and diluted to 10 ml with deionized water. The elements Cu, Pb and Zn were determined in the acid solution by Atomic Absorption. All sample pulps from the grid are stored at the Acme Analytical Laboratory in Vancouver. Sample results from the geochemical program are plotted on the accompanying 1:10,000 scale Geochemical Values and Contour Maps (Maps 3, 4 and 5).

Contour intervals for copper, lead and zinc were calculated from mean plus increasing standard deviations. From previous experience in these rock types, lead response appears to be the best indicator of stratiform sulfide mineralization followed by zinc.


FIGURE 2
J.M. May 1982
TENAS OPTION
CUMULATIVE FREQUENCY PLOTS
FOR COPPER, LEAD & ZINC
COPPER
LEAD
ZINC
ZINC
COPPER
LEAD
3SD
2SD
1SD
b
CUMULATIVE FREQUENCY %
99.99 99.9 99.8 99.5 99 98 95 90 80 70 60 50 40 30 20 10 5 2 1 0.5 0.2 0.1 0.05 0.01
0.01 0.05 0.1 0.2 0.5 1 2 5 10 20 30 40 50 60 70 80 90 95 98 99 99.5 99.8 99.9 99.99

Cu, Pb and Zn cumulative frequency plots are shown in Figure 2 on logarithmic probability paper. Cu and Pb give a reasonably straight line indicating a log-normal distribution and the data is treated accordingly and contour intervals were established at the following intervals:

	Cumulative Frequency	Cu ppm	Pb ppm
Background	50%	28	20
Mean +1 Standard Deviation	14%	50	35
Mean +2 Standard Deviation	2.5%	85	60
Mean +3 Standard Deviation	0.1%	155	100

Zn has a pronounced curvilinear plot indicating a normal distribution. The histogram plot for Zn also indicates it is normally distributed. Thus the contour intervals for Zn were established assuming a normal distribution at the following intervals:

	Zn ppm
Background	113
Mean +1 Standard Deviation	165
Mean +2 Standard Deviation	220
Mean +3 Standard Deviation	270

7.1 Copper Contours and Geochemical Values

With a background of 50 ppm, the copper data and contours are shown in Map 3. The best anomaly is centred on line 575E at 156N with a high value of 225 ppm. Metabasite of the Vangorda Formation (Ꞓ Ovb) outcrops in the immediate area. Other low order anomalies which occur in the western part of the grid are certainly line biased and it is probable that many of these are associated with metabasite occurrences.

7.2 Lead Contours and Geochemical Values

Pb values and contours are shown in Map 4 and once again the contour pattern suggests a line biased nature west of 520E.

The anomaly centered on line 540E, 156N has a high value of 485 ppm (25 times background). This is the location of DDH 75-01, drilled to discover the source of the original anomaly. This hole did test the favourable Mt. Mye - Vangorda contact horizon but did not encounter any mineralization. Similarly, the anomaly on 570E at 158N, with a high of 385 ppm is the site for DDH 75-02 and ET 81-01. While not extensive there is a high value at 585E, 154N of 413 ppm. These three anomalies are possibly related as they all occur at similar stratigraphic horizons and have values which are of the same order of magnitude above background.

An isolated, poorly defined anomaly of 100 ppm at line 445E, 158N is apparently well up in the Vangorda section. Another anomaly with a high of 205 ppm at 475E, 136S occurs at the correct stratigraphic interval but is somewhat isolated and gains little support from surrounding values.

7.3 Zn Contours and Geochemical Values

As in Cu and Pb, a pronounced line bias is apparent in the Western sector of the grid. Generally Zn shows wider dispersion and slightly higher contrast than Pb. As well, the Zn values show a broad correlation with the Mt. Mye - Vangorda contact, except for the area between 600E and 640E which may be covered by thicker overburden.

The two anomalies centered on line 570E and 540E with high values of 2700 and 800 ppm respectively may be continuous but for an interval of assumed thicker overburden. These two Zn highs are coincident with Pb anomalies. An isolated high value of 800 ppm occurs at 580E, 156N and is presumed to relate to the anomaly on 570E, despite a discontinuity along line 575E. In addition the high Zn values on 580E correlate well with a Pb high on 585E at 154N.

The anomaly between line 445 and 460E, with a high of 665 ppm, is coincident with a Pb high of 100 ppm. Lack of outcrop in the immediate area

precludes a definitive assessment of the stratigraphic section, but this anomaly may be near the Mt. Mye - Vangorda contact. Alternatively this anomaly may occur proximal to metabasites of Mt. Mye which commonly contain disseminated pyrrhotite. Many of the low order Zn anomalies appear to be related to metabasite occurrences.

8.0 GEOPHYSICAL SURVEY

A reconnaissance spectral IP survey was undertaken on 7 lines with an electrode interval of 500 ft. In addition a survey was completed along the base line with an electrode interval of 1,000 ft. Complete results of this survey by Phoenix Geophysics are given in Appendix I.

The spectral IP survey was planned to locate metallic mineralization that might be present. Extensive tests over graphitic hosted sulfides indicated the possibility of being able to descriminate between sulfide mineralization or graphitic phyllite. It was hoped that descrimination of a similar nature would be achieved in the Tenas survey. However, the data obtained was not sufficient to allow detailed descrimination. Detailed discussion of results are given in the Appendix.

In general the survey was able to pinpoint the contact between the Mt. Mye and Vangorda formations and is represented by the sharp contact in resistivity on all lines. A peculiar feature is the apparent resistivity difference between rocks of Mt. Mye affinity and rocks of the Vangorda formation. The Vangorda Formtion shows as a relatively high resistivity while those of Mt. Mye show low resistivity. This phenomenon may be due to the presence of 1-2% disseminated pyrrhotite, particularly within the metabasite.

Each line has similar anomalies which are thought to be related. The best appear to occur on either line 565E or line 550E where there are coincident IP and resistivity anomalies. The fact that these anomalies appear in each line, as well as others, suggest that they are related to strtigraphic units and possibly not indicative of mineralization. The inversion of the spectral IP plots for this data is somewhat inconclusive, indicating both graphite and sulfides.

The survey along the base line indicates the lower resistivity Mt. Mye Formation to the west of 530E and the higher resistivity Vangorda Formation to the east. In addition, there is a strong, narrow, shallow resistivity anomaly centered at 510E. The spectral plots suggest the source may be graphitic.

9.0 1981 DRILL RESULTS

During 1981, 3 diamond drill holes totalling 1,417.6 m were completed on the Tenas claims. All holes were NQ in size and collared vertically. Complete logs are on file at Cyprus Anvil and summary logs are provided in Appendix II. Core from the 1981 drilling has all been removed and is presently in the core storage facilities at the Grum camp near Faro.

ET81-01 was collared at 570E, 156N to evaluate the coincident Pb-Zn anomaly and to test the occurrence of some weak mineralization within the graphitic sections of 75-02. 75-02, an angle hole, did not pass through the Mt. Mye - Vangorda contact so it did not adequately test the surface geochemical anomaly. Drilled to a total depth of 461.8 m, ET81-01 was terminated in Mt. Mye phyllites. Sparse sphalerite mineralization within very siliceous graphitic phyllite was observed between 197.8 and 198.1 m as well as between 200.5 and 201.4 m. The sphalerite was red brown and appeared to be stratiform within siliceous horizons of the graphitic sequence. The mineralization and lithologies are like those either up or down dip from massive sulfides at either Faro or the Grum deposits.

In addition to the observed mineralization, several horizons of white mica envelope lithology were encountered, notably from 173.0 to 196.2 m. This alteration sequence again is characteristically associated with more massive sulfide mineralization within the Anvil district. In 81-01 it consists of bleached ϵOvp with quartz-chlorite (pyrrhotite) carbonate veinlets. Other than the quartz noted in the veinlets the alteration was not siliceous.

Based on the results of ET81-01, it was decided to test the downdip extension of the mineralization by stepping southwest 500 ft. and drilling another hole, ET81-02. This second hole encountered similar lithologies and was stopped at 458.4 m, well within the Mt. Mye phyllites. Trace amounts of red brown sphalerite were once again observed as stratiform lenses within very siliceous, graphitic phyllites.

ET81-03 tested the strike extension of the mineralization encountered in 81-01 and 81-02. Once again trace amounts of red-brown stratiform sphalerite were observed within siliceous graphitic phyllites. The only difference between this and the other two holes was the presence of finely disseminated pyrite within the graphitic phyllite. This hole was stopped at 497.4 m, well within the Mt. Mye Formation.

10.0 CONCLUSIONS

Previous drilling programs within the Tenas area were guided primarily by geochemical and geophysical targets. It has been shown that holes did not adequately test the favourable stratigraphic targets, and that only three happened to penetrate the Mt. Mye - Vangorda contact, a known host to stratiform mineralization.

The 1981 drilling program indicated the presence of a mineralizing system similar to that observed around most of the deposits in the Anvil district. The combined presence of stratiform sphalerite within siliceous graphitic phyllites or quartzites and the alteration assemblages suggests the area drilled has need for more drilling.

The geochemical survey, while not adding new information, did tend to clarify the anomalies that were previously known. Without the new survey it would have been very difficult to correlate between anomalies and geology. The geophysical survey did help in the interpretation of geology with respect to the Mt. Mye - Vangorda contact.

The 2.0 m gal. gravity Pelly Anomaly remains somewhat enignatic, despite having been drilled. This gravity high occurs in association with some vein type mineralization, which may be remobilized from a stratiform deposit at depth. There is evidence of a high thermal gradient in the area with the presence of calc-silicates.

11.0 RECOMMENDATIONS

Future work is governed partly by assessment work requirements. Those claims within the Watson Lake Mining District need most of the work for assessment purposes. In addition, further work should recognize that pre-1981 work was done without fully understanding the significance of detailed stratigraphy.

The following 1982 program is recommended as part of the ongoing evaluation of the Tenas Option. A major objective of this program is to enable a decision to be made by the end of 1982 as to whether or not the option should be retained.

1. Integration of all existing data using the new orthophoto maps at a scale of 1:10,000.

2. Finish detailed mapping to pinpoint the favourable contact in a structural framework.

3. Barium analysis should be carried out on soil samples that have high Pb or Zn values.

4. Some additional soil sampling and trenching should be carried out over the coincident Pb-Zn anomaly between 445E and 460E at

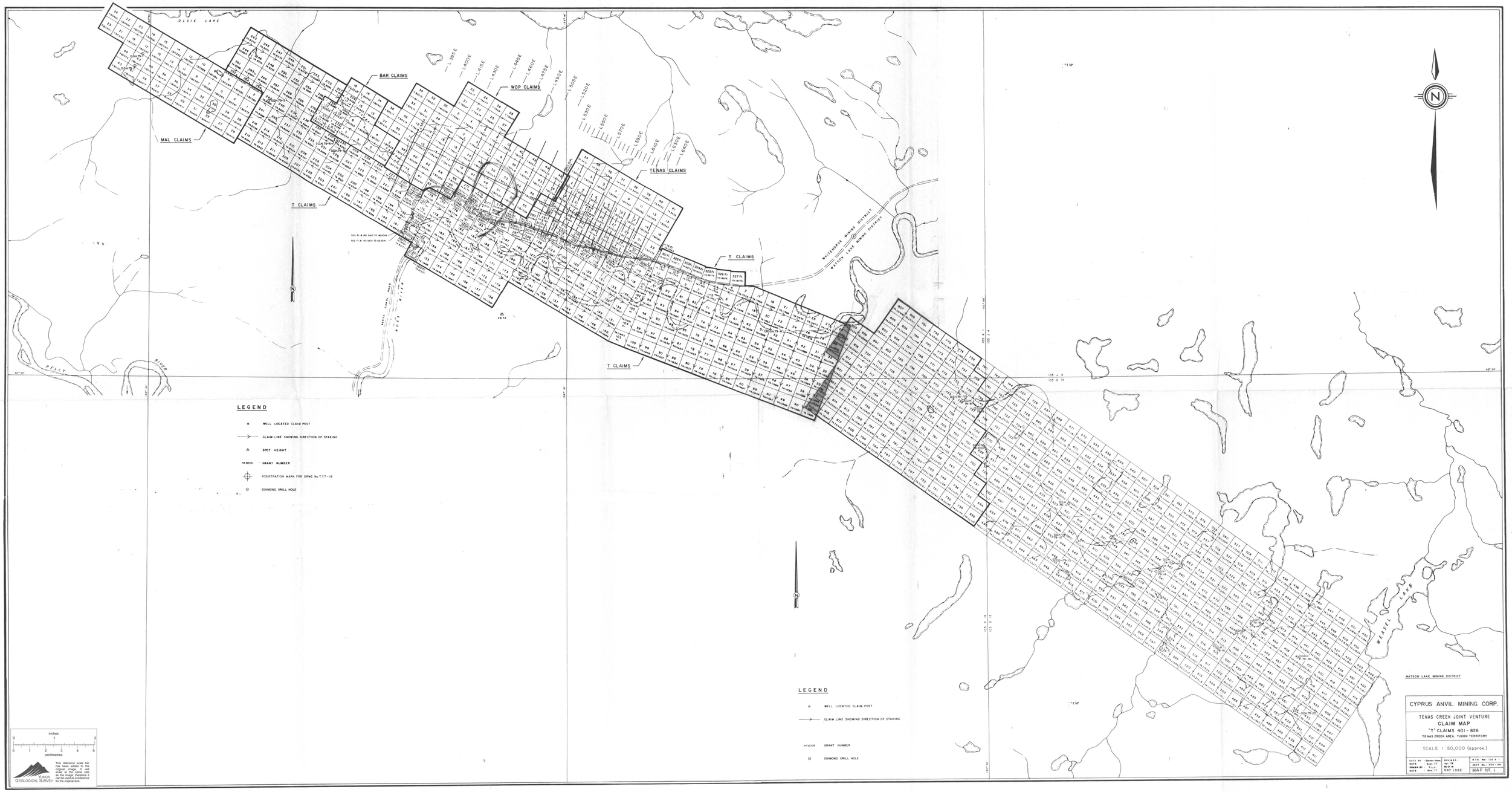
5. Two holes are recommended to follow-up the mineralization and alteration encountered in the 1981 drilling. At least one of these holes should be drilled well downdip of 81-02 and 81-03.

6. At least one hole designed to penetrate the favourable contact in the Pelly gravity anomaly. This one or two hole program here would satisfy much needed work within the Watson Lake Mining District, thereby nullifying a possible payment of some $9,000 in 1983 for payments in lieu.

Map 1

Claim Map and Grid Location

1:50,000



LEGEND

- WELL LOCATED CLAIM POST
- CLAIM LINE SHOWING DIRECTION OF STAKING
- SPOT HEIGHT
- 1A 83/3 - GRANT NUMBER
- REGISTRATION MARK FOR DRWG No. T.77-19
- DIAMOND DRILL HOLE

LEGEND

- WELL LOCATED CLAIM POST
- CLAIM LINE SHOWING DIRECTION OF STAKING
- 1A 112/6 GRANT NUMBER
- DIAMOND DRILL HOLE

WATSON LAKE MINING DISTRICT

CYPRUS ANVIL MINING CORP.

TENAS CREEK JOINT VENTURE

CLAIM MAP

"T" CLAIMS 401 - 826

TENAS CREEK AREA, YUKON TERRITORY

SCALE 1 : 50,000 (approx.)

DATA BY	Canam Assoc.	REVISED	N.T.S. No.: 105 K 1
DATE	Sept. '77	Jan. '78	
DRAWN BY	N. J.	Feb. '78	ACCT. No.: 328-04
DATE	Nov. '77	MAY. 1982	MAP NR. 1

inches
0 1 2
centimetres
0 1 2 3 4 5

YUKON GEOLOGICAL SURVEY

This reference scale bar was accurate for the original image. It will scale at the same rate as the original and hence it can be used as a reference for the original size.

Map 2

Geology

1:10,000

CRETACEOUS

Kgd — Biotite granodiorite quartz monzonite.

PENNSYLVANIAN - PERMIAN
Anvil Range Group

PPav — Medium to dark green, massive to fragmental finely crystalline alkali basalt.

DEVONIAN - MISSIPPIAN
Earn Group

DMet — Beige, phyllitic chert and carbonaceous phyllite and slate; includes pebble conglomerate.

ORDOVICIAN - SILURIAN
Menzie Creek Formation

OSmc — Chloritic phyllite, chlorite - mottled metabasalt and metabasite.

CAMBRIAN - ORDOVICIAN
Vangorda Formation

€Ovp — Calcareous muscovite - chlorite ± biotite phyllite.

€Ovcs — Calc - silicate phyllite equivalent of €Ovp.

€Ovb — Dark green, variably calcareous, massive metabasite.

€Ovcp — Laminarly banded, variably calcareous, chloritic phyllite.

€Ovgp — Variably calcareous, graphitic phyllite.

€Ovpm — Phyllitic marble and silicated marble.

€Ovm — Non - calcareous muscovite - chlorite ± biotite phyllite (possibly = HCmmp)

HADRYNIAN - CAMBRIAN
Mt. Mye Formation

HCmmp — Non - calcareous, grey - brown biotite - muscovite andalusite schist with lesser phyllitic equivalents.

HCmmb — Dark green variably calcareous, massive to foliated metabasite.

• 3820 Station Number

Outcrop Boundary

Geological Contact

Steep Fault

⊙ Diamond Drill Hole Location

inches
0 1 2
centimetres
0 1 2 3 4 5

YUKON GEOLOGICAL SURVEY

This reference scale bar was plotted at the original image & will scale at the same ratio as the image, therefore it can be used as a reference for the original size.

Scale 1:10,000
0 100 200 300 400 500 1000 M

CYPRUS ANVIL MINING CORPORATION

MAL, BAR, WOP, TENAS, BELL AND T MINERAL CLAIMS - TENAS OPTION
Whitehorse & Watson Lake Mining Districts

GEOLOGY

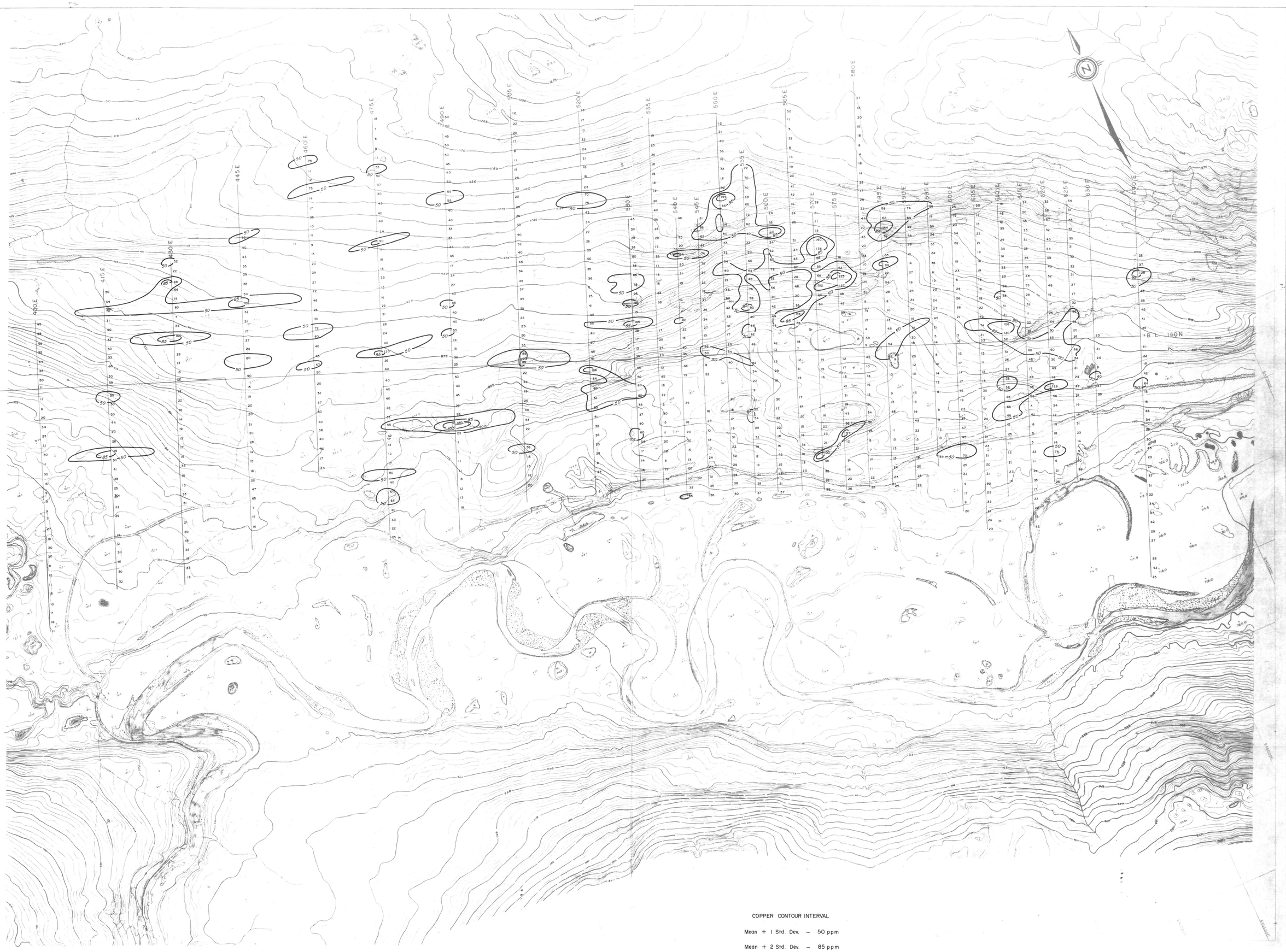
NTS 105 E - 1, 2, & F - 15
SURVEY BY: J.M.
DRAWN BY: C. L. C.

DATE: MAY 1982
MAP N°.2

Map 3

Copper Geochemical Values
and Contours

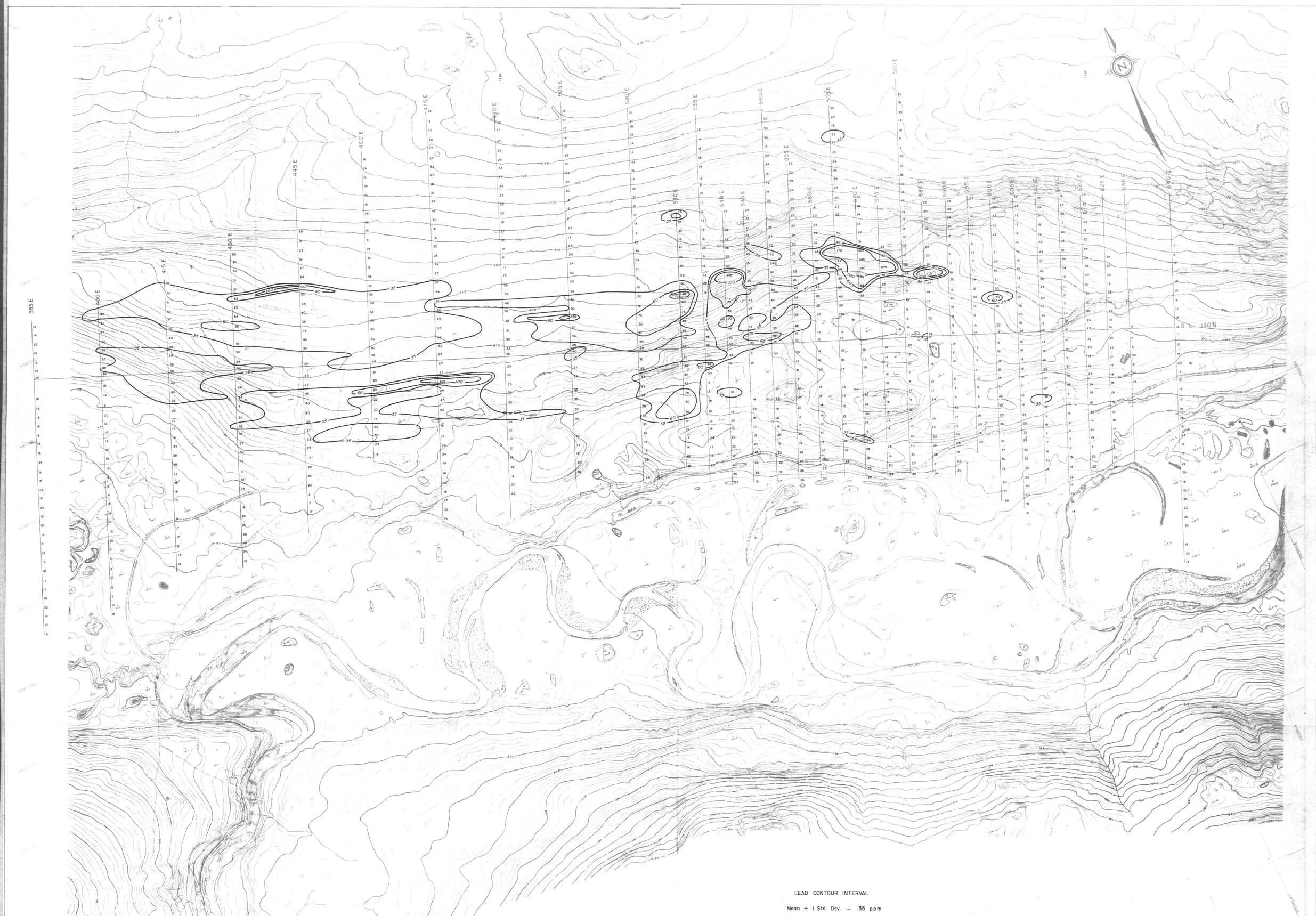
1:10,000


385 E
400 E
415 E
430 E
445 E
460 E
475 E
490 E
505 E
520 E
535 E
550 E
565 E
580 E
595 E
610 E
625 E
640 E
655 E
670 E
685 E

Map 4

Lead Geochemical Values
and Contours

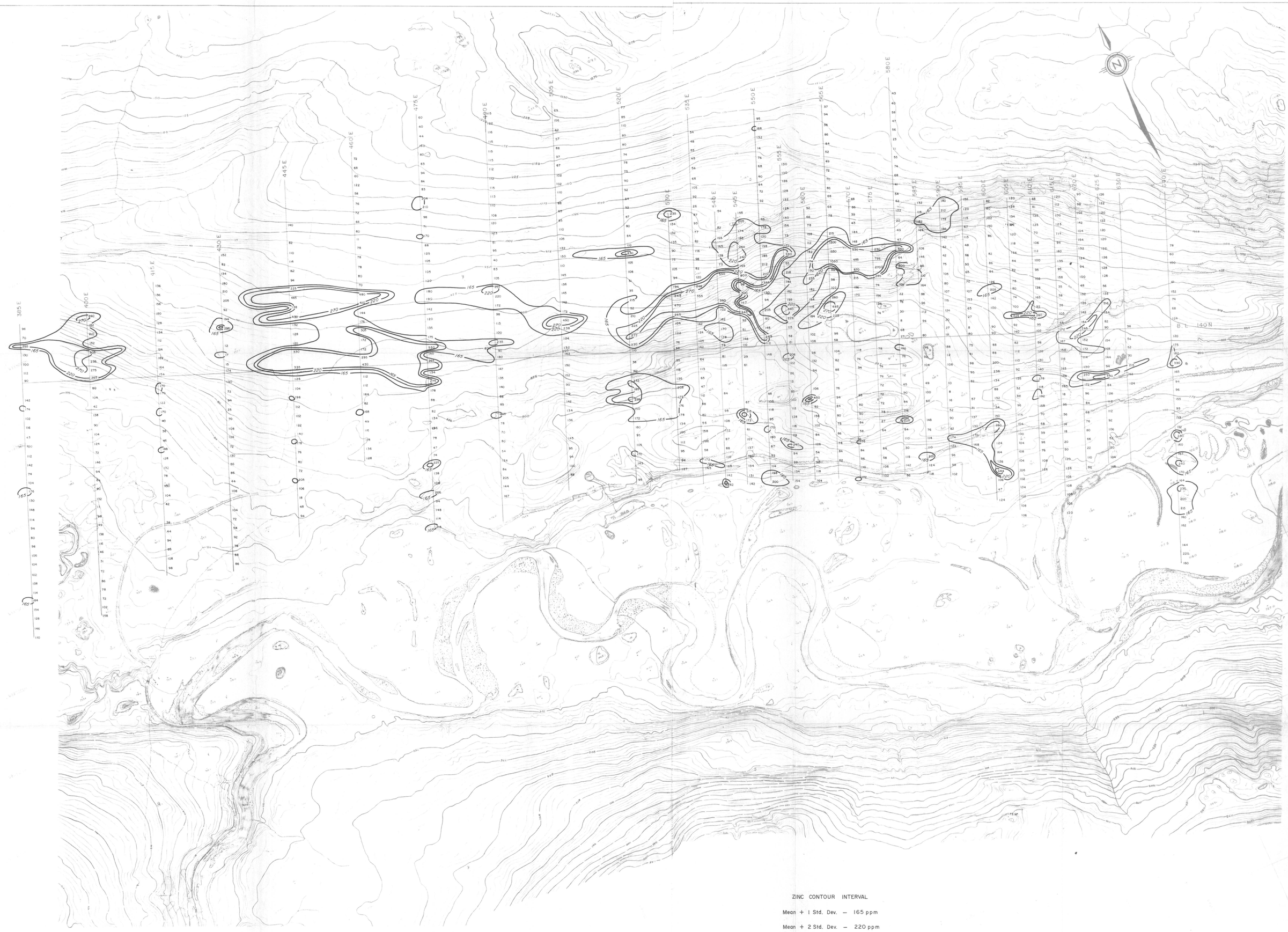
1:10,000


385E
400E
415E
430E
445E
460E
475E
490E
505E
520E
535E
550E
565E
580E
595E
610E
625E
640E
655E
670E
685E
700E
715E
730E
745E
760E
775E
790E
805E
820E
835E
850E
865E
880E
895E
910E
925E
940E
955E
970E
985E

Map 5

Zinc Geochemical Values
and Contours

1:10,000


385 E
400 E
415 E
430 E
445 E
460 E
475 E
490 E
505 E
520 E
535 E
550 E
565 E
580 E
595 E
610 E
625 E
640 E
655 E
670 E
685 E

APPENDIX I

GEOPHYSICAL REPORT

TABLE OF CONTENTS

Part A:	Report	13 pages	Page
1.	Introduction		1
2.	Presentation of Results		2
3.	Discussion of Results		4
4.	Conclusions and Recommendations		8
5.	Certificate - P.G. Hallof		13
6.	Appendix		
Part B:	Illustrations	63 pieces	
	Plan Map (in pocket)	Dwg. S.I.P.P. 3109	
	SIP Data Plots	Dwgs. SIP 1104-1 to -3 Dwgs. SIP 1105-1 to -4 Dwgs. SIP 1106-1 to -6 Dwgs. SIP 1107-1 to -11 Dwgs. SIP 1108-1 to -8 Dwgs. SIP 1109-1 to -11 Dwgs. SIP 1110-1 to -9 Dwgs. SIP 1111-1 to -10	

PHOENIX GEOPHYSICS LIMITED

REPORT ON THE
RECONNAISSANCE SPECTRAL IP SURVEY
TENAS PROJECT
WHITEHORSE MINING DISTRICT, Y.T.
FOR
CYPRUS ANVIL MINING CORPORATION

---

1. INTRODUCTION

At the request of Dr. David S. Jennings, Chief Geologist, we have completed a reconnaissance Spectral IP Survey on widely spaced lines at the Tenas Project, on behalf of Cyprus Anvil Mining Corporation. The area of interest chosen for the survey lies to the east of the main mining area at Faro, in the Whitehorse Mining District of the Yukon Territory.

The reconnaissance geologic map of the area shows that favourable host rocks from the Faro District strike roughly east-west across the reconnaissance grid. The spectral IP survey was planned to locate any unknown zones of metallic mineralization that might be present. Further, previous Test Surveys with the Spectral IP technique, in the vicinity of the known ore zones, have shown that the sources of the Spectral IP anomalies detected can often be established as being sulphide

mineralization or graphitic phyllite. This separation is made, based upon the time-constant of the Cole-Cole Dispersion that best approximates the IP effect measured.

2. PRESENTATION OF RESULTS

When the IPV-3 is used in the field, the complete results are stored on tape cassettes, using the CP-1 Computer, which is a major part of the system. These tape cassettes can then be used to plot the data in the field using the HP85, portable computer. In the office, the tape cassettes are used to process the data through an HP9845, portable computer. As outlined in the attached technical paper, the processing consists of the removal of inductive coupling effects from the spectral data and the determination of the electrical parameters of the Cole-Cole dispersion that best fits the measured data.

This processing is applied to the spectral data obtained for each dipole pair along the lines. The various parameters (both measured and calculated) are also plotted in "pseudosection" form by the computer. A copy of all of the relevant data is enclosed in Volume II of the report. Certain spectral plots and pseudosections have been extracted for discussion in this portion of the report.

Line	Electrode Intervals	Dwg. No.
580E	500'	SIP 1104-1 to -3
565E	500'	SIP 1105-1 to -4
550E	500'	SIP 1106-1 to -6
535E	500'	SIP 1107-1 to -11
505E	500'	SIP 1108-1 to -8
475E	500'	SIP 1109-1 to -11
445E	500'	SIP 1110-1 to -9

Also enclosed with this report is Dwg. SI.P.P. 3109 a plan map of the lines surveyed at a scale of 1" = 833' or 1:10,000. The definite, probable and possible Induced Polarization anomalies are indicated by bars, in the manner shown on the legend, on this plan map as well as on the data plots. These bars represent the surface projection of the anomalous zones as interpreted from the location of the transmitter and receiver electrodes when the anomalous values were measured.

Since the Induced Polarization measurement is essentially an averaging process, as are all potential methods, it is frequently difficult to exactly pinpoint the source of an anomaly. Certainly, no anomaly can be located with more accuracy than the electrode interval length; i.e. when using 500' electrode intervals the position of a narrow sulphide body can only be determined to lie between two stations 500' apart. In order to definitely locate, and fully evaluate, a narrow, shallow source it is necessary to use shorter electrode intervals. In order to locate sources at some depth, larger electrode intervals must be used, with a corresponding increase in the uncertainties of location. Therefore, while the centre of the indicated anomaly probably corresponds fairly well with source, the length of the indicated anomaly along the line should not be taken to represent the exact edges of the anomalous material.

The topographic and geologic information shown on Dwg. SI.P.P. 3109 has been taken from maps made available by the staff of Cyrpus Anvil Mining Corporation.

3. DISCUSSION OF RESULTS

The reconnaissance spectral IP survey at the Tenas Project has given results that are of interest. Definite phase IP anomalies have been detected on all of the lines surveyed; on several lines more than one anomaly was located. Some of the anomalous patterns indicate a shallow source (i.e. anomalous for n = 1). In other cases the results suggest a source at considerable depth.

Line 580E

This is the easternmost line surveyed. There is a shallow anomaly centered at the north end of the data (155N). The source of this anomaly could be better located, and evaluated, by repeating the measurements with shorter electrode intervals and by extending the data to the north. The inversion of the spectral data for D6;N1 gives a time-constant value of 0.45 sec. This does not suggest that graphite is the source.

At the south end of the data there is the suggestion of a deep source at about 120N to 125N. This anomaly cannot be evaluated with the present data; further work would be necessary. The spectral results for D2;N4 gives a moderate apparent resistivity and a time-constant of 4.3 seconds.

The source of the deep anomaly is indicated to lie within, or beneath, the higher resistivity rock unit. The apparent resistivity pseudeosection clearly indicated the contact to be at 150N, near surface. To the north, the apparent resistivities are appreciably lower in magnitude. At some points there are anomalous IP effects within this rock unit; at other places there are none.

This resistivity contact can be easily interpreted on each of the north-south lines we have surveyed. The interpreted contacts have been plotted on the plan map (Dwg. SI.P.P. 3109) and then correlated from line to line.

Line 565E

On this line there is a shallow, narrow, source at about 155N to 160N; this anomaly can be better evaluated only by using shorter electrode intervals. The spectral results for D7;N1 and D7;N3 give time-constants in the range from 0.35 to 2.1 seconds.

The contour pattern suggests a possible second, deeper source, centered at about 150N. This location would be approximately under the northern edge of the high resistivity rock unit. The anomaly pattern is small and sharp; the anomaly shape may suggest that the line passes near the end of a relatively small source. Further detailed measurements would be necessary to better locate, and evaluate, the source.

Line 550E

The deep source on Line 565E may correlate with the much stronger, larger, deep anomaly centered at 155N to 160N on Line 550N. The source of this anomaly appears to lie well within the lower resistivity rock unit. The pattern for this definite, deep source is incomplete. The measurements would have to be extended to the north. The spectral time-constant characteristics for this anomaly are fairly large. However, they are poorly determined and better data is necessary.

There is a slight suggestion in the apparent resistivity data and in the phase shift data, of a second anomaly at considerable depth.

The source would be located beneath the high resistivity rock unit, centered at about 140N to 145N.

Line 535E

There is a similar, very deep anomalous pattern on this line that is somewhat more pronounced than 1500 feet to the east. On Line 535E, the source would have to be centered, at considerable depth, at about 135N to 145N.

The shallow anomaly centered at 155N to 160N on this line is more easily interpreted. The apparent resistivity measured for n = 1 is quite low. The shallow source could be better located, and evaluated, using shorter electrode intervals. The spectral plots for D6;N1, D7;N1; D7;N2 and D8;N3 range from 2.1 seconds to 54 seconds. Measurements with shorter electrode intervals would be more discriminating.

Line 505E

This line lies 3000 feet to the west; the contact with the high resistivity rocks is farther to the south (at about 130N). This interpretation requires an off-set between Line 505E and Line 535E. As we shall discuss later, the measurements along Line 140N Baseline confirm the shift in the contact at about this point.

The apparent resistivity and phase IP data on Line 505E suggest a complex, multiple source in the interval 125N to 150N. It is possible that the survey line is passing more parallel than perpendicular to the source. Further, detailed measurements would be necessary to clarify the location of the source, or sources.

The inversion of the spectral IP plots for the deep anomaly at 125N to 130N show time-constants that range from 0.06 seconds to 0.51 seconds. This result is important, and detailed measurements with

shorter electrode intervals should give rise to more reliable spectra that would permit a better interpretation for the northern portion of the anomaly.

Line 475E

A distance of 3000 feet to the west, the pseudosection for Line 475E indicates two, relatively distinct sources within the lower resistivity rocks. There is a strong, deep source centered at 145N to 150N and a narrow, shallow source centered at 135N to 140N.

The inversion of the spectral plots D4; D6 and D7 shows that the time-constants for these two IP dispersions are fairly small for the shallow source and large for the deeper source.

Detailed measurements are warranted to further investigate the sources of the two anomalies. Better data should lead to better determinations for the time-constant.

Line 445E

The deep anomaly outlined on Line 475E may correlate with the even deeper, stronger anomaly centered at about 135N to 140N on this line. This position for the source would be beneath the edge of the higher resistivity rock unit.

This is one of the more definite deep anomalies located during the reconnaissance survey at Tenas Creek and further investigation is warranted.

The spectral inversion for the dipole pair within the deep anomaly (D4;N2, D4;N4) give time-constants that suggest sulphide mineralization as the source. The measurements at less depth to the north (D5;N1, D7;N2, D7;N3, D8;N1) all give much larger values of time-constant that suggest graphitic material as the source.

Baseline 140N

This east-west line was surveyed using X = 305 meters. The apparent resistivity results show the lower resistivity rock unit to the west of about 530E and the higher resistivity rock unit to the east. This position for the contact agrees relatively well with the off-set previously predicted between Line 505E and Line 535E.

In addition, there is a strong, narrow, shallow resistivity anomaly centered at 510E. There are IP effects here; the pattern suggests that the line crosses the source at approximately right angles and the anomaly correlates with the complex source previously described in Line 505E. The sources should be better located, and evaluated by making measurements using shorter electrode intervals on lines parallel to Baseline 140N.

The spectral plots for the dipole-pair within the anomaly show large values, suggesting that the source may be graphitic. However, the values are poorly determined since the measurements were noisy due to low voltages. Detailed measurements with shorter electrode intervals will give large voltage levels and the spectral plots should be more accurately determined.

4. CONCLUSIONS AND RECOMMENDATIONS

The lines used for the reconnaissance survey at the Tenas Project are 1500 feet and 3000 feet apart. An electrode interval of X = 500 feet was used for the survey and the correlation between lines is possible due to the fact that the patterns show similarities from line to line.

As shown on the plan map, Dwg. No. SI.P.P. 3109, the area of the survey is underlain by volcanic rocks. There is only limited outcrop,

presumably because of recent sediment distributed in the river valley. The contact between high resistivity rocks to the south and lower resistivity rocks to the north, has been interpreted from the data plots and transferred to the plan map. This interpreted contact does not correlate exactly with the approximate contacts shown on the geologic map. It would be worthwhile to discover which of the volcanic rock units correlates with the high resistivity rock unit, some further reconnaissance geologic mapping could be accomplished using straightforward resistivity techniques.

As shown on the Spectral IP pseudosections, some of the low resistivity rock unit, to the north of the interpreted contact, has broad, weak IP effects. However, there are numerous strong IP anomalies, with associated resistivity lows, within this zone. The anomalies have been shown on the plan map. An attempt has been made to correlate these anomalies from line to line. The correlations have been made, based upon the character of the anomalous values and the indicated depth to the source. Because of the distance between the survey lines, this may not be correct.

In the case of most of the anomalies, the reconnaissance spectral IP results are not definitive enough to permit a discrimination interpretation. The purpose of the reconnaissance survey was primarily to locate anomalous zones; further detailed measurements would be necessary to better locate and evaluate the source of the anomalies. In addition, greater care must be taken to obtain more reliable spectral information on at least one line across each anomalous zone. With accurate spectral IP data for several dipole-dipole pairs in an anomalous pattern, it should be possible to determine the time-constant

of the IP effect from that source.

The nature of the detailed measurements required will depend upon whether the data measured with X = 500' indicates the source to be shallow, or at depth.

a) For the shallow source, the n = 1 measurement with X = 500' is anomalous. The most definte examples from the reconnaissance survey at the Tenas Project are centered at Line 565E, 157+50N; Line 535E, 155N; Line 475E, 137+50N. The detailed measurements should be of three types:

i) The measurements over the anomaly with the spectral system should be repeated with X = 300', and even shorter electrode intervals. The electrode interval should be shortened until the maximum apparent IP effect <u>is not</u> measured for n = 1.

ii) Closely spaced parallel lines should also be surveyed with this short electrode interval.

iii) On one of the lines of this small grid, time should be taken to make an accurate set of spectral measurements. This will be made somewhat easier by the fact that the voltages measured for the short electrode intervals will be larger in magnitude.

b) For the deep sources, the highest IP effects and the lowest apparent resistivities are measured for the larger values of (n). The more definite of the deep anomalies are centered at Line 550E, 155N to 165N; Line 475E, 145N to 155N; Line 445N,

130N to 140N. Because the sources of these anomalies are at depth, they will be difficult to intersect with a single drill hole. Further, the drilling will be expensive. Detailed measurements are necessary, and warranted, to obtain the best location for the source that is possible. Detailed measurements of several types are warranted.

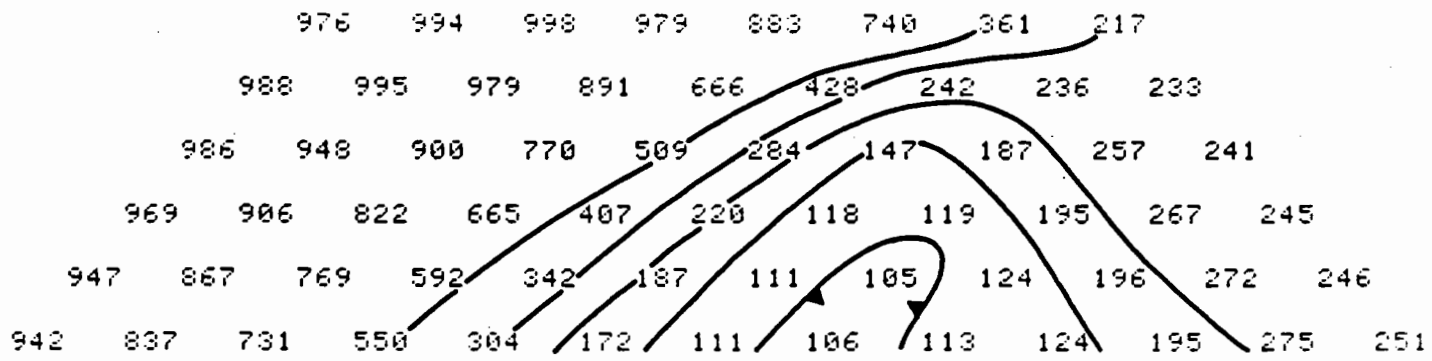
i) The X = 500' measurements should be repeated with the electrode positions shifted 250 feet. This data will confirm the presence of the deep source.

ii) Lines 500 feet and 1000 feet to the east and west of the discovery lines should be surveyed to determine the variations, along strike, of the source. Several of the anomalous patterns for the deep sources, measured with X = 500', suggest that the line may pass near the end of the deep source. The attached theoretical results for sources with infinite strike length show much broader patterns than were measured.

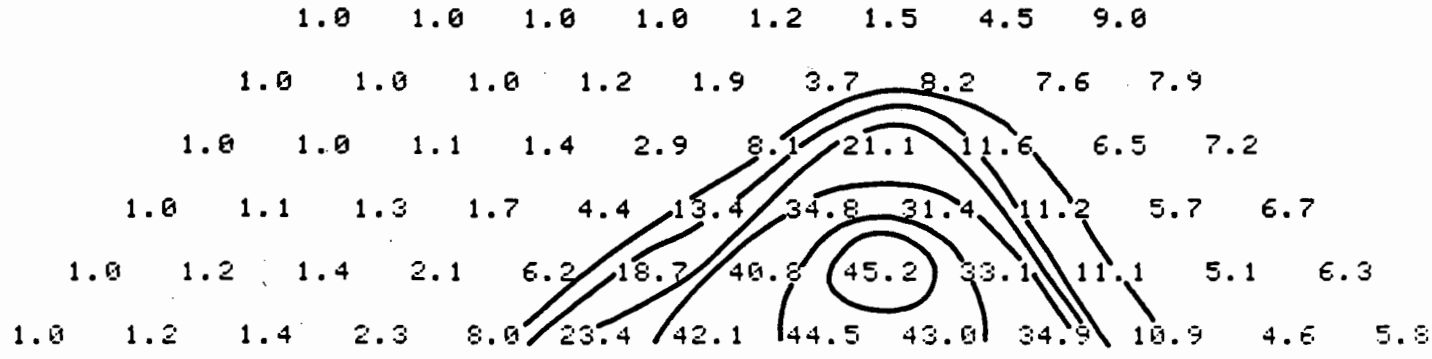
iii) The survey lines necessarily cross the strike of the geologic formation, and the resistivity patterns vary accordingly. When a deep source has been located on several parallel lines, a perpendicular line should be surveyed directly over the source and parallel to its apparent

Fig. I

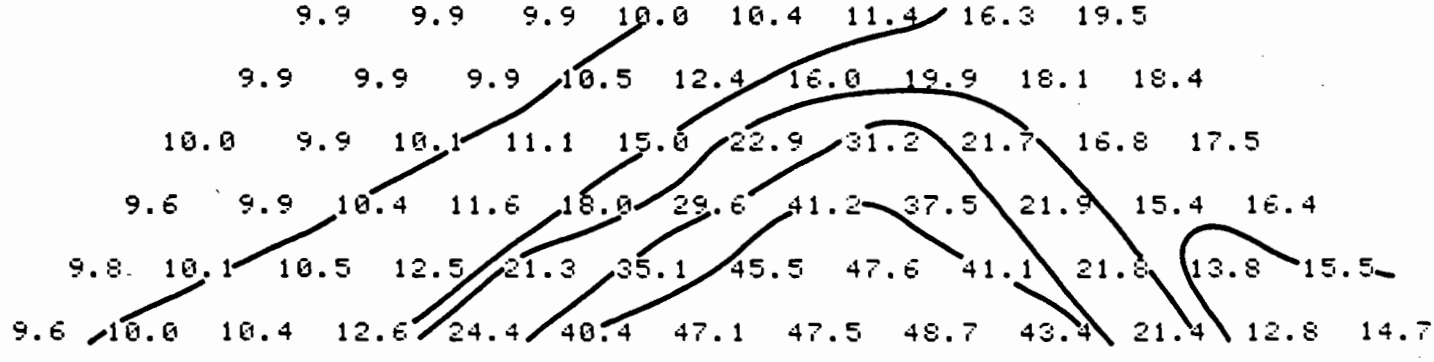
APPARENT RESISTIVITY

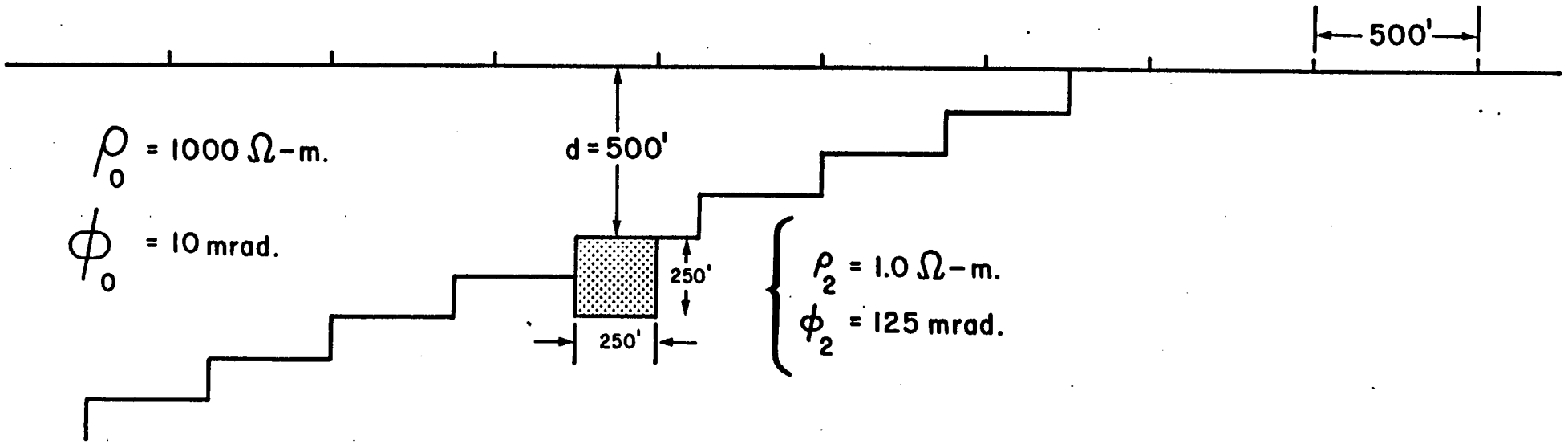


APPARENT METAL FACTOR



APPARENT PHASE





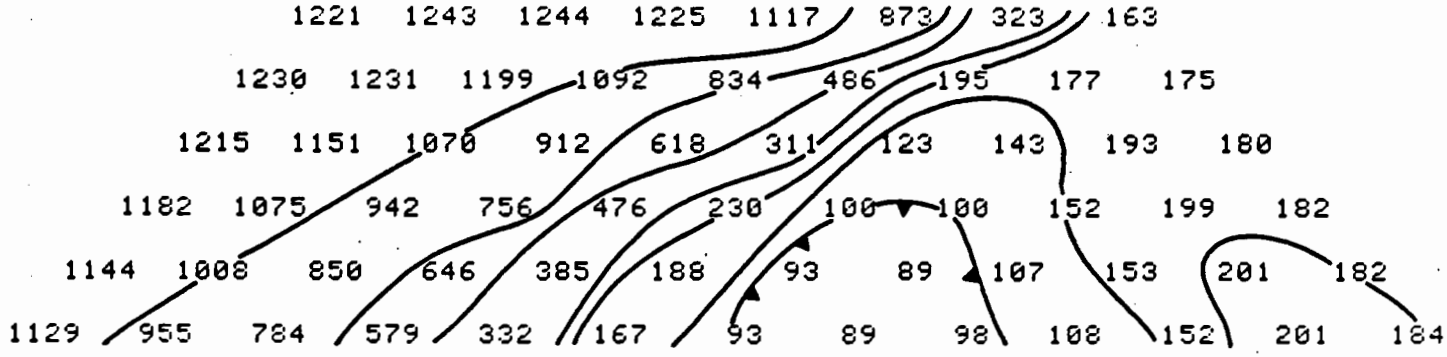
ρ_1 = 200 Ω-m.

ϕ_1 = 20 mrad.

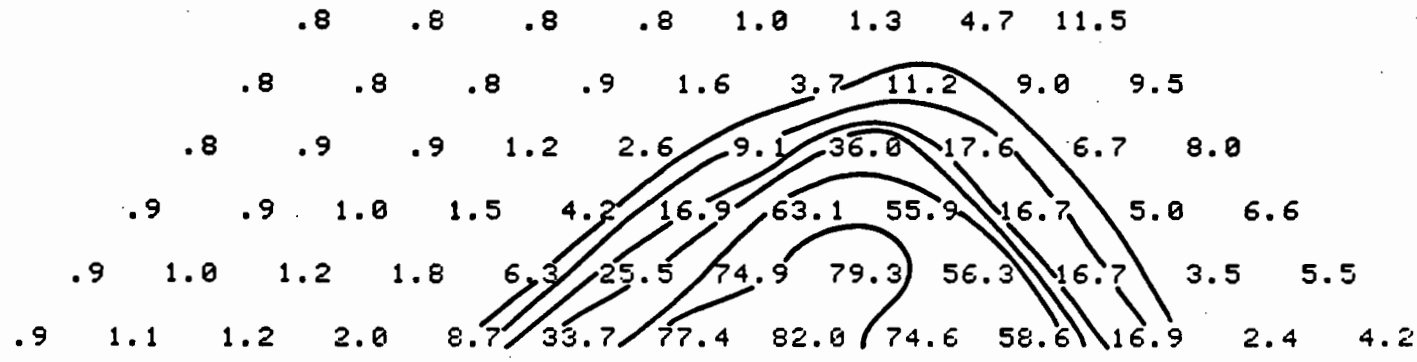
Fig. 1

Fig. II

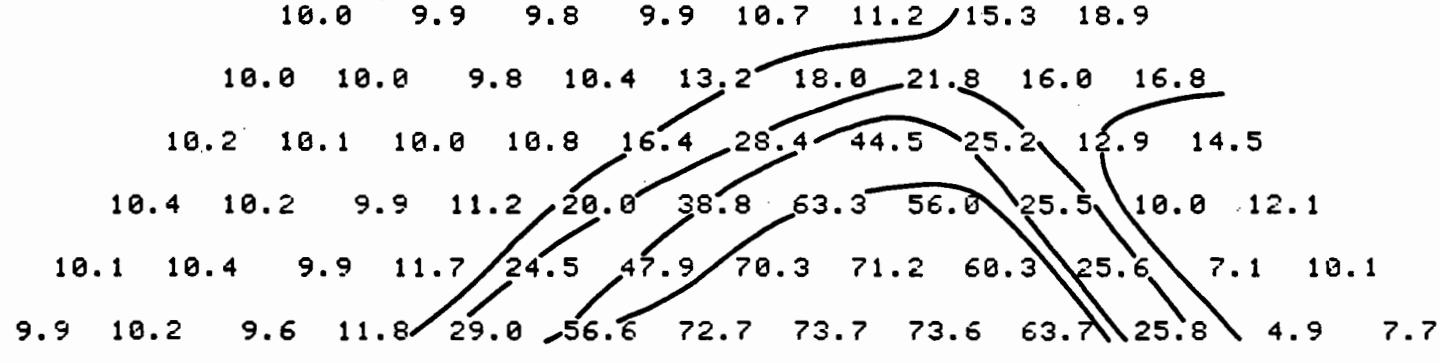
APPARENT RESISTIVITY

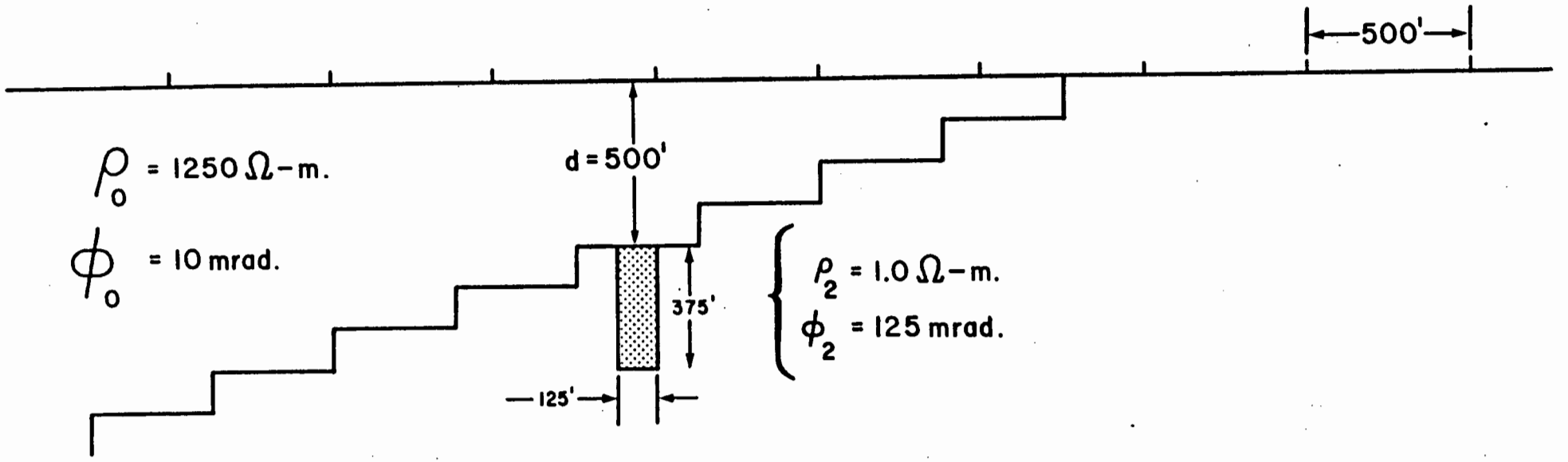


APPARENT METAL FACTOR



APPARENT PHASE





ρ_1 = 200 Ω-m.

ϕ_1 = 20 mrad.

Fig. II

iii) cont'd.

strike. This further data will even better locate the strongest part of the anomaly.

iv) An attempt should be made to measure fully reliable spectral data for the deep sources, on one line. For this check, it may be necessary to use a heavier, more powerful transmitter current source. This may slow the progress of the field work but it should result in interpretable spectral plots.

With this detailed data in hand, it would be possible to locate drill holes to test the sources of the anomalies at the Tenas Project. Further, with good spectral plots it will be possible to make interpretations concerning the time-constant magnitudes for the IP effects from the various sources. These results will provide an excellent test for the usefulness of the spectral IP techniques in reconnaissance exploration in the Anvil Area.

PHOENIX GEOPHYSICS LIMITED

Philip G. Hallof, Ph.D., P.Eng.
Geophysicist

Dated: January 21, 1982

CERTIFICATE

I, Philip George Hallof, of the City of Toronto, Province of Ontario, do hereby certify that:

1. I am a geophysicist residing at Suite 3505, 2045 Lakeshore Blvd. W., Toronto, Ontario.

2. I am a graduate of the Massachusetts Institute of Technology with a B.Sc. Degree (1952) in Geology and Geophysics, and a Ph.D. Degree (1957) in Geophysics.

3. I am a member of the Society of Exploration Geophysicists and the European Association of the Exploration Geophysicists.

4. I am a Professional Geophysicist, registered in the Province of Ontario, the Province of British Columbia and the State of Arizona.

5. I have no direct or indirect interest, nor do I expect to receive any interest directly or indirectly, in the property or securities of Cyprus Anvil Mining Corporation or any affiliate.

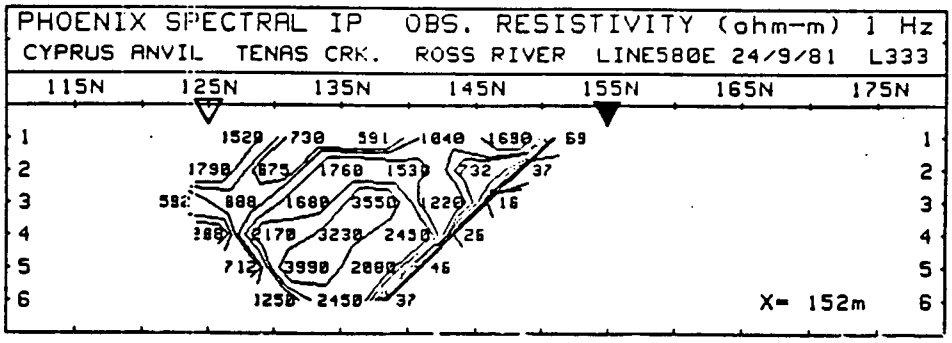
6. The statements made in this report are based on a study of published geological literature and unpublished private reports.

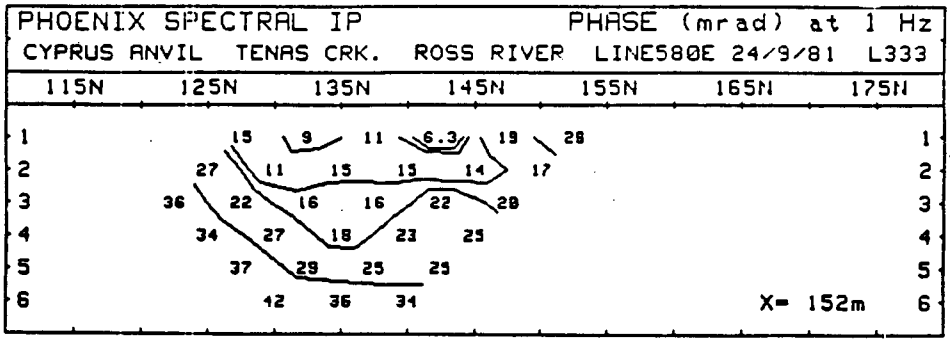
7. Permission is granted to use in whole or in part for assessment and qualification requirements but nor for advertising purposes.

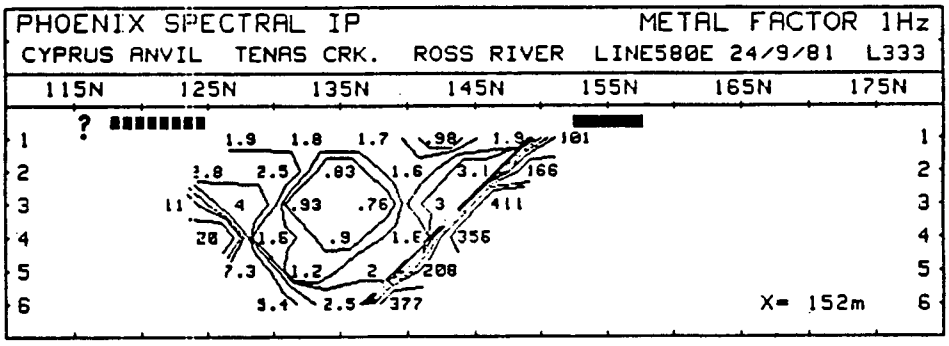
Dated at Toronto

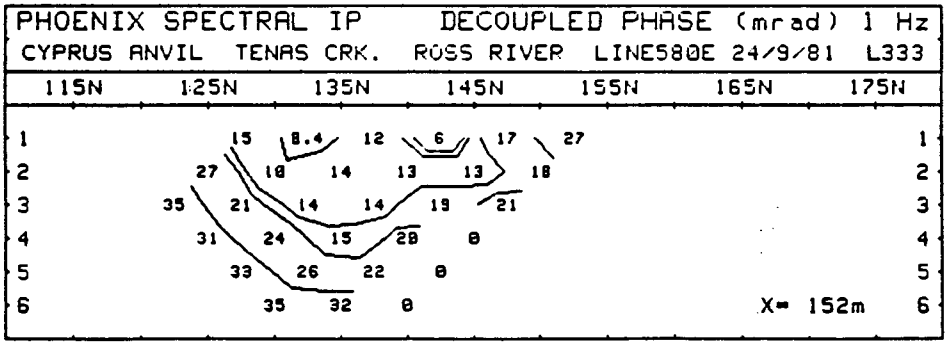
This 21st day of January, 1982

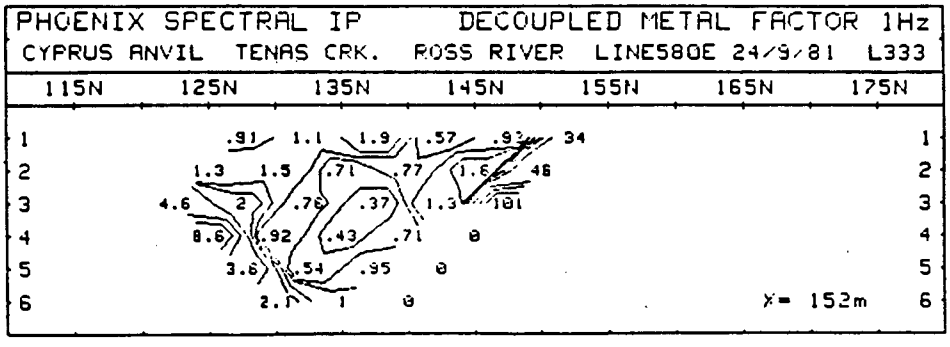
Philip G. Hallof, Ph.D., P.Eng.


PHOENIX SPECTRAL IP OBS. RESISTIVITY (ohm-m) 1 Hz
CYPRUS ANVIL TENAS CRK. ROSS RIVER LINE580E 24/9/81 L333
115N 125N 135N 145N 155N 165N 175N
1 2 3 4 5 6
1520 730 591 1040 1690 69
1790 675 1760 1530 732 37
592 888 1680 3550 1220 16
288 2170 3230 2450 26
712 3990 2880 46
1250 2450 37
X= 152m


PHOENIX SPECTRAL IP PHASE (mrad) at 1 Hz
CYPRUS ANVIL TENAS CRK. ROSS RIVER LINE580E 24/9/81 L333
115N 125N 135N 145N 155N 165N 175N
1 2 3 4 5 6
15 9 11 6.3 19 28
27 11 15 15 14 17
36 22 16 16 22 28
34 27 18 23 25
37 29 25 25
42 36 34
X= 152m

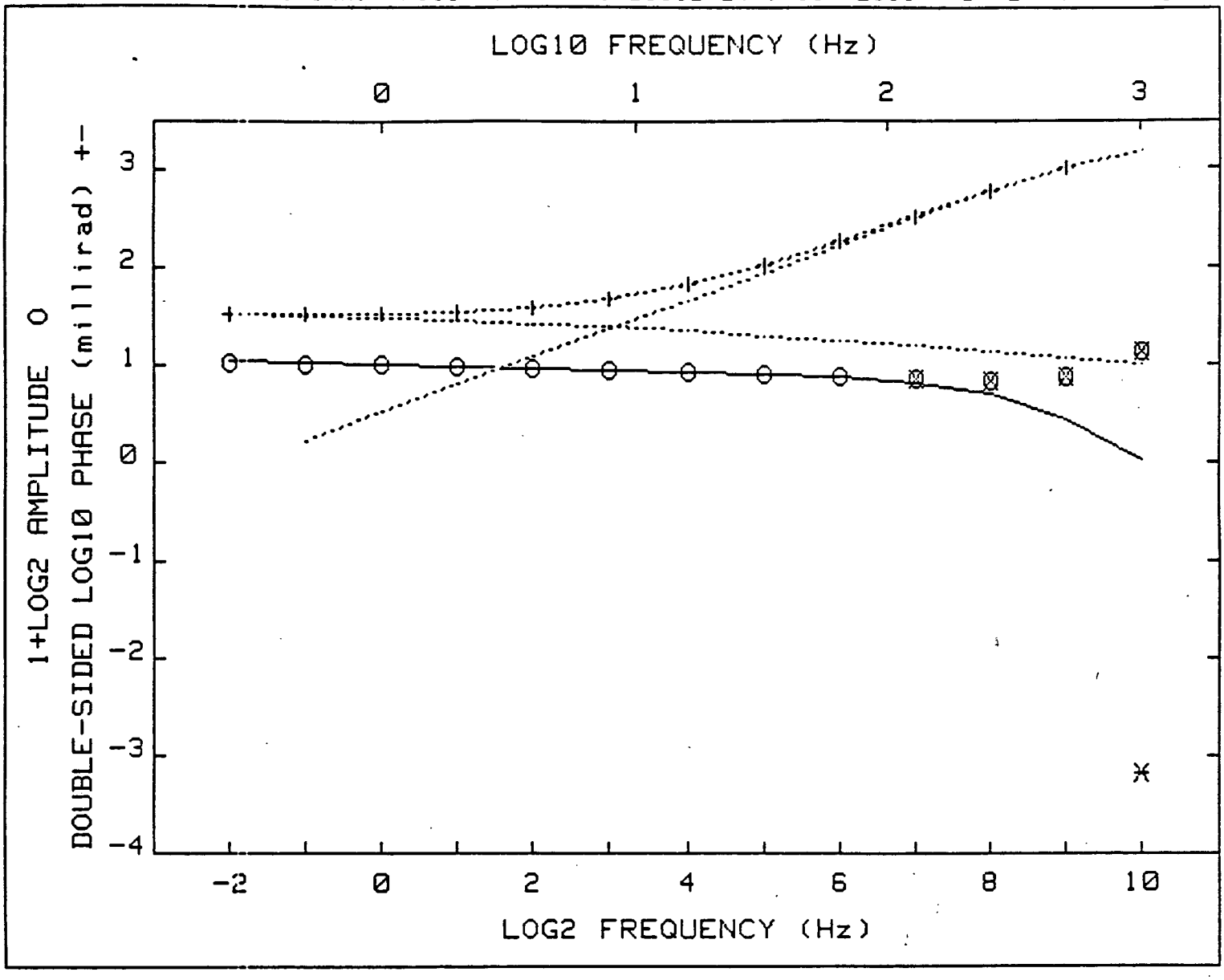

PHOENIX SPECTRAL IP METAL FACTOR 1Hz
CYPRUS ANVIL TENAS CRK. ROSS RIVER LINE580E 24/9/81 L333
115N 125N 135N 145N 155N 165N 175N
1 2 3 4 5 6
? ■■■■■■■■
1.9 1.8 1.7 .98 1.9 101
3.8 2.5 .83 1.6 3.1 166
11 4 .93 .76 3 411
28 1.6 .9 1.6 356
7.3 1.2 2 208
3.4 2.5 377
X= 152m


PHOENIX SPECTRAL IP DECOUPLED PHASE (mrad) 1 Hz
CYPRUS ANVIL TENAS CRK. ROSS RIVER LINE580E 24/9/81 L333
115N 125N 135N 145N 155N 165N 175N
1 2 3 4 5 6
15 8.4 12 6 17 27
27 18 14 13 13 18
35 21 14 14 19 21
31 24 15 28 0
33 26 22 0
35 32 0
X= 152m


PHOENIX SPECTRAL IP DECOUPLED METAL FACTOR 1Hz
CYPRUS ANVIL TENAS CRK. ROSS RIVER LINE580E 24/9/81 L333
115N 125N 135N 145N 155N 165N 175N
1 2 3 4 5 6
.91 1.1 1.9 .57 .92 34
1.3 1.5 .71 .77 1.6 46
4.6 2 .78 .37 1.3 101
8.6 .92 .43 .71 0
3.6 .54 .95 0
2.1 1 0
X= 152m

DWG. NO. - S.I.P. - 1104 - 2

CYPRUS ANVIL TENAS CRK. ROSS RIVER LINE580E 24/9/81 L333 D= 2 N=4 X=152m



CRL: Number of dispersions= 2
C1=.25 M2=1 fixed

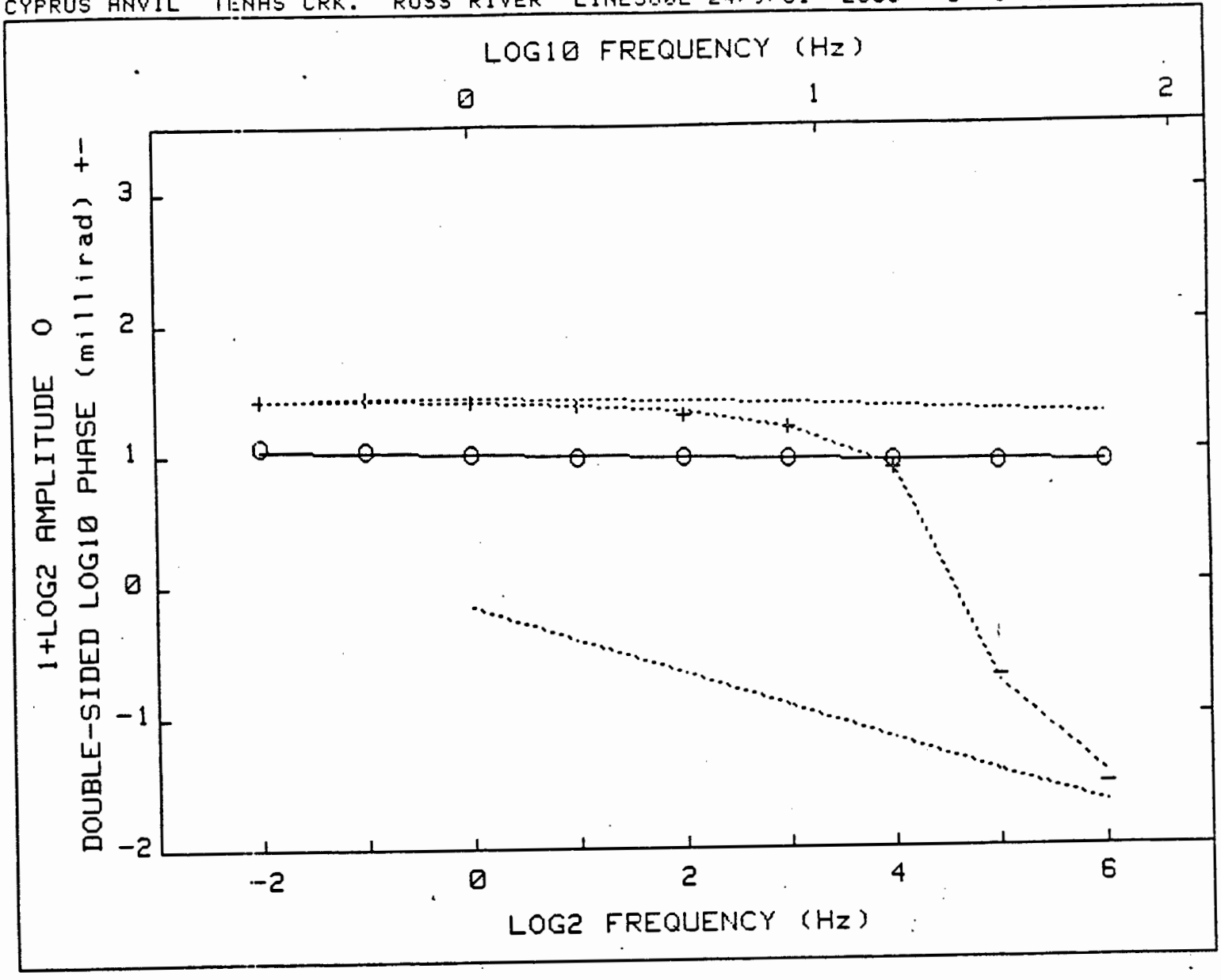
Iter	Lambda	Rchsq	R0	M1	T1	T2	C2
0	1.E-02	.00678	1.265	.301	3.2E+00	3.9E-04	.928
1	1.E-02	.00003	1.250	.290	3.2E+00	2.7E-04	.930
2	1.E-03	.00002	1.253	.291	3.4E+00	2.8E-04	.935
3	1.E-04	.00002	1.259	.293	4.0E+00	2.7E-04	.932
4	1.E-05	.00002	1.262	.294	4.3E+00	2.7E-04	.931

Pct Std Deviations	.8	1.3	28.9	1.3	.6	
Correlation Matrix	1.000					
	.970	1.000				
	.982	.936	1.000			
	-.815	-.783	-.811	1.000		
	-.719	-.603	-.763	.836	1.000	

Apparent Resistivity Measured at 1 Hz is 287.5
Apparent Resistivity Calculated from Inductive Coupling is 410.0

DWG. NO. – S.I.P. – 1104 – 3

CYPRUS ANVIL TENAS CRK. ROSS RIVER LINE580E 24/9/81 L333 D= 6 N=1 X=152m

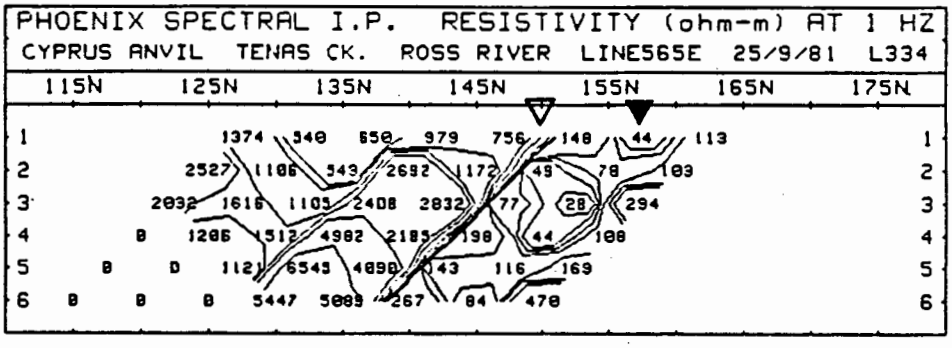


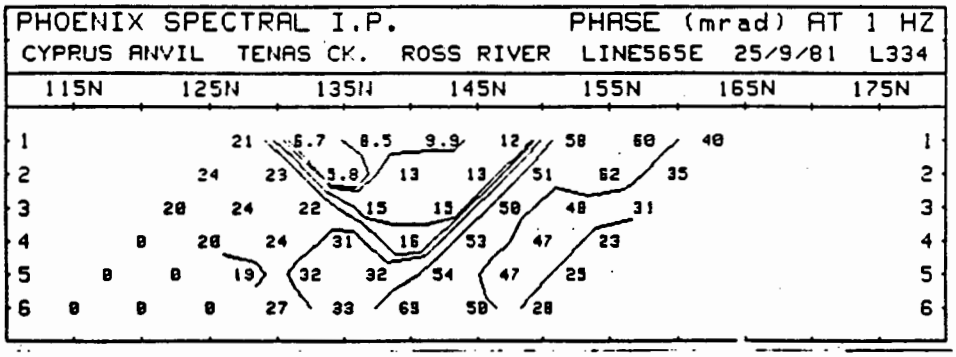
CRL: Number of dispersions= 2 Negative.
C1=.25 M2=1 fixed

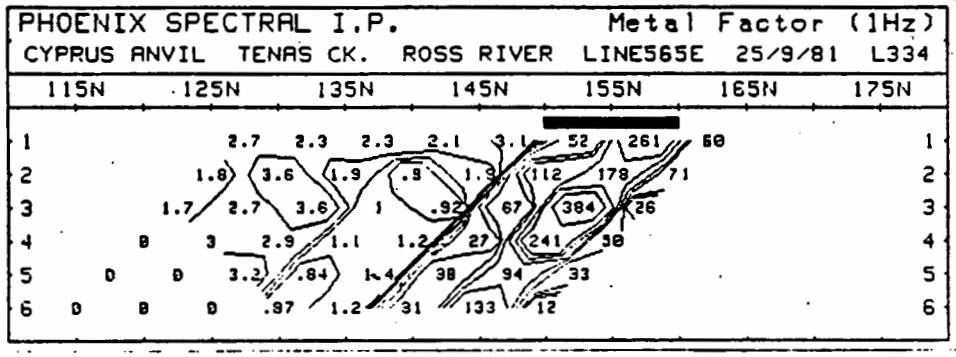
Iter	Lambda	Rchsq	R0	M1	T1	T2	C2
0	1.E-02	.00661	1.080	.217	4.9E-01	5.3E-05	.866
1	1.E-02	.00069	1.159	.239	4.6E-01	5.4E-05	.835
2	1.E-02	.00069	1.159	.238	4.5E-01	5.4E-05	.834

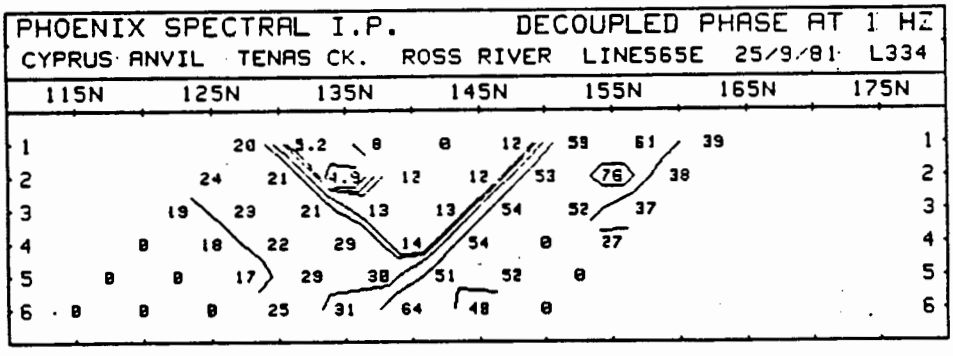
Pct Std Deviations	2.0	2.8	195.7	20.1	8.5	
Correlation Matrix	1.000					
	.162	1.000				
	.928	-.059	1.000			
	.544	-.535	.690	1.000		
	.737	-.428	.875	.949	1.000	

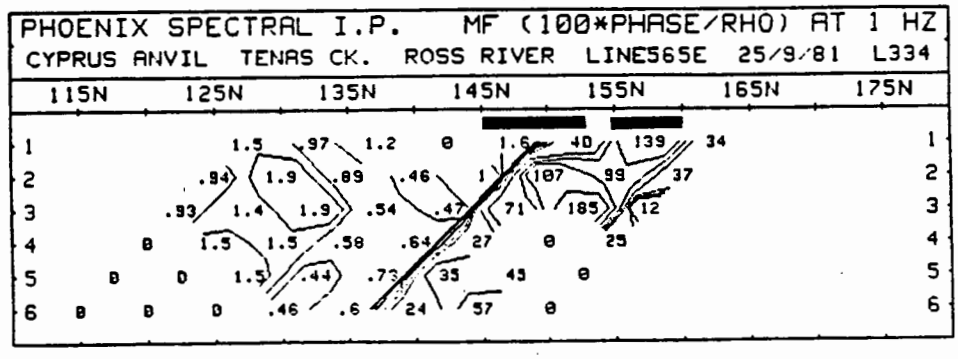
Apparent Resistivity Measured at 1 Hz is 68.96
Apparent Resistivity Calculated from Inductive Coupling is 177.3


PHOENIX SPECTRAL I.P. RESISTIVITY (ohm-m) AT 1 HZ
CYPRUS ANVIL TENAS CK. ROSS RIVER LINE565E 25/9/81 L334
115N 125N 135N 145N 155N 165N 175N
1374 540 650 979 756 148 44 113
2527 1106 543 2692 1172 49 78 103
2032 1616 1101 2408 2832 77 28 294
1206 1512 4982 2185 198 44 108
112 6545 4898 143 116 169
5447 5089 267 84 478


PHOENIX SPECTRAL I.P. PHASE (mrad) AT 1 HZ
CYPRUS ANVIL TENAS CK. ROSS RIVER LINE565E 25/9/81 L334
115N 125N 135N 145N 155N 165N 175N
21 5.7 8.5 3.9 12 58 60 40
24 23 5.8 13 13 51 52 35
20 24 22 15 15 50 48 31
20 24 31 16 53 47 23
19 32 32 54 47 25
27 33 65 50 28

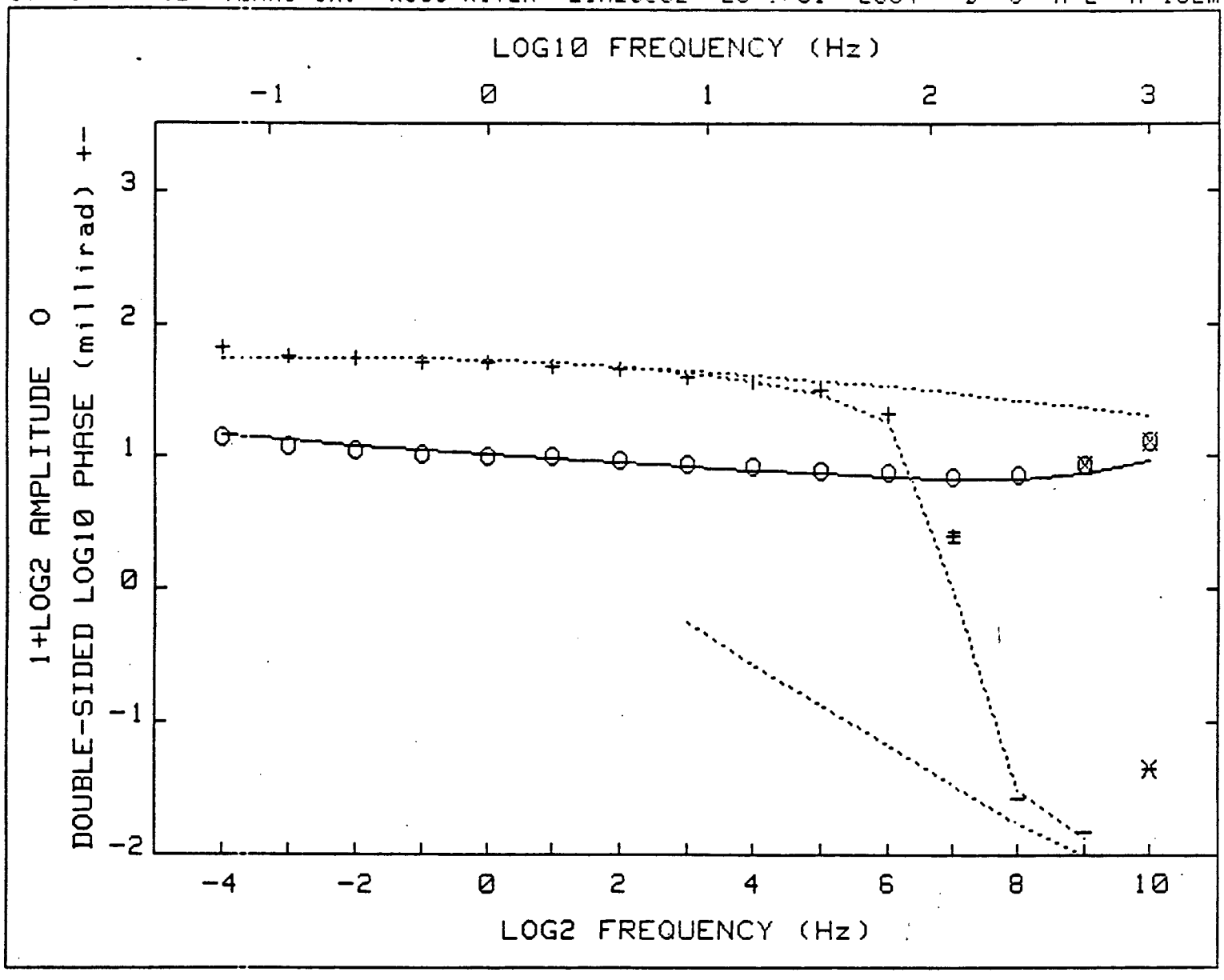

PHOENIX SPECTRAL I.P. Metal Factor (1Hz)
CYPRUS ANVIL TENAS CK. ROSS RIVER LINE565E 25/9/81 L334
115N 125N 135N 145N 155N 165N 175N
2.7 2.3 2.3 2.1 52 261 60
1.8 3.6 1.9 .8 112 178 71
1.7 2.7 3.6 1 .92 67 384 26
3 2.9 1.1 1.2 27 241 30
3.2 .84 38 94 33
.97 1.2 31 133 12


PHOENIX SPECTRAL I.P. DECOUPLED PHASE AT 1 HZ
CYPRUS ANVIL TENAS CK. ROSS RIVER LINE565E 25/9/81 L334
115N 125N 135N 145N 155N 165N 175N
20 3.2 12 59 61 39
24 21 4.3 12 12 53 76 38
19 23 21 13 13 54 52 37
18 22 29 14 54 27
17 29 38 51 52
25 31 64 48


PHOENIX SPECTRAL I.P. MF (100*PHASE/RHO) AT 1 HZ
CYPRUS ANVIL TENAS CK. ROSS RIVER LINE565E 25/9/81 L334
115N 125N 135N 145N 155N 165N 175N
1.5 .97 1.2 1.6 40 139 34
.94 1.9 .89 .46 107 99 37
.93 1.4 1.9 .54 .47 71 185 12
1.5 1.5 .58 .64 27 25
1.5 .44 .73 35 45
.46 .6 24 57

DWG. NO. - S.I.P - 1105-2

CYPRUS ANVIL TEMAS CK. ROSS RIVER LINE565E 25/9/81 L334 D= 6 N=2 X=152m



CRL: Number of dispersions= 2 Negative.
C1=.25 C2=1 fixed

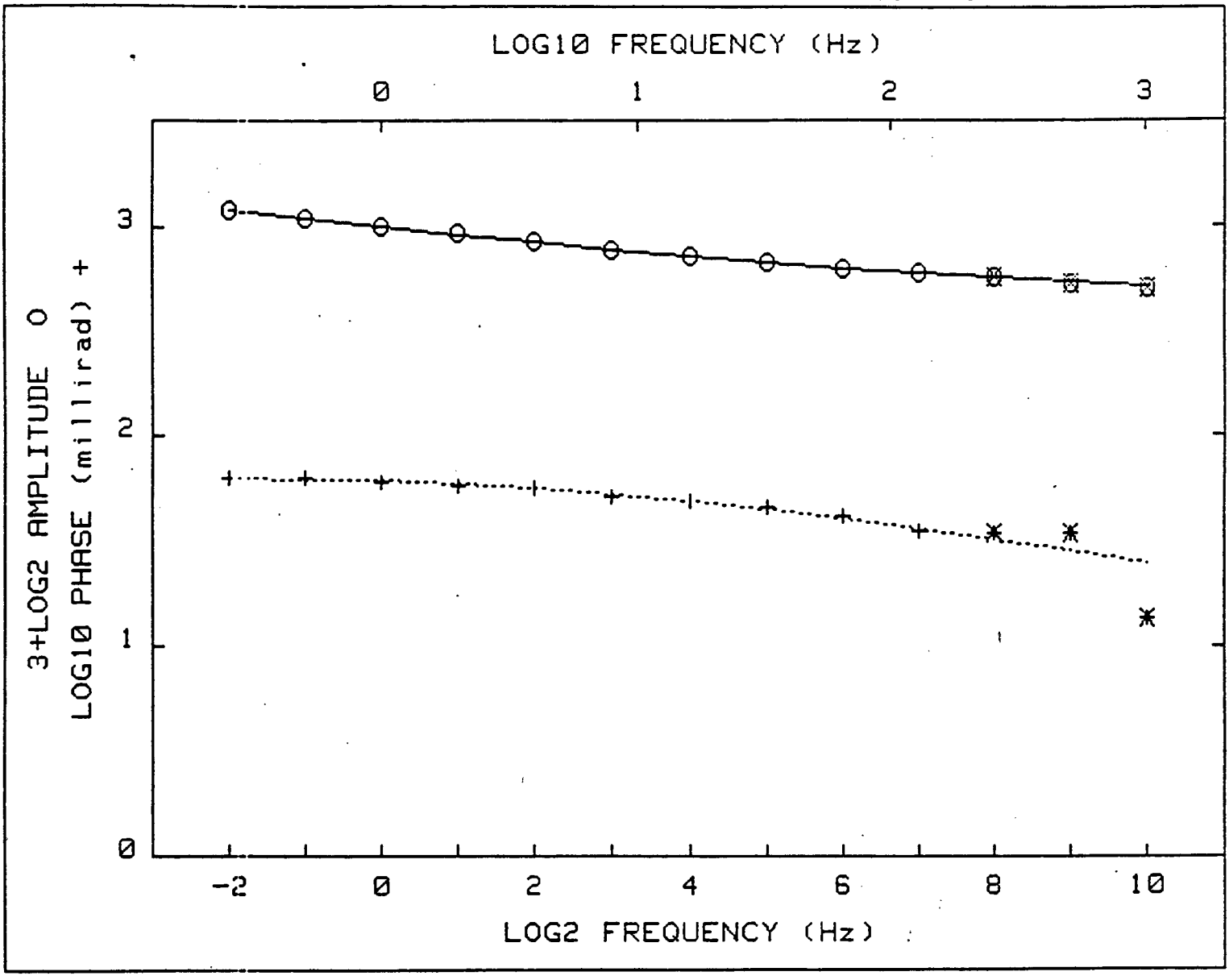
Iter	Lambda	Rchsq	R0	M1	T1	M2	T2
0	1.E-02	.00854	1.423	.426	2.6E+00	.165	1.5E-04
1	1.E+03	.00854	1.423	.428	2.6E+00	.165	1.5E-04

Pct Std Deviations	2.9	1.0	99.7	75.5	105.7
Correlation Matrix	1.000				
	.296	1.000			
	.759	.186	1.000		
	.283	-.005	.347	1.000	
	-.384	-.015	-.482	-.977	1.000

Apparent Resistivity Measured at 1 Hz is 49.27
Apparent Resistivity Calculated from Inductive Coupling is 1867

DWG. NO. - S.I.P - 1105 - 3

CYPRUS ANVIL TENAS CK. ROSS RIVER LINE565E 25/9/81 L334 D= 7 N=1 X=152m



CRL: Number of dispersions= 2 Negative.
C1=.25 M2=0 T2=0 C2=0 fixed

Iter	Lambda	Rchsq	R0	M1	T1
0	1.E-02	.01008	1.280	.405	2.4E+00
1	1.E-02	.00015	1.447	.475	2.2E+00
2	1.E-03	.00004	1.452	.471	2.2E+00
3	1.E-04	.00004	1.451	.471	2.1E+00

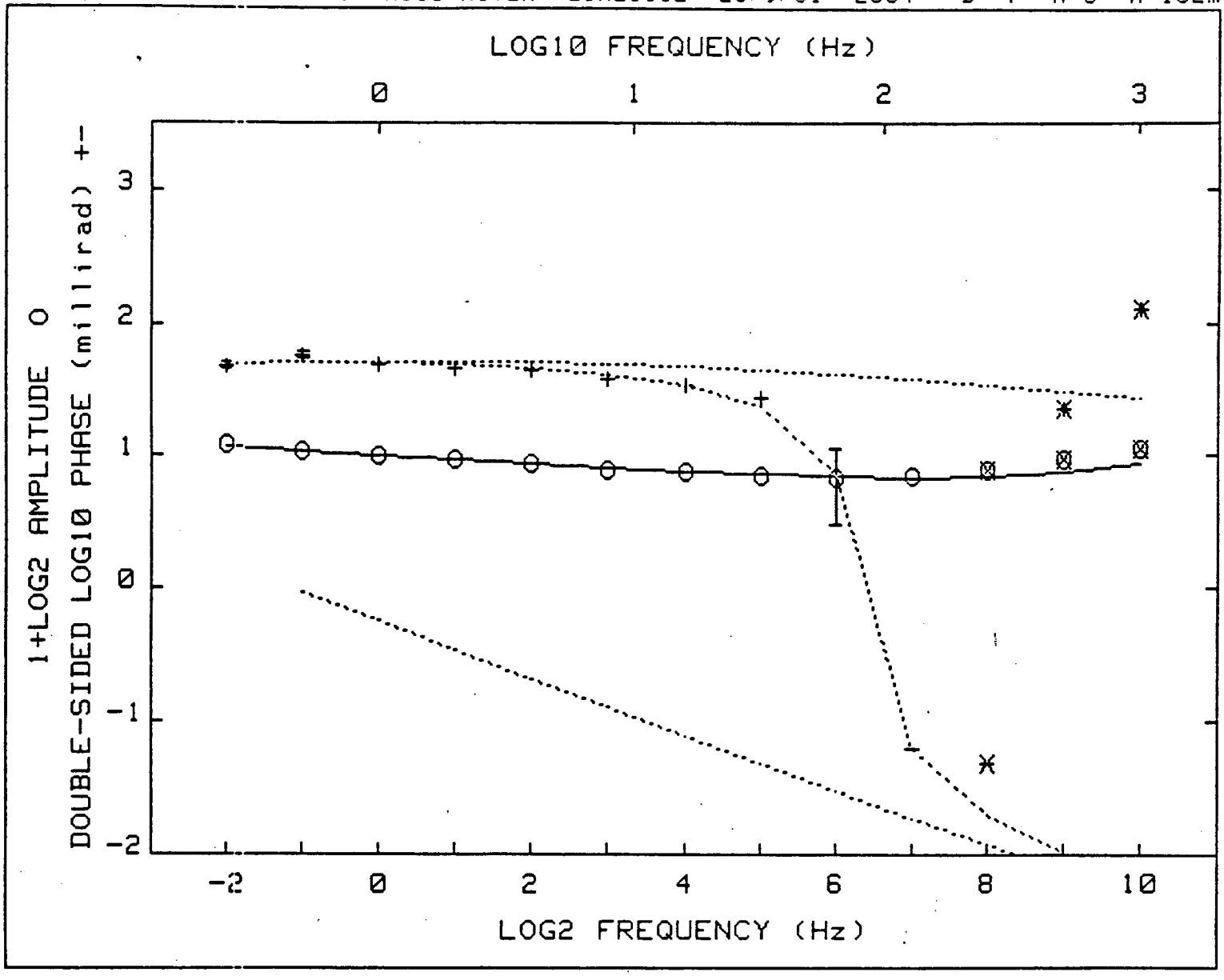
Pct Std Deviations	.7	.7	10.6

Correlation Matrix	1.000		
	.952	1.000	
	.950	.890	1.000

Apparent Resistivity Measured at 1 Hz is 43.82
Apparent Resistivity Calculated from Inductive Coupling is 0.000

DWG. NO. - S.I.P. - 1105 - 4

CYPRUS ANVIL TENAS CK. ROSS RIVER LINE565E 25/9/81 L334 D= 7 N=3 X=152m

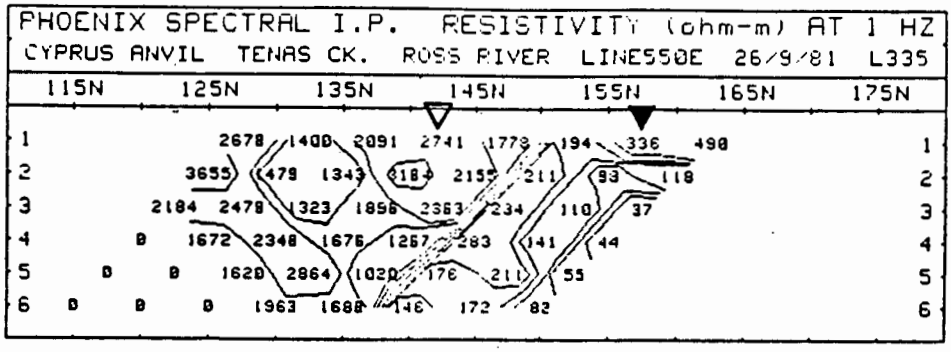


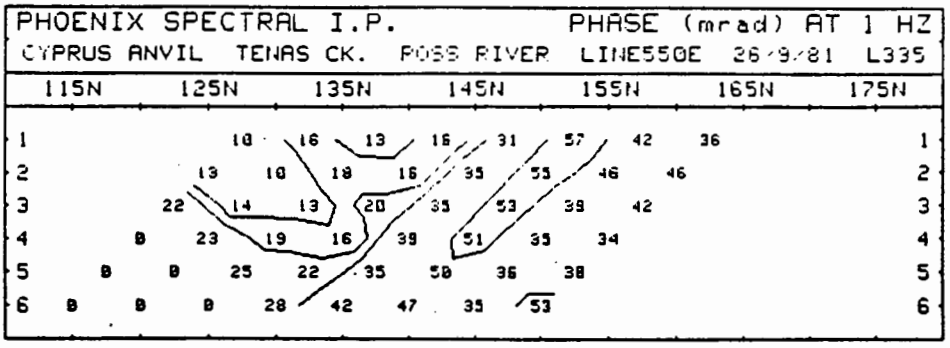
CRL: Number of dispersions= 2 Negative.
C1=.25 M2=1 fixed

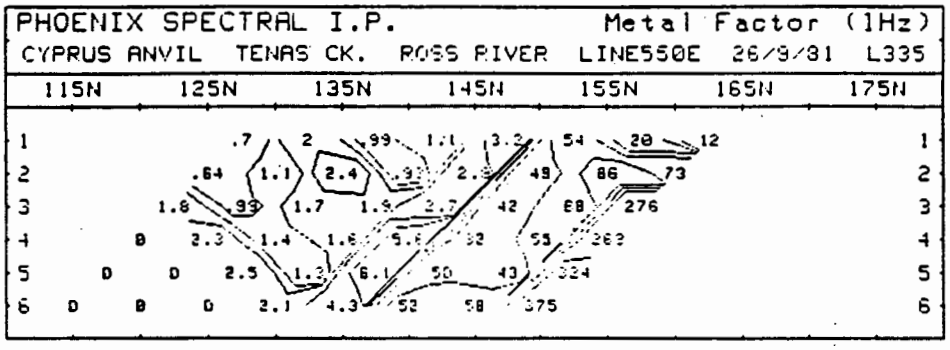
Iter	Lambda	Rchsq	R0	M1	T1	T2	C2
0	1.E-02	.00245	1.256	.483	6.3E-02	3.5E-06	.415
1	1.E-02	.00135	1.252	.456	7.0E-02	5.8E-06	.490
2	1.E-03	.00108	1.257	.429	1.1E-01	7.7E-06	.553
3	1.E-04	.00098	1.272	.415	2.0E-01	9.3E-06	.611
4	1.E-05	.00087	1.279	.413	2.5E-01	1.1E-05	.642
5	1.E-06	.00081	1.284	.411	2.9E-01	1.2E-05	.662
6	1.E-07	.00079	1.286	.409	3.2E-01	1.2E-05	.676
7	1.E-08	.00077	1.288	.408	3.4E-01	1.3E-05	.685
8	1.E-09	.00077	1.289	.408	3.5E-01	1.3E-05	.691

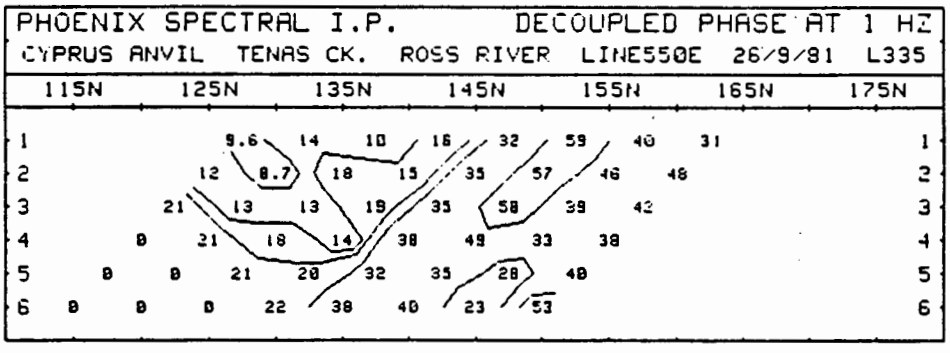
Pct Std Deviations	2.4	2.1	98.3	14.3	5.8	
Correlation Matrix	1.000					
	.138	1.000				
	.923	-.156	1.000			
	.077	-.561	.228	1.000		
	.612	-.554	.787	.763	1.000	

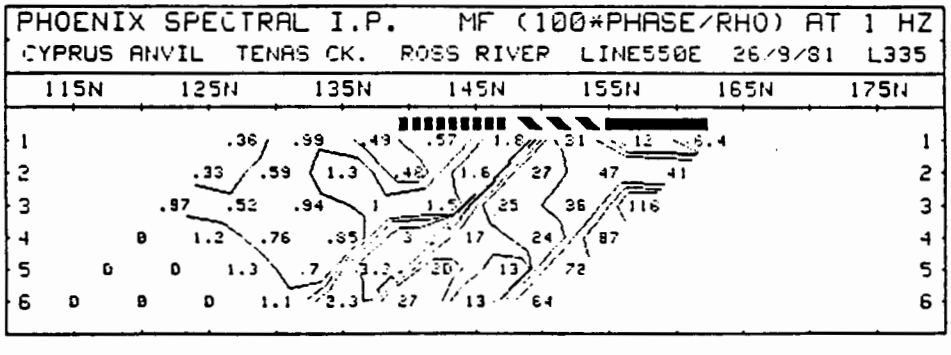
DWG. NO. - S.I.P - 1106 - 1





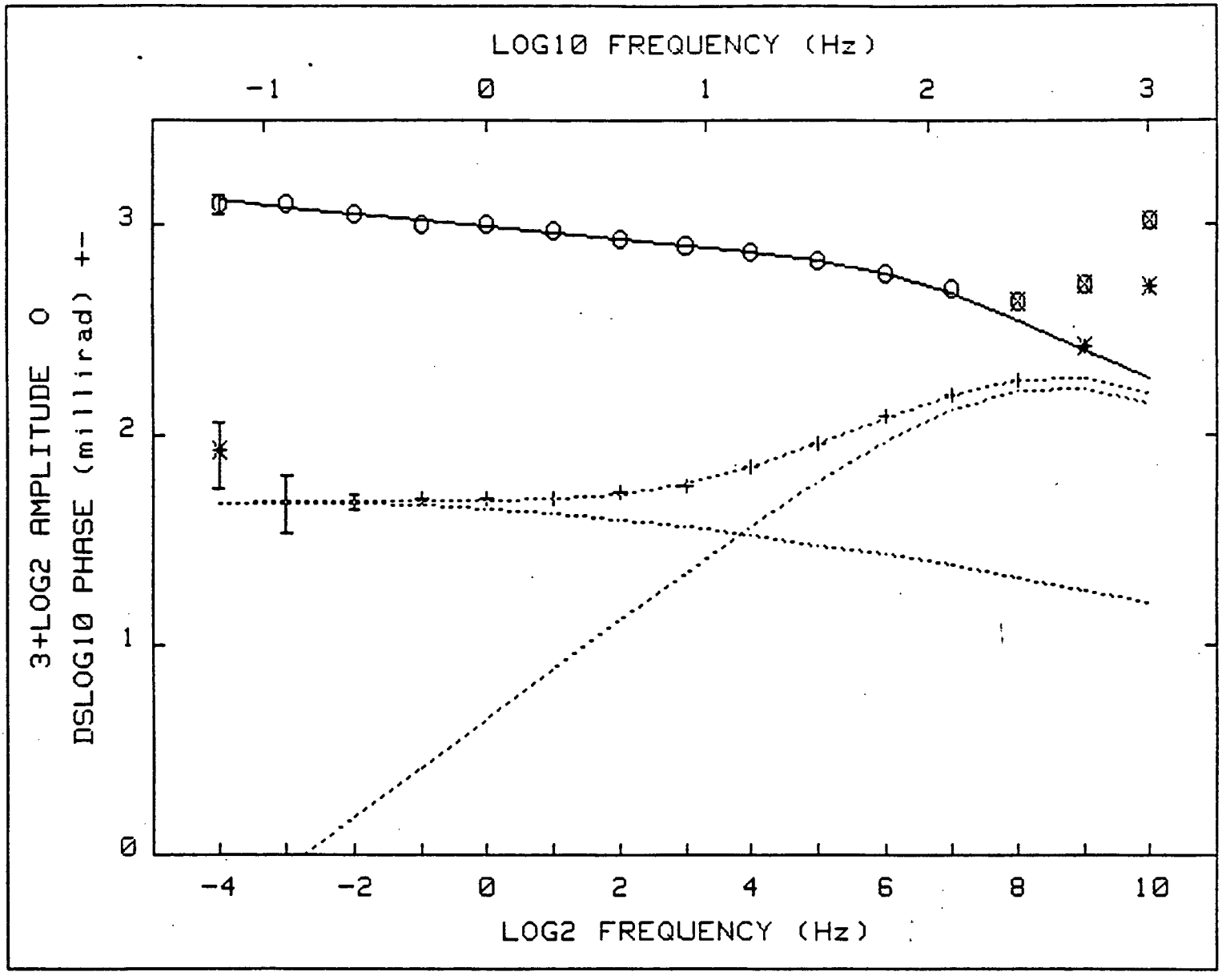






DWG. NO. - S.I.P - 1106 - 2

CYPRUS ANVIL TENAS CK. ROSS RIVER LINE550E 26/9/81 L335 D= 6 N=5 X=152m

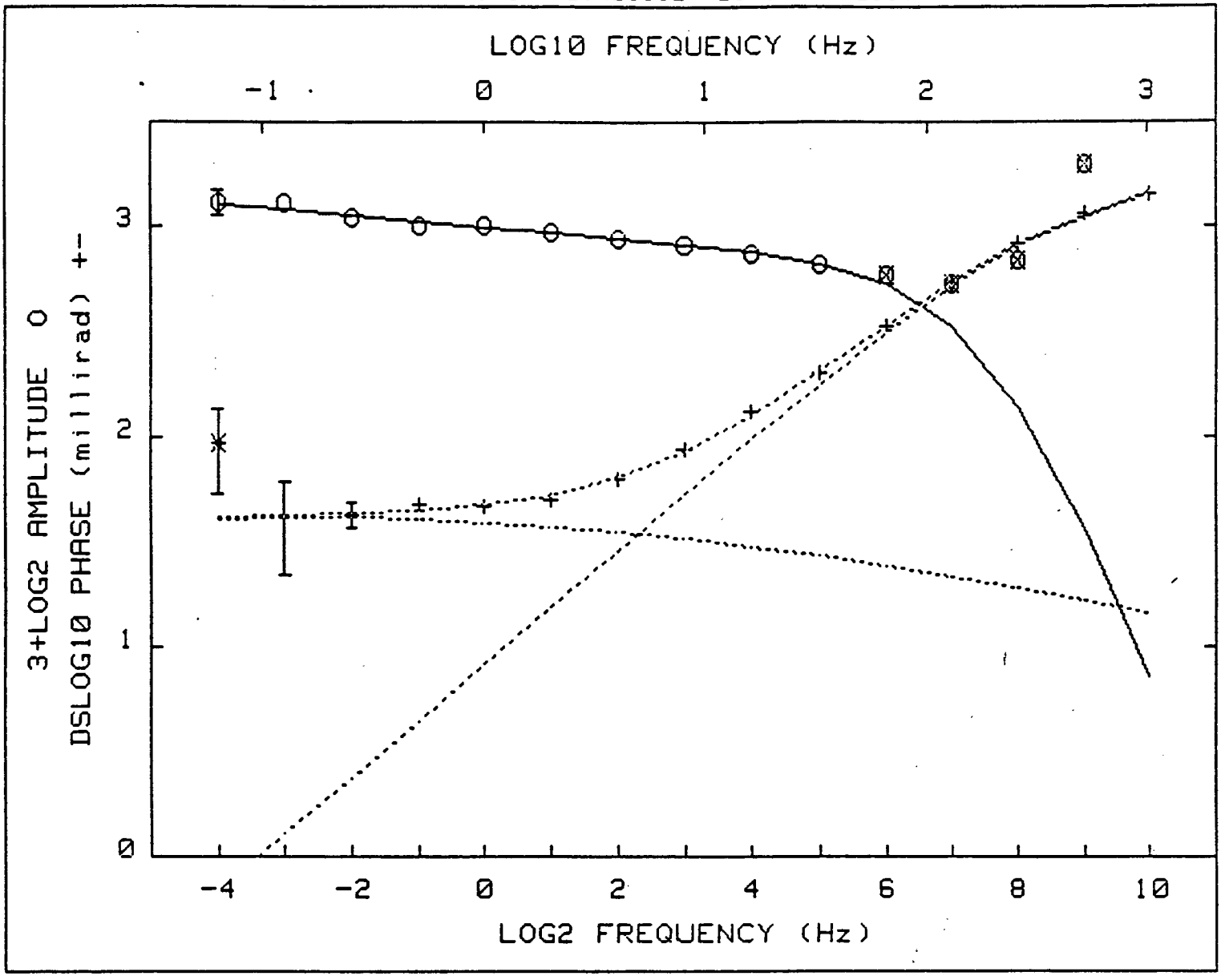


CRL: Number of dispersions= 2
C1=.25 fixed

Iter	Lambda	Rchsq	R0	M1	T1	M2	T2	C2
0	1.E-02	.00025	1.441	.392	1.9E+01	.502	1.2E-04	.578
1	1.E-02	.00023	1.438	.389	1.9E+01	.485	1.3E-04	.568
2	1.E-03	.00020	1.444	.393	1.9E+01	.415	1.9E-04	.591
3	1.E-03	.00018	1.444	.396	1.8E+01	.360	2.7E-04	.622
4	1.E-03	.00016	1.439	.397	1.6E+01	.322	3.5E-04	.652
5	1.E-04	.00014	1.375	.384	5.3E+00	.266	5.6E-04	.729
6	1.E-05	.00012	1.357	.384	3.3E+00	.251	5.9E-04	.763
7	1.E-06	.00012	1.359	.385	3.5E+00	.251	5.9E-04	.763

Pct Std Deviations	2.3	1.5	89.0	10.7	19.4	6.4	
Correlation Matrix	1.000						
	.681	1.000					
	.979	.547	1.000				
	.584	-.028	.672	1.000			
	-.500	.020	-.573	-.971	1.000		
	-.718	-.088	-.796	-.951	.901	1.000	

CYPRUS ANVIL TENAS CK. ROSS RIVER LINE550E 26/9/81 L335 D= 6 N=6 X=152m



CRL: Number of dispersions= 2
C1=.25 fixed

Iter	Lambda	Rchsq	R0	M1	T1	M2	T2	C2
0	1.E-02	.00024	1.293	.342	2.0E+00	.736	7.2E-04	.887
1	1.E-02	.00022	1.290	.341	2.1E+00	.742	7.1E-04	.877
2	1.E-03	.00022	1.294	.341	2.3E+00	.743	7.1E-04	.874

Pct Std Deviations	2.3	1.9	119.1	2.5	5.6	2.5	

Correlation Matrix

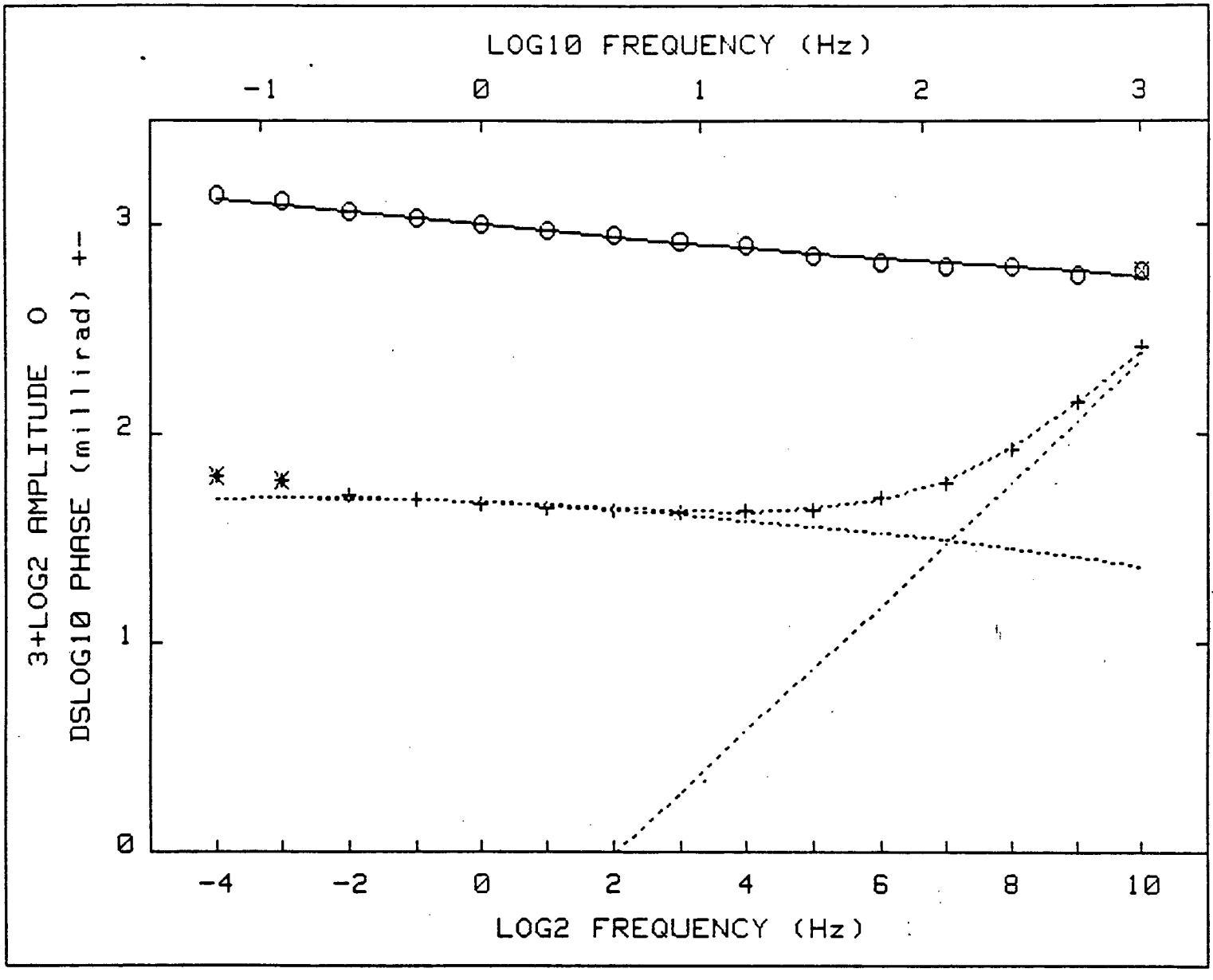
1.000						
.546	1.000					
.971	.383	1.000				
-.025	-.547	.076	1.000			
-.260	.130	-.298	-.833	1.000		
-.639	.101	-.715	-.639	.727	1.000	

Apparent Resistivity Measured at 1 Hz is 146.1

Apparent Resistivity Calculated from Inductive Coupling is 338.0

DWG. NO. - S.I.P. - 1106-4

CYPRUS ANVIL TENAS CK. ROSS RIVER LINE550E 26/9/81 L335 D= 8 N=2 X=152m



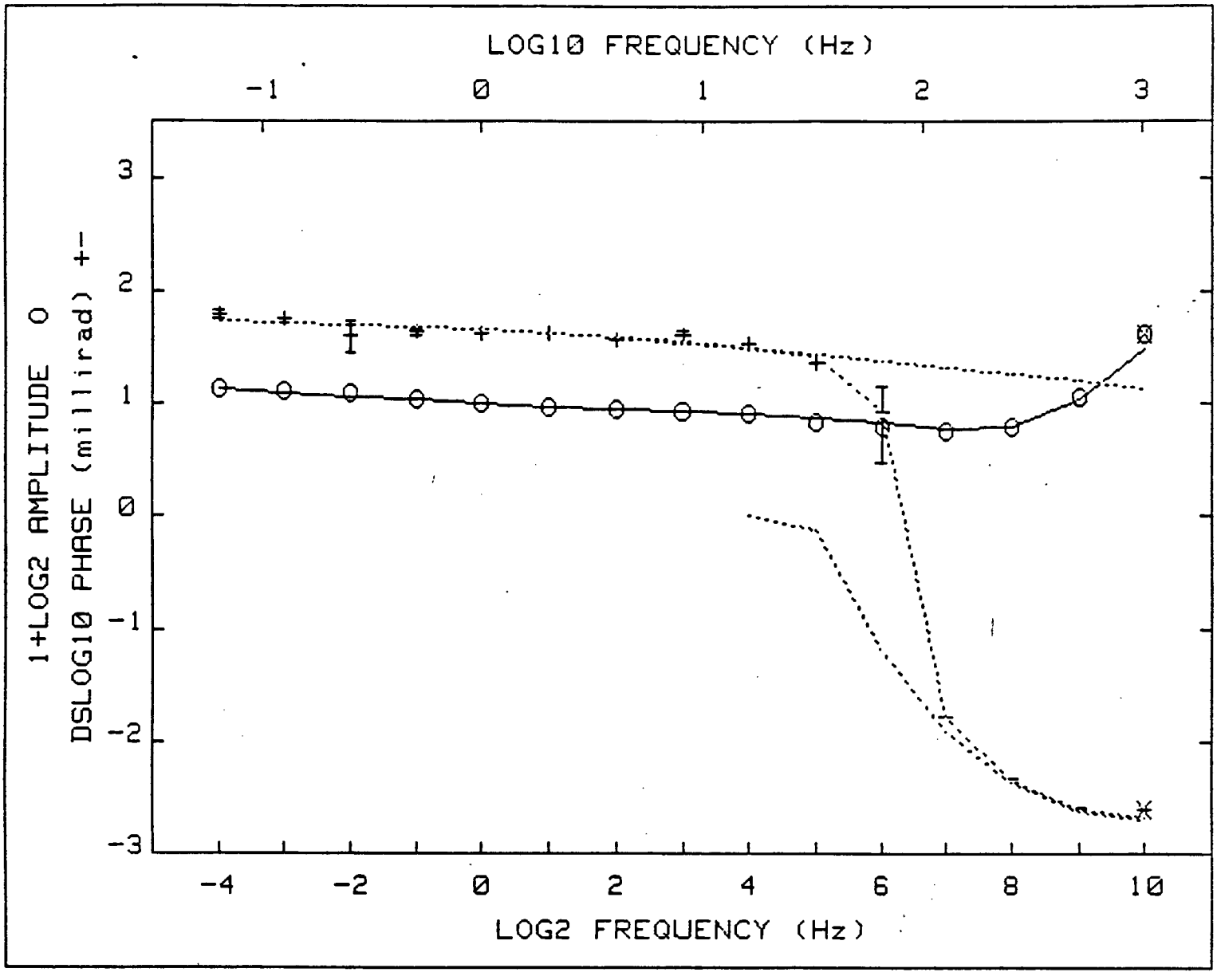
CRL: Number of dispersions= 2
M2=1 fixed

Iter	Lambda	Rchsq	R0	M1	T1	C1	T2	C2
0	1.E-02	.00022	1.345	.393	1.8E+00	.250	2.0E-05	.922
1	1.E-02	.00021	1.354	.404	1.8E+00	.240	2.0E-05	.940
2	1.E-03	.00020	1.383	.424	2.4E+00	.226	2.0E-05	.956
3	1.E-03	.00019	1.401	.433	3.0E+00	.220	2.0E-05	.960
4	1.E-03	.00019	1.417	.441	3.7E+00	.215	2.0E-05	.962
5	1.E-03	.00019	1.430	.448	4.3E+00	.211	2.0E-05	.963
6	1.E-03	.00018	1.442	.454	4.9E+00	.208	2.0E-05	.965
7	1.E-03	.00018	1.453	.459	5.6E+00	.206	2.0E-05	.966

Pct Std Deviations	16.5	28.2	1133.5	34.6	15.6	5.2	
Correlation Matrix	1.000						
	.996	1.000					
	.998	.990	1.000				
	-.988	-.997	-.978	1.000			
	-.816	-.783	-.836	.758	1.000		
	.687	.733	.651	-.759	-.166	1.000	

DWG. NO. - S.I.P - 1106 - 5

CYPRUS ANVIL TENAS CK. ROSS RIVER LINE550E 26/9/81 L335 D= 8 N=3 X=152m



CRL: Number of dispersions= 3 Negative.
C1=.25 C2=1 M3=1 C3=1 fixed

Iter	Lambda	Rchsq	R0	M1	T1	M2	T2	T3
0	1.E-02	.00142	1.466	.418	1.4E+01	.073	1.5E-03	1.0E-04
1	1.E-02	.00142	1.466	.418	1.4E+01	.073	1.5E-03	1.0E-04

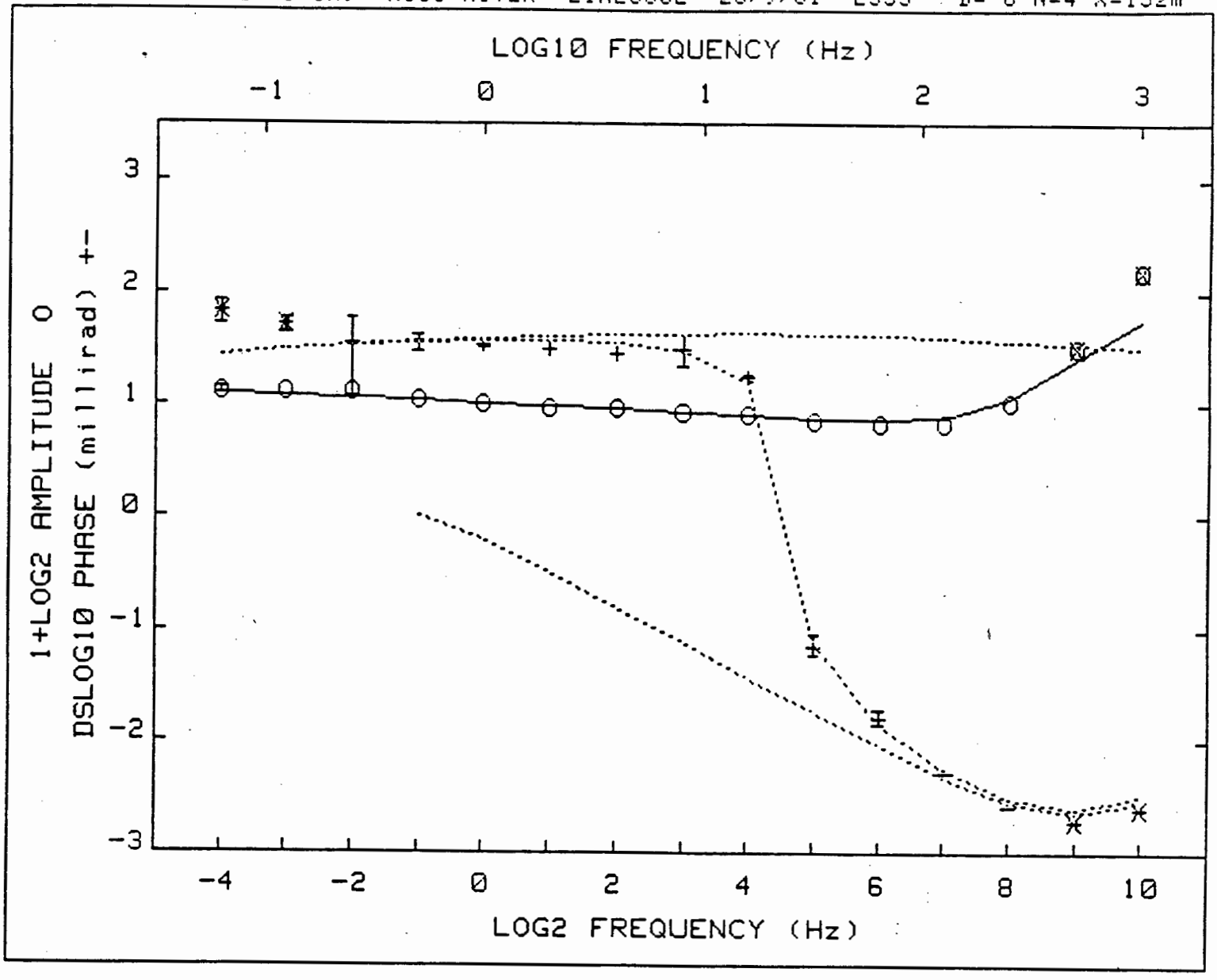
Pct Std Deviations	4.9	5.6	131.3	18.6	19.2	10.7	
Correlation Matrix	1.000						
	.974	1.000					
	.965	.922	1.000				
	-.437	-.387	-.463	1.000			
	.397	.317	.467	-.924	1.000		
	-.681	-.632	-.703	.925	-.800	1.000	

Apparent Resistivity Measured at 1 Hz is 36.52

Apparent Resistivity Calculated from Inductive Coupling is 782.6

DWG. NO. - S.I.P - 1106 - 6

CYPRUS ANVIL TENAS CK. ROSS RIVER LINE550E 26/9/81 L335 D= 8 N=4 X=152m



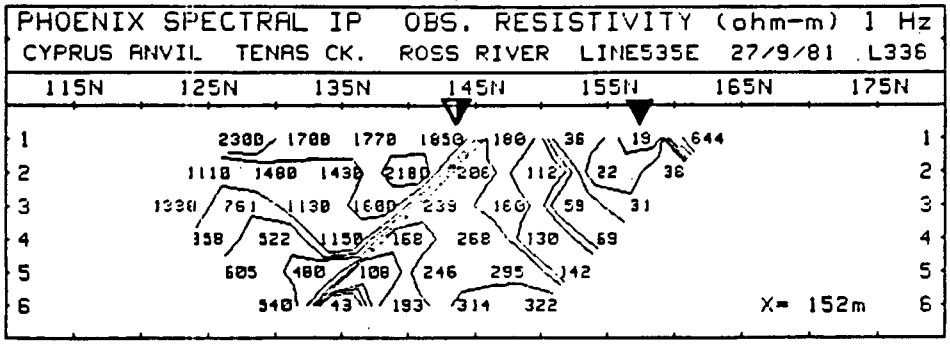
CRL: Number of dispersions= 2 Negative.
C1=.25 M2=1 C2=1 fixed

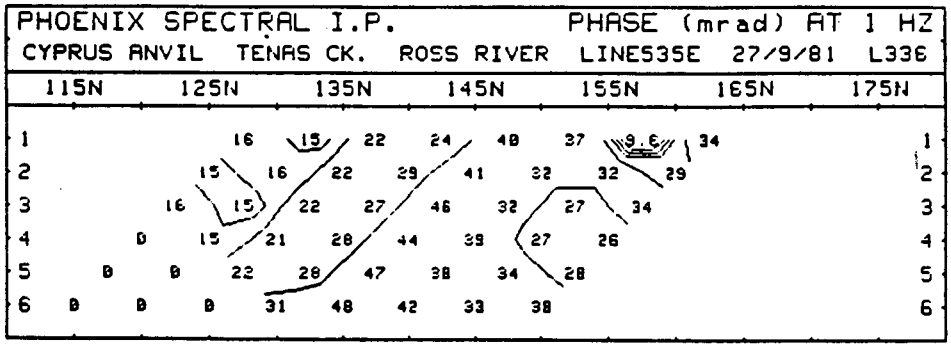
Iter	Lambda	Rchsq	R0	M1	T1	T2
0	1.E-02	.00660	1.210	.318	3.0E-01	1.9E-04
1	1.E-02	.00340	1.213	.337	1.8E-01	1.8E-04
2	1.E-03	.00267	1.168	.337	4.3E-02	2.1E-04
3	1.E-04	.00244	1.164	.350	2.7E-02	2.2E-04
4	1.E-05	.00244	1.164	.351	2.7E-02	2.2E-04

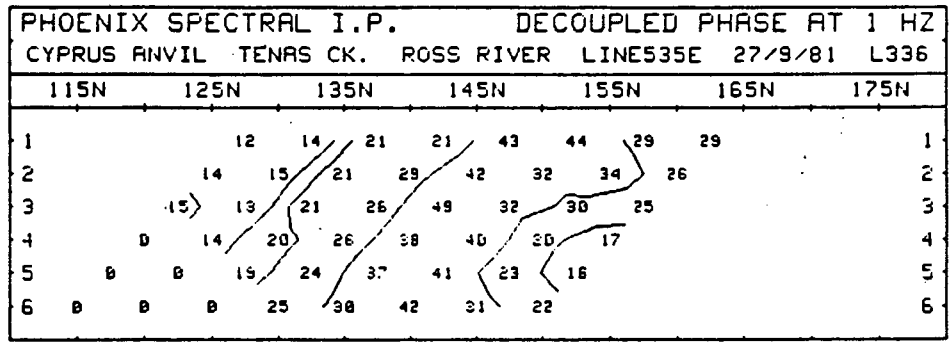
Pct Std Deviations	2.0	4.8	137.2	7.5	
Correlation Matrix	1.000				
	-.455	1.000			
	.826	-.763	1.000		
	-.674	.885	-.899	1.000	

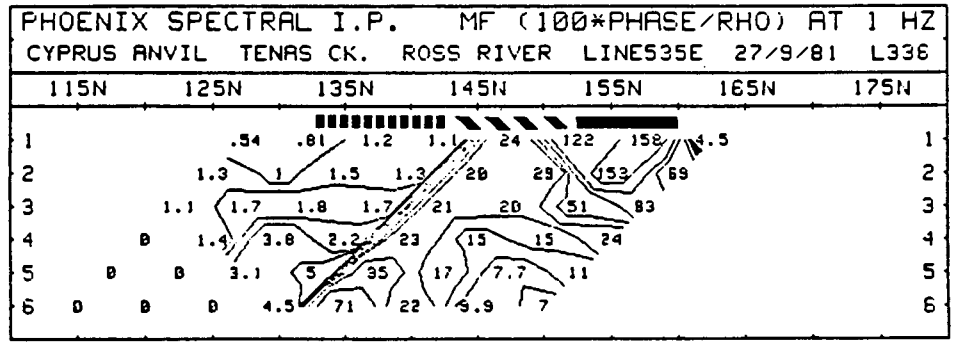
Apparent Resistivity Measured at 1 Hz is 43.62

Apparent Resistivity Calculated from Inductive Coupling is 642.0


PHOENIX SPECTRAL IP OBS. RESISTIVITY (ohm-m) 1 Hz
CYPRUS ANVIL TENAS CK. ROSS RIVER LINE535E 27/9/81 L336
115N 125N 135N 145N 155N 165N 175N
1 2 3 4 5 6
2300 1700 1770 1650 180 36 19 644
1110 1480 1430 210 206 112 22 36
1330 761 1130 160 239 180 59 31
358 522 1150 168 268 130 69
605 480 108 246 295 142
340 43 193 314 322
X= 152m

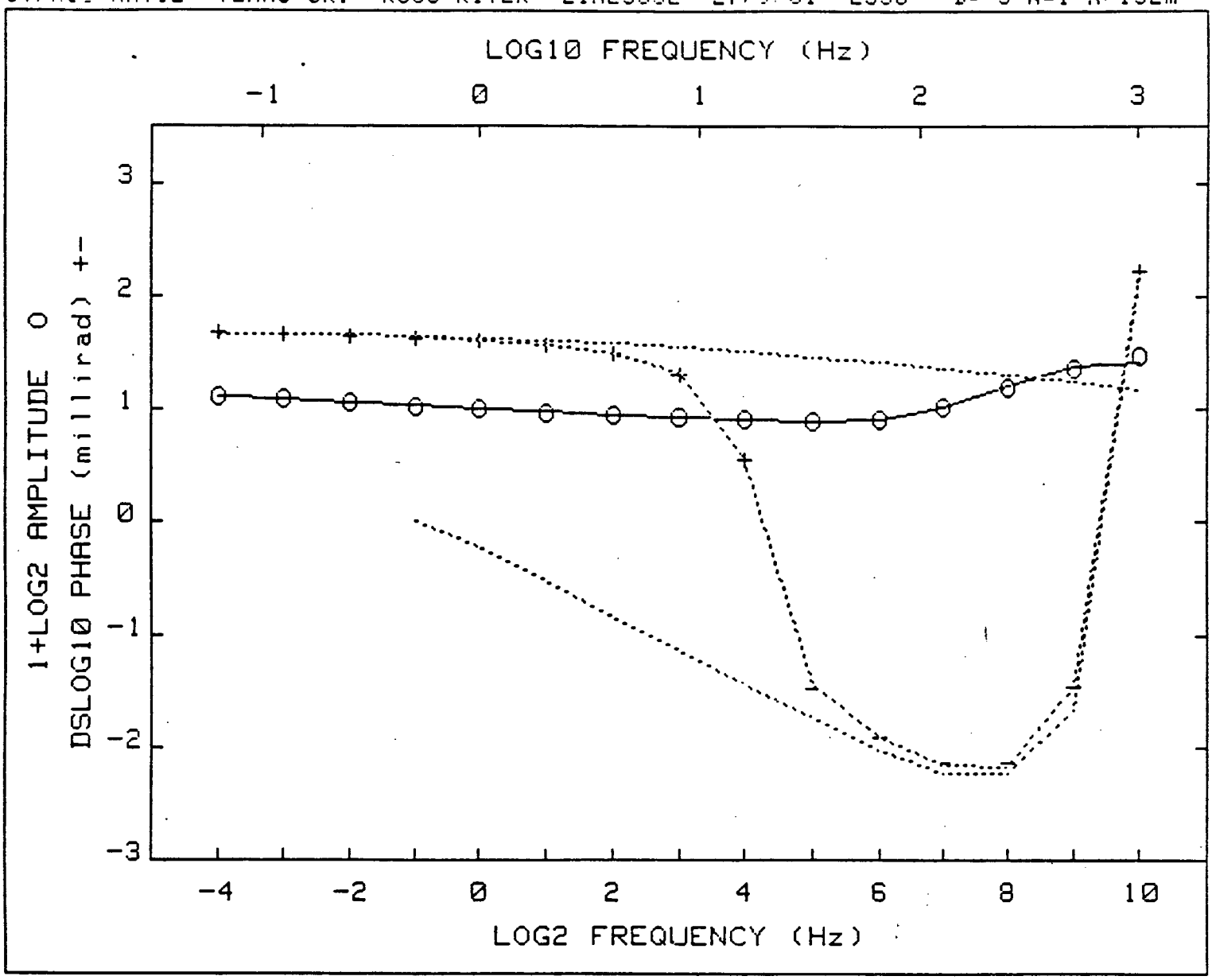

PHOENIX SPECTRAL I.P. PHASE (mrad) AT 1 HZ
CYPRUS ANVIL TENAS CK. ROSS RIVER LINE535E 27/9/81 L336
115N 125N 135N 145N 155N 165N 175N
1 2 3 4 5 6
16 15 22 24 40 37 9.6 34
15 16 22 29 41 32 32 29
16 15 22 27 46 32 27 34
0 15 21 28 44 39 27 26
0 0 22 28 47 38 34 28
0 0 0 31 48 42 33 38


PHOENIX SPECTRAL I.P. DECOUPLED PHASE AT 1 HZ
CYPRUS ANVIL TENAS CK. ROSS RIVER LINE535E 27/9/81 L336
115N 125N 135N 145N 155N 165N 175N
1 2 3 4 5 6
12 14 21 21 43 44 29 29
14 15 21 29 42 32 34 26
15 13 21 26 49 32 30 25
0 14 20 26 38 40 30 17
0 0 19 24 37 41 23 16
0 0 0 25 38 42 31 22


PHOENIX SPECTRAL I.P. MF (100*PHASE/RHO) AT 1 HZ
CYPRUS ANVIL TENAS CK. ROSS RIVER LINE535E 27/9/81 L336
115N 125N 135N 145N 155N 165N 175N
1 2 3 4 5 6
.54 .81 1.2 1.1 24 122 158 4.5
1.3 1 1.5 1.3 20 29 153 69
1.1 1.7 1.8 1.7 21 20 51 83
0 1.4 3.8 2.2 23 15 15 24
0 0 3.1 5 35 17 7.7 11
0 0 0 4.5 71 22 9.9 7

DWG. NO. - S.I.P. - 1107 - 2

CYPRUS ANVIL TENAS CK. ROSS RIVER LINE535E 27/9/81 L336 D= 5 N=1 X=152m



CRL: Number of dispersions= 3 Negative.
C1=.25 M2=1 C2=1 C3=1 fixed

Iter	Lambda	Rchsq	R0	M1	T1	T2	M3	T3
0	1.E-02	.00856	1.506	.456	2.7E+01	3.8E-05	.375	5.8E-04
1	1.E-02	.00077	1.457	.412	1.7E+01	4.2E-05	.385	5.4E-04
2	1.E-03	.00048	1.355	.375	4.9E+00	4.4E-05	.417	5.6E-04
3	1.E-04	.00033	1.349	.372	3.8E+00	4.4E-05	.420	5.7E-04
4	1.E-05	.00033	1.349	.372	3.7E+00	4.4E-05	.420	5.7E-04

	R0	M1	T1	T2	M3	T3
Pct Std Deviations	1.3	1.8	28.9	5.1	3.0	2.3

Correlation Matrix

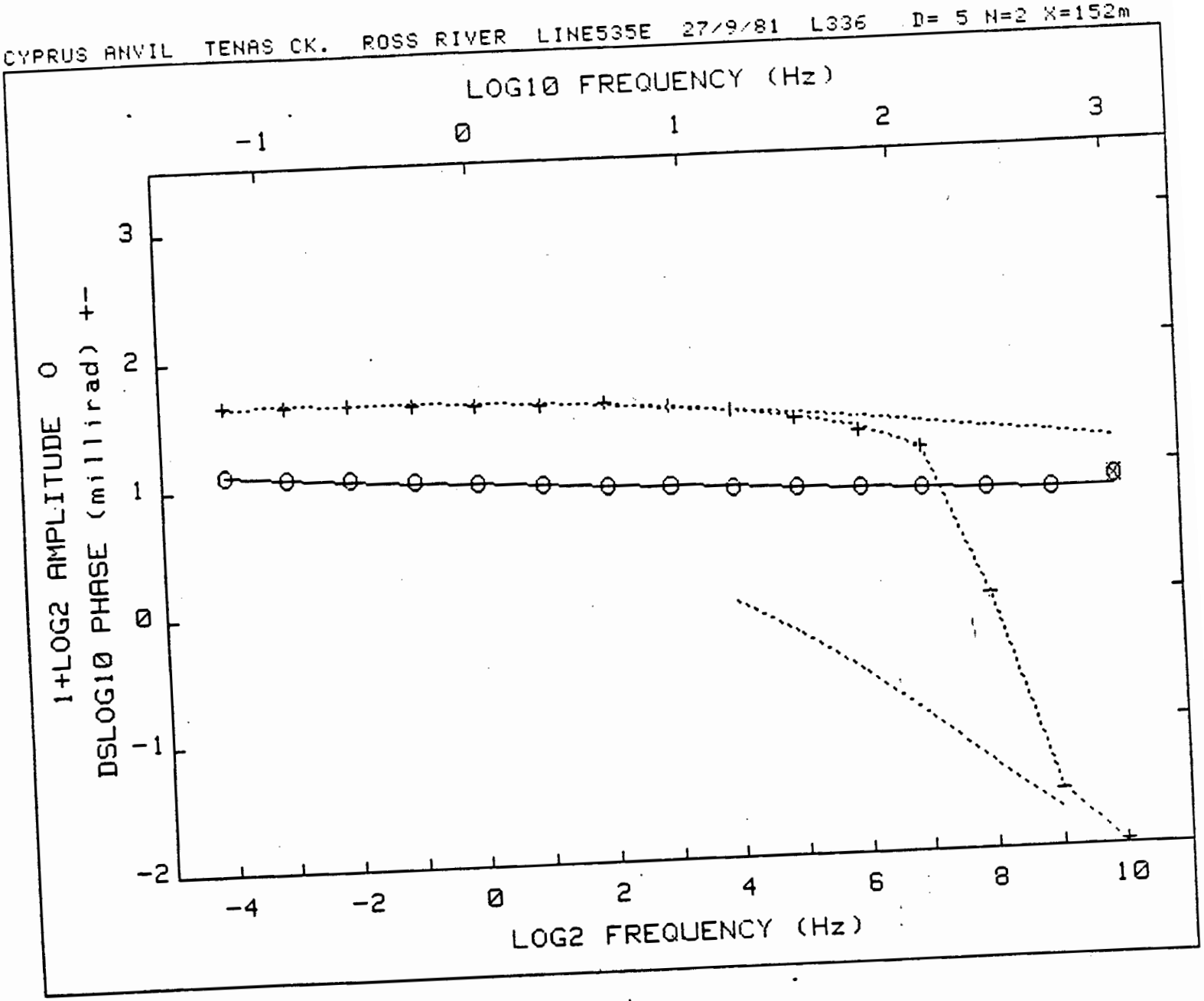
	1.000					
	.925	1.000				
	.940	.863	1.000			
	-.184	-.210	-.086	1.000		
	-.476	-.442	-.428	.919	1.000	
	-.298	-.168	-.459	-.785	-.534	1.000

Apparent Resistivity Measured at 1 Hz is 179.8

Apparent Resistivity Calculated from Inductive Coupling is 387.5

DWG. NO. – S.I.P. – 1107 – 3

CYPRUS ANVIL TENAS CK. ROSS RIVER LINE535E 27/9/81 L336 D= 5 N=2 X=152m



CRL: Number of dispersions= 3 Negative.
C1=.25 C2=1 M3=1 C3=1 fixed

Iter	Lambda	Rchsq	R0	M1	T1	M2	T2	T3
0	1.E-02	.00046	1.317	.357	2.4E+00	.012	8.3E-04	1.3E-05
1	1.E-02	.00019	1.317	.361	2.5E+00	.011	6.0E-04	1.2E-05
2	1.E-03	.00017	1.321	.362	2.7E+00	.011	5.3E-04	1.2E-05
3	1.E-01	.00017	1.321	.362	2.7E+00	.011	5.3E-04	1.2E-05
Pct Std Deviations			.8	1.2	20.6	3.7	15.8	2.4

Correlation Matrix

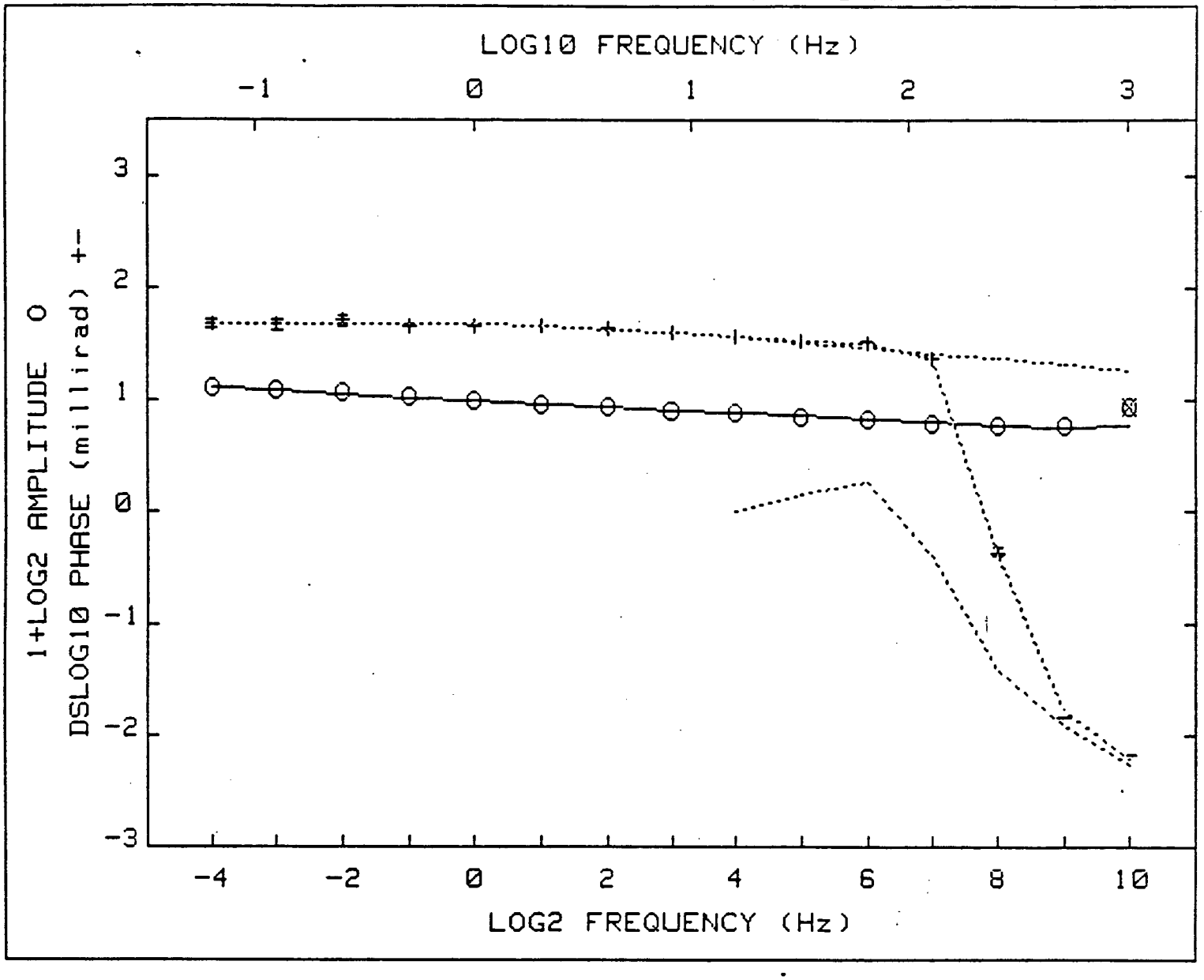
1.000						
.898	1.000					
.905	.775	1.000				
-.885	-.986	-.764	1.000			
.607	.414	.753	-.414	1.000		
-.765	-.668	-.835	.664	-.578	1.000	

Apparent Resistivity Measured at 1 Hz is 206.3

Apparent Resistivity Calculated from Inductive Coupling is 7673

DWG. NO. - S.I.P - 1107 - 4

CYPRUS ANVIL TENAS CK. ROSS RIVER LINE535E 27/9/81 L336 D= 5 N=3 X=152m



CRL: Number of dispersions= 3 Negative.
C1=.25 C2=1 M3=1 C3=1 fixed

Iter	Lambda	Rchsq	R0	M1	T1	M2	T2	T3
0	1.E-02	.00039	1.355	.387	2.4E+00	.029	8.6E-04	1.9E-05
1	1.E-02	.00031	1.347	.389	2.3E+00	.029	8.5E-04	1.9E-05
2	1.E-03	.00031	1.344	.389	2.2E+00	.029	8.5E-04	1.9E-05

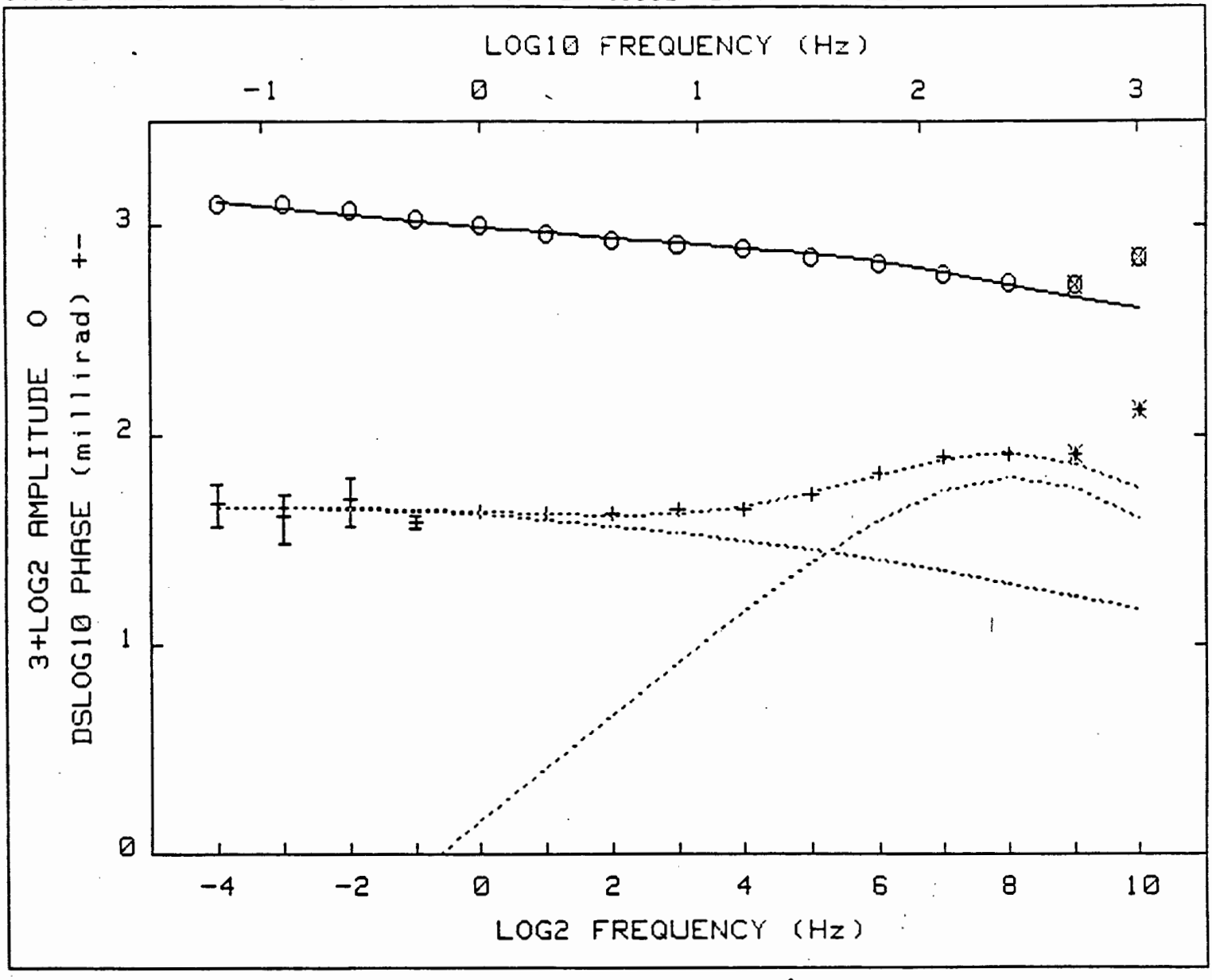
Pct Std Deviations	1.3	1.5	32.3	7.1	9.5	3.7	
Correlation Matrix	1.000						
	.871	1.000					
	.914	.718	1.000				
	.159	-.016	.262	1.000			
	.301	.123	.399	-.353	1.000		
	-.466	-.382	-.505	.644	-.815	1.000	

Apparent Resistivity Measured at 1 Hz is 239.0

Apparent Resistivity Calculated from Inductive Coupling is 3482

DWG. NO. – S.I.P. – 1107 – 5

CYPRUS ANVIL TENAS CK. ROSS RIVER LINE535E 27/9/81 L336 D= 5 N=4 X=152m



CRL: Number of dispersions= 2
C1=.25 fixed

Iter	Lambda	Rchsq	R0	M1	T1	M2	T2	C2
0	1.E-02	.00059	1.310	.367	1.7E+00	.076	9.3E-04	1.000
1	1.E-02	.00055	1.310	.366	1.8E+00	.082	8.6E-04	.938
2	1.E-03	.00053	1.321	.365	2.4E+00	.091	7.8E-04	.880
3	1.E-04	.00052	1.333	.367	3.2E+00	.097	7.3E-04	.843
4	1.E-05	.00052	1.337	.367	3.5E+00	.099	7.1E-04	.831
Pct Std Deviations			2.4	2.3	101.4	22.2	30.7	13.6

Correlation Matrix

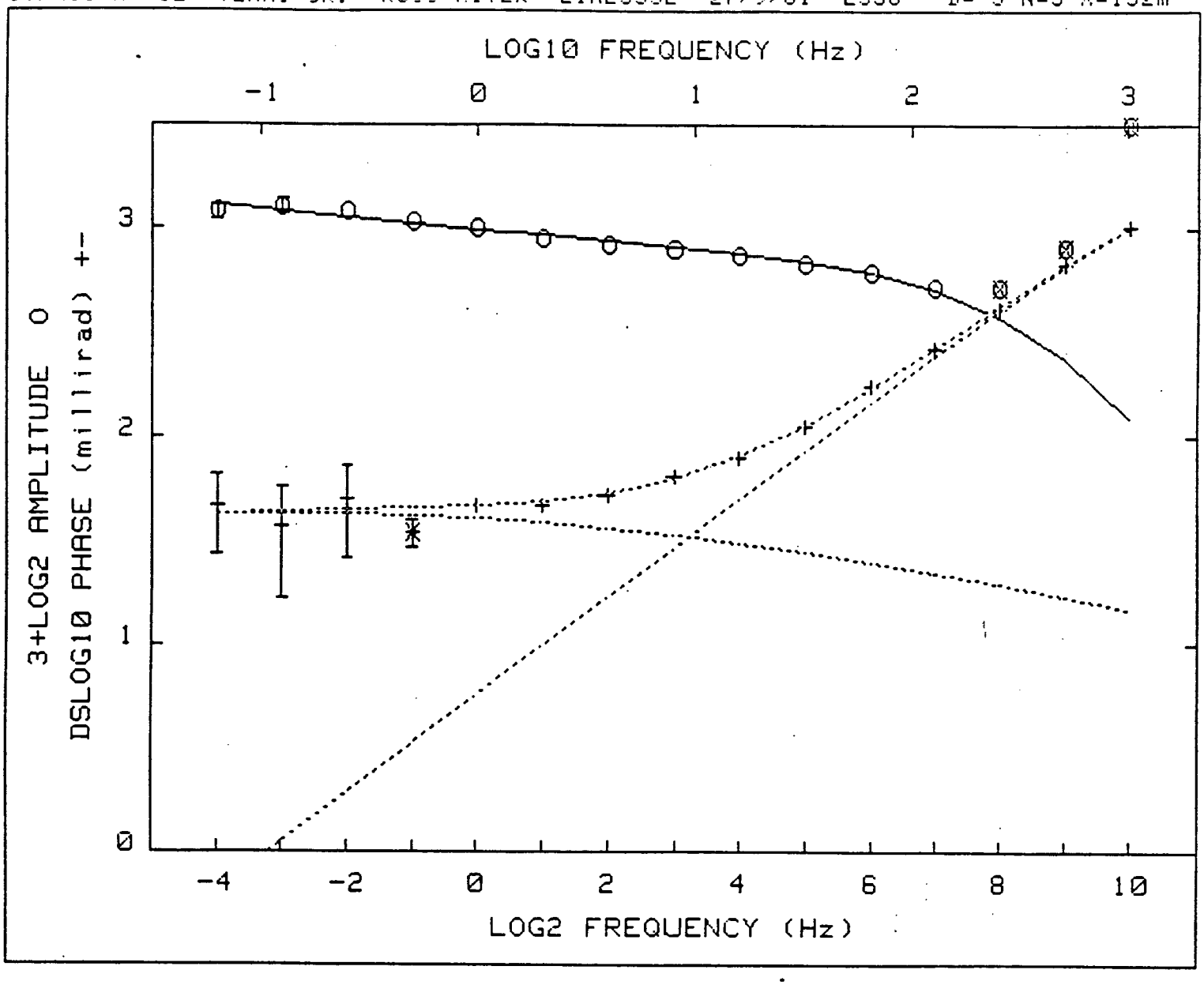
1.000						
.712	1.000					
.948	.522	1.000				
.547	-.001	.675	1.000			
-.305	.037	-.389	-.882	1.000		
-.583	-.032	-.701	-.958	.829	1.000	

Apparent Resistivity Measured at 1 Hz is 167.7

Apparent Resistivity Calculated from Inductive Coupling is 1073

DWG. NO. - S.I.P. - 1107-6

CYPRUS ANVIL TENAS CK. ROSS RIVER LINE535E 27/9/81 L336 D= 5 N=5 X=152m



CRL: Number of dispersions= 2
C1=.25 M2=1 fixed

Iter	Lambda	Rchsq	R0	M1	T1	T2	C2
0	1.E-02	.00076	1.321	.342	4.7E+00	1.4E-04	.743
1	1.E-02	.00067	1.332	.354	4.5E+00	1.4E-04	.749
2	1.E-03	.00066	1.320	.353	3.4E+00	1.4E-04	.755
3	1.E-04	.00066	1.309	.351	2.5E+00	1.4E-04	.762
Pct Std Deviations			2.8	2.8	137.3	6.2	3.5

Correlation Matrix

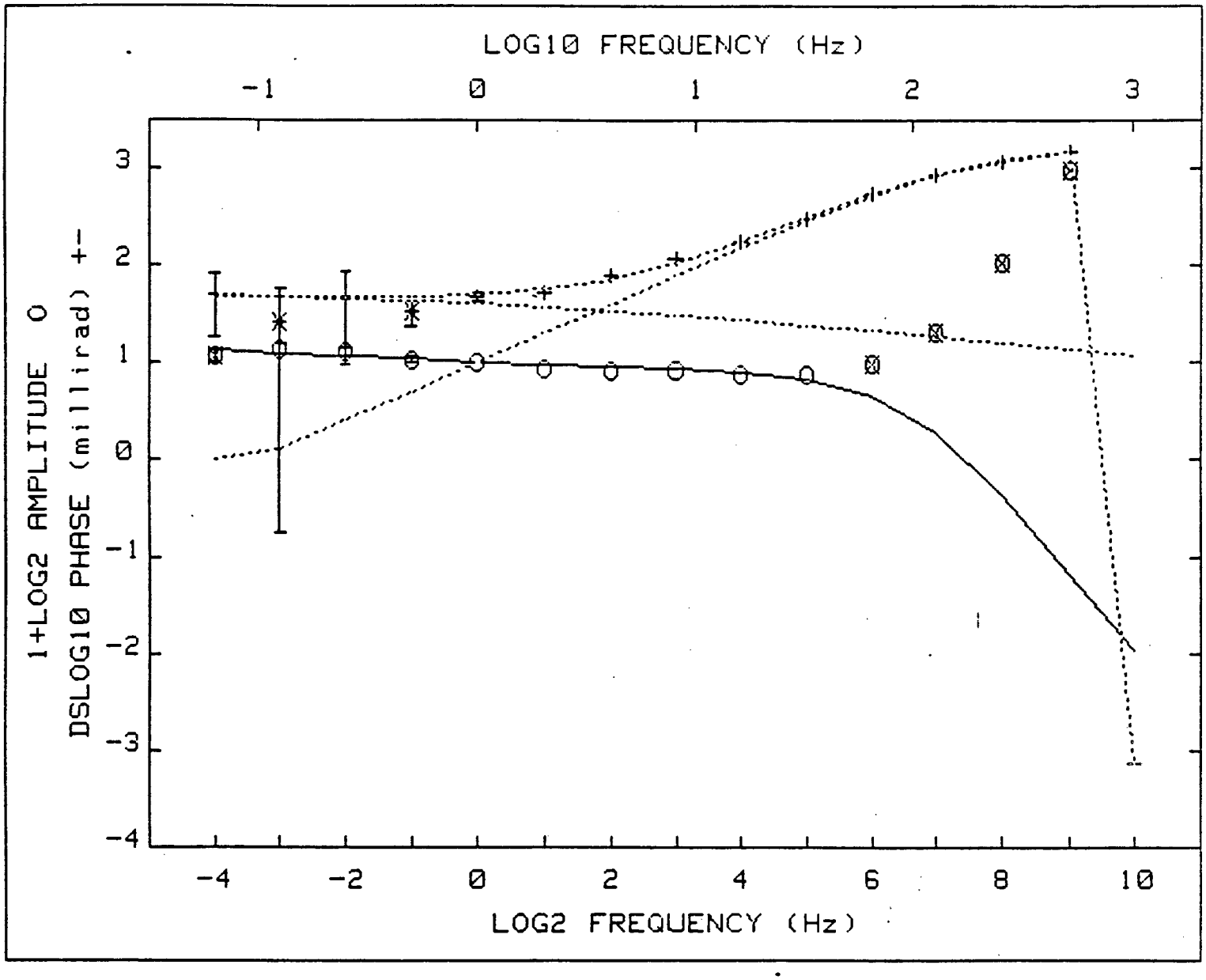
1.000					
.668	1.000				
.949	.471	1.000			
-.599	-.477	-.544	1.000		
-.669	-.080	-.751	.652	1.000	

Apparent Resistivity Measured at 1 Hz is 108.3

Apparent Resistivity Calculated from Inductive Coupling is 558.0

DWG. NO. - S.I.P. - 1107-7

CYPRUS ANVIL TENAS CK. ROSS RIVER LINE535E 27/9/81 L336 D= 5 N=6 X=152m



CRL: Number of dispersions= 2
C1=.25 fixed

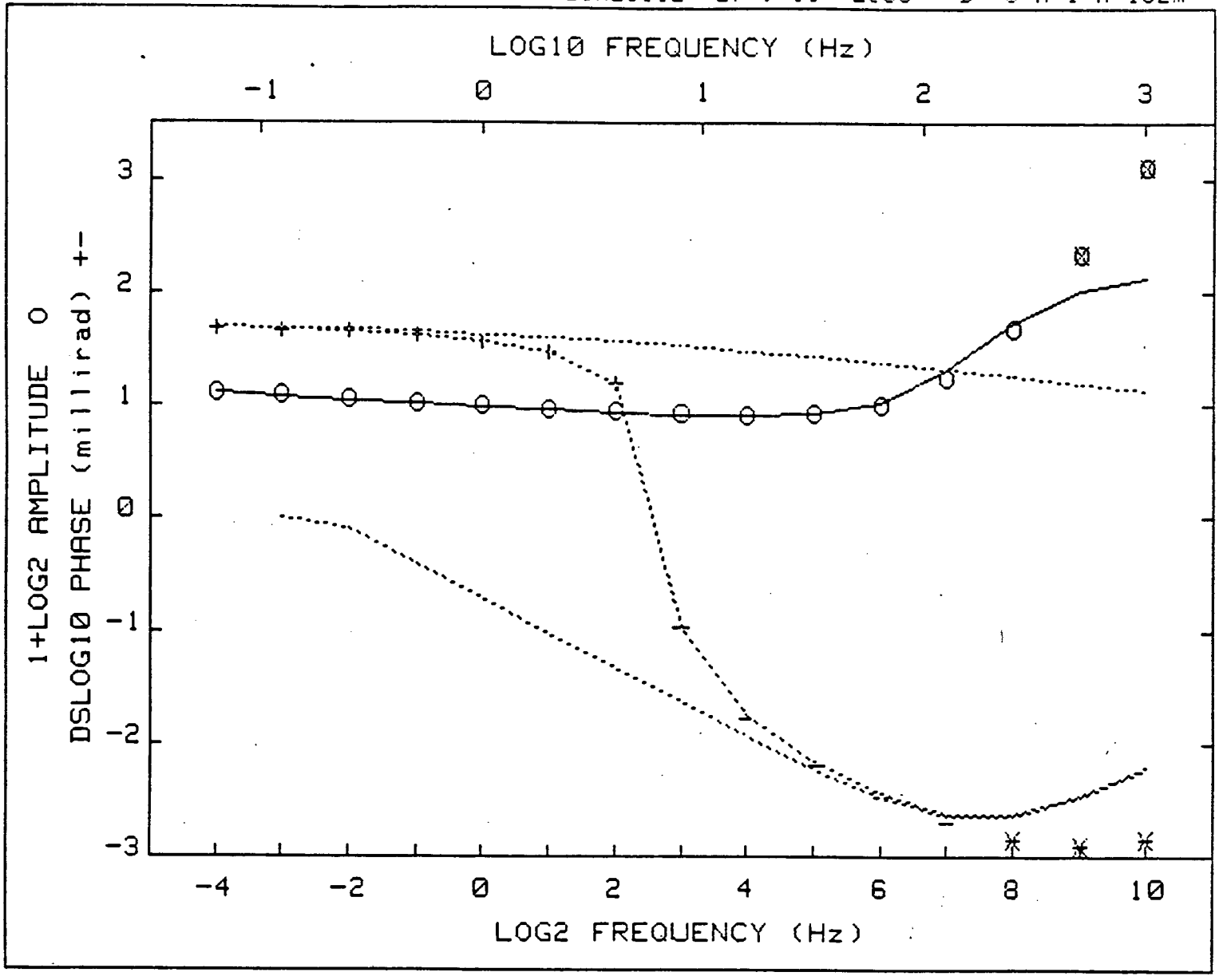
Iter	Lambda	Rchsq	R0	M1	T1	M2	T2	C2
0	1.E-02	.00087	1.445	.392	1.8E+01	.667	1.4E-03	.953
1	1.E-02	.00085	1.451	.394	1.8E+01	.660	1.4E-03	.957
2	1.E-03	.00085	1.449	.394	1.7E+01	.661	1.4E-03	.958

Pct Std Deviations	7.0	7.7	318.9	5.4	6.6	3.4	
Correlation Matrix	1.000						
	.961	1.000					
	.975	.896	1.000				
	-.869	-.931	-.804	1.000			
	-.070	-.019	-.076	-.276	1.000		
	-.543	-.376	-.611	.128	.573	1.000	

Apparent Resistivity Measured at 1 Hz is 42.72

Apparent Resistivity Calculated from Inductive Coupling is 260.8

CYPRUS ANVIL TENAS CK. ROSS RIVER LINE535E 27/9/81 L336 D= 6 N=1 X=152m



CRL: Number of dispersions= 2 Negative.
C1=.25 M2=1 fixed

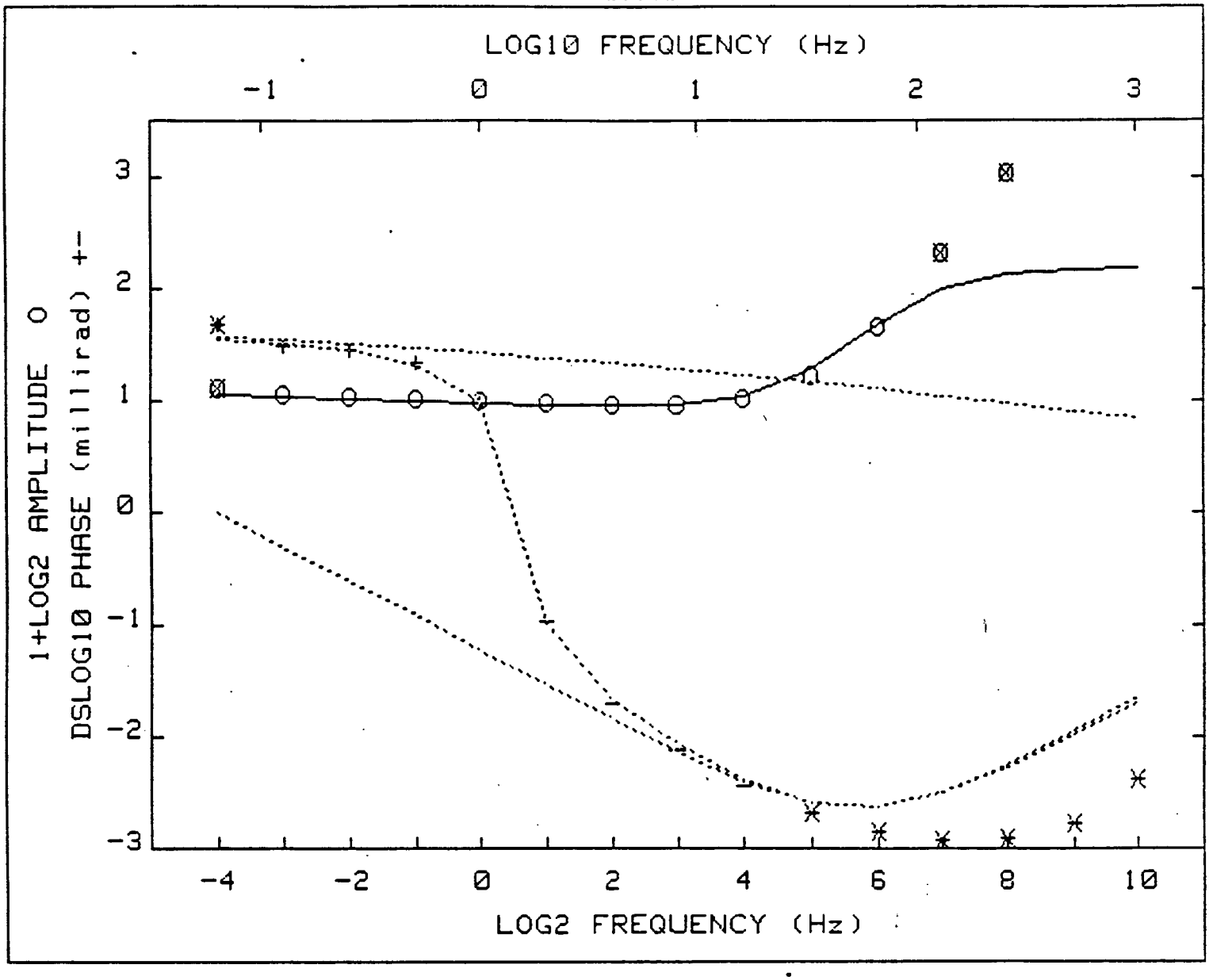
Iter	Lambda	Rchsq	R0	M1	T1	T2	C2
0	1.E-02	.00167	1.275	.367	1.0E+00	6.3E-04	.963
1	1.E-02	.00146	1.295	.368	1.5E+00	6.1E-04	.968
2	1.E-03	.00117	1.347	.374	5.0E+00	5.8E-04	.988
3	1.E-04	.00107	1.386	.390	8.7E+00	5.6E-04	.993
4	1.E-05	.00107	1.395	.393	9.4E+00	5.6E-04	.993
Pct Std Deviations			3.6	4.3	103.5	5.8	1.8
Correlation Matrix			1.000				
			.936	1.000			
			.952	.845	1.000		
			-.786	-.758	-.729	1.000	
			.324	.131	.508	.160	1.000

Apparent Resistivity Measured at 1 Hz is 35.76

Apparent Resistivity Calculated from Inductive Coupling is 30.36

DWG. NO. - S.I.P. - 1107 - 9

CYPRUS ANVIL TENAS CK. ROSS RIVER LINE535E 27/9/81 L336 D= 7 N=1 X=152m



CRL: Number of dispersions= 2 Negative.
C1=.25 M2=1 C2=1 fixed

Iter	Lambda	Rchsq	R0	M1	T1	T2
0	1.E-02	.00123	1.330	.318	4.4E+01	2.0E-03
1	1.E-02	.00113	1.340	.324	4.5E+01	2.0E-03
2	1.E-03	.00112	1.352	.329	5.4E+01	2.0E-03

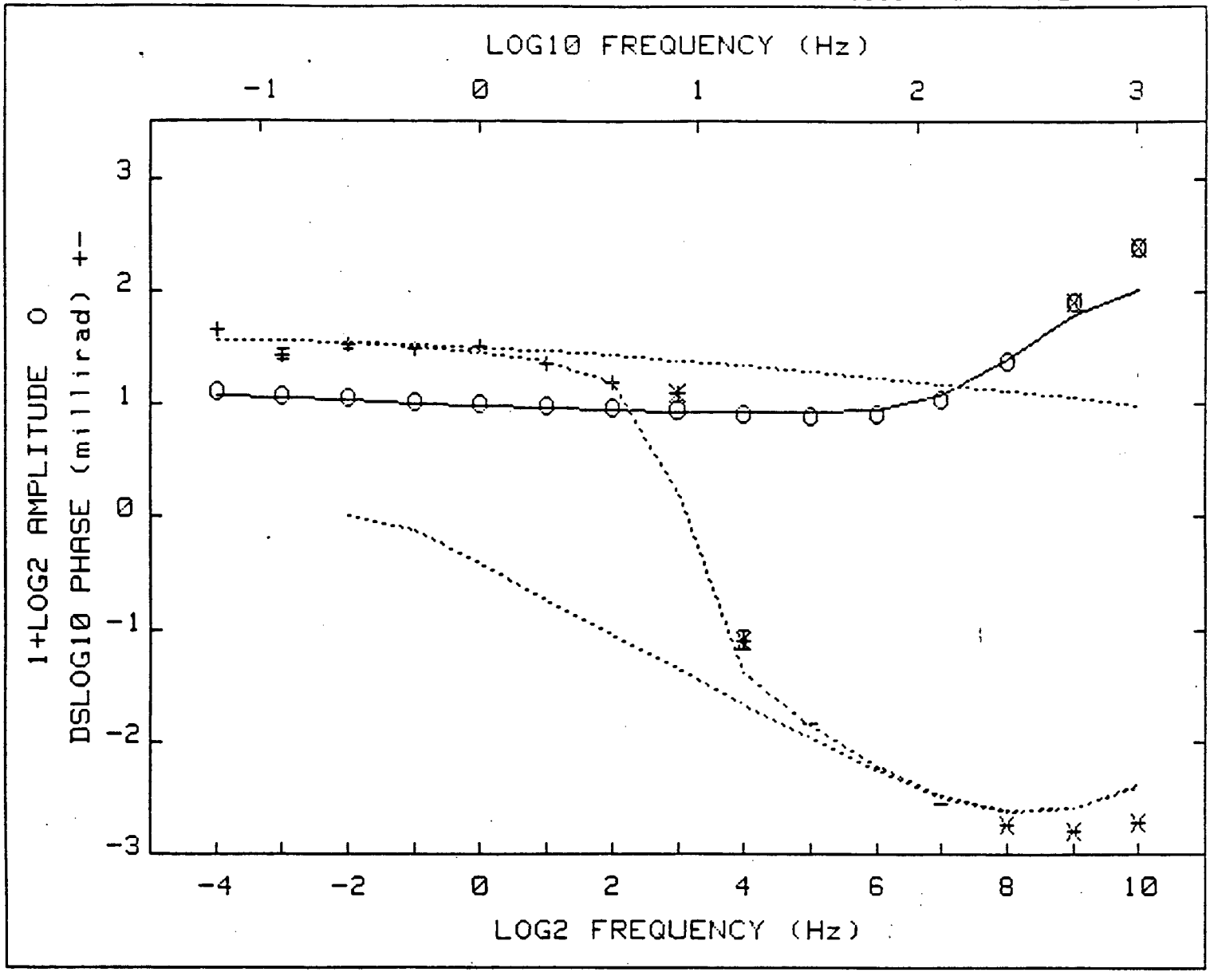
Pct Std Deviations	7.8	14.5	345.1	10.8	
Correlation Matrix	1.000				
	.992	1.000			
	.992	.988	1.000		
	-.967	-.951	-.980	1.000	

Apparent Resistivity Measured at 1 Hz is 18.63

Apparent Resistivity Calculated from Inductive Coupling is 8.816

DWG. NO. - S.I.P. - 1107 - 10

CYPRUS ANVIL TENAS CK. ROSS RIVER LINE535E 27/9/81 L336 D= 7 N=2 X=152m



CRL: Number of dispersions= 2 Negative.
C1=.25 M2=1 C2=1 fixed

Iter	Lambda	Rchsq	R0	M1	T1	T2
0	1.E-02	.00337	1.248	.296	2.5E+00	3.1E-04
1	1.E-02	.00225	1.246	.295	3.3E+00	3.5E-04
2	1.E-03	.00211	1.275	.307	6.9E+00	3.4E-04
3	1.E-04	.00208	1.294	.315	9.6E+00	3.3E-04
4	1.E-05	.00208	1.297	.316	1.0E+01	3.3E-04

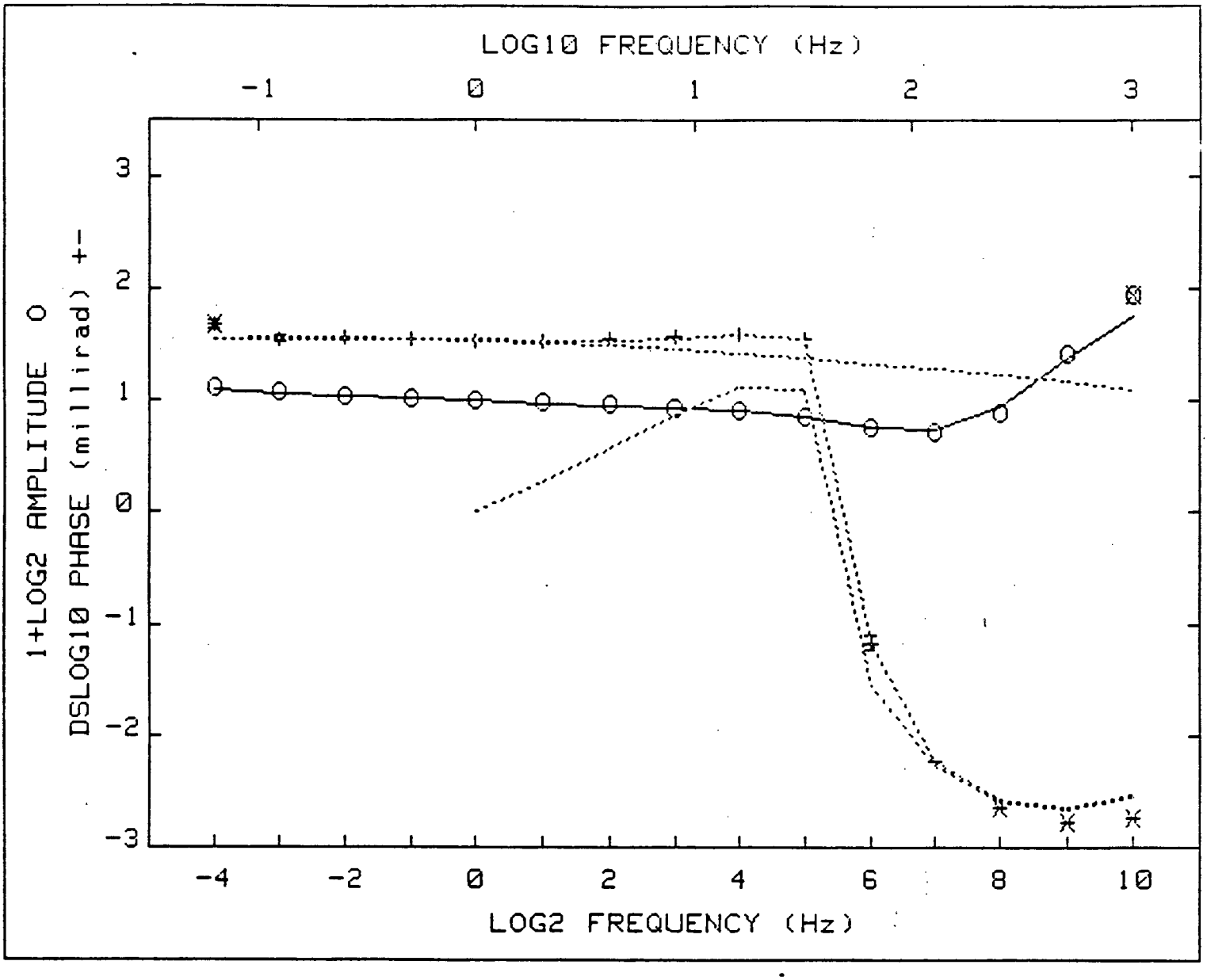
Pct Std Deviations	4.1	7.3	155.9	7.4	
Correlation Matrix	1.000				
	.957	1.000			
	.953	.925	1.000		
	-.751	-.668	-.760	1.000	

Apparent Resistivity Measured at 1 Hz is 21.92

Apparent Resistivity Calculated from Inductive Coupling is 137.2

DWG. NO. - S.I.P - 1107-11

CYPRUS ANVIL TENAS CK. ROSS RIVER LINE535E 27/9/81 L336 D= 8 N=3 X=152m



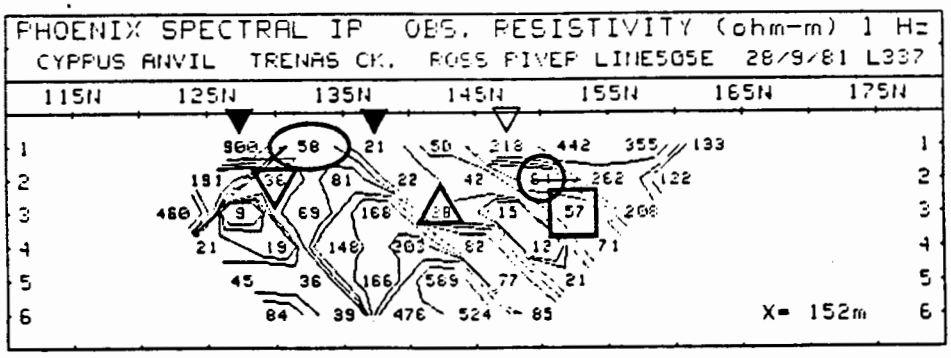
CRL: Number of dispersions= 3 Negative.
C1=.25 C2=1 M3=1 C3=1 fixed

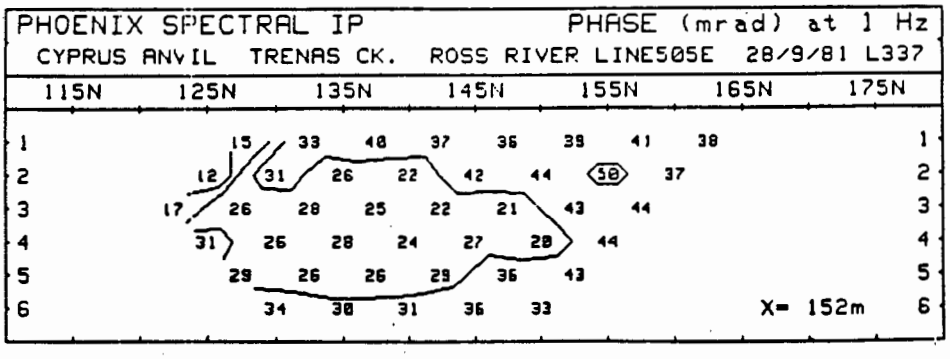
Iter	Lambda	Rchsq	R0	M1	T1	M2	T2	T3
0	1.E-02	.02331	1.478	.476	3.4E+01	.105	2.5E-03	2.0E-04
1	1.E-02	.00238	1.365	.368	2.8E+01	.124	2.8E-03	2.0E-04
2	1.E-03	.00056	1.311	.328	1.1E+01	.126	2.8E-03	2.1E-04
3	1.E-04	.00045	1.243	.300	2.5E+00	.132	2.7E-03	2.3E-04
4	1.E-05	.00040	1.246	.304	2.1E+00	.130	2.6E-03	2.3E-04
5	1.E-02	.00040	1.246	.304	2.1E+00	.130	2.6E-03	2.3E-04

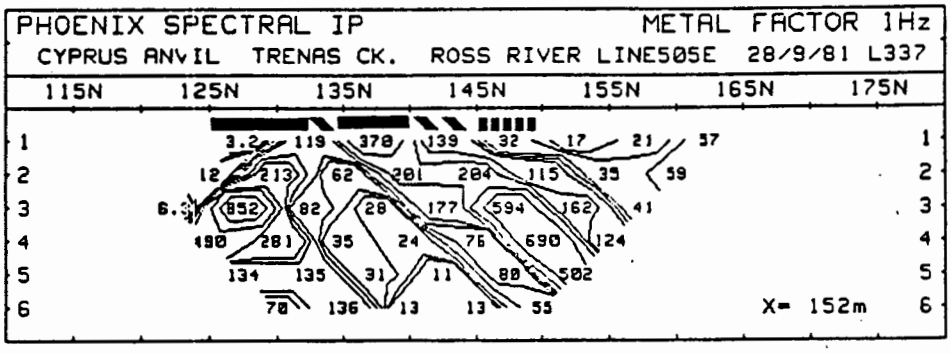
Pct Std Deviations	1.9	2.6	84.0	6.0	6.0	5.0	
Correlation Matrix	1.000						
	.875	1.000					
	.955	.772	1.000				
	-.354	-.270	-.311	1.000			
	.483	.233	.520	-.804	1.000		
	-.628	-.467	-.620	.931	-.867	1.000	

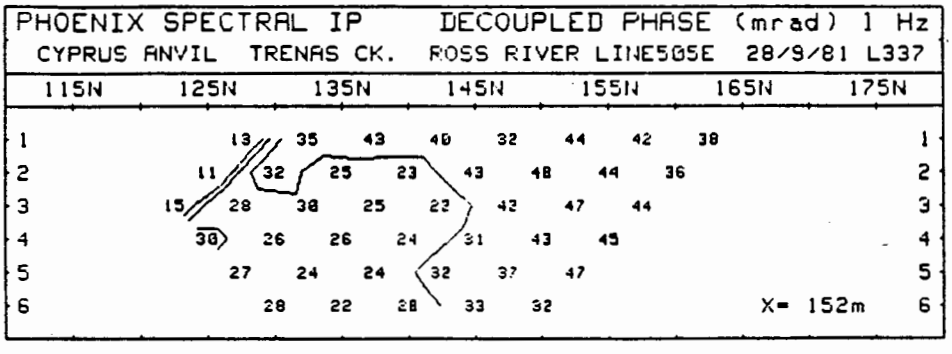
Apparent Resistivity Measured at 1 Hz is 30.72

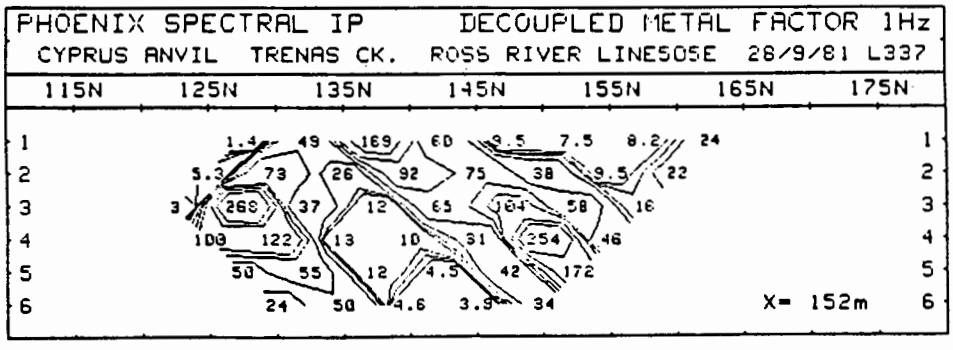
Apparent Resistivity Calculated from Inductive Coupling is 248.3


PHOENIX SPECTRAL IP OBS. RESISTIVITY (ohm-m) 1 Hz
CYPRUS ANVIL TRENAS CK. ROSS RIVER LINE505E 28/9/81 L337
115N 125N 135N 145N 155N 165N 175N
X= 152m


PHOENIX SPECTRAL IP PHASE (mrad) at 1 Hz
CYPRUS ANVIL TRENAS CK. ROSS RIVER LINE505E 28/9/81 L337
115N 125N 135N 145N 155N 165N 175N
X= 152m

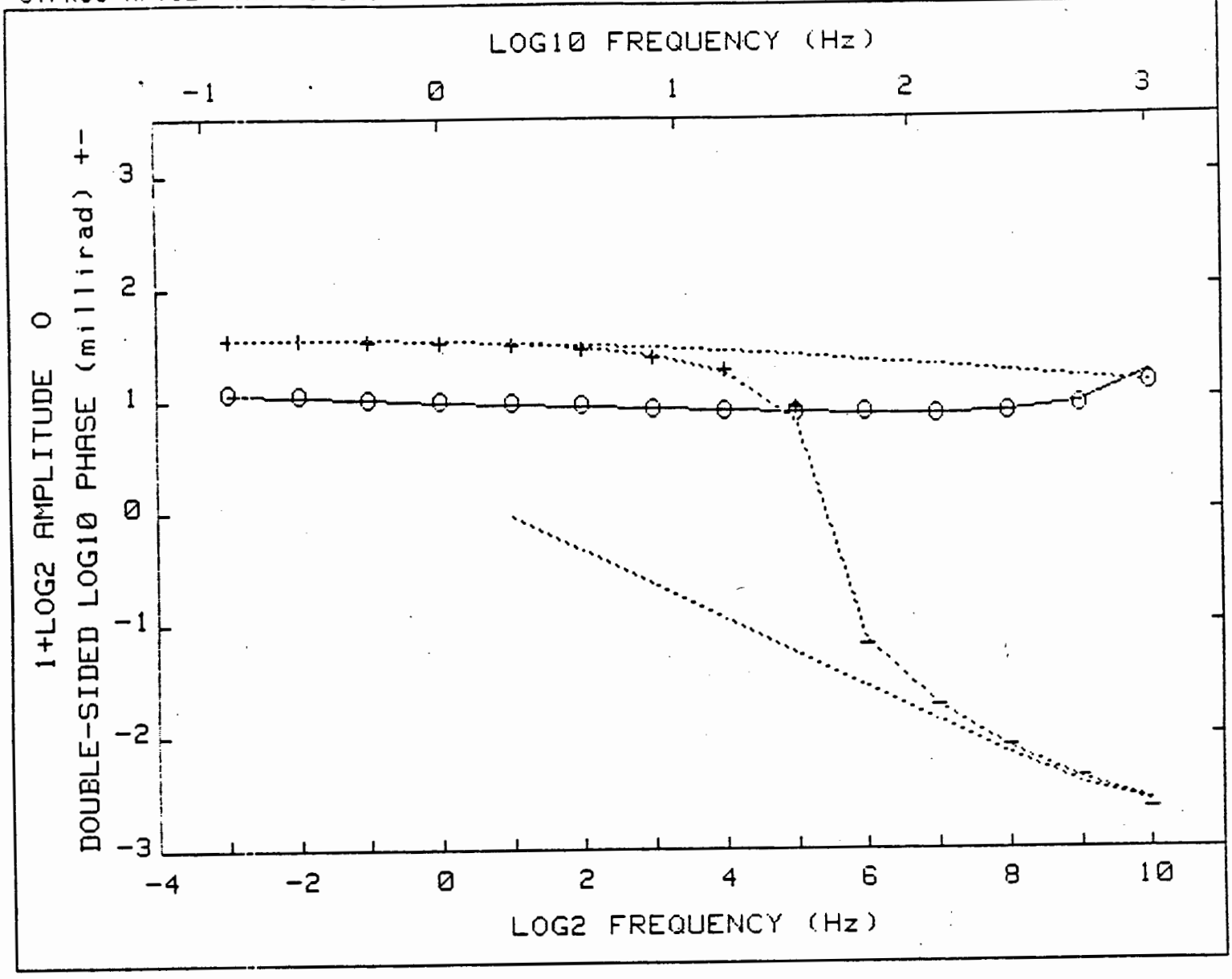

PHOENIX SPECTRAL IP METAL FACTOR 1Hz
CYPRUS ANVIL TRENAS CK. ROSS RIVER LINE505E 28/9/81 L337
115N 125N 135N 145N 155N 165N 175N
X= 152m


PHOENIX SPECTRAL IP DECOUPLED PHASE (mrad) 1 Hz
CYPRUS ANVIL TRENAS CK. ROSS RIVER LINE505E 28/9/81 L337
115N 125N 135N 145N 155N 165N 175N
X= 152m


PHOENIX SPECTRAL IP DECOUPLED METAL FACTOR 1Hz
CYPRUS ANVIL TRENAS CK. ROSS RIVER LINE505E 28/9/81 L337
115N 125N 135N 145N 155N 165N 175N
X= 152m

DWG. NO. - S.I.P - 1108 - 2

CYPRUS ANVIL TRENAS CK. ROSS RIVER LINE505E 28/9/81 L337 D= 2 N=1 X=152m



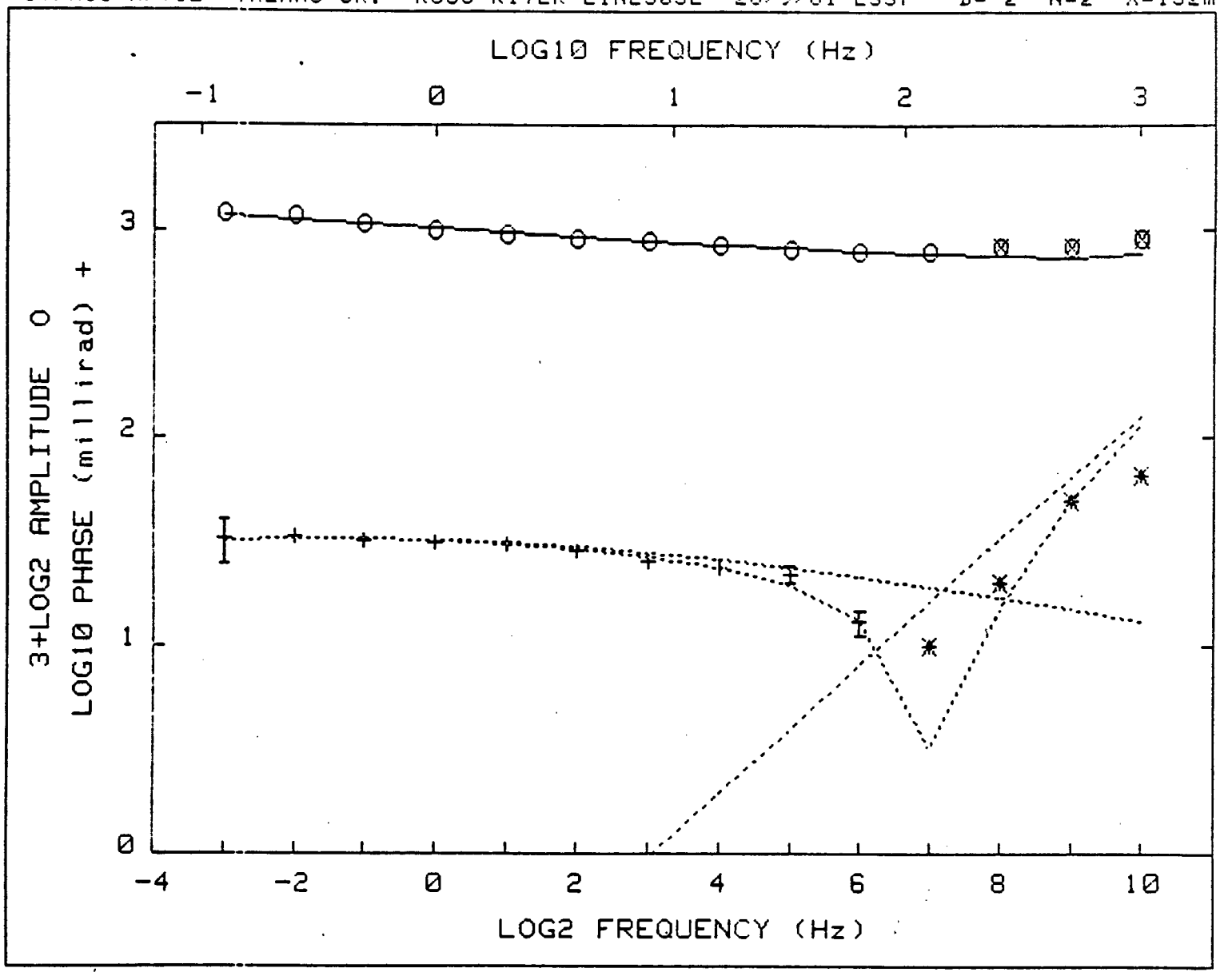
CRL: Number of dispersions= 2 Negative.
C1=.25 M2=1 fixed

Iter	Lambda	Rchsq	R0	M1	T1	T2	C2
0	1.E-02	.21417	1.000	.150	1.0E+00	8.0E-05	1.000
1	1.E-02	.02138	1.175	.244	5.1E+00	4.3E-05	1.000
2	1.E-03	.00510	1.230	.296	1.6E+00	7.3E-05	1.000
3	1.E-04	.00131	1.231	.300	1.6E+00	6.7E-05	1.000
4	1.E+00	.00129	1.234	.302	1.6E+00	6.7E-05	1.000
5	1.E+01	.00123	1.235	.303	1.6E+00	6.7E-05	1.000
6	1.E+01	.00119	1.235	.304	1.6E+00	6.7E-05	1.000
7	1.E+01	.00116	1.236	.304	1.6E+00	6.7E-05	1.000
8	1.E+01	.00114	1.236	.304	1.6E+00	6.7E-05	1.000
9	1.E+01	.00112	1.236	.305	1.6E+00	6.7E-05	1.000

Pct Std Deviations		2.1	3.5	77.7	5.4	2.3
Correlation Matrix	1.000					
	.885	1.000				
	.916	.781	1.000			
	-.211	-.325	-.083	1.000		
	.471	.215	.668	.620	1.000	

DWG. NO. – S.I.P. – 1108 -3

CYPRUS ANVIL TRENAS CK. ROSS RIVER LINE505E 28/9/81 L337 D= 2 N=2 X=152m



CRL: Number of dispersions= 2 Negative.
C1=.25 M2=1 C2=1 fixed

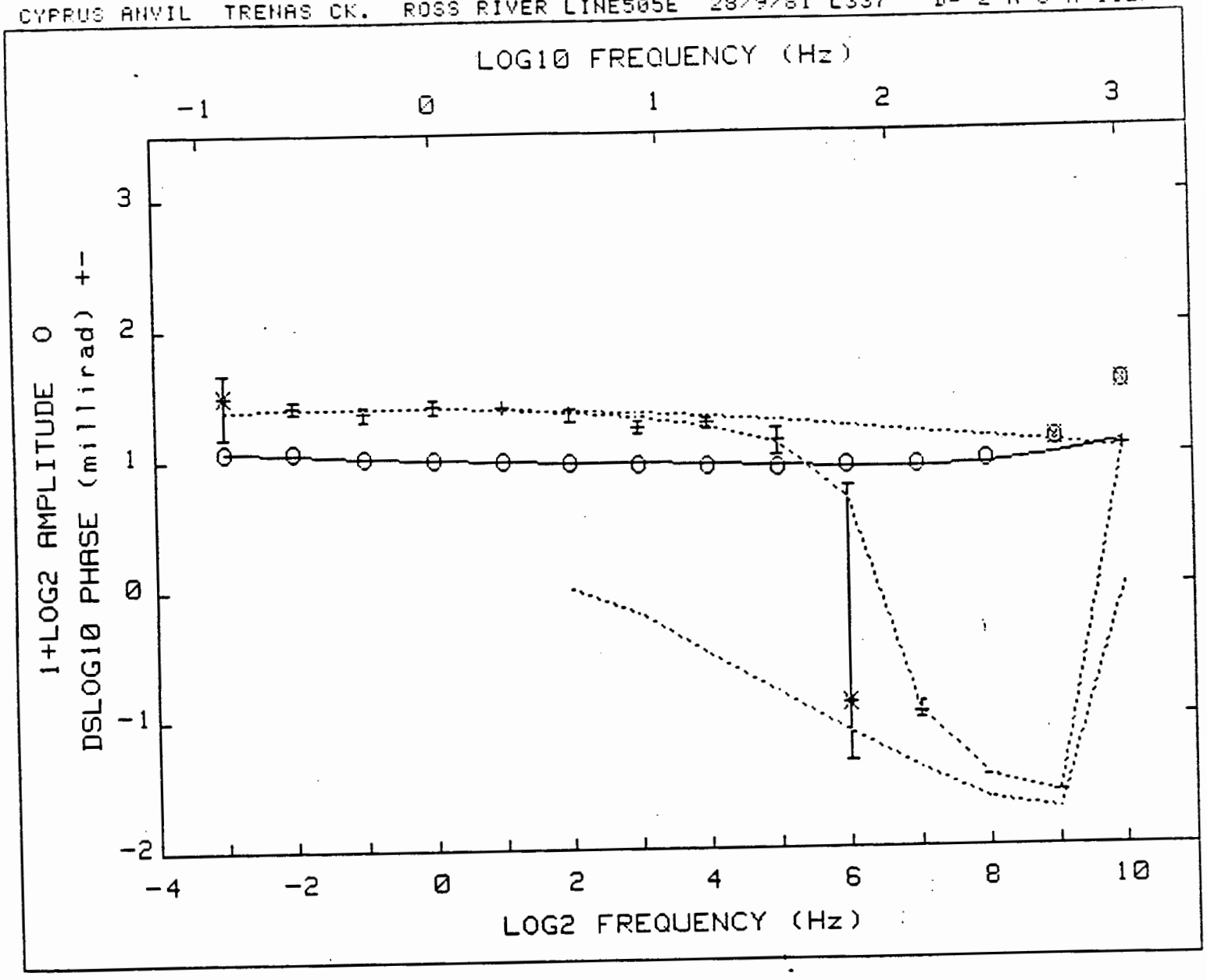
Iter	Lambda	Rchsq	R0	M1	T1	T2
0	1.E-02	.00164	1.174	.286	1.4E-01	3.4E-05
1	1.E-02	.00076	1.174	.274	2.2E-01	2.6E-05
2	1.E-03	.00040	1.198	.274	6.4E-01	1.8E-05
3	1.E-04	.00029	1.212	.281	9.3E-01	1.6E-05
4	1.E-05	.00029	1.213	.282	9.6E-01	1.5E-05

Pct Std Deviations	.9	1.6	35.1	13.3	
Correlation Matrix	1.000				
	.816	1.000			
	.875	.690	1.000		
	-.591	-.287	-.797	1.000	

Apparent Resistivity Measured at 1 Hz is 36.20
Apparent Resistivity Calculated from Inductive Coupling is 2961

DWG. NO. - S.I.P. - 1108 - 4

CYPRUS ANVIL TRENAS CK. ROSS RIVER LINE505E 28/9/81 L337 D= 2 N=3 X=152m



CRL: Number of dispersions= 3 Negative.
C1=.25 M2=1 C2=1 C3=1 fixed

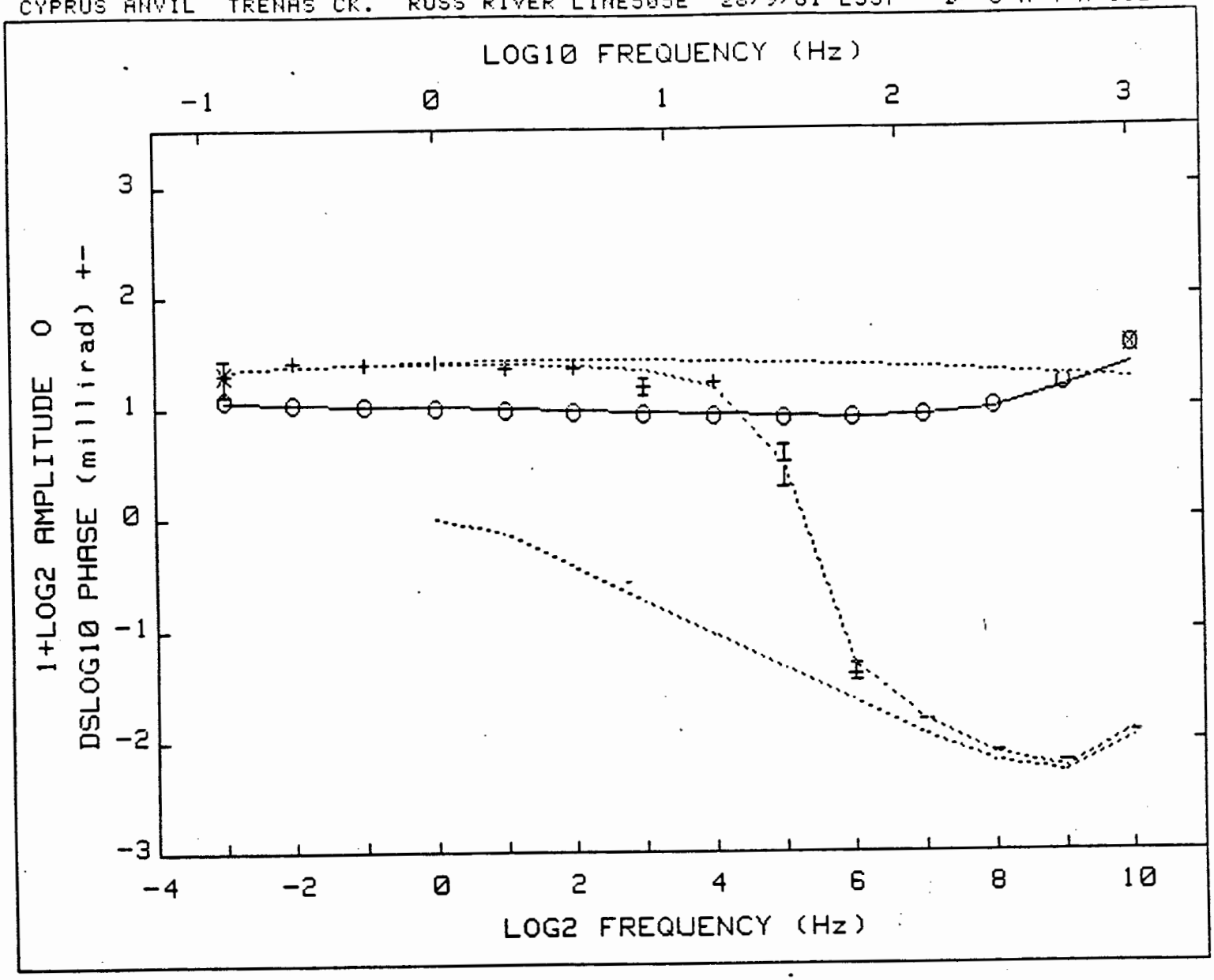
Iter	Lambda	Rchsq	R0	M1	T1	T2	M3	T3
0	1.E-02	.00074	1.167	.224	5.6E-01	1.6E-05	.211	2.0E-04
1	1.E-02	.00067	1.159	.225	5.6E-01	1.6E-05	.210	2.0E-04
2	1.E-03	.00067	1.159	.225	5.6E-01	1.6E-05	.210	2.0E-04
Pct Std Deviations			1.2	2.8	56.7	15.0	13.4	9.5
Correlation Matrix			1.000					
			.834	1.000				
			.862	.785	1.000			
			.188	.076	.277	1.000		
			.140	.038	.216	.997	1.000	
			-.297	-.168	-.409	-.982	-.970	1.000

Apparent Resistivity Measured at 1 Hz is 8.980

Apparent Resistivity Calculated from Inductive Coupling is 5251

DWG. NO. - S.I.P - 1108 - 5

CYPRUS ANVIL TRENAS CK. ROSS RIVER LINE505E 28/9/81 L337 D= 3 N=4 X=152m



CRL: Number of dispersions= 3 Negative.
C1=.25 M2=1 C2=1 M3=1 C3=1 fixed

Iter	Lambda	Rchsq	R0	M1	T1	T2	T3
0	1.E-02	.00193	1.118	.238	4.2E-02	7.4E-05	1.7E-04
1	1.E-02	.00190	1.120	.238	4.7E-02	7.5E-05	1.7E-04
2	1.E-03	.00188	1.124	.238	5.8E-02	7.5E-05	1.7E-04
3	1.E-04	.00188	1.125	.238	6.1E-02	7.5E-05	1.7E-04
Pct Std Deviations			1.4	2.5	77.1	3.9	3.1

Correlation Matrix

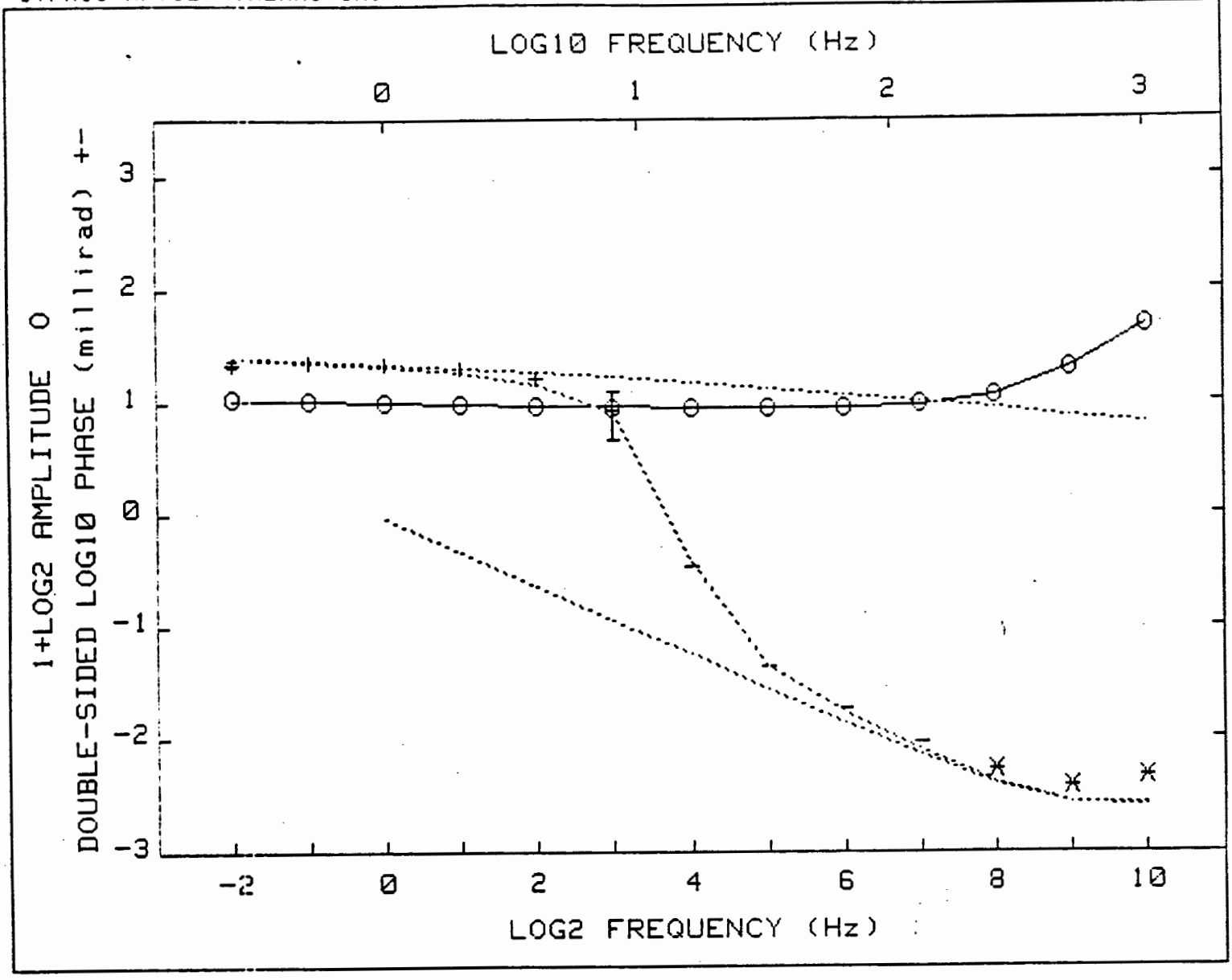
1.000					
.256	1.000				
.752	.044	1.000			
.238	-.093	.372	1.000		
-.396	.436	-.641	.223	1.000	

Apparent Resistivity Measured at 1 Hz is 18.77

Apparent Resistivity Calculated from Inductive Coupling is 1857

DWG. NO. - S.I.P. - 1108-6

CYPRUS ANVIL TRENAS CK. ROSS RIVER LINE505E 28/9/81 L337 D= 5 N=3 X=152m



CRL: Number of dispersions= 2 Negative.
C1=.25 M2=1 C2=1 fixed

Iter	Lambda	Rchsq	R0	M1	T1	T2
0	1.E-02	.00097	1.222	.243	1.1E+01	1.4E-04
1	1.E-02	.00097	1.221	.242	1.2E+01	1.4E-04

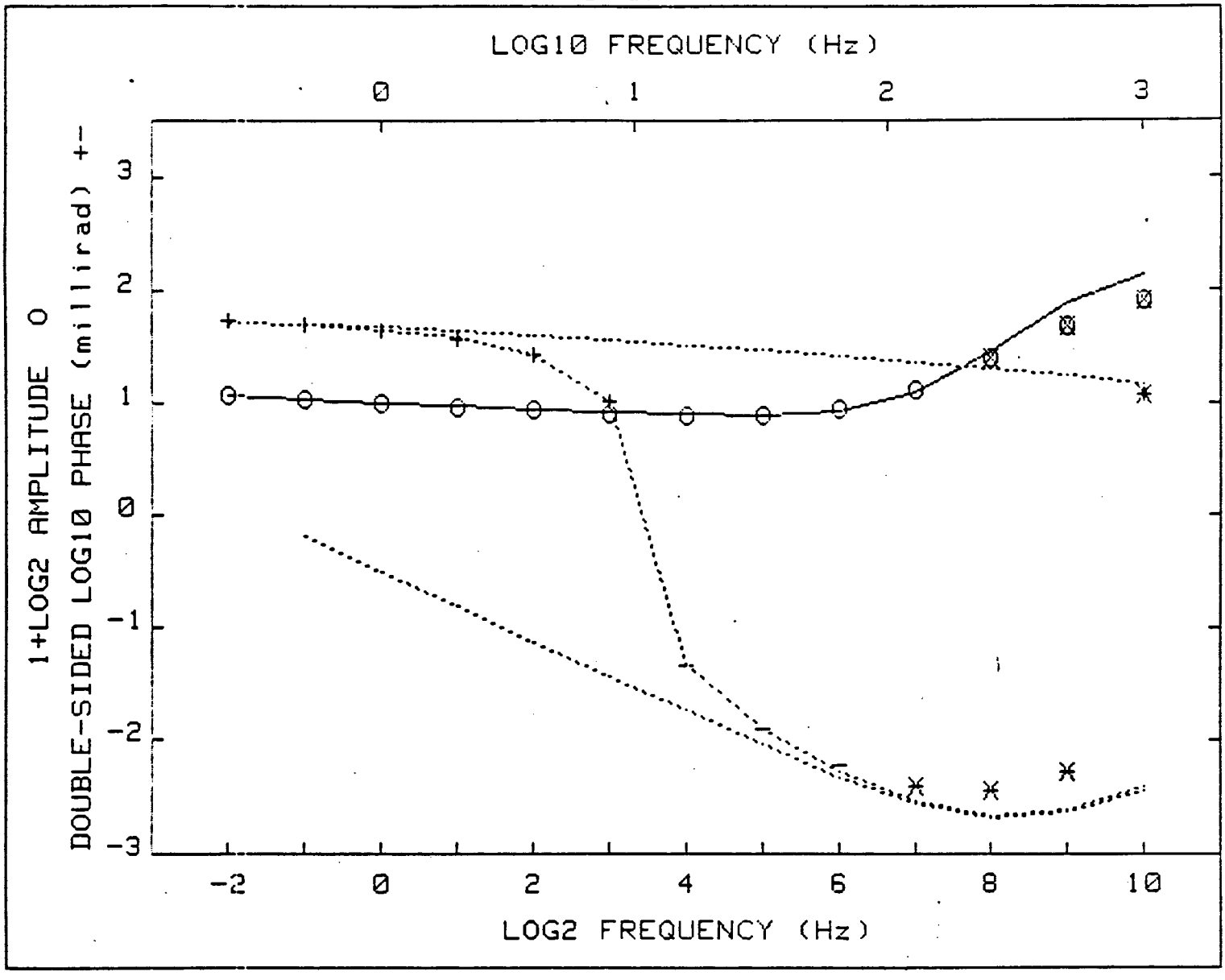
Pct Std Deviations	3.1	8.7	114.4	5.5

Correlation Matrix

1.000			
.975	1.000		
.974	.975	1.000	
-.904	-.874	-.952	1.000

Apparent Resistivity Measured at 1 Hz is 27.78
Apparent Resistivity Calculated from Inductive Coupling is 613.1

CYPRUS ANVIL TRENAS CK. ROSS RIVER LINE505E 28/9/81 L337 D= 6 N=2 X=152m



CRL: Number of dispersions= 2 Negative.
C1=.25 M2=1 C2=1 fixed

Iter	Lambda	Rchsq	R0	M1	T1	T2
0	1.E-02	.00045	1.501	.433	1.5E+01	3.2E-04
1	1.E-02	.00037	1.509	.438	1.4E+01	3.3E-04
2	1.E-03	.00037	1.499	.435	1.3E+01	3.4E-04

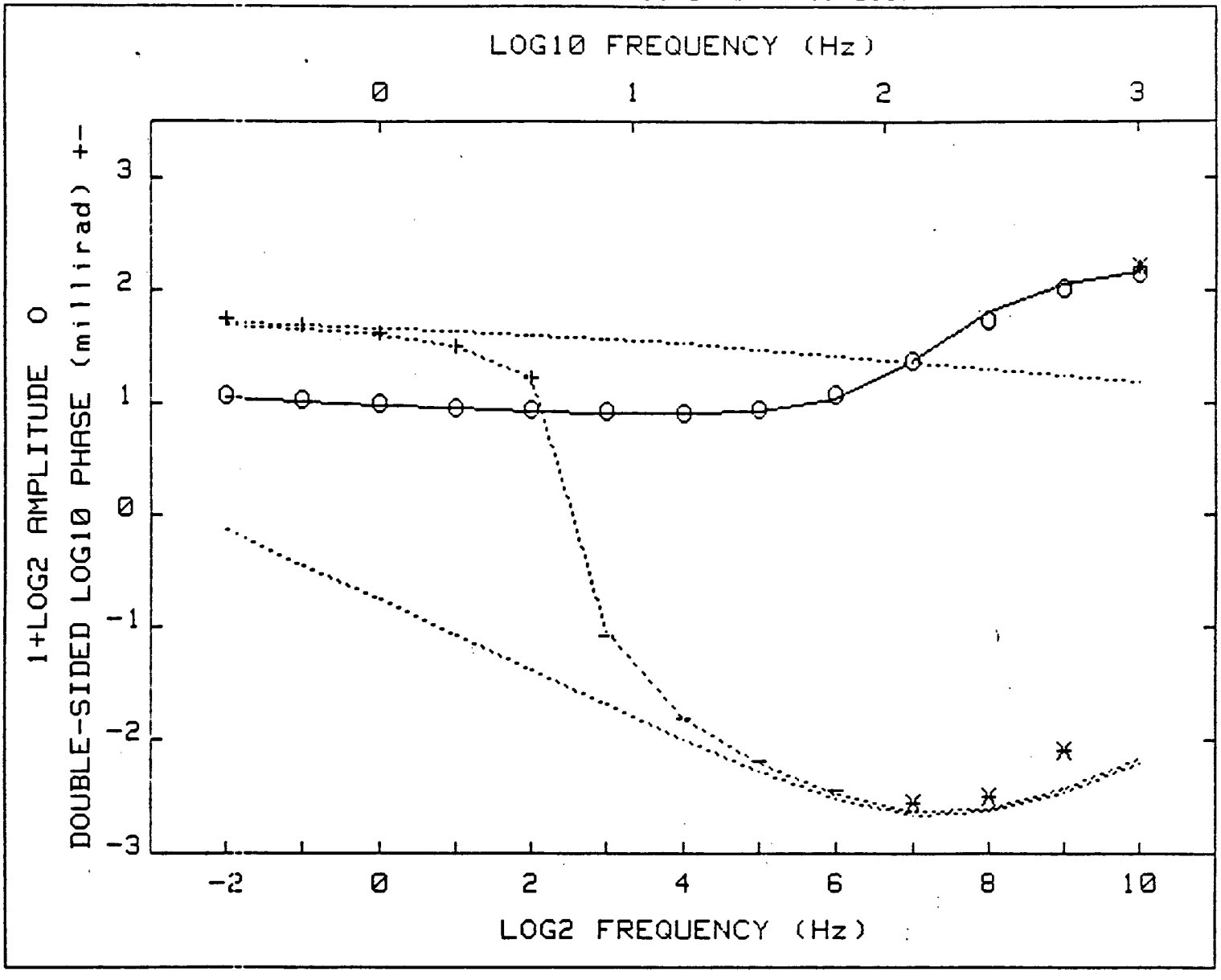
Pct Std Deviations	4.0	4.5	75.3	5.6

Correlation Matrix

1.000			
.990	1.000		
.987	.977	1.000	
-.942	-.917	-.970	1.000

Apparent Resistivity Measured at 1 Hz is 83.92
Apparent Resistivity Calculated from Inductive Coupling is 135.1

CYPRUS ANVIL TRENAS CK. ROSS RIVER LINE505E 28/9/81 L337 D= 7 N=3 X=152m



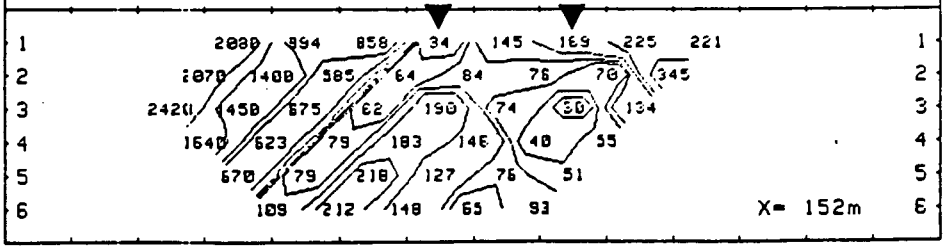
CRL: Number of dispersions= 2 Negative.
C1=.25 M2=1 C2=1 fixed

Iter	Lambda	Rchsq	R0	M1	T1	T2
0	1.E-02	.19193	1.322	.382	1.1E+00	5.1E-04
1	1.E-02	.01035	1.319	.346	4.8E+00	6.8E-04
2	1.E-03	.00126	1.425	.417	9.9E+00	6.1E-04
3	1.E-04	.00101	1.428	.415	7.7E+00	6.2E-04
4	1.E-02	.00101	1.428	.415	7.8E+00	6.3E-04

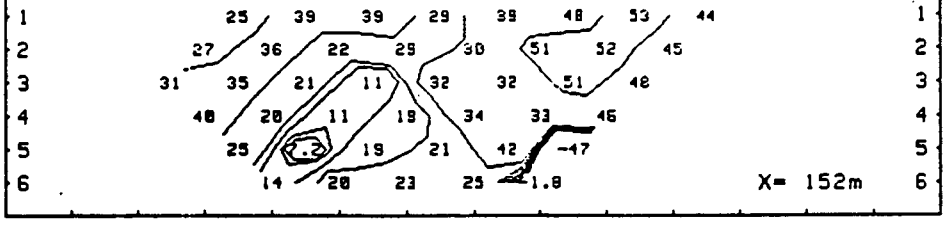
Pct Std Deviations	2.7	3.4	62.7	4.7	
Correlation Matrix	1.000				
	.930	1.000			
	.947	.865	1.000		
	-.855	-.705	-.934	1.000	

Apparent Resistivity Measured at 1 Hz is 56.88
Apparent Resistivity Calculated from Inductive Coupling is 136.3

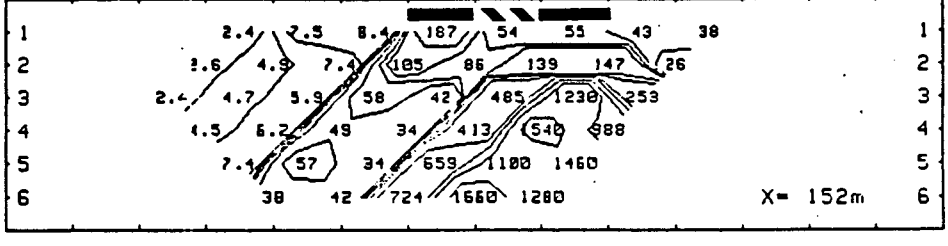
PHOENIX SPECTRAL IP OBS. RESISTIVITY (ohm-m) 1 Hz
CYPRUS ANVIL TENAS CK. ROSS RIVER LINE475E 29/9/81 L338



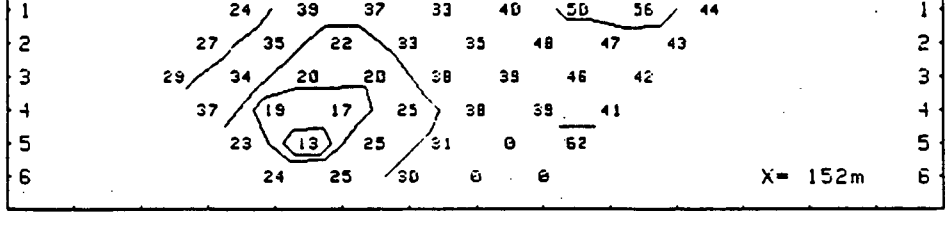
PHOENIX SPECTRAL IP PHASE (mrad) at 1 Hz
CYPRUS ANVIL TENAS CK. ROSS RIVER LINE475E 29/9/81 L338



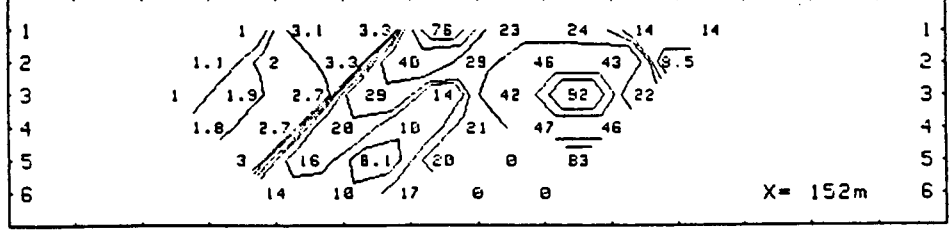
PHOENIX SPECTRAL IP METAL FACTOR 1Hz
CYPRUS ANVIL TENAS CK. ROSS RIVER LINE475E 29/9/81 L338



PHOENIX SPECTRAL IP DECOUPLED PHASE (mrad) 1 Hz
CYPRUS ANVIL TENAS CK. ROSS RIVER LINE475E 29/9/81 L338

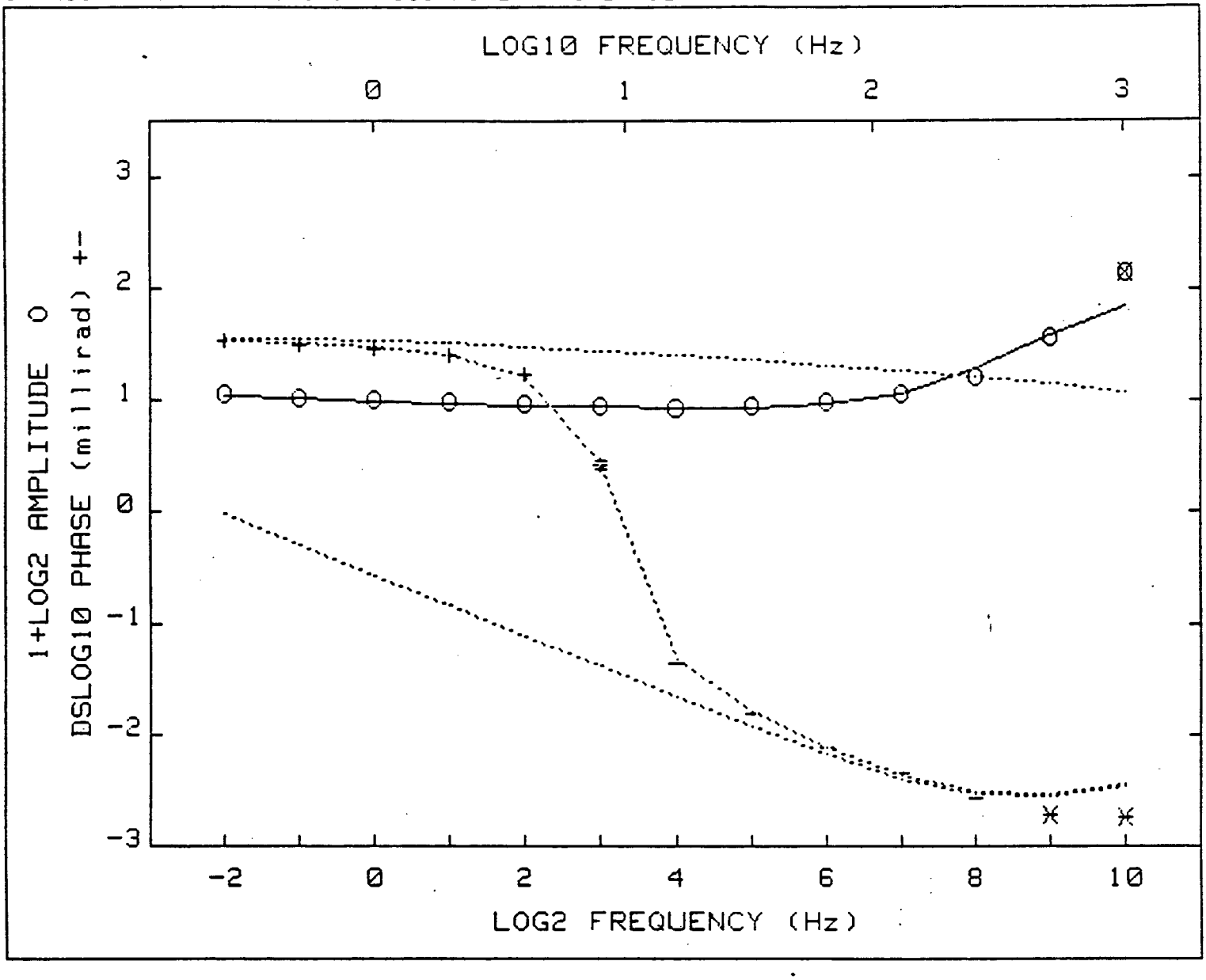


PHOENIX SPECTRAL IP DECOUPLED METAL FACTOR 1Hz
CYPRUS ANVIL TENAS CK. ROSS RIVER LINE475E 29/9/81 L338



DWG. NO. - S.I.P. - 1109-2

CYPRUS ANVIL TENAS CK. ROSS RIVER LINE475E 29/9/81 L338 D= 4 N=1 X=152m



CRL: Number of dispersions= 2 Negative.
C1=.25 M2=1 fixed

Iter	Lambda	Rchsq	R0	M1	T1	T2	C2
0	1.E-02	.00087	1.260	.305	3.8E+00	2.5E-04	.911
1	1.E-01	.00085	1.260	.307	3.8E+00	2.4E-04	.906
2	1.E-02	.00082	1.260	.307	3.7E+00	2.4E-04	.903
3	1.E-03	.00081	1.252	.304	3.1E+00	2.4E-04	.901
4	1.E-04	.00081	1.242	.300	2.4E+00	2.4E-04	.897
Pct Std Deviations			3.7	5.9	183.9	6.3	1.7

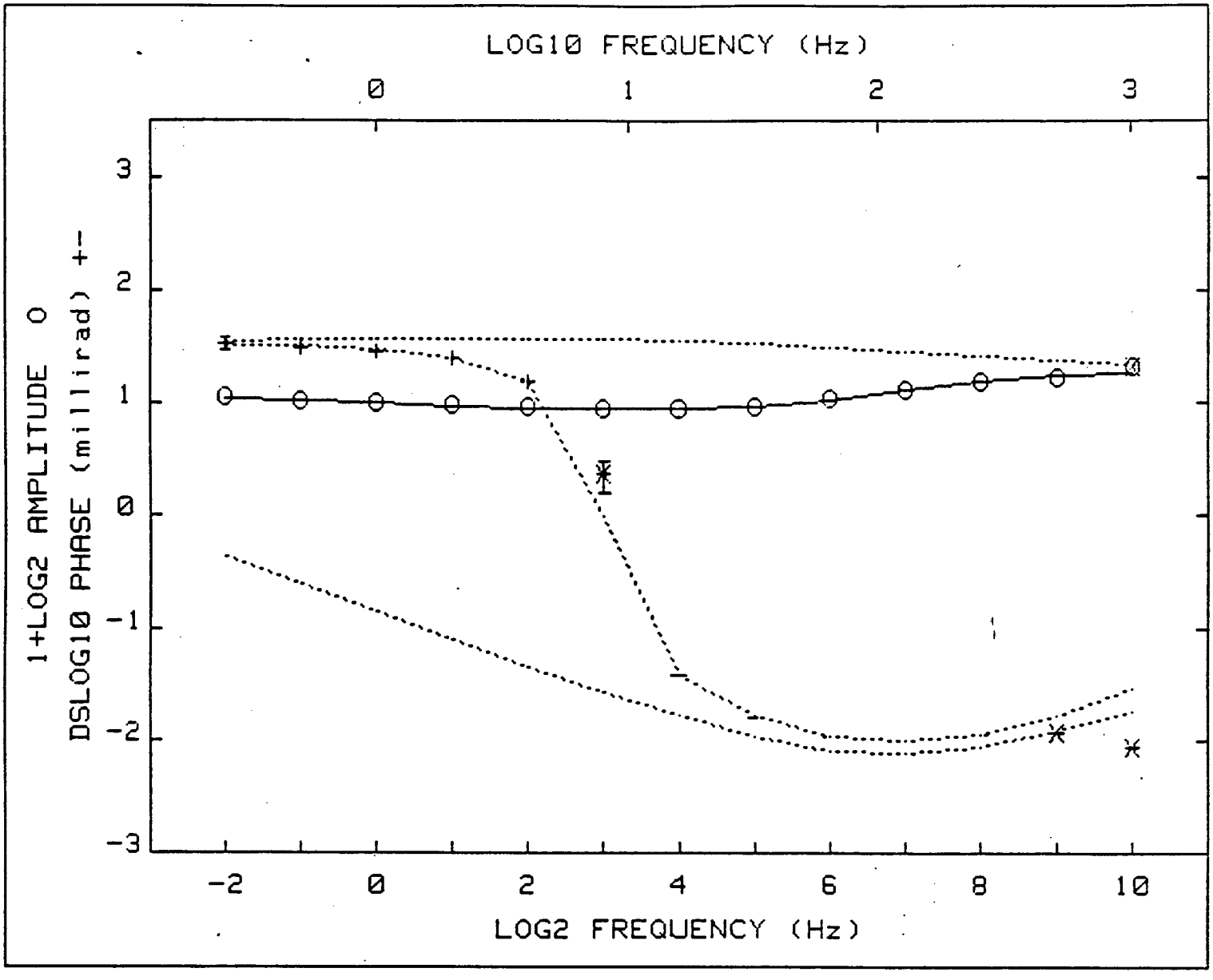
Correlation Matrix

1.000					
.957	1.000				
.969	.909	1.000			
-.827	-.807	-.785	1.000		
.615	.463	.749	-.240	1.000	

Apparent Resistivity Measured at 1 Hz is 34.16

Apparent Resistivity Calculated from Inductive Coupling is 50.30

CYPRUS ANVIL TENAS CK. ROSS RIVER LINE475E 29/9/81 L338 D= 4 N=2 X=152m



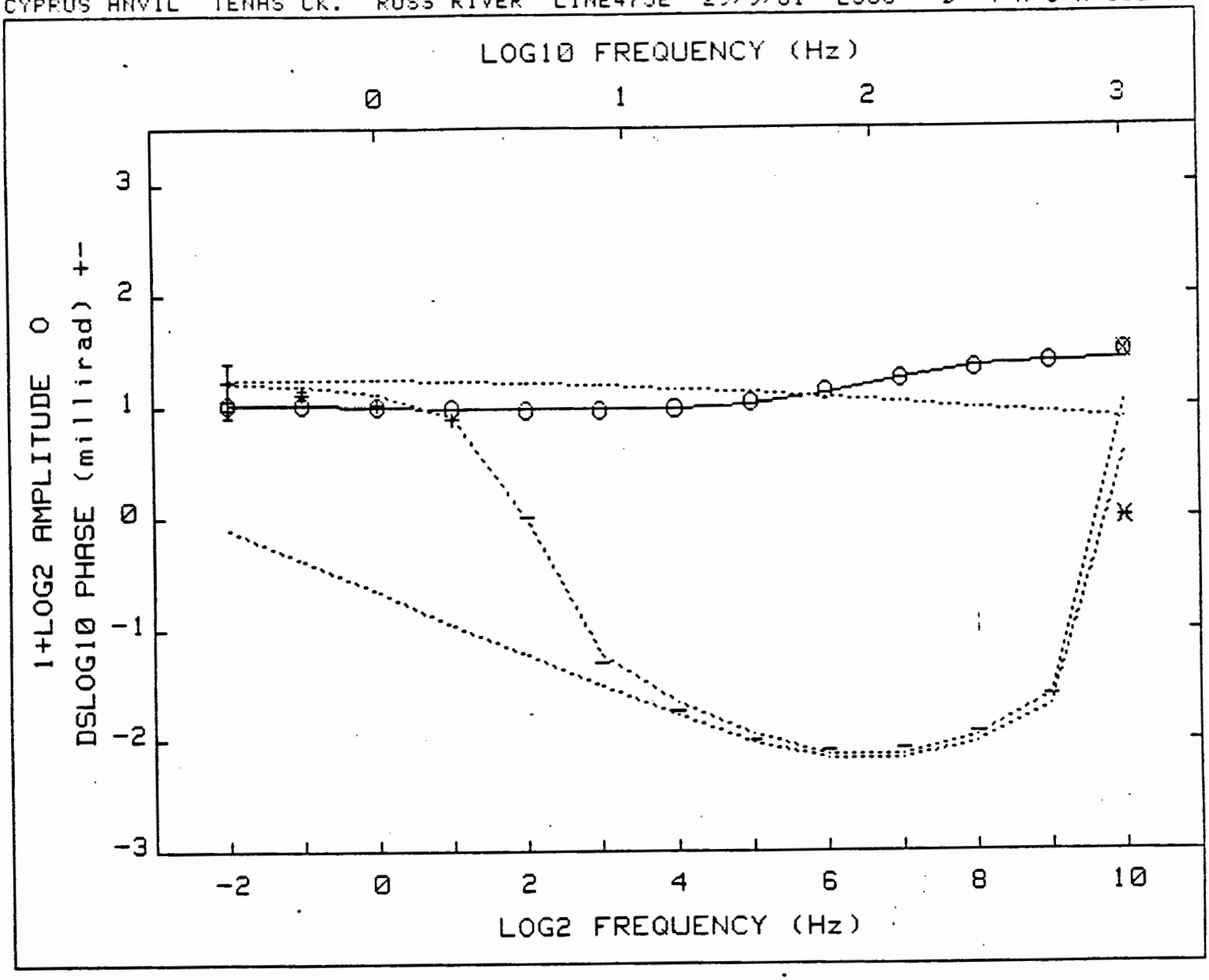
CRL: Number of dispersions= 2 Negative.
C1=.25 fixed

Iter	Lambda	Rchsq	R0	M1	T1	M2	T2	C2
0	1.E-02	.00064	1.320	.332	1.0E+01	.232	1.3E-03	.899
1	1.E-02	.00061	1.313	.330	8.7E+00	.235	1.3E-03	.895
2	1.E-03	.00043	1.256	.309	3.0E+00	.254	1.3E-03	.876
3	1.E-03	.00030	1.229	.302	1.4E+00	.268	1.3E-03	.859
4	1.E-03	.00024	1.212	.302	7.5E-01	.280	1.3E-03	.844
5	1.E-03	.00021	1.202	.303	4.9E-01	.290	1.3E-03	.833
6	1.E-04	.00019	1.181	.308	2.1E-01	.311	1.2E-03	.810
7	1.E-05	.00018	1.178	.314	1.6E-01	.318	1.2E-03	.803
8	1.E+00	.00018	1.178	.314	1.6E-01	.318	1.2E-03	.803

Pct Std Deviations	1.2	4.2	108.0	7.0	4.6	3.2	
Correlation Matrix	1.000						
	-.747	1.000					
	.935	-.910	1.000				
	-.826	.949	-.940	1.000			
	.326	-.554	.435	-.672	1.000		
	.664	-.941	.930	-.936	.738	1.000	

DWG. NO. - S.I.P. - 1109 - 4

CYPRUS ANVIL TENAS CK. ROSS RIVER LINE475E 29/9/81 L338 D= 4 N=3 X=152m



CRL: Number of dispersions= 3 Negative.
C1=.25 M2=1 C2=1 fixed

Iter	Lambda	Rchsq	R0	M1	T1	T2	M3	T3	C3
0	1.E-02	.00170	1.106	.164	5.4E-01	8.2E-06	.366	1.4E-03	.932
1	1.E+03	.00170	1.106	.164	5.4E-01	8.2E-06	.366	1.4E-03	.932
Pct Std Deviations			1.6	5.3	244.4	87.3	11.1	13.4	5.6

Correlation Matrix

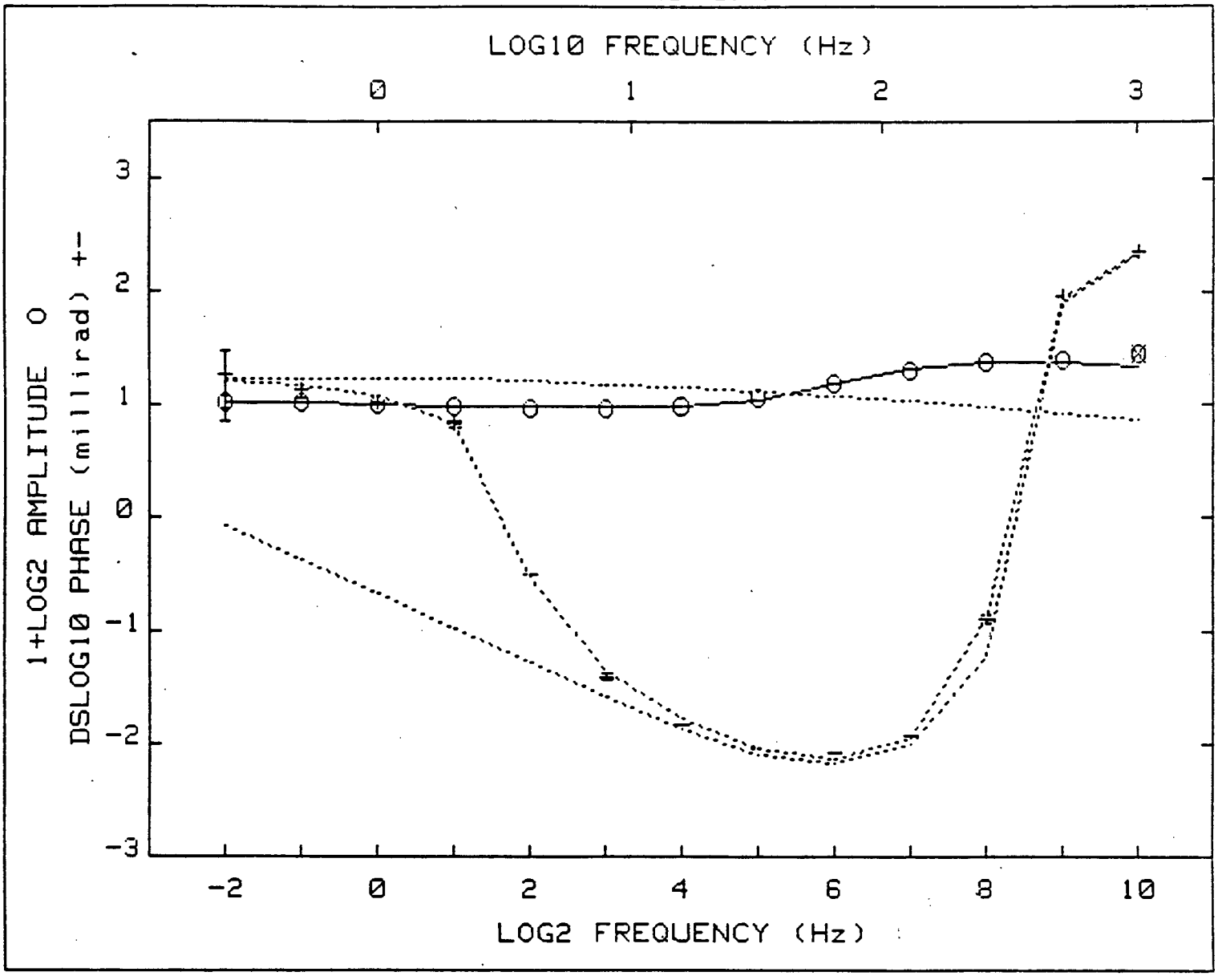
1.000							
.063	1.000						
.793	-.282	1.000					
-.500	.461	-.686	1.000				
-.616	.456	-.796	.939	1.000			
.498	-.441	.701	-.949	-.930	1.000		
.607	-.618	.915	-.801	-.857	.820	1.000	

Apparent Resistivity Measured at 1 Hz is 61.53

Apparent Resistivity Calculated from Inductive Coupling is 134.9

DWG. NO. - S.I.P - 1109-5

CYPRUS ANVIL TENAS CK. ROSS RIVER LINE475E 29/9/81 L338 D= 4 N=4 X=152m



CRL: Number of dispersions= 3 Negative.
C1=.25 M2=1 C2=1 C3=1 fixed

Iter	Lambda	Rchsq	R0	M1	T1	T2	M3	T3
0	1.E-02	.00124	1.107	.159	4.6E-01	4.6E-05	.345	2.2E-03
1	1.E-02	.00118	1.100	.158	4.6E-01	4.6E-05	.343	2.2E-03
2	1.E-03	.00118	1.100	.158	4.7E-01	4.6E-05	.343	2.2E-03

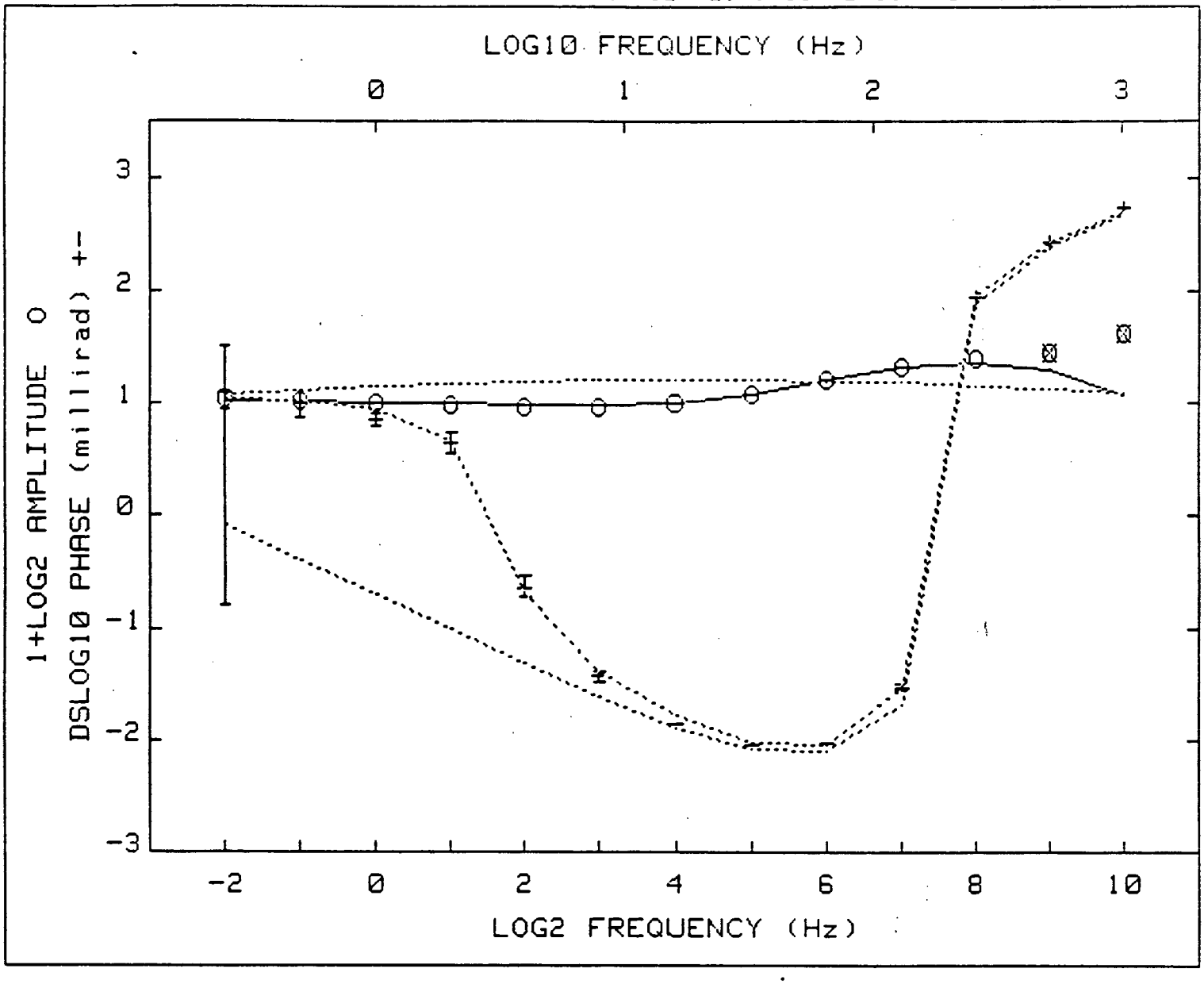
Pct Std Deviations	1.7	3.3	207.7	5.9	4.3	3.4	
Correlation Matrix	1.000						
	.575	1.000					
	.899	.524	1.000				
	-.104	-.149	-.024	1.000			
	-.729	-.290	-.781	.577	1.000		
	-.440	.039	-.584	-.704	.134	1.000	

Apparent Resistivity Measured at 1 Hz is 79.48

Apparent Resistivity Calculated from Inductive Coupling is 188.8

DWG. NO. - S.I.P - 1109 - 6

CYPRUS ANVIL TENAS CK. ROSS RIVER LINE475E 29/9/81 L338 D= 4 N=5 X=152m



CRL: Number of dispersions= 3 Negative.
C1=.25 M2=1 C2=1 C3=1 fixed

Iter	Lambda	Rchsq	R0	M1	T1	T2	M3	T3
0	1.E-02	.00183	1.069	.130	1.0E-01	1.2E-04	.354	2.3E-03
1	1.E-02	.00181	1.068	.130	8.6E-02	1.2E-04	.355	2.3E-03
2	1.E-03	.00172	1.062	.134	3.8E-02	1.2E-04	.360	2.4E-03
3	1.E-04	.00167	1.056	.144	1.4E-02	1.2E-04	.367	2.4E-03
4	1.E-05	.00161	1.056	.148	1.2E-02	1.2E-04	.368	2.4E-03
5	1.E-06	.00160	1.056	.149	1.1E-02	1.2E-04	.369	2.4E-03

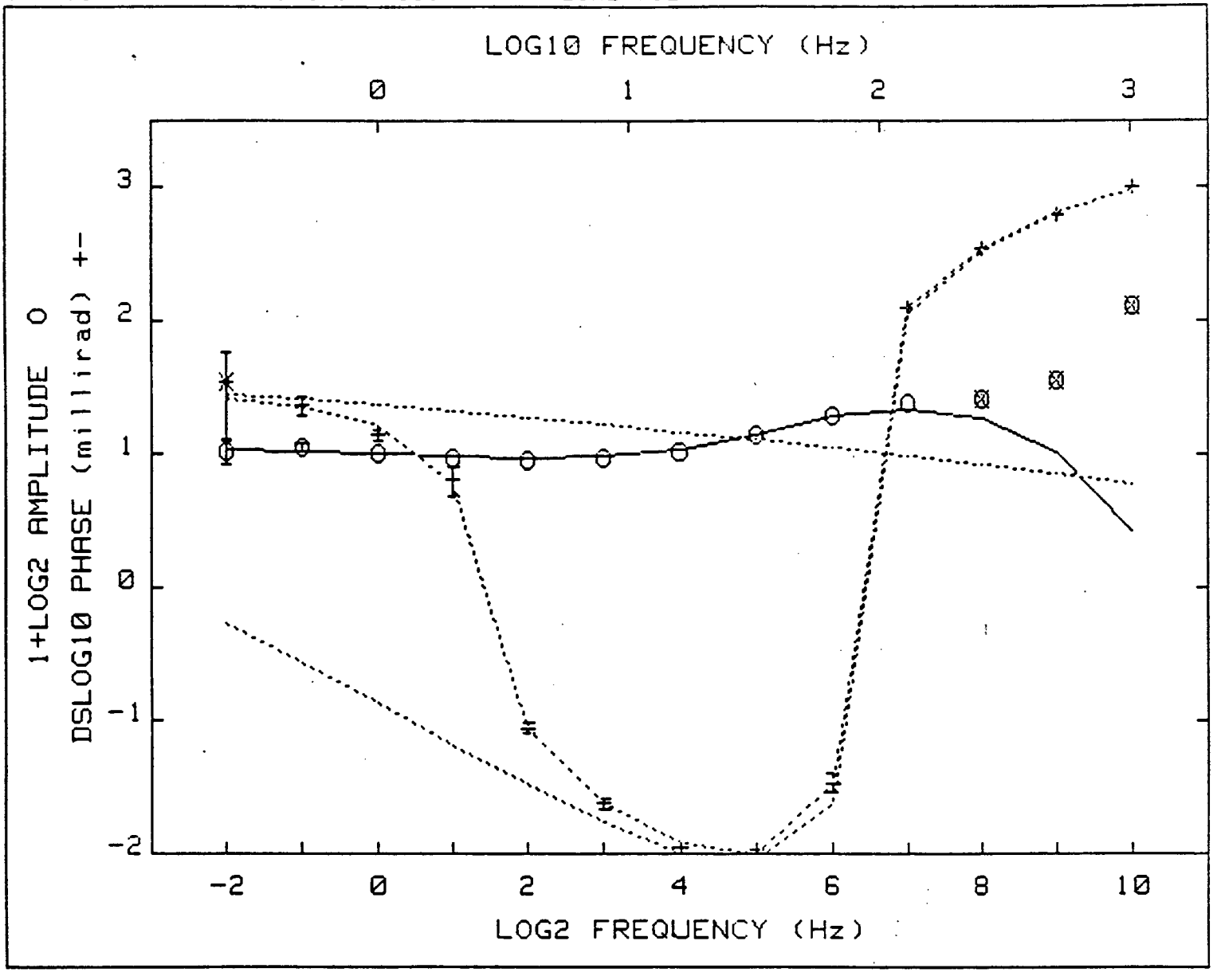
Pct Std Deviations	1.1	16.8	402.1	7.5	4.8	4.3	
Correlation Matrix	1.000						
	-.612	1.000					
	.646	-.978	1.000				
	.034	-.218	.195	1.000			
	-.456	.605	-.597	.575	1.000		
	-.276	.624	-.553	-.745	-.148	1.000	

Apparent Resistivity Measured at 1 Hz is 78.65

Apparent Resistivity Calculated from Inductive Coupling is 222.8

DWG. NO. - S.I.P - 1109-7

CYPRUS ANVIL TENAS CK. ROSS RIVER LINE475E 29/9/81 L338 D= 4 N=6 X=152m



CRL: Number of dispersions= 3 Negative.
C1=.25 M2=1 C2=1 C3=1 fixed

Iter	Lambda	Rchsq	R0	M1	T1	T2	M3	T3
0	1.E-02	.00118	1.621	.422	9.0E+02	2.0E-04	.241	3.9E-03
1	1.E-02	.00101	1.572	.405	7.8E+02	2.1E-04	.245	3.9E-03
2	1.E-03	.00087	1.439	.357	2.6E+02	2.3E-04	.271	3.9E-03
3	1.E-04	.00083	1.311	.299	5.9E+01	2.6E-04	.306	3.8E-03
4	1.E-05	.00065	1.318	.296	5.1E+01	2.6E-04	.307	3.8E-03
5	1.E-06	.00065	1.318	.296	5.1E+01	2.6E-04	.308	3.8E-03

Pct Std Deviations	4.3	9.7	134.3	7.5	6.1	2.6

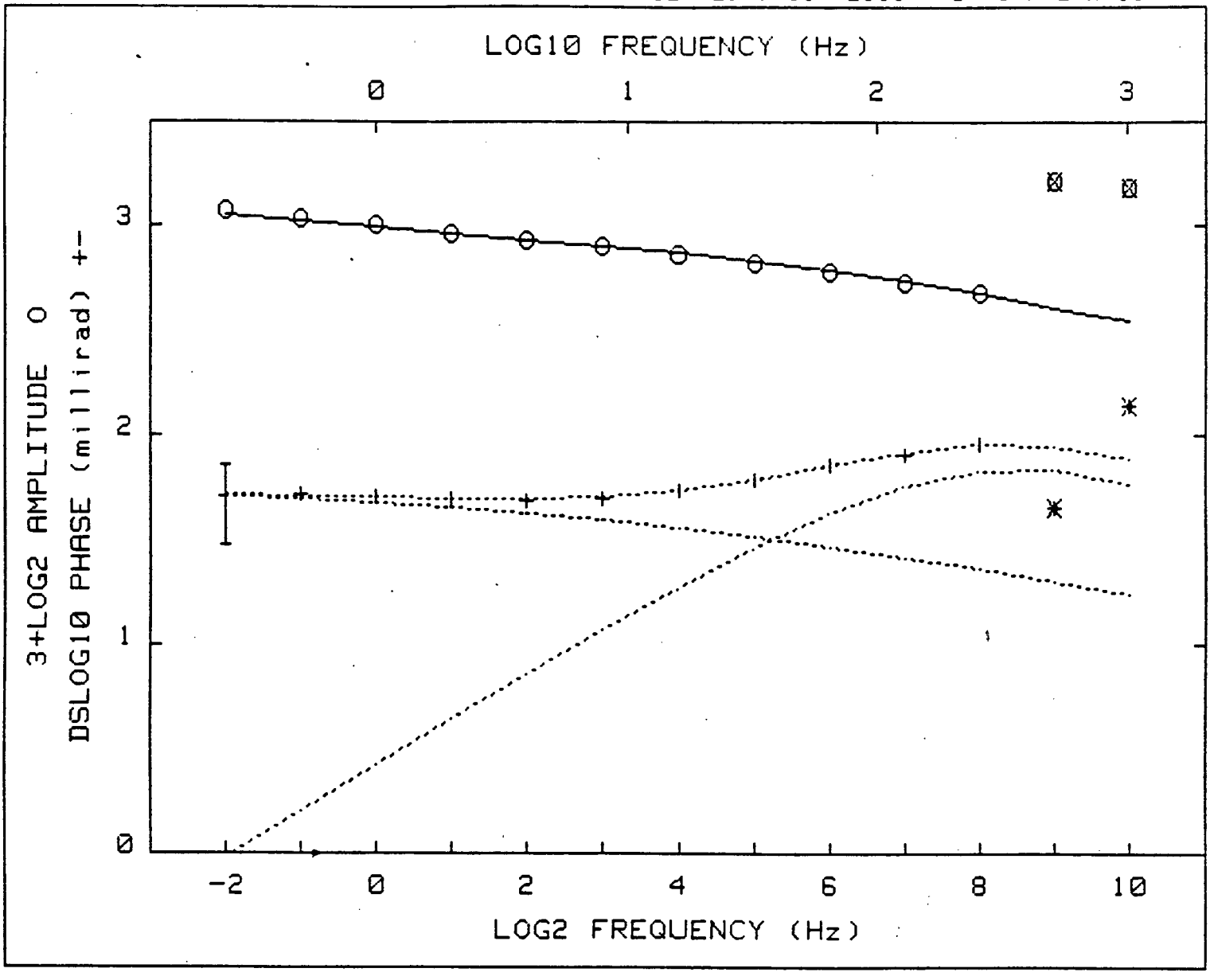
Correlation Matrix

1.000						
.988	1.000					
.983	.980	1.000				
-.750	-.752	-.727	1.000			
-.867	-.862	-.862	.959	1.000		
-.066	-.035	-.143	-.468	-.286	1.000	

Apparent Resistivity Measured at 1 Hz is 108.8

Apparent Resistivity Calculated from Inductive Coupling is 232.6

CYPRUS ANVIL TENAS CK. ROSS RIVER LINE475E 29/9/81 L338 D= 6 N=2 X=152m



CRL: Number of dispersions= 2
C1=.25 fixed

Iter	Lambda	Rchsq	R0	M1	T1	M2	T2	C2
0	1.E-02	.00010	1.379	.405	3.4E+00	.123	5.3E-04	.711
1	1.E+03	.00010	1.379	.405	3.4E+00	.123	5.3E-04	.711

Pct Std Deviations	3.2	2.1	125.1	21.3	32.9	12.7

Correlation Matrix

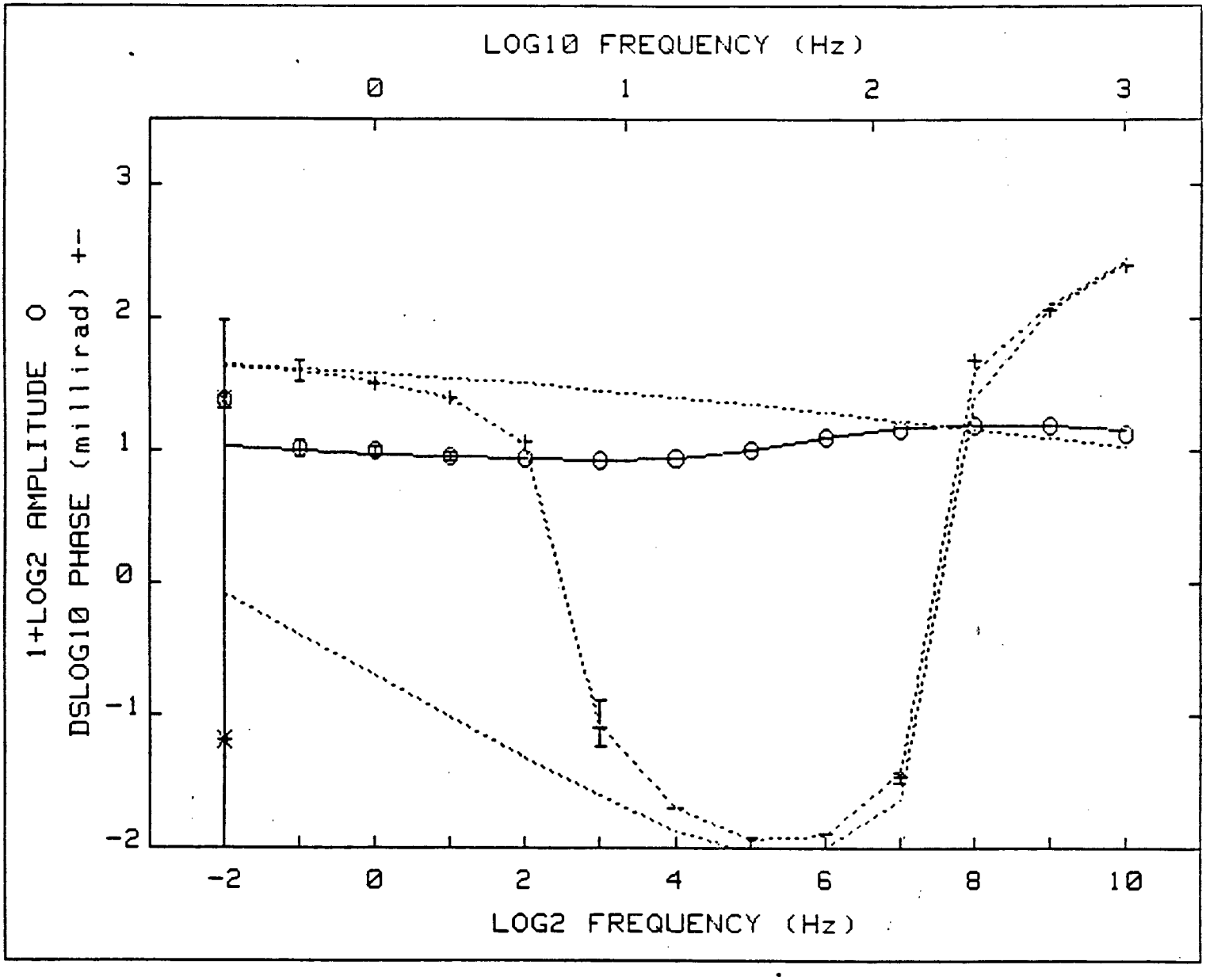
1.000						
.832	1.000					
.984	.742	1.000				
.717	.287	.787	1.000			
-.535	-.150	-.598	-.946	1.000		
-.770	-.344	-.833	-.983	.901	1.000	

Apparent Resistivity Measured at 1 Hz is 75.78

Apparent Resistivity Calculated from Inductive Coupling is 206.9

DWG. NO. - S.I.P - 1109 -9

CYPRUS ANVIL TENAS CK. ROSS RIVER LINE475E 29/9/81 L338 D= 6 N=3 X=152m



CRL: Number of dispersions= 3 Negative.
C1=.25 M2=1 C2=1 C3=1 fixed

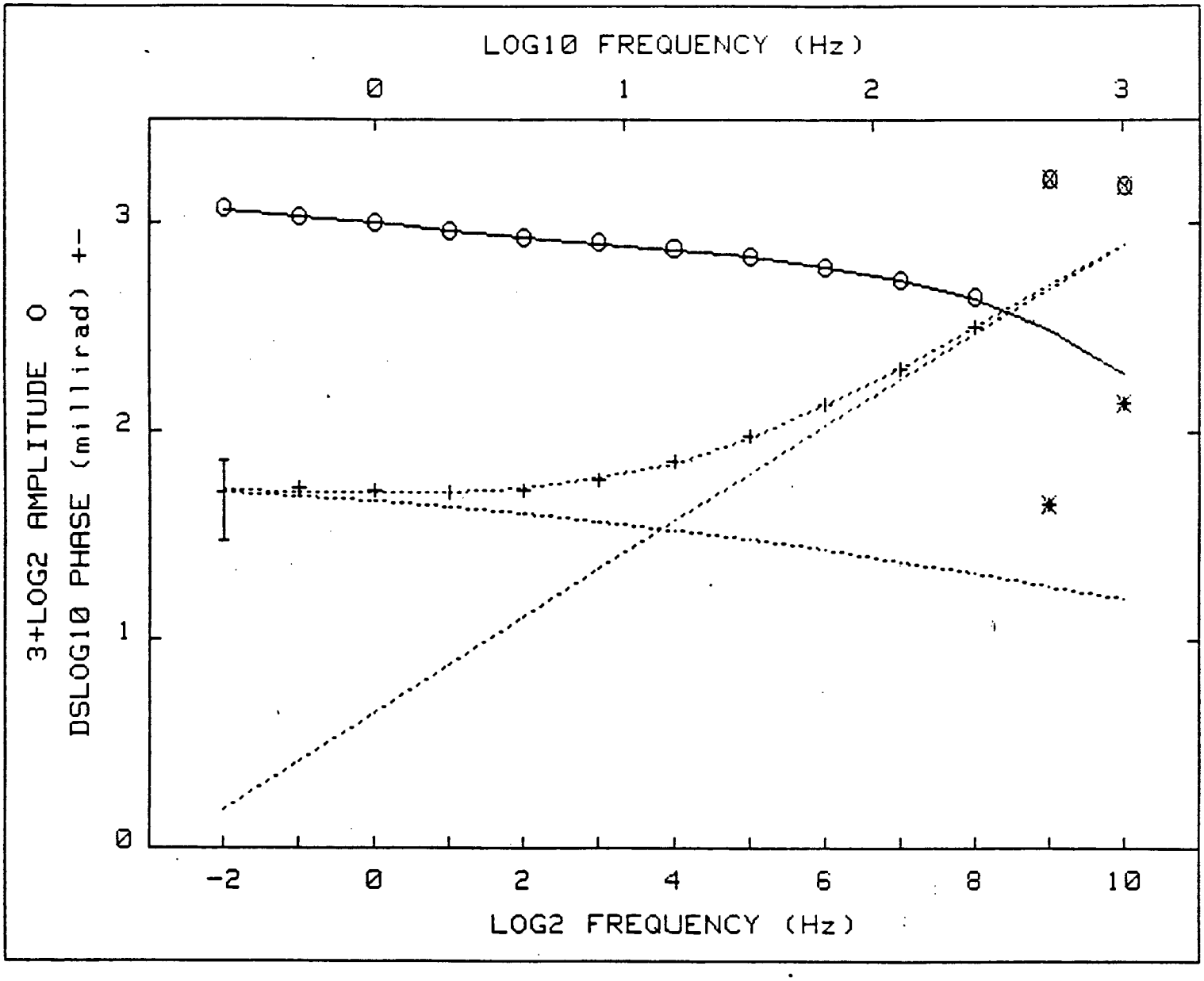
Iter	Lambda	Rchsq	R0	M1	T1	T2	M3	T3
0	1.E-02	.00086	1.476	.413	3.9E+01	3.4E-05	.174	3.3E-03
1	1.E-02	.00085	1.470	.411	3.8E+01	3.4E-05	.174	3.3E-03

Pct Std Deviations	13.5	18.0	525.4	13.1	16.1	2.7	
Correlation Matrix	1.000						
	.998	1.000					
	.996	.994	1.000				
	-.948	-.948	-.941	1.000			
	-.989	-.986	-.992	.963	1.000		
	-.460	-.444	-.496	.263	.428	1.000	

Apparent Resistivity Measured at 1 Hz is 73.62

Apparent Resistivity Calculated from Inductive Coupling is 150.2

CYPRUS ANVIL TENAS CK. ROSS RIVER LINE475E 29/9/81 L338 D= 7 N=2 X=152m



CRL: Number of dispersions= 2
C1=.25 M2=1 fixed

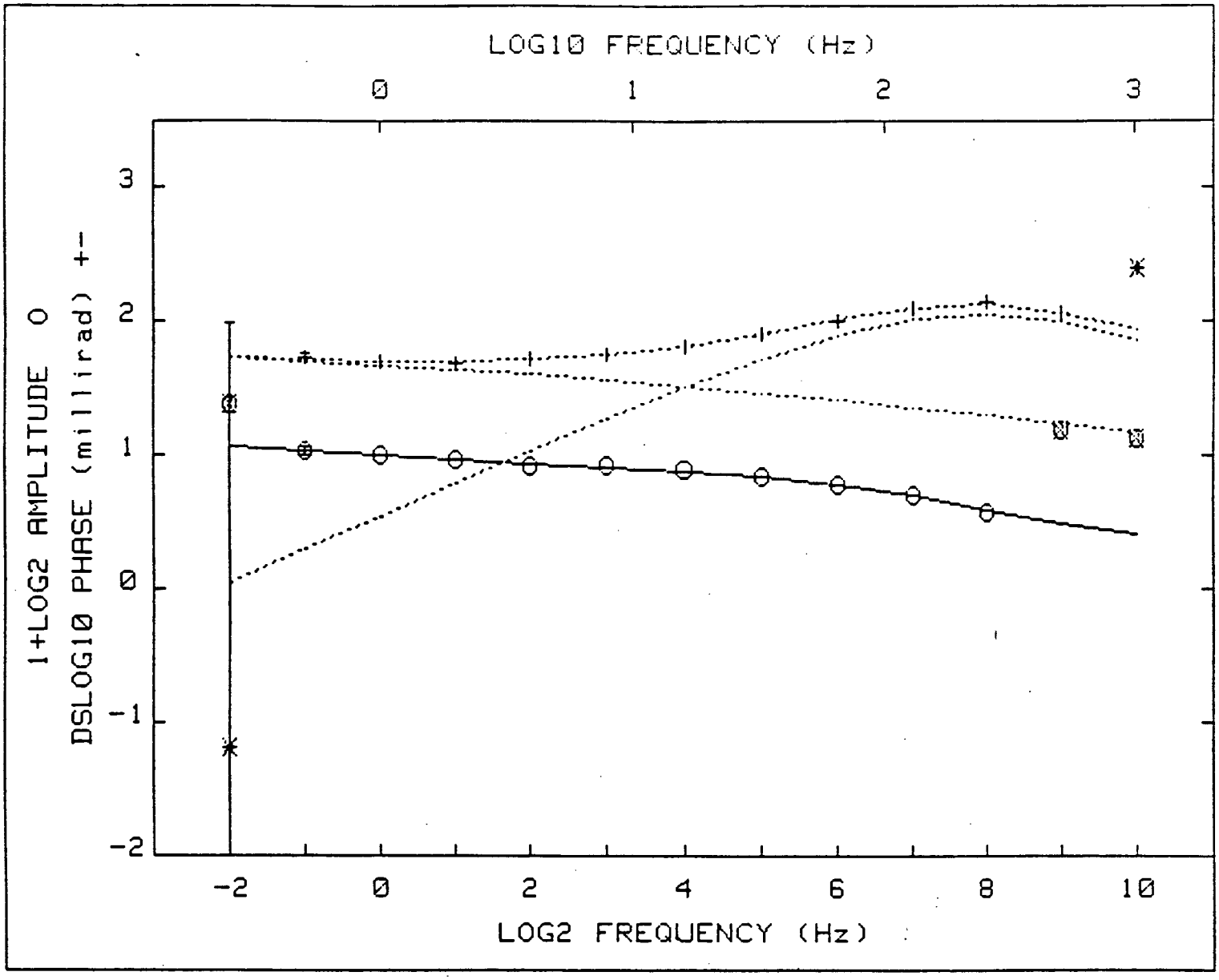
Iter	Lambda	Rchsq	R0	M1	T1	T2	C2
0	1.E-02	.00011	1.543	.445	2.8E+01	6.5E-05	.715
1	1.E-02	.00011	1.540	.443	2.8E+01	6.4E-05	.709
2	1.E-03	.00010	1.520	.437	2.2E+01	6.6E-05	.713
3	1.E-04	.00009	1.440	.414	9.1E+00	7.4E-05	.733
4	1.E-05	.00008	1.415	.408	6.0E+00	7.7E-05	.745
5	1.E-06	.00007	1.417	.408	6.0E+00	7.7E-05	.745

Pct Std Deviations	2.6	2.5	71.0	7.0	2.4	
Correlation Matrix	1.000					
	.964	1.000				
	.985	.917	1.000			
	-.790	-.679	-.824	1.000		
	-.708	-.539	-.774	.945	1.000	

Apparent Resistivity Measured at 1 Hz is 70.25

Apparent Resistivity Calculated from Inductive Coupling is 213.1

CYPRUS ANVIL TENAS CK. ROSS RIVER LINE475E 29/9/81 L338 D= 7 N=3 X=152m



CRL: Number of dispersions= 2
C1=.25 fixed

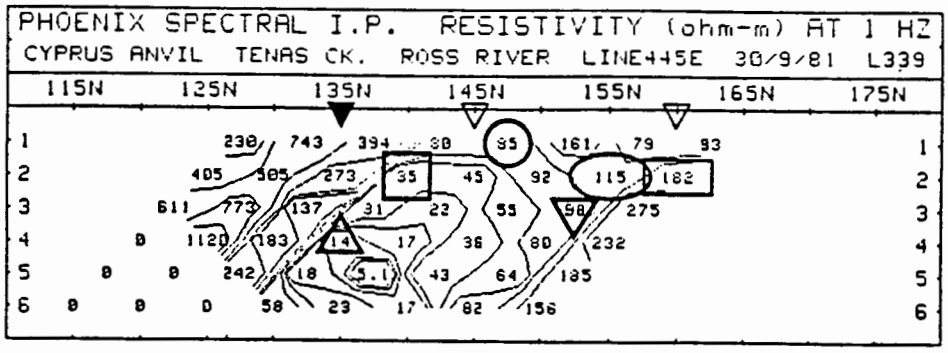
Iter	Lambda	Rchsq	R0	M1	T1	M2	T2	C2
0	1.E-02	.00043	1.679	.486	7.7E+01	.169	7.1E-04	.727
1	1.E-02	.00019	1.682	.487	7.7E+01	.155	8.4E-04	.749
2	1.E-03	.00017	1.682	.488	7.2E+01	.151	8.8E-04	.770
3	1.E-04	.00016	1.618	.471	4.4E+01	.154	8.7E-04	.777
4	1.E-04	.00016	1.576	.459	3.0E+01	.156	8.7E-04	.784
5	1.E-05	.00016	1.509	.440	1.6E+01	.159	8.7E-04	.795
6	1.E-06	.00016	1.499	.437	1.4E+01	.158	8.7E-04	.800
Pct Std Deviations			9.3	9.5	322.7	4.7	5.2	4.8

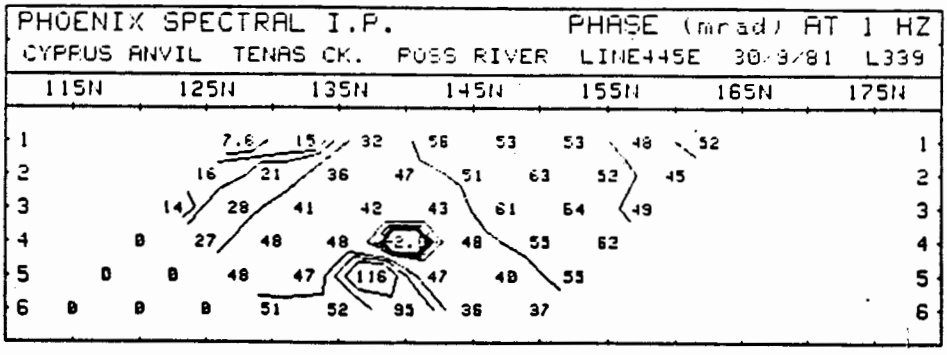
Correlation Matrix

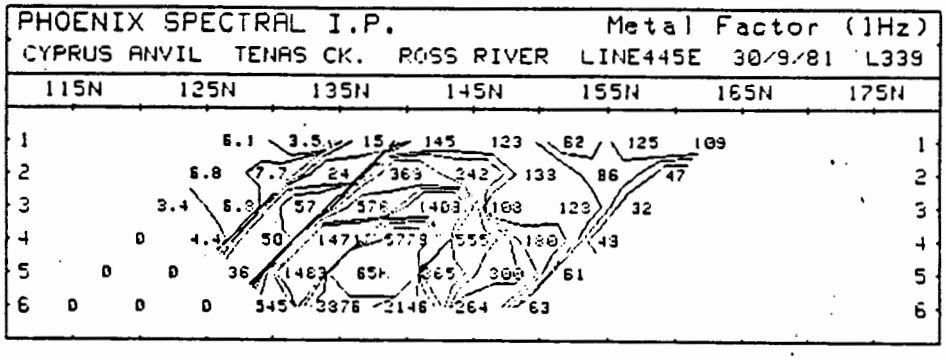
1.000						
.995	1.000					
.995	.984	1.000				
-.556	-.618	-.499	1.000			
.107	.120	.094	-.509	1.000		
-.713	-.658	-.751	-.123	.315	1.000	

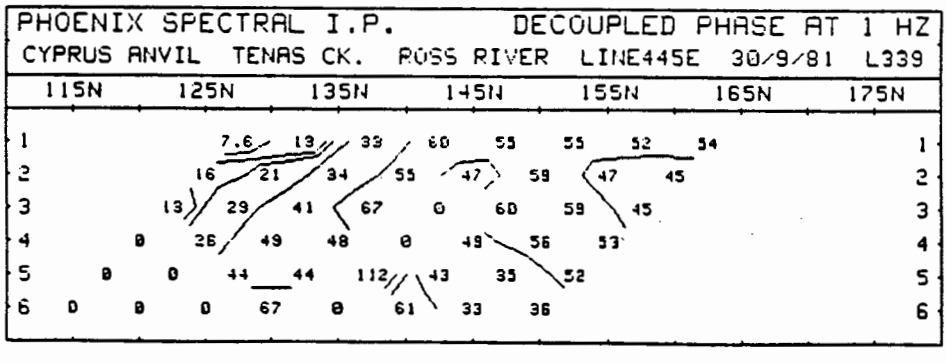
Apparent Resistivity Measured at 1 Hz is 29.75

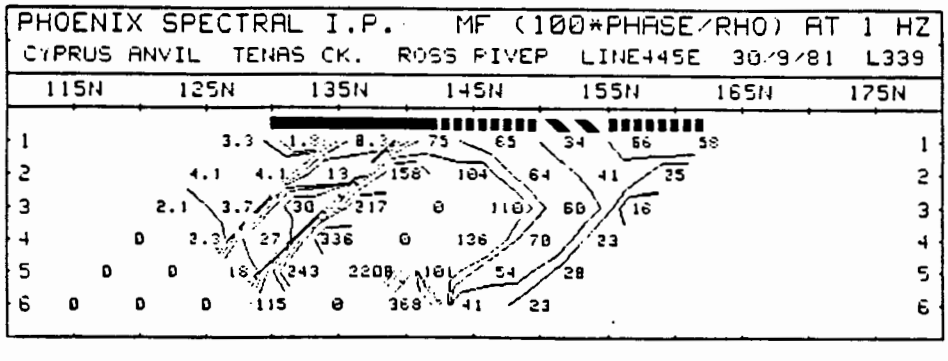
Apparent Resistivity Calculated from Inductive Coupling is 28.5


PHOENIX SPECTRAL I.P. RESISTIVITY (ohm-m) AT 1 HZ
CYPRUS ANVIL TENAS CK. ROSS RIVER LINE445E 30/9/81 L339
115N 125N 135N 145N 155N 165N 175N


PHOENIX SPECTRAL I.P. PHASE (mrad) AT 1 HZ
CYPRUS ANVIL TENAS CK. ROSS RIVER LINE445E 30/9/81 L339
115N 125N 135N 145N 155N 165N 175N

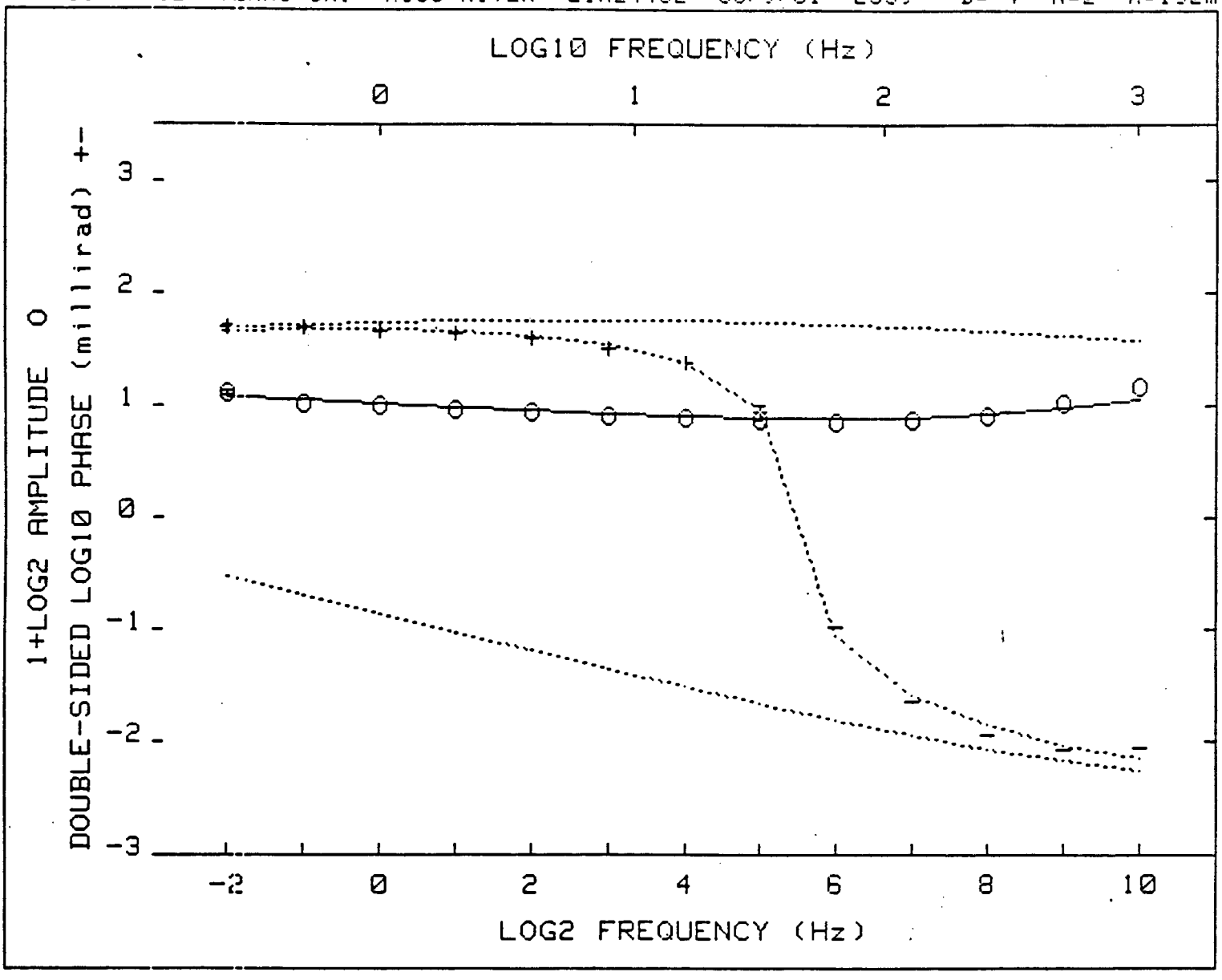

PHOENIX SPECTRAL I.P. Metal Factor (1Hz)
CYPRUS ANVIL TENAS CK. ROSS RIVER LINE445E 30/9/81 L339
115N 125N 135N 145N 155N 165N 175N


PHOENIX SPECTRAL I.P. DECOUPLED PHASE AT 1 HZ
CYPRUS ANVIL TENAS CK. ROSS RIVER LINE445E 30/9/81 L339
115N 125N 135N 145N 155N 165N 175N


PHOENIX SPECTRAL I.P. MF (100*PHASE/RHO) AT 1 HZ
CYPRUS ANVIL TENAS CK. ROSS RIVER LINE445E 30/9/81 L339
115N 125N 135N 145N 155N 165N 175N

DWG. NO. – S.I.P. – 1110 – 2

CYPRUS ANVIL TENAS CK. ROSS RIVER LINE445E 30/9/81 L339 D= 4 N=2 X=152m



CRL: Number of dispersions= 2 Negative.
C1=.25 M2=1 fixed

Iter	Lambda	Rchsq	R0	M1	T1	T2	C2
0	1.E-02	.58558	1.399	.458	1.0E+00	2.2E-04	.976
1	1.E-02	.02733	1.138	.278	2.0E-01	4.8E-05	.881
2	1.E-03	.00769	1.242	.416	9.3E-02	2.0E-05	.616
3	1.E-04	.00376	1.254	.447	6.1E-02	1.4E-05	.513
4	1.E-05	.00363	1.267	.436	9.9E-02	1.3E-05	.522
5	1.E-06	.00363	1.265	.441	9.0E-02	1.3E-05	.518
Pct Std Deviations			4.2	12.7	453.2	27.6	12.7

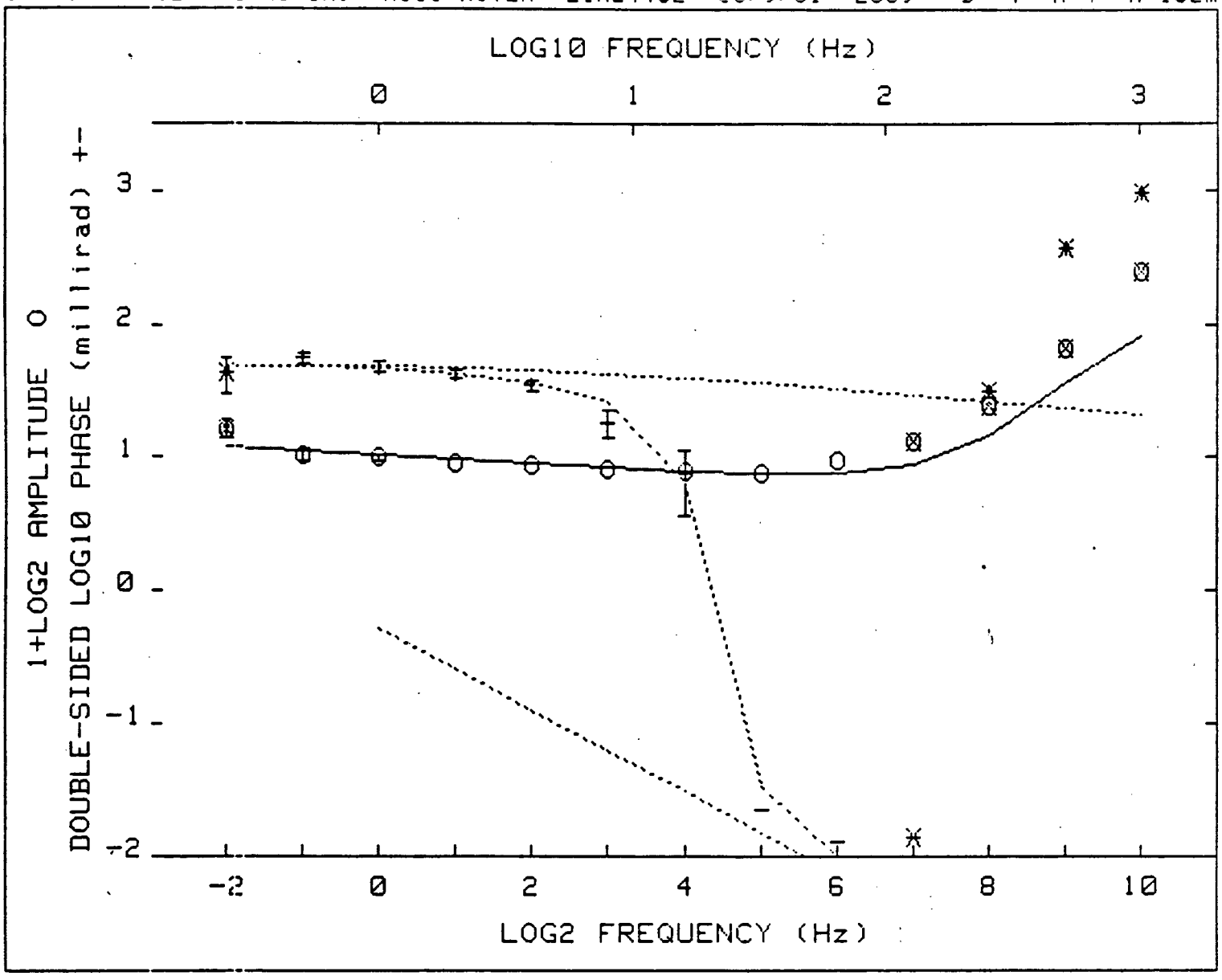
Correlation Matrix

1.000					
-.615	1.000				
.893	-.877	1.000			
-.791	.500	-.763	1.000		
.602	-.958	.841	-.332	1.000	

Apparent Resistivity Measured at 1 Hz is 34.74
Apparent Resistivity Calculated from Inductive Coupling is 212.8

DWG. NO. - S.I.P. - 1110 - 3

CYPRUS ANVIL TENAS CK. ROSS RIVER LINE445E 30/9/81 L339 D= 4 N=4 X=152m



CRL: Number of dispersions= 2 Negative.
C1=.25 M2=1 C2=1 fixed

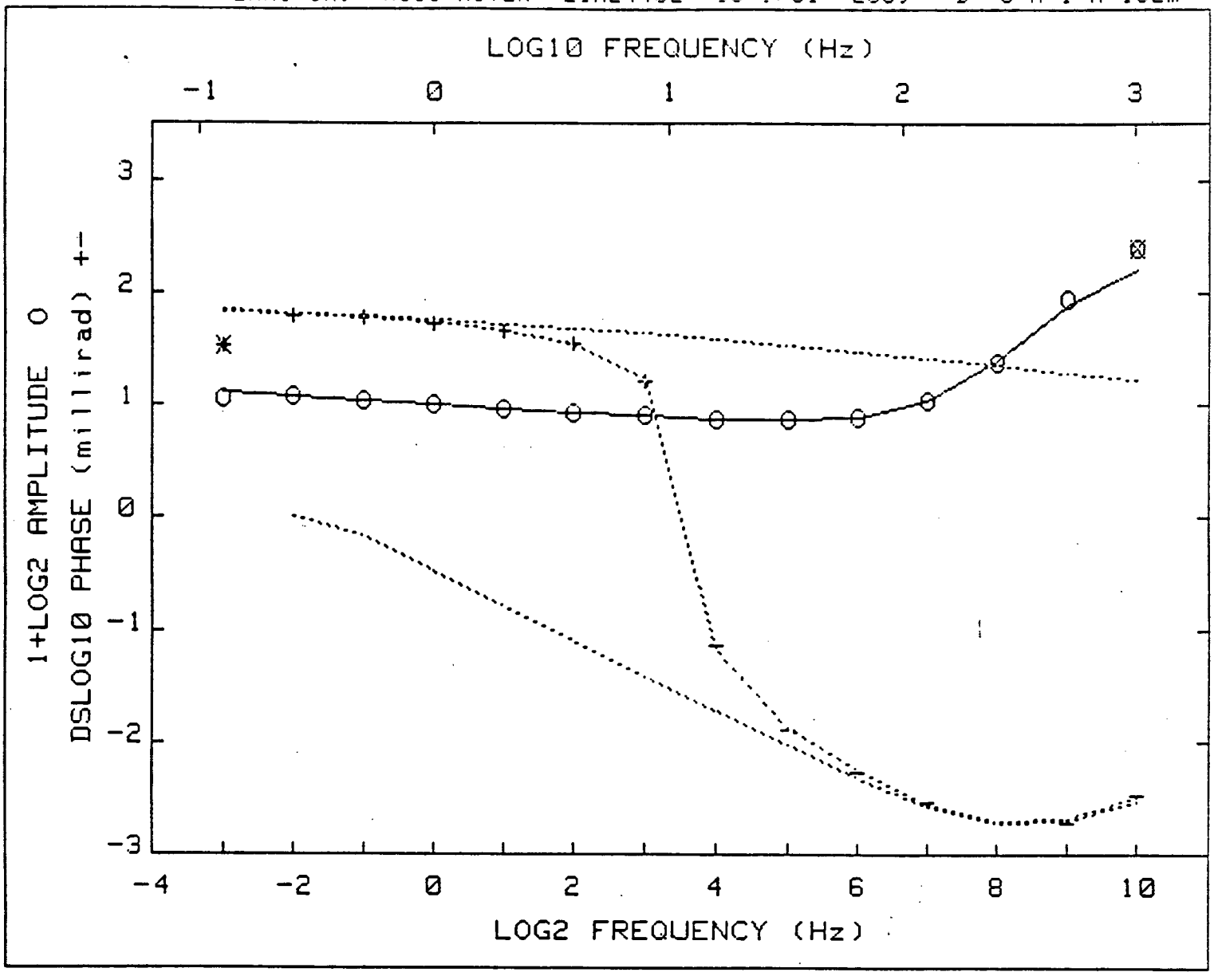
Iter	Lambda	Rchsq	R0	M1	T1	T2
0	1.E-02	.00739	1.323	.385	1.0E+00	2.3E-04
1	1.E-02	.00734	1.335	.391	1.1E+00	2.3E-04

Pct Std Deviations	10.8	12.2	790.7	23.3	
Correlation Matrix	1.000				
	.944	1.000			
	.962	.900	1.000		
	-.861	-.730	-.946	1.000	

Apparent Resistivity Measured at 1 Hz is 14.40
Apparent Resistivity Calculated from Inductive Coupling is 606.0

DWG. NO. - S.I.P - 1110 - 4

CYPRUS ANVIL TENAS CK. ROSS RIVER LINE445E 30/9/81 L339 D= 5 N=1 X=152m



CRL: Number of dispersions= 2 Negative.
C1=.25 M2=1 C2=1 fixed

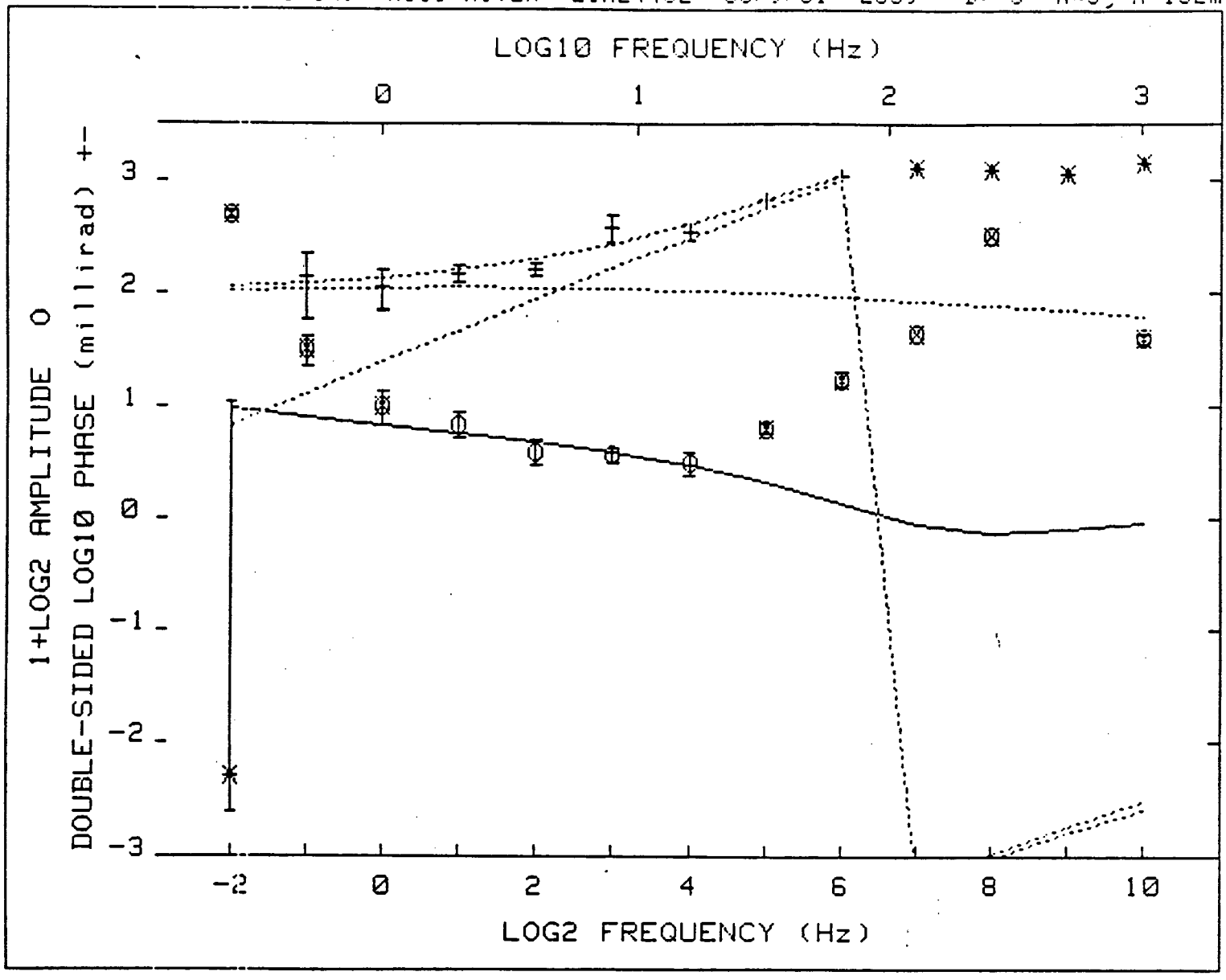
Iter	Lambda	Rchsq	R0	M1	T1	T2
0	1.E-02	.00159	1.547	.472	1.2E+01	3.3E-04
1	1.E-02	.00079	1.609	.495	1.7E+01	3.0E-04
2	1.E-03	.00060	1.696	.518	3.2E+01	2.9E-04
3	1.E-04	.00058	1.723	.524	3.7E+01	2.8E-04
4	1.E+00	.00058	1.723	.524	3.7E+01	2.8E-04

Pct Std Deviations	3.1	2.6	40.0	3.8	
Correlation Matrix	1.000				
	.975	1.000			
	.963	.927	1.000		
	-.902	-.841	-.942	1.000	

Apparent Resistivity Measured at 1 Hz is 85.09

Apparent Resistivity Calculated from Inductive Coupling is 61.43

CYPRUS ANVIL TENAS CK. ROSS RIVER LINE445E 30/9/81 L339 D= 5 N=5, X=152m



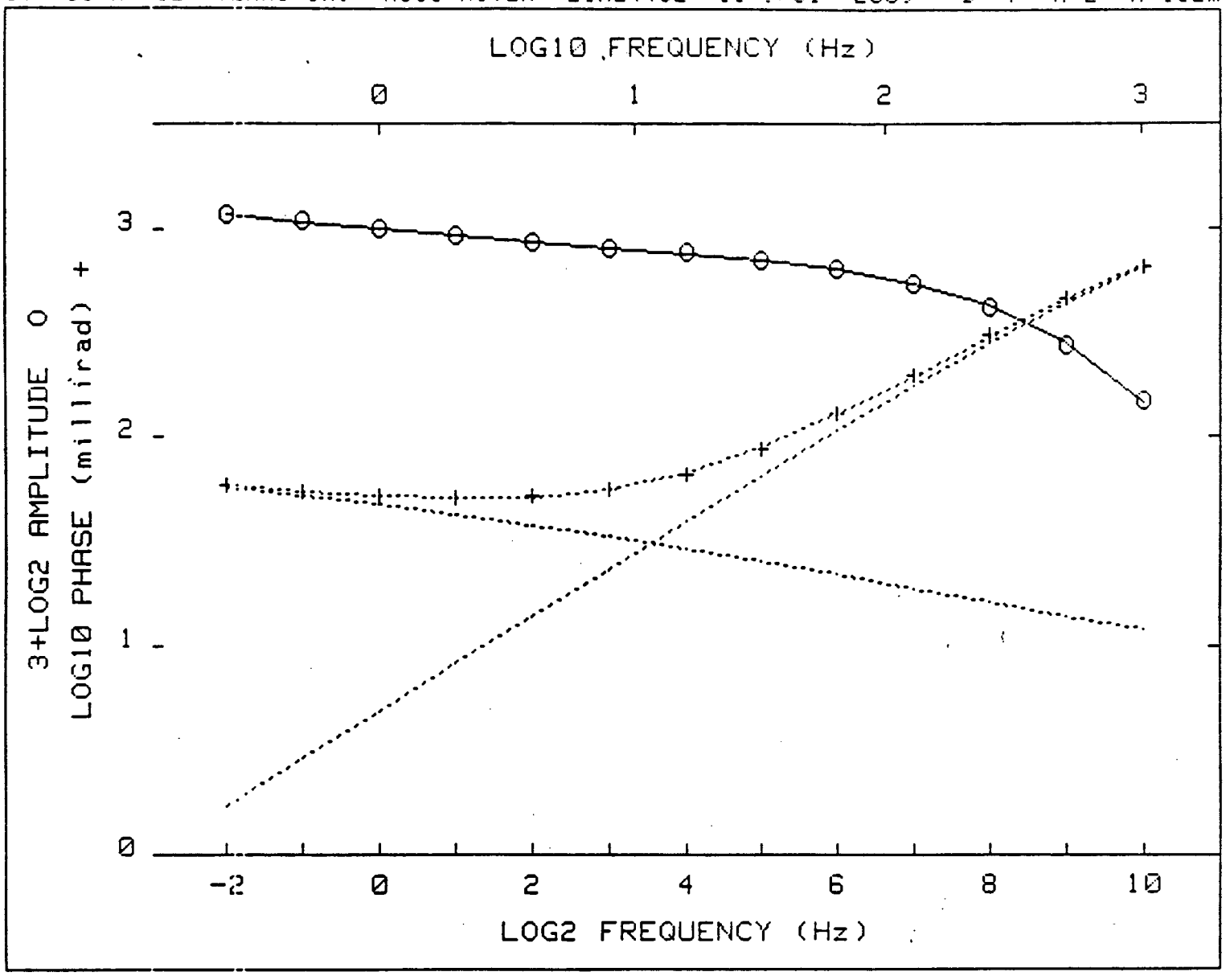
CRL: Number of dispersions= 2
T1=1 C1=.25 fixed

Iter	Lambda	Rchsq	R0	M1	M2	T2	C2
0	1.E-02	.07482	1.540	.690	.241	2.0E-03	.878
1	1.E-02	.01022	1.612	.725	.523	3.0E-03	.948
2	1.E-03	.00829	1.543	.690	.629	2.1E-03	.879
3	1.E-04	.00826	1.539	.687	.708	1.7E-03	.863

Pct Std Deviations	14.8	23.8	999.9	999.9	72.5	
Correlation Matrix	1.000					
	.950	1.000				
	-.707	-.797	1.000			
	.650	.748	-.995	1.000		
	.743	.865	-.963	.955	1.000	

Apparent Resistivity Measured at 1 Hz is 5.060
Apparent Resistivity Calculated from Inductive Coupling is 99.74

CYPRUS ANVIL TENAS CK. ROSS RIVER LINE445E 30/9/81 L339 D= 7 N=2 X=152m



CRL: Number of dispersions= 2
C1=.25 fixed

Iter	Lambda	Rchsq	R0	M1	T1	M2	T2	C2
0	1.E-02	.01086	1.949	.577	1.2E+02	.337	3.2E-04	.830
1	1.E-02	.00123	1.772	.518	1.3E+02	.479	1.7E-04	.736
2	1.E-03	.00007	1.787	.517	1.4E+02	.579	1.2E-04	.731
3	1.E-04	.00004	1.819	.526	1.7E+02	.577	1.2E-04	.737
4	1.E-05	.00004	1.845	.532	2.0E+02	.571	1.2E-04	.736
Pct Std Deviations			5.7	4.7	82.6	4.8	3.9	1.2

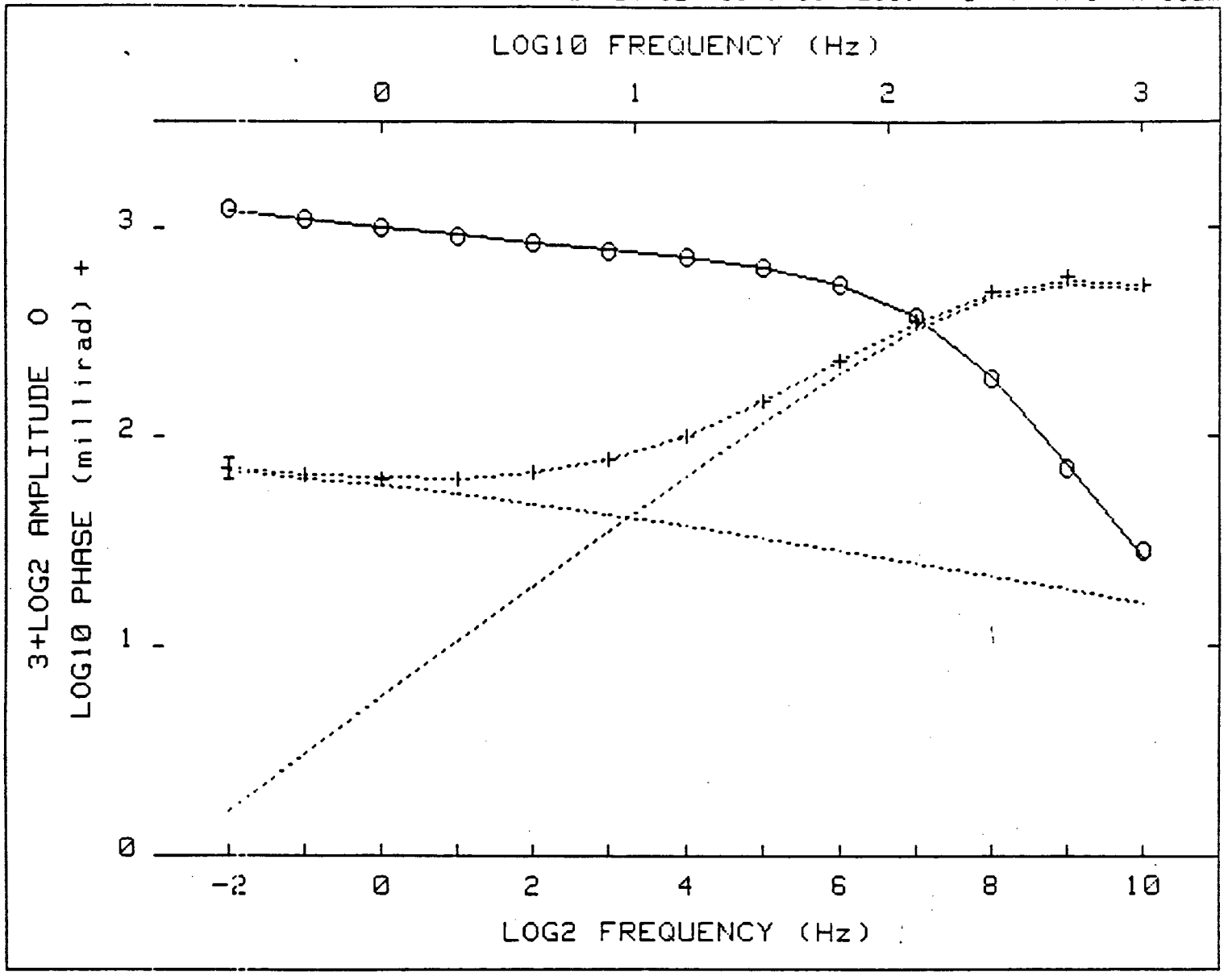
Correlation Matrix

1.000						
.999	1.000					
.997	.994	1.000				
-.919	-.924	-.903	1.000			
-.406	-.394	-.434	.034	1.000		
-.675	-.653	-.704	.412	.817	1.000	

Apparent Resistivity Measured at 1 Hz is 115.5
Apparent Resistivity Calculated from Inductive Coupling is 231.8

DWG. NO. - SIP - 1110 - 7

CYPRUS ANVIL TENAS CK. ROSS RIVER LINE445E 30/9/81 L339 D= 7 N=3 X=152m



CRL: Number of dispersions= 2
C1=.25 fixed

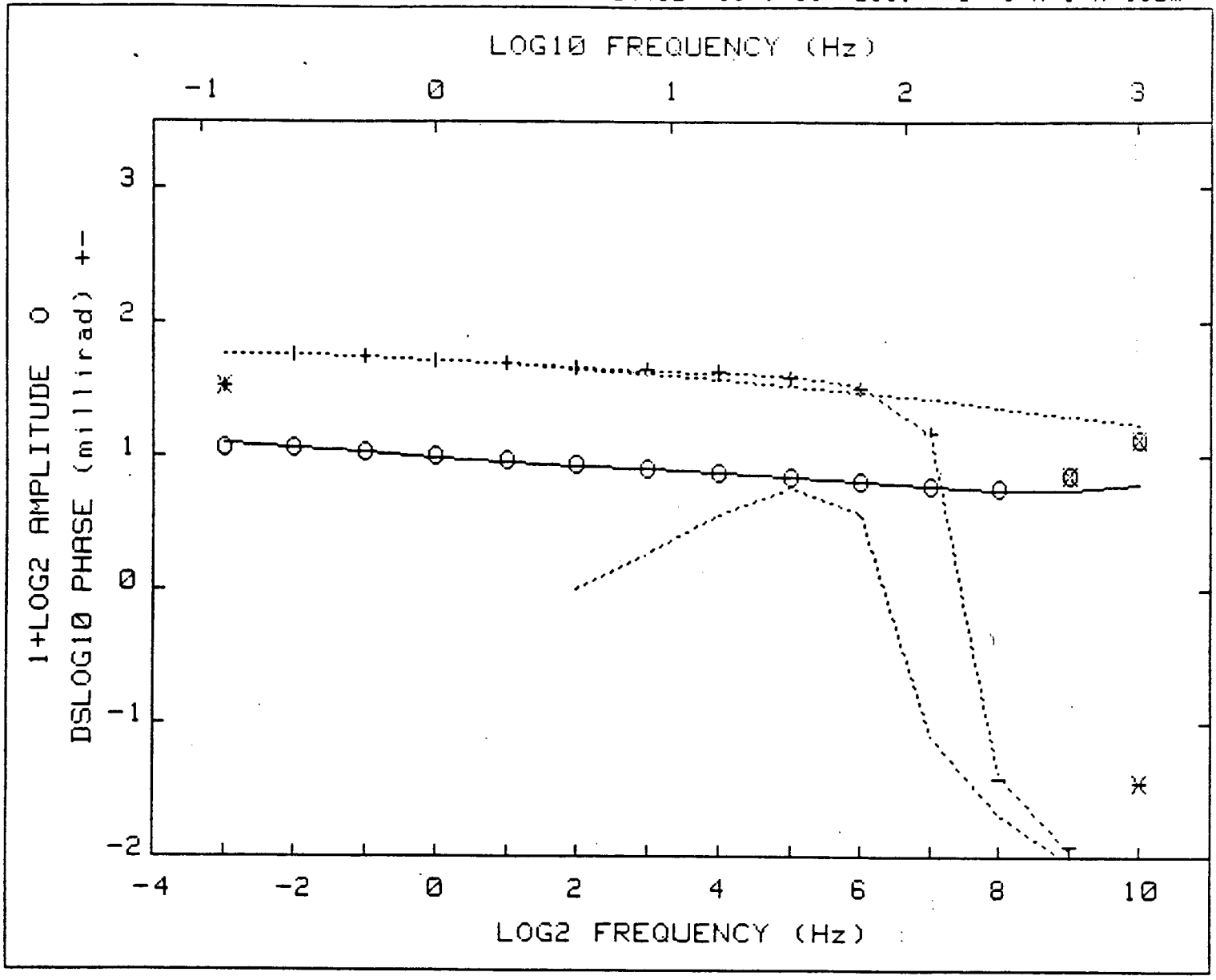
Iter	Lambda	Rchsq	R0	M1	T1	M2	T2	C2
0	1.E-02	.06770	1.845	.532	2.0E+02	.571	1.2E-04	.736
1	1.E-02	.03069	1.893	.549	2.1E+02	.296	6.1E-04	.641
2	1.E-03	.00487	2.070	.625	1.3E+02	.295	6.2E-04	.987
3	1.E-04	.00187	1.749	.548	4.3E+01	.365	6.4E-04	.875
4	1.E-05	.00010	1.877	.560	8.7E+01	.348	6.4E-04	.858
5	1.E-06	.00010	1.898	.564	9.6E+01	.344	6.4E-04	.859

Pct Std Deviations	7.7	5.4	123.2	6.6	1.6	1.1	
Correlation Matrix	1.000						
	.998	1.000					
	.996	.990	1.000				
	-.985	-.990	-.974	1.000			
	.175	.166	.171	-.262	1.000		
	-.610	-.581	-.642	.491	.208	1.000	

Apparent Resistivity Measured at 1 Hz is 98.24
Apparent Resistivity Calculated from Inductive Coupling is 236.8

DWG. NO. - S.I.P - 1110 - 8

CYPRUS ANVIL TENAS CK. ROSS RIVER LINE445E 30/9/81 L339 D= 8 N=1 X=152m



CRL: Number of dispersions= 3 Negative.
C1=.25 C2=1 M3=1 C3=1 fixed

Iter	Lambda	Rchsq	R0	M1	T1	M2	T2	T3
0	1.E-02	.02227	1.301	.297	5.5E+00	.100	1.0E-02	1.9E-05
1	1.E-01	.01454	1.405	.437	5.2E+00	.048	8.2E-03	1.8E-05
2	1.E-02	.00222	1.455	.453	4.4E+00	.021	4.7E-03	2.0E-05
3	1.E-03	.00048	1.434	.441	3.7E+00	.016	2.2E-03	2.1E-05
4	1.E-04	.00035	1.478	.448	7.2E+00	.022	2.1E-03	2.1E-05
5	1.E-05	.00029	1.492	.453	8.2E+00	.021	2.2E-03	2.0E-05
6	1.E-06	.00029	1.491	.453	8.1E+00	.021	2.2E-03	2.0E-05

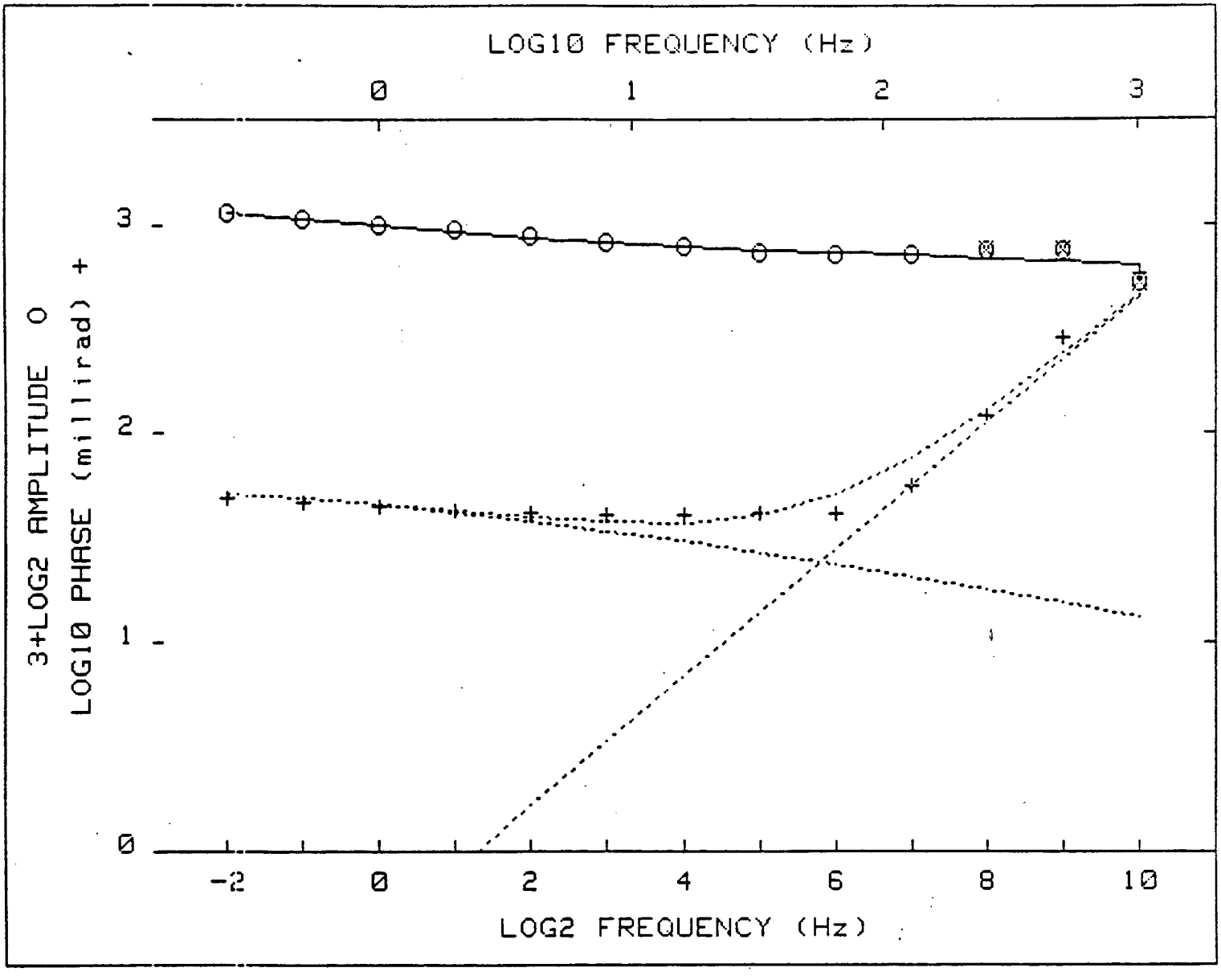
Pct Std Deviations	3.9	3.8	85.5	8.4	11.1	5.8	
Correlation Matrix	1.000						
	.985	1.000					
	.984	.954	1.000				
	.546	.442	.635	1.000			
	.366	.297	.416	.461	1.000		
	-.906	-.880	-.917	-.451	-.586	1.000	

Apparent Resistivity Measured at 1 Hz is 32.0

Apparent Resistivity Calculated from Inductive Limit is 34.2

DWG. NO. - S.I.P. - 1110 - 9

CYPRUS ANVIL TENAS CK. ROSS RIVER LINE445E 30/9/81 L339 D= 8 N=2 X=152m

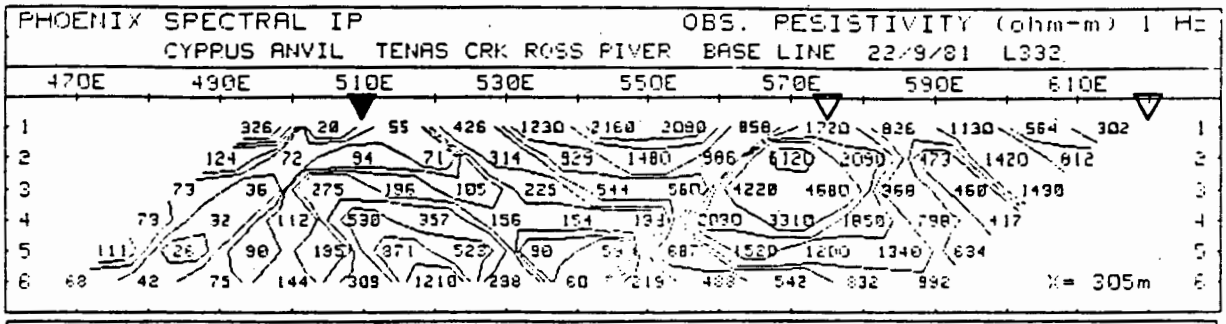


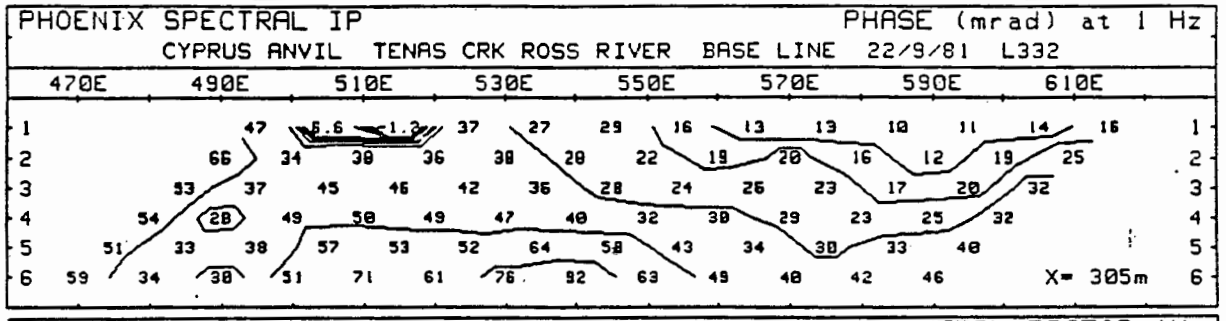
CRL: Number of dispersions= 2
C1=.25 M2=1 C2=1 fixed

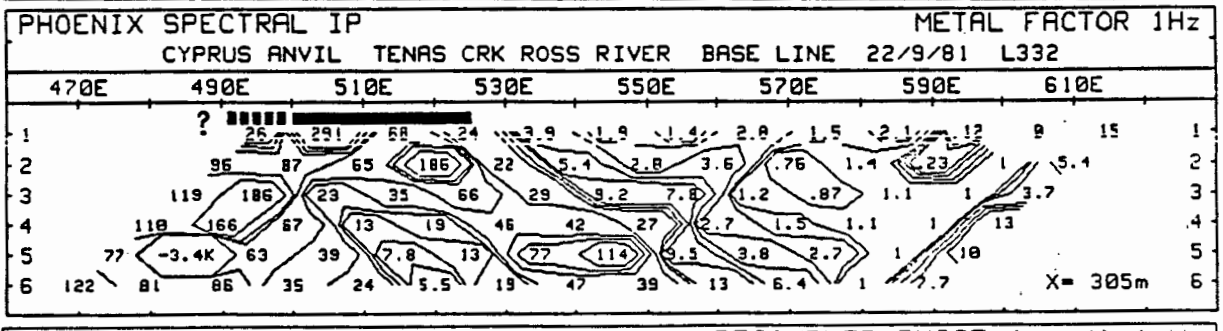
Iter	Lambda	Rchsq	R0	M1	T1	T2
0	1.E-02	.00248	1.502	.433	2.1E+01	4.2E-05
1	1.E-02	.00248	1.503	.433	2.1E+01	4.2E-05

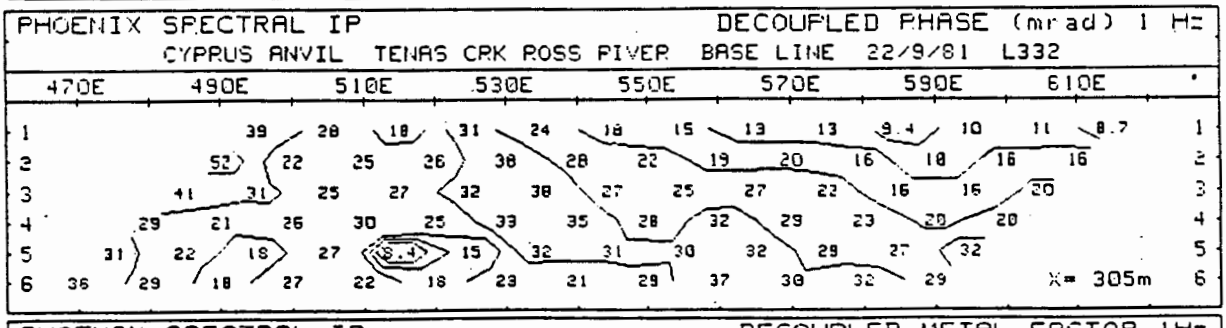
Pct Std Deviations	11.2	13.6	350.1	11.0	
Correlation Matrix	1.000				
	.992	1.000			
	.983	.975	1.000		
	-.769	-.787	-.729	1.000	

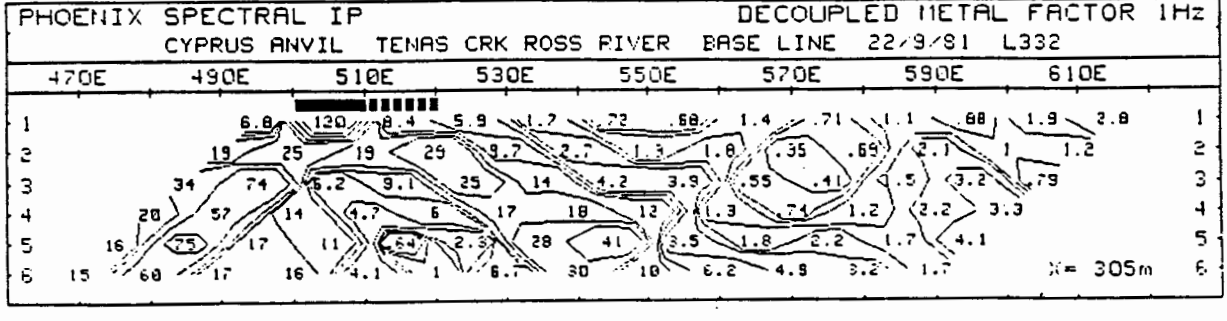
Apparent Resistivity Measured at 1 Hz is 181.6
Apparent Resistivity Calculated from Inductive Coupling is 1079


PHOENIX SPECTRAL IP
OBS. RESISTIVITY (ohm-m) 1 Hz
CYPRUS ANVIL TENAS CRK ROSS RIVER BASE LINE 22/9/81 L332
470E 490E 510E 530E 550E 570E 590E 610E
X= 305m


PHOENIX SPECTRAL IP
PHASE (mrad) at 1 Hz
CYPRUS ANVIL TENAS CRK ROSS RIVER BASE LINE 22/9/81 L332
470E 490E 510E 530E 550E 570E 590E 610E
X= 305m

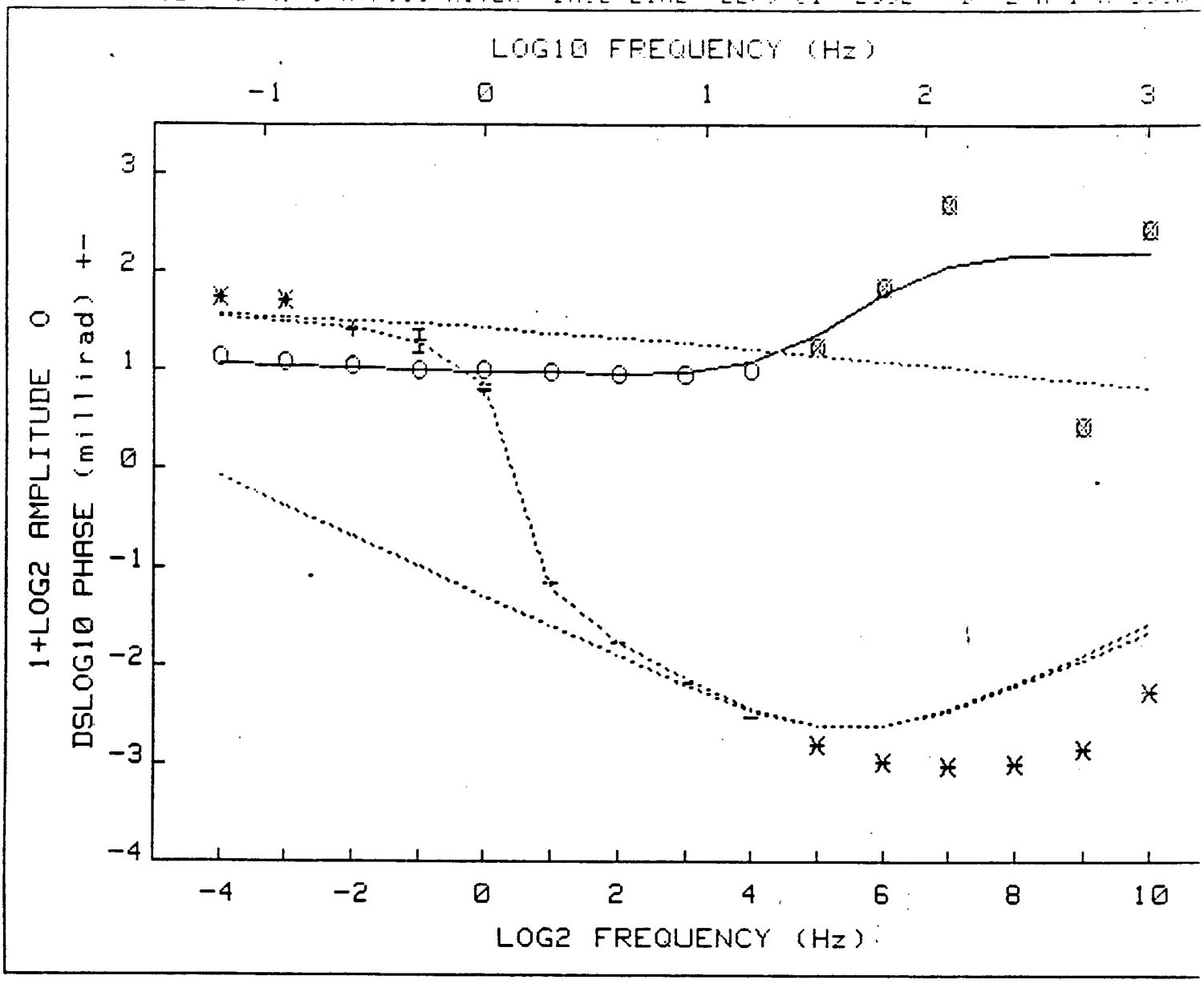

PHOENIX SPECTRAL IP
METAL FACTOR 1Hz
CYPRUS ANVIL TENAS CRK ROSS RIVER BASE LINE 22/9/81 L332
470E 490E 510E 530E 550E 570E 590E 610E
X= 305m


PHOENIX SPECTRAL IP
DECOUPLED PHASE (mrad) 1 Hz
CYPRUS ANVIL TENAS CRK ROSS RIVER BASE LINE 22/9/81 L332
470E 490E 510E 530E 550E 570E 590E 610E
X= 305m


PHOENIX SPECTRAL IP
DECOUPLED METAL FACTOR 1Hz
CYPRUS ANVIL TENAS CRK ROSS RIVER BASE LINE 22/9/81 L332
470E 490E 510E 530E 550E 570E 590E 610E
X= 305m

DWG. NO. - S.I.P. - IIII - 2

CYPRUS ANVIL TEXAS CPI POSS RIVER BASE LINE 22/9/91 L332 D= 2 N=1 I=30[illegible]



CRL: Number of dispersions= 2 Negative.
C1=.25 M2=1 C2=1 fixed

Iter	Lambda	Rchsq	R0	M1	T1	T2
0	1.E-02	.00246	1.379	.337	6.8E+01	2.3E-03
1	1.E-02	.00246	1.383	.338	7.0E+01	2.3E-03

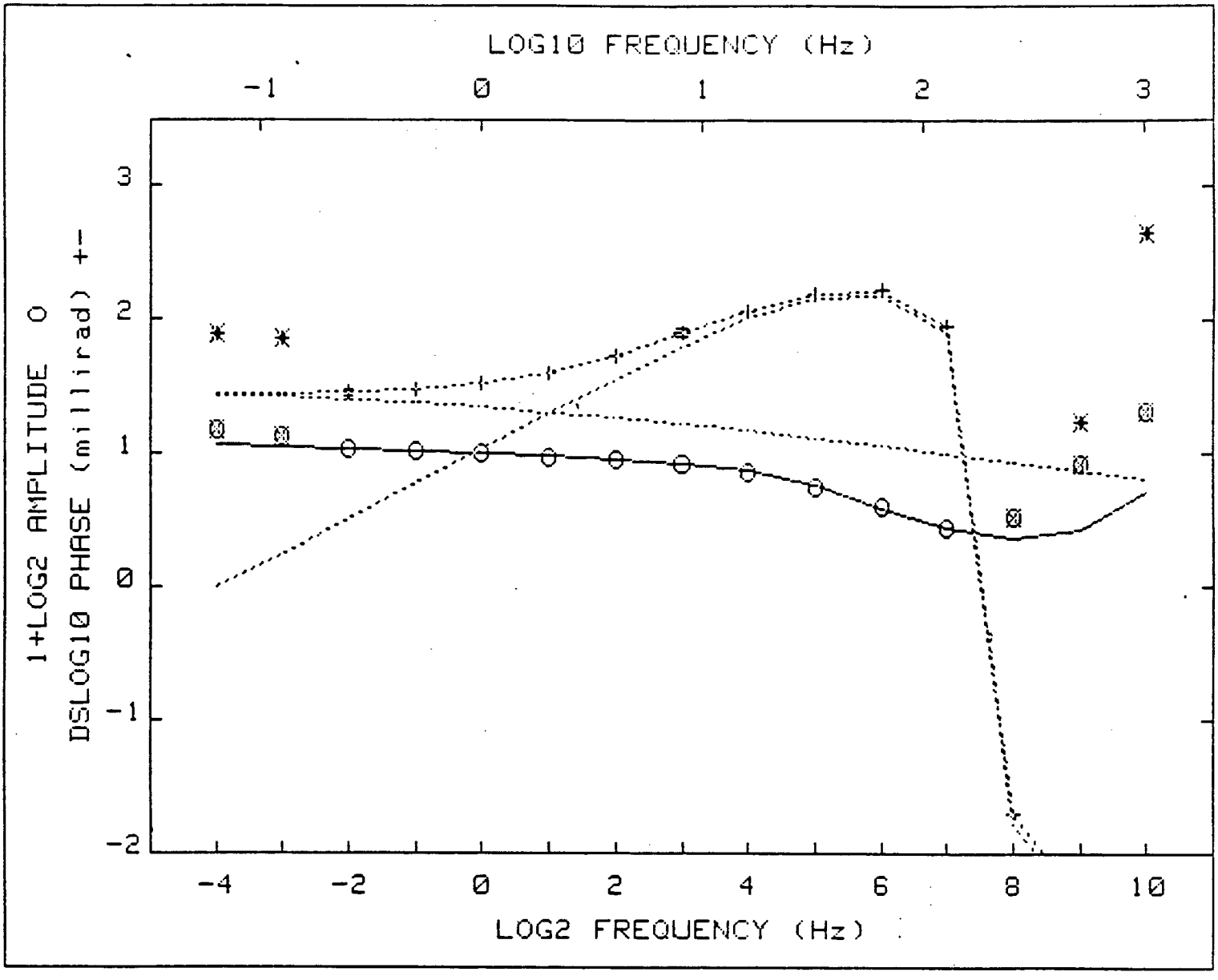
Pct Std Deviations	24.7	47.8	5792.4	32.6	
Correlation Matrix	1.000				
	.998	1.000			
	.997	.997	1.000		
	-.984	-.980	-.991	1.000	

Apparent Resistivity Measured at 1 Hz is 20.17

Apparent Resistivity Calculated from Inductive Coupling is 30.55

DWG. NO. - S.I.P - 1111 - 3

CYPRUS ANVIL TENAS CRK ROSS RIVER BASE LINE 22/9/81 L332 D= 2 N=2 X=305m



CRL: Number of dispersions= 3 Negative.
C1=.25 M3=1 C3=1 fixed

Iter	Lambda	Rchsq	R0	M1	T1	M2	T2	C2	T3
0	1.E-02	.00011	1.231	.246	1.3E+01	.280	3.4E-03	.879	5.5E-05
1	1.E-02	.00011	1.231	.247	1.3E+01	.280	3.4E-03	.879	5.5E-05

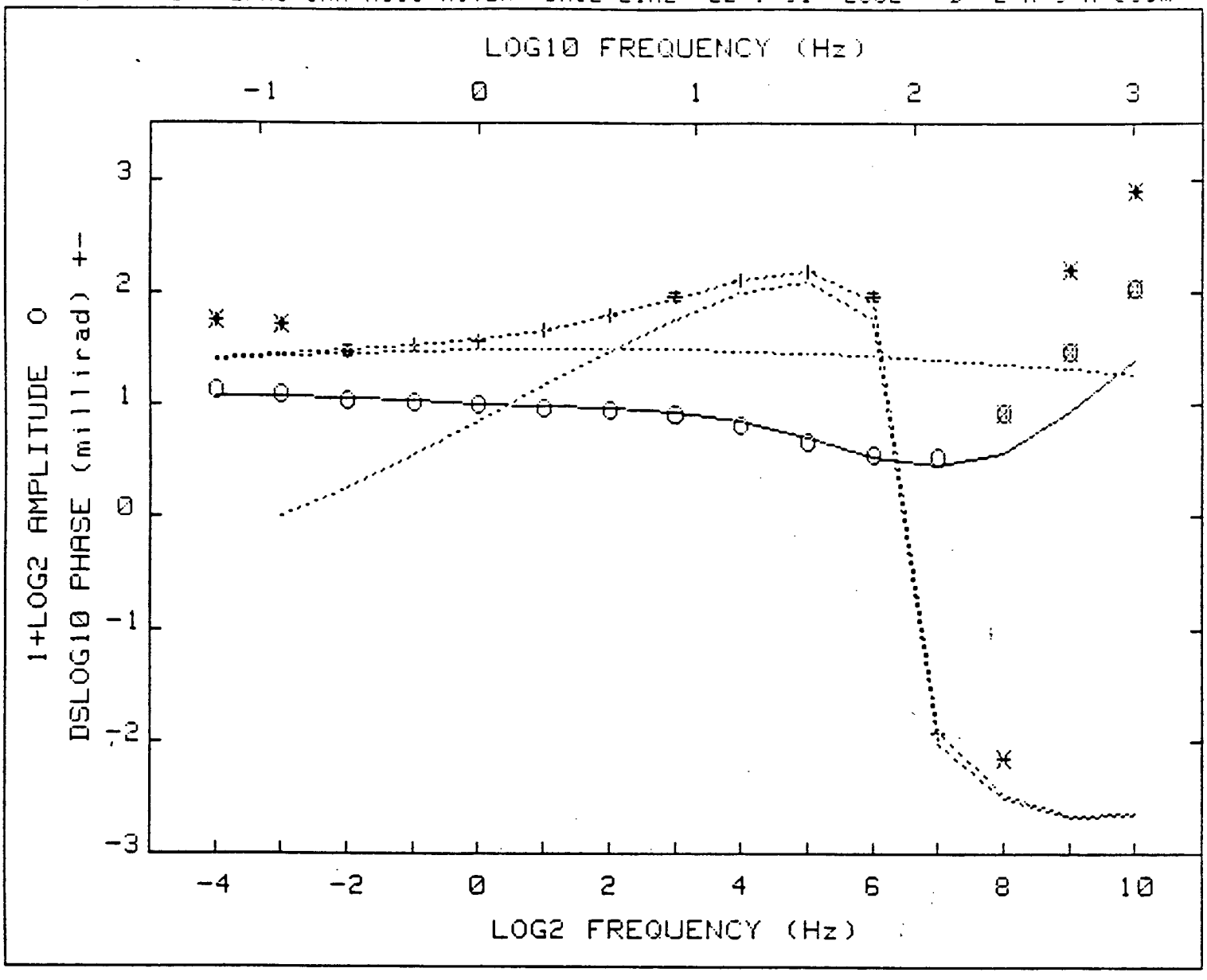
Pct Std Deviations	5.3	12.0	482.5	2.6	2.8	2.4	4.9	
Correlation Matrix	1.000							
	.994	1.000						
	.995	.983	1.000					
	-.571	-.636	-.520	1.000				
	-.064	-.043	-.089	-.510	1.000			
	-.753	-.697	-.789	-.048	.478	1.000		
	-.826	-.850	-.802	.872	-.447	.321	1.000	

Apparent Resistivity Measured at 1 Hz is 72.23

Apparent Resistivity Calculated from Inductive Coupling is 3329

DWG. NO. - S.I.P - 1111 - 4

CYPRUS ANVIL TENAS CRK ROSS RIVER BASE LINE 22/9/81 L332 D= 2 N=3 X=305m



CRL: Number of dispersions= 3 Negative.
C1=.25 C2=1 M3=1 C3=1 fixed

Iter	Lambda	Rchsq	R0	M1	T1	M2	T2	T3
0	1.E-02	.00114	1.148	.269	1.1E-01	.232	4.9E-03	1.6E-04
1	1.E-02	.00109	1.156	.271	1.1E-01	.232	5.0E-03	1.6E-04
2	1.E-03	.00109	1.156	.271	1.1E-01	.232	5.0E-03	1.6E-04

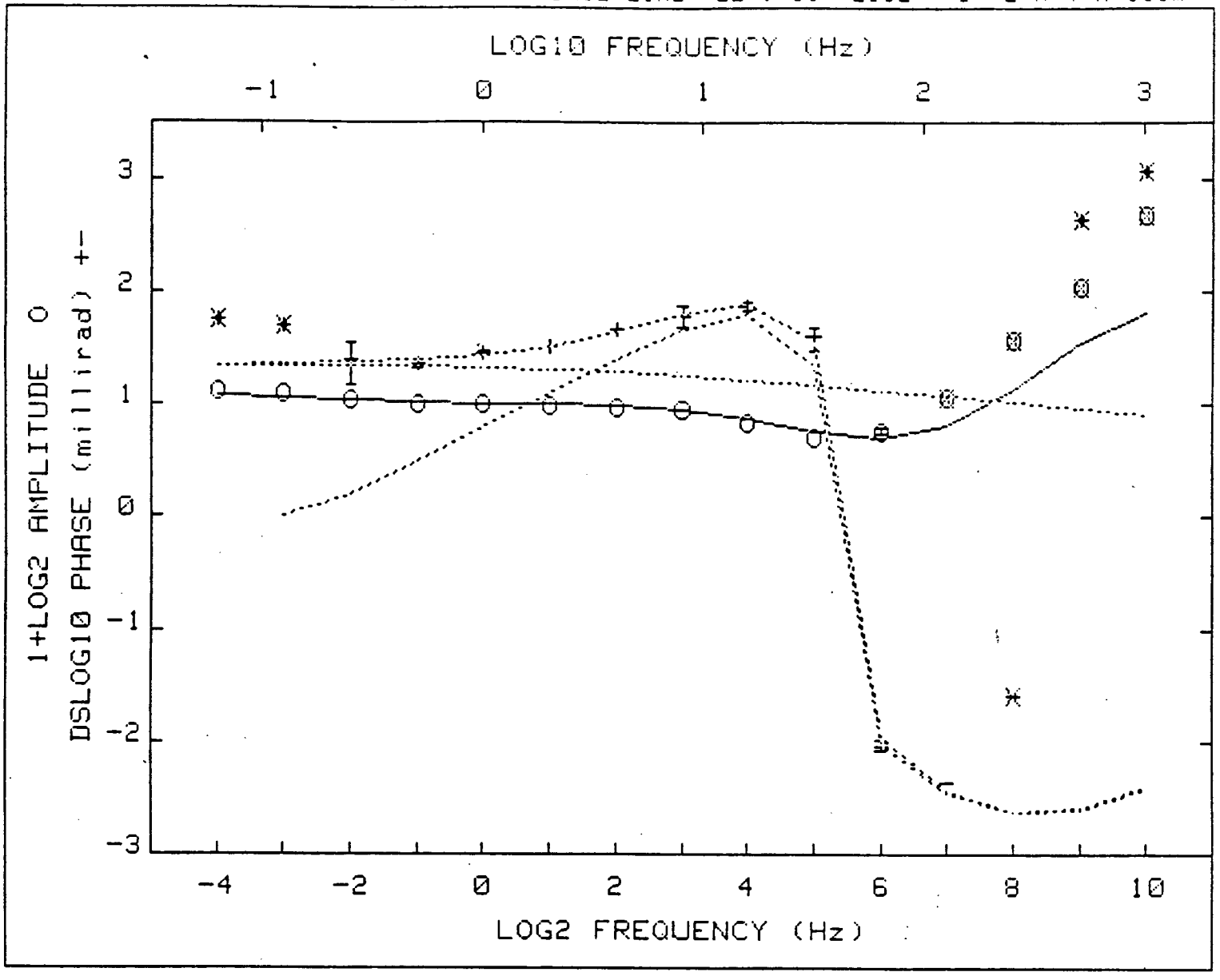
Pct Std Deviations	2.9	12.8	823.8	5.2	7.7	9.9	
Correlation Matrix	1.000						
	-.805	1.000					
	.948	-.929	1.000				
	.547	-.737	.636	1.000			
	.452	-.611	.519	.211	1.000		
	-.783	.807	-.838	-.309	-.772	1.000	

Apparent Resistivity Measured at 1 Hz is 35.75

Apparent Resistivity Calculated from Inductive Coupling is 2203

DWG. NO. – S.I.P – 1111 –5

CYPRUS ANVIL TENAS CRK ROSS RIVER BASE LINE 22/9/81 L332 D= 2 N=4 X=305m



CRL: Number of dispersions= 3 Negative.
C1=.25 C2=1 M3=1 C3=1 fixed

Iter	Lambda	Rchsq	R0	M1	T1	M2	T2	T3
0	1.E-02	.00229	1.135	.198	1.3E+00	.172	7.0E-03	3.3E-04
1	1.E-02	.00197	1.152	.199	1.3E+00	.169	7.1E-03	3.3E-04
2	1.E-03	.00197	1.153	.199	1.4E+00	.169	7.1E-03	3.3E-04

Pct Std Deviations	6.5	10.6	4113.6	6.2	11.4	14.0

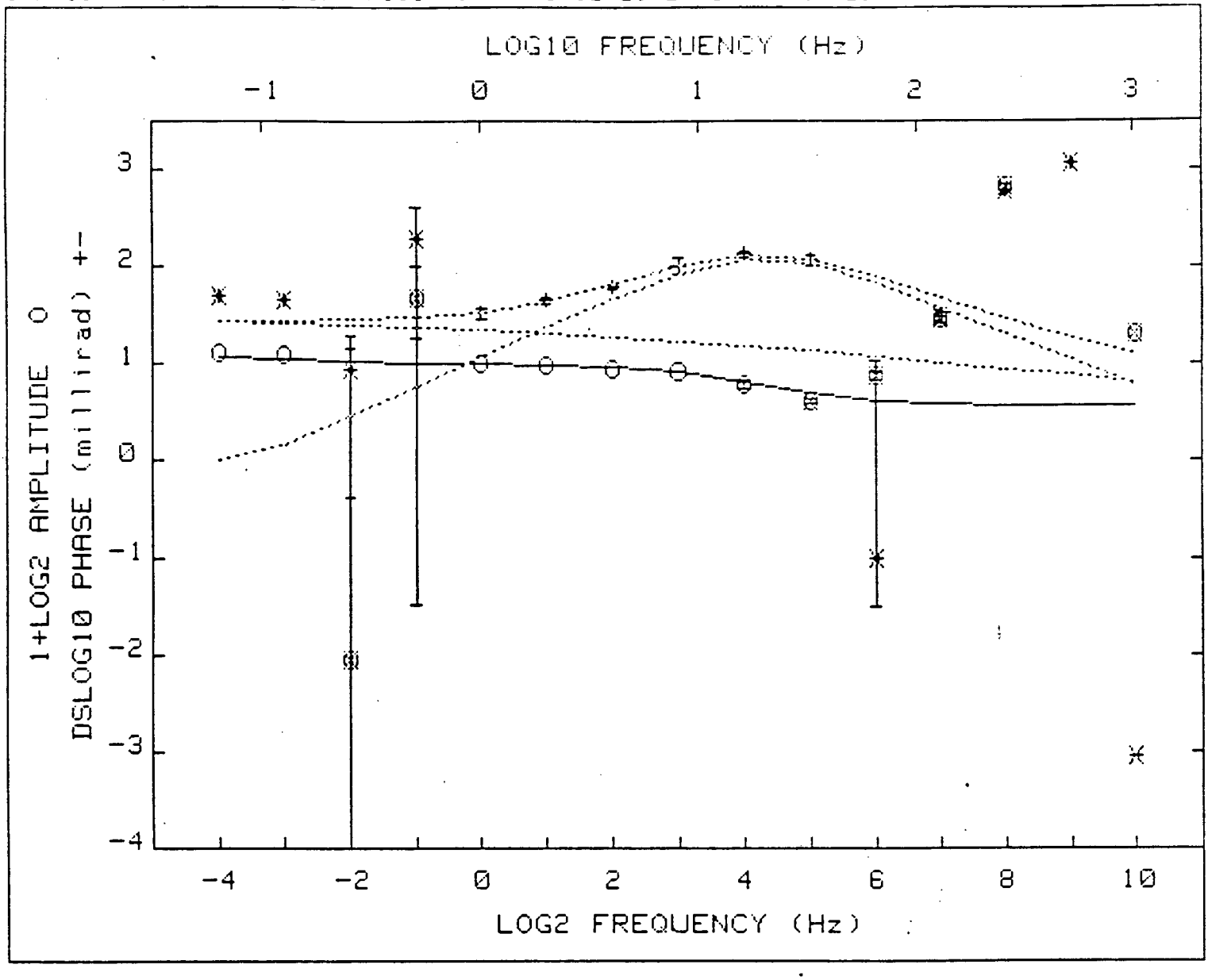
Correlation Matrix

1.000						
.837	1.000					
.980	.767	1.000				
-.212	-.349	-.183	1.000			
.560	.247	.606	-.394	1.000		
-.800	-.610	-.822	.604	-.792	1.000	

Apparent Resistivity Measured at 1 Hz is 32.32

Apparent Resistivity Calculated from Inductive Coupling is 1720

CYPRUS ANVIL TEM83 CPA FOSS RIVER BASE LINE 22/9/81 L332 D= 2 N=5 X=305m



CRL: Number of dispersions= 2
C1=.25 C2=1 fixed

Iter	Lambda	Rchsq	R0	M1	T1	M2	T2
0	1.E-02	.00100	1.231	.247	1.0E+01	.166	9.1E-03
1	1.E-02	.00099	1.222	.243	1.0E+01	.164	9.3E-03
2	1.E-03	.00099	1.225	.244	1.1E+01	.164	9.4E-03

Pct Std Deviations	54.5	208.7	9999.9	35.0	9.7

Correlation Matrix

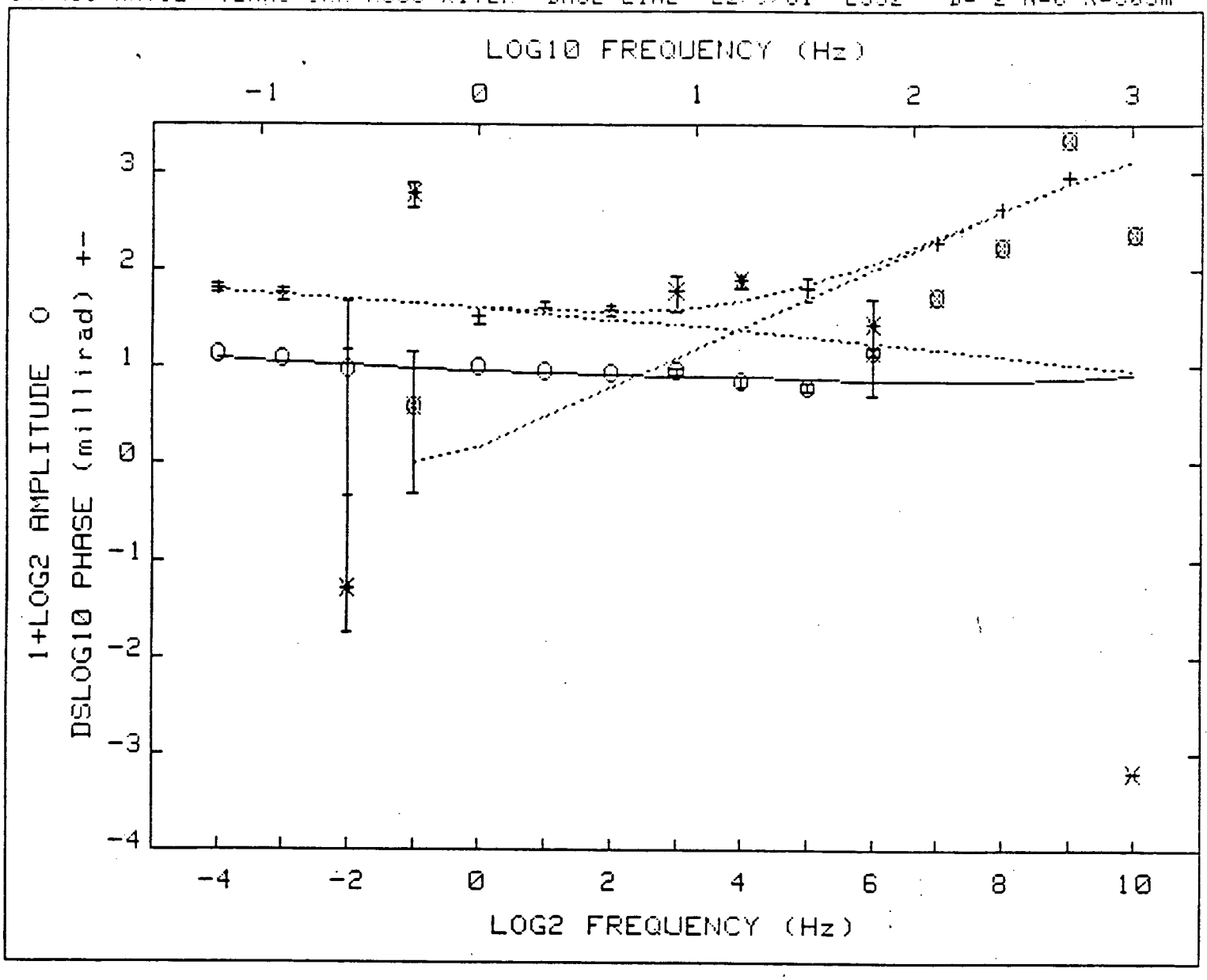
1.000				
.999	1.000			
.999	.996	1.000		
-.982	-.986	-.975	1.000	
.381	.356	.403	-.367	1.000

Apparent Resistivity Measured at 1 Hz is 25.80

Apparent Resistivity Calculated from Inductive Coupling is 517.9

DWG. NO. - S.I.P. - IIII - 7

CYPRUS ANVIL TENAS CRK ROSS RIVER BASE LINE 22/9/81 L332 D= 2 N=6 X=305m



CRL: Number of dispersions= 2
C1=.25 M2=1 C2=1 fixed

Iter	Lambda	Rchsq	R0	M1	T1	T2
0	1.E-02	.00303	1.905	.544	6.9E+02	1.2E-04
1	1.E-02	.00300	1.905	.544	7.0E+02	1.2E-04

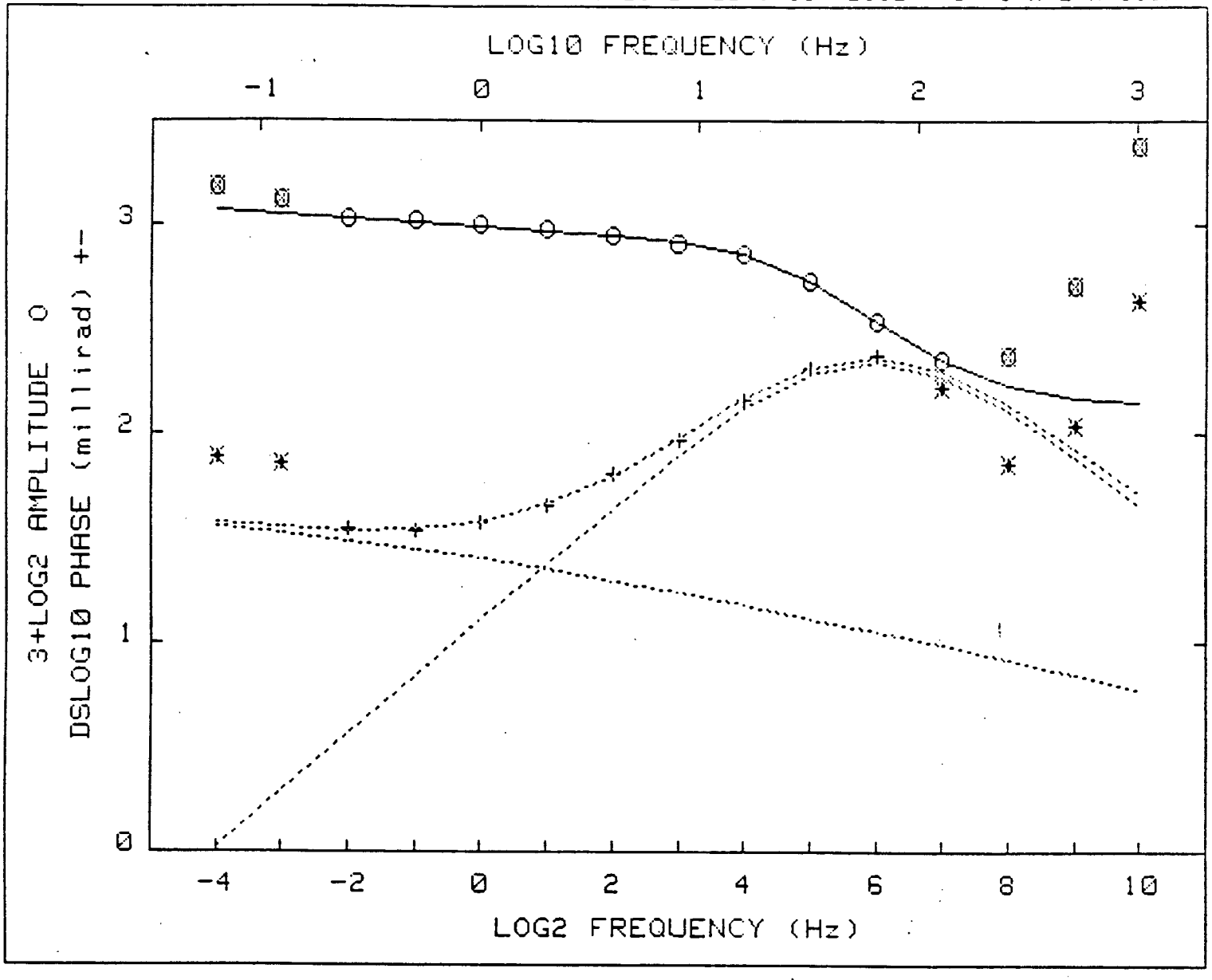
Pct Std Deviations	34.3	27.2	1555.9	33.2	
Correlation Matrix	1.000				
	.998	1.000			
	.993	.990	1.000		
	-.964	-.967	-.951	1.000	

Apparent Resistivity Measured at 1 Hz is 41.58

Apparent Resistivity Calculated from Inductive Coupling is 9120

DWG. NO. - S.I.P. - IIII - 8

CYPRUS ANVIL TENAS CRK ROSS RIVER BASE LINE 22/9/81 L332 D= 3 N=2 X=305m



CRL: Number of dispersions= 2
C1=.25 fixed

Iter	Lambda	Rchsq	R0	M1	T1	M2	T2	C2
0	1.E-02	.00004	1.430	.352	1.6E+02	.274	3.6E-03	.894
1	1.E-02	.00004	1.430	.352	1.6E+02	.274	3.5E-03	.893
2	1.E-03	.00004	1.432	.353	1.6E+02	.274	3.5E-03	.893
Pct Std Deviations			9.9	17.2	423.4	7.3	3.3	1.9

Correlation Matrix

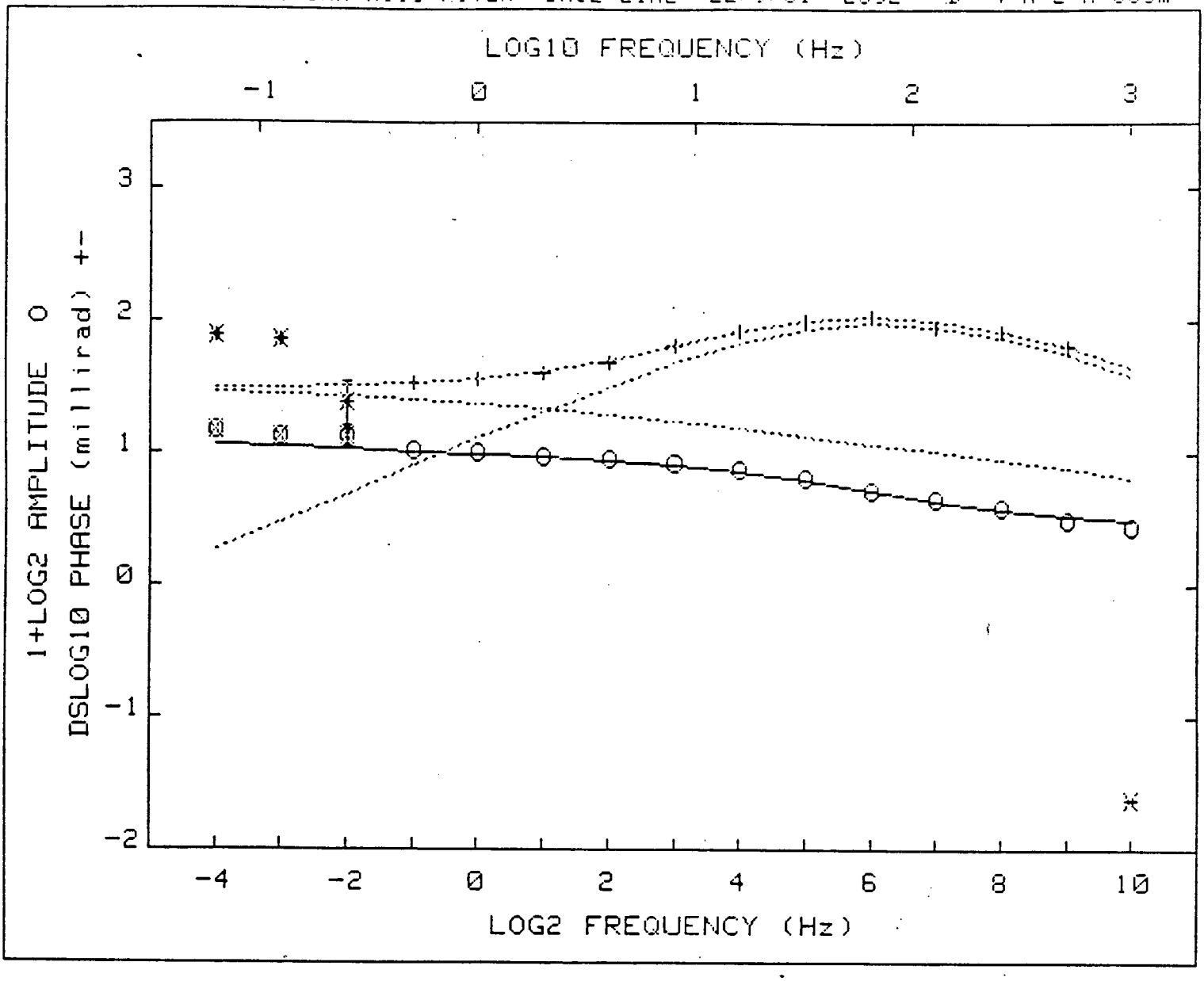
1.000						
1.000	1.000					
.999	.997	1.000				
-.960	-.964	-.950	1.000			
-.342	-.336	-.363	.094	1.000		
-.764	-.753	-.786	.573	.746	1.000	

Apparent Resistivity Measured at 1 Hz is 93.99

Apparent Resistivity Calculated from Inductive Coupling is 131.2

DWG. NO. - S.I.P - IIII - 9

CYPRUS ANVIL TENAS CRK ROSS RIVER BASE LINE 22/9/81 L332 D= 4 N=2 X=305m



CRL: Number of dispersions= 2
C1=.25 fixed

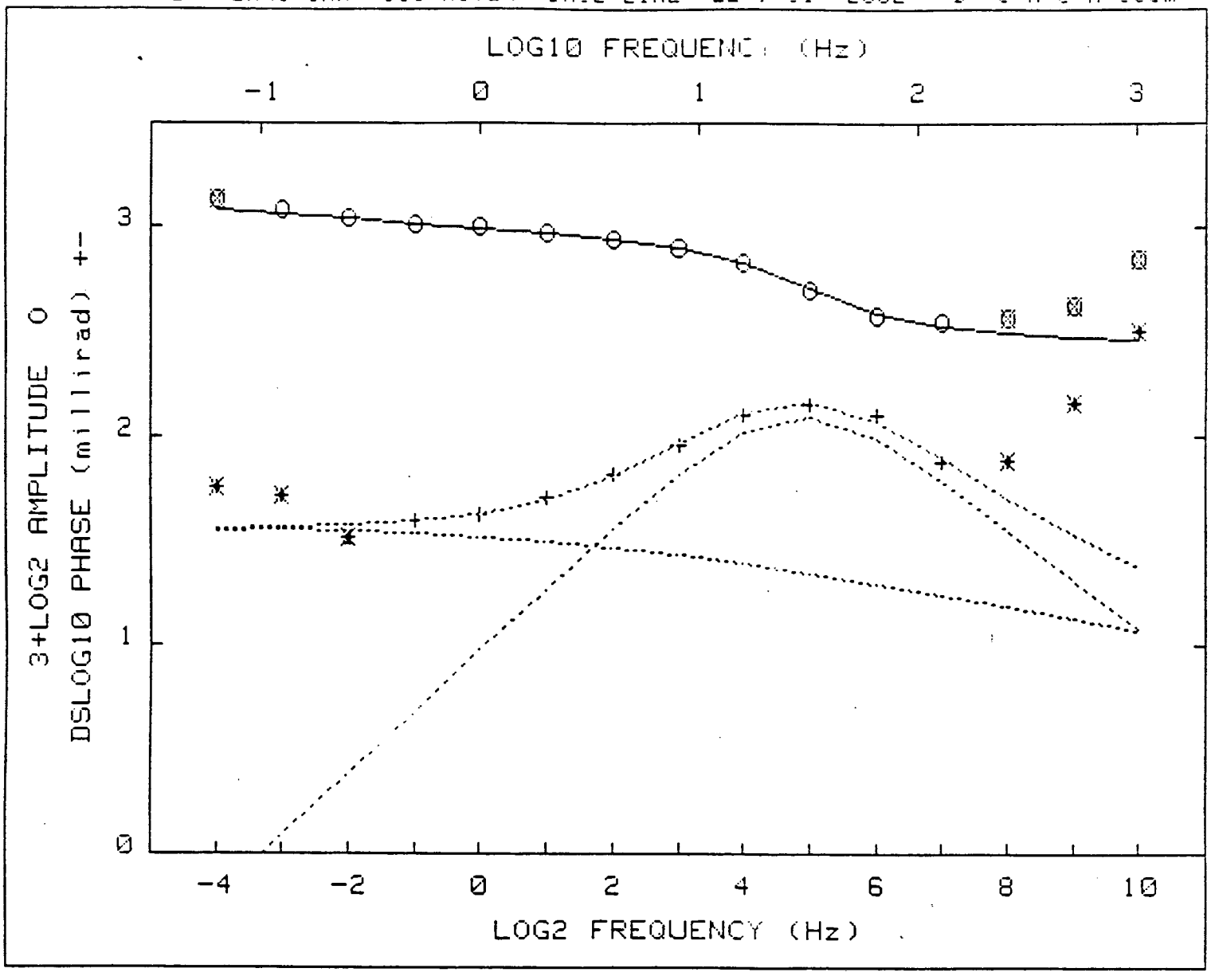
Iter	Lambda	Rchsq	R0	M1	T1	M2	T2	C2
0	1.E-02	.00054	1.265	.272	1.7E+01	.197	2.8E-03	.715
1	1.E-02	.00052	1.258	.265	1.7E+01	.201	2.8E-03	.702
2	1.E-03	.00052	1.259	.265	1.9E+01	.202	2.8E-03	.701

Pct Std Deviations	37.3	96.2	9999.9	11.0	10.5	10.3
Correlation Matrix	1.000					
	.998	1.000				
	.998	.994	1.000			
	-.830	-.861	-.802	1.000		
	.754	.730	.769	-.480	1.000	
	-.880	-.955	-.900	.502	-.738	1.000

Apparent Resistivity Measured at 1 Hz is 71.01

Apparent Resistivity Calculated from Inductive Coupling is 69.73

CYPRUS ANVIL TENAS CRK FOSS RIVER BASE LINE 22 F 81 L332 D= 5 N=3 X=305m



CRL: Number of dispersions= 2
C1=.25 fixed

Iter	Lambda	Rchsq	R0	M1	T1	M2	T2	C2
0	1.E-02	.00023	1.2?1	.297	3.0E+00	.174	?.2E-03	.937
1	1.E-02	.00020	1.2?5	.303	3.0E+00	.169	?.3E-03	.963
2	1.E-03	.00020	1.2?5	.303	3.0E+00	.169	?.3E-03	.963
Pct Std Deviations			11.?	13.2	3758.0	5.1	2.9	5.7

Correlation Matrix

1.000					
.?31	1.000				
.?97	.966	1.000			
.?33	.546	.730	1.000		
.?12	-.042	.049	.203	1.000	
-.?3?	-.817	-.919	-.872	-.092	1.000

Apparent Resistivity Measured at 1 Hz is 105.1

Apparent Resistivity Calculated from Inductive Coupling is 286.6

RECENT AND FUTURE ADVANCES IN THE INDUCED POLARIZATION METHOD

by

Philip G. Hallof, Ph.D., and William H. Pelton, Ph.D.

Prepared for Presentation
at the Prospectors and Developers Convention
Royal York Hotel, Toronto
March 8th to March 11th, 1981

- -

RECENT AND FUTURE ADVANCES IN THE INDUCED POLARIZATION METHOD

BY

Philip G. Hallof, Ph.D., and William H. Pelton, Ph.D.

INTRODUCTION

The induced polarization (IP) method was introduced into Canadian exploration practice in the period from 1955 to 1960. Two measurement techniques were widely used, the pulse-transient method (time domain) and the variable frequency method (frequency domain). In the fifteen years following 1960, striking improvements were made in both frequency domain and time domain IP equipment, but only limited progress was made in a better understanding of the IP phenomenon, its source, and how to use it.

However, in the five year period since 1975, considerable progress has been made in our understanding of the IP method. Beginning with an understanding of the exact equivalence of the IP measurements in the phase-domain, the frequency-domain and the time-domain (see Figure 1), we have progressed to the study of the IP effect over the entire frequency range of interest. These studies have led to a greatly advanced understanding of the IP method in at least three important areas:-

i) Our understanding of the IP phenomenon itself has been vastly increased. A greater knowledge of the source of the IP effect and its detailed behavior has suggested additional uses for the method, beyond the simple detection of anomalies.

ii) A better idea of what we wanted to measure, and modern solid-state electronics, have resulted in greatly improved measurement techniques and instrumentation.

iii) The advent of smaller, less expensive digital computers has greatly helped with the interpretation of IP field data. Rapid forward problem solutions and the possibility of direct inversion of IP field data have made it possible for the geophysicists to give the exploration geologist a much better picture of just what the source of a particular IP anomaly might be.

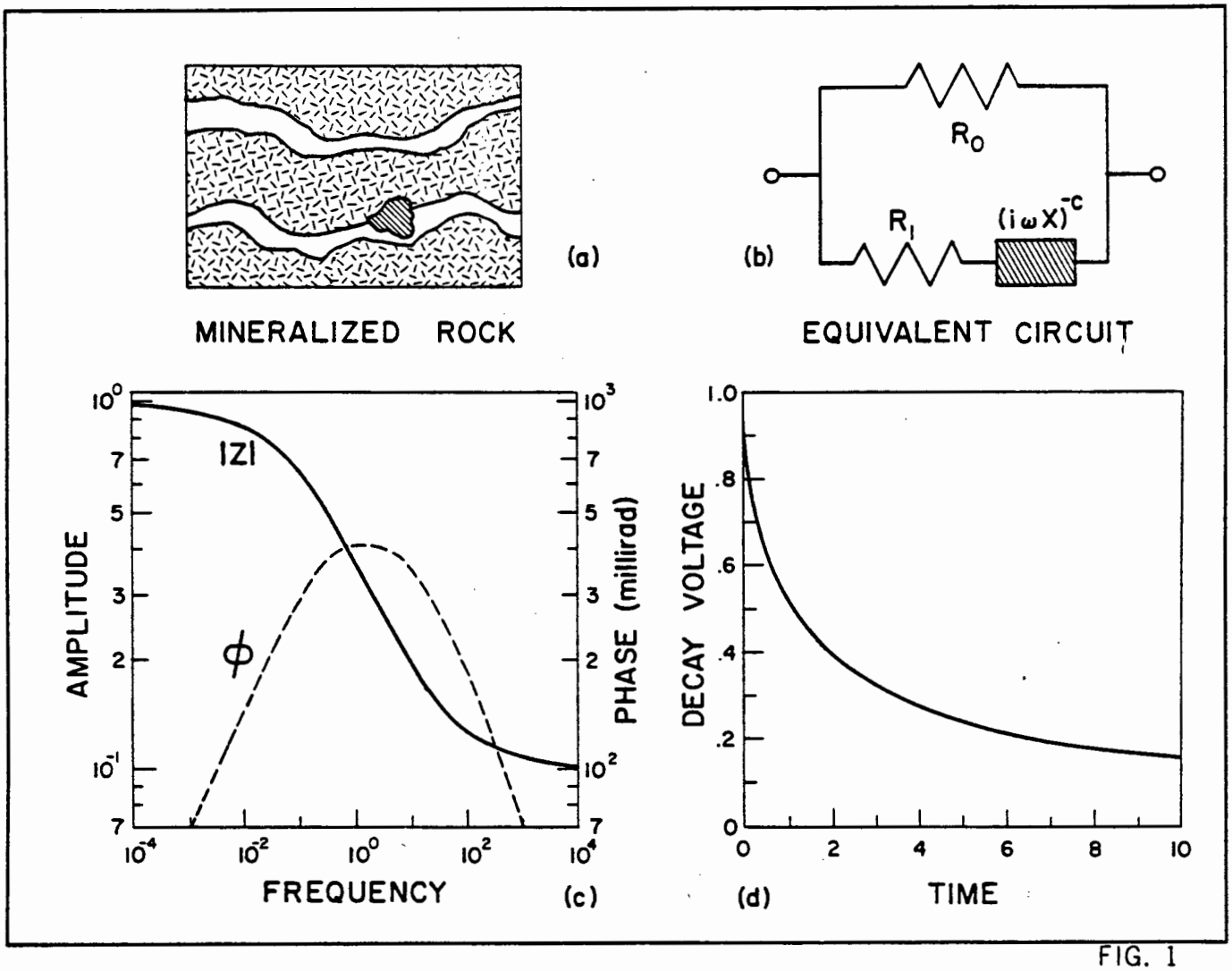


FIG. 1

WHAT IS THE NATURE OF THE IP EFFECT

Spectral induced polarization measurements (the measurement of the phase shifts over a wide frequency range) in open-pit mines, gave the first information concerning the detailed nature of the IP phenomenon. It became clear that four parameters, not just two (resistivity and IP

effect) were necessary to completely describe the IP effect.

The equation shown on Figure 2 and Figure 3 is formally known as the Cole-Cole Dispersion Equation; the four electrical parameters are:

Ro - the dc resistivity value

m - the IP effect (in non-dimensional form)

τ - the time constant of the IP effect

c - the exponent of the frequency (ω)

Since the very beginning of our experience with spectral IP measurements, we have found that these four parameters, and the Cole-Cole equation will adequately describe any IP effect that has been measured. The first measurements were made using one meter electrode intervals, within open-pit mines. The circles on Figure 4 and Figure 5 show the data points measured over massive graphite and massive sulphides at the Anvil Mine. As the solid line curves on the drawings show, the measured data points can be almost exactly replaced using a Cole-Cole Dispersion.

The four parameters obtained by the computer inversion of the graphite data are typical of those that have been measured over all graphite deposits. The IP effect is very large and the time constant (τ) is much greater than 1.0 seconds.

Large IP effects are also measured over massive sulphide sources. However, invariably the time constant value for (τ) is less than 1.0 seconds. The measurements shown on Figure 6 are for a massive sulphide source at the Kidd Creek Mine; again there is a large IP effect, and a small time constant.

The critical frequency (Fc) for a Cole-Cole Dispersion is defined as that frequency for which the maximum phase-shift is measured. An examination of the equation and curves in Figure 2 shows that as the time-constant (τ) is increased by a factor of ten, the critical frequency (Fc) will decrease by a factor of ten. Therefore, we can expect that for the spectral IP response of polarizable sources (Fc) will be inversely proportional to (τ).

An understanding of the physical parameters that affect the time-constant (τ) of a spectral IP response has come from two areas of research. One is the study of the spectral IP response from artificial rocks; these samples are prepared using metallic particles of known material and size (see Figure 8 for example). The second line of attack has been to formulate the mathematical expressions that might describe the macro-characteristics of conduction in a mineralized rock, with certain simplifying assumptions. Initially spherical particles were assumed for this work and an example of the predicted spectral results is shown on Figure 7.

We have shown these two different sets of data, because they are very similar in character. Further, they show the same result that all of

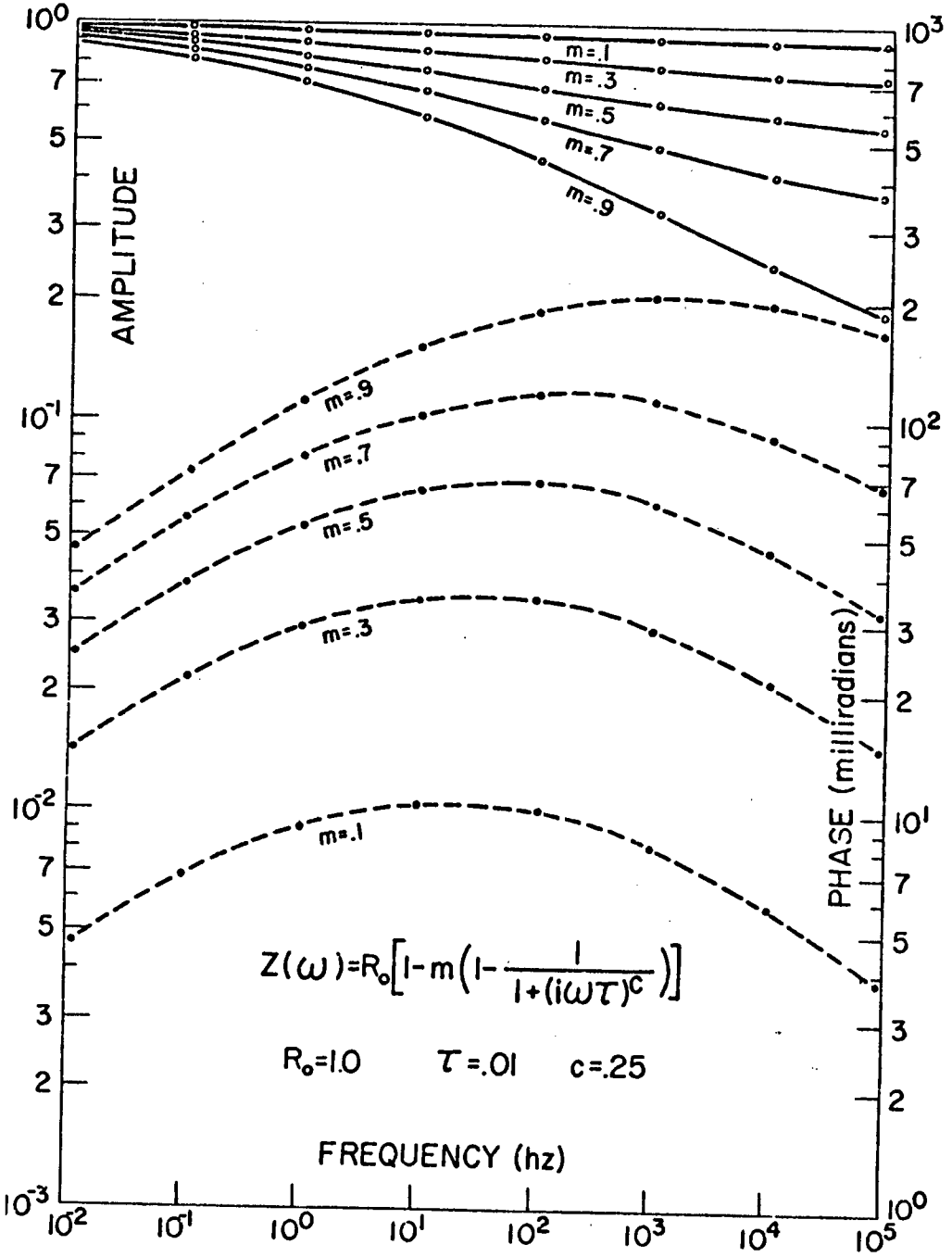

AMPLITUDE
PHASE (milliradians)
m=.1
m=.3
m=.5
m=.7
m=.9
m=.9
m=.7
m=.5
m=.3
m=.1
$Z(\omega)=R_o\left[1-m\left(1-\frac{1}{1+(i\omega\tau)^c}\right)\right]$
R_o=1.0 τ=.01 c=.25
FREQUENCY (hz)

FIG. 2

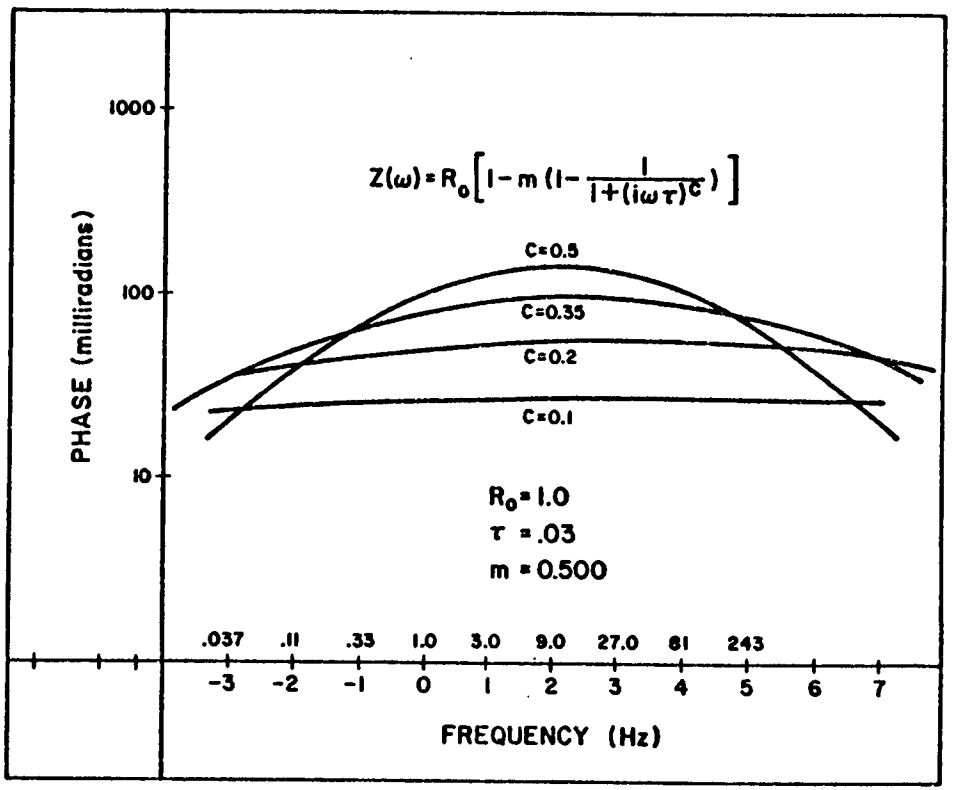

PHASE (milliradians)
1000
100
10
$Z(\omega)=R_o\left[1-m\left(1-\frac{1}{1+(i\omega\tau)^c}\right)\right]$
C=0.5
C=0.35
C=0.2
C=0.1
R_o=1.0
τ=.03
m=0.500
.037 .11 .33 1.0 3.0 9.0 27.0 81 243
-3 -2 -1 0 1 2 3 4 5 6 7
FREQUENCY (Hz)

FIG. 3

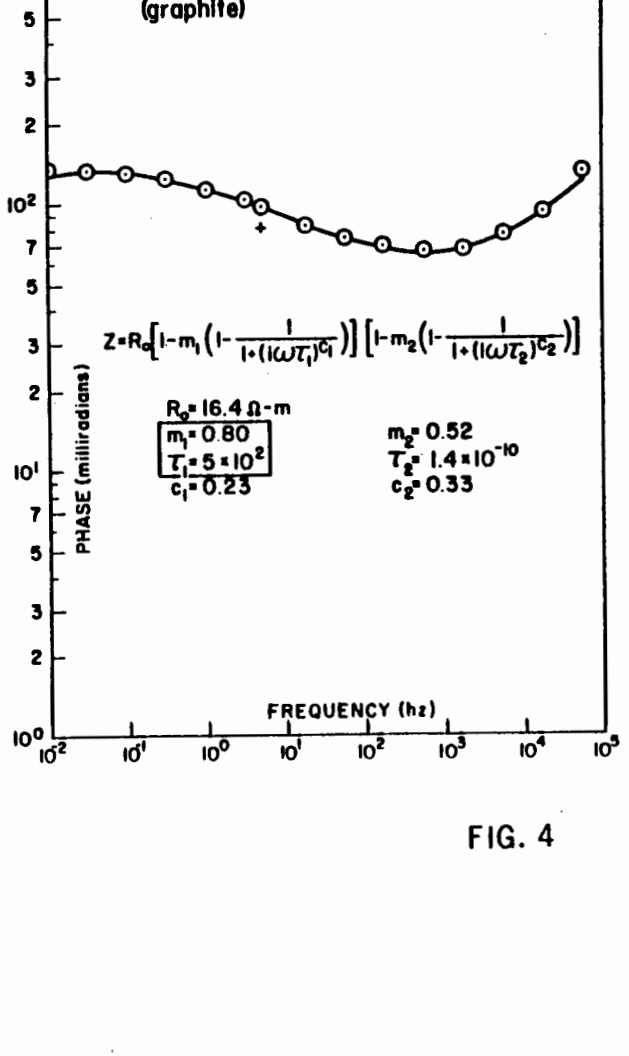


FIG. 4

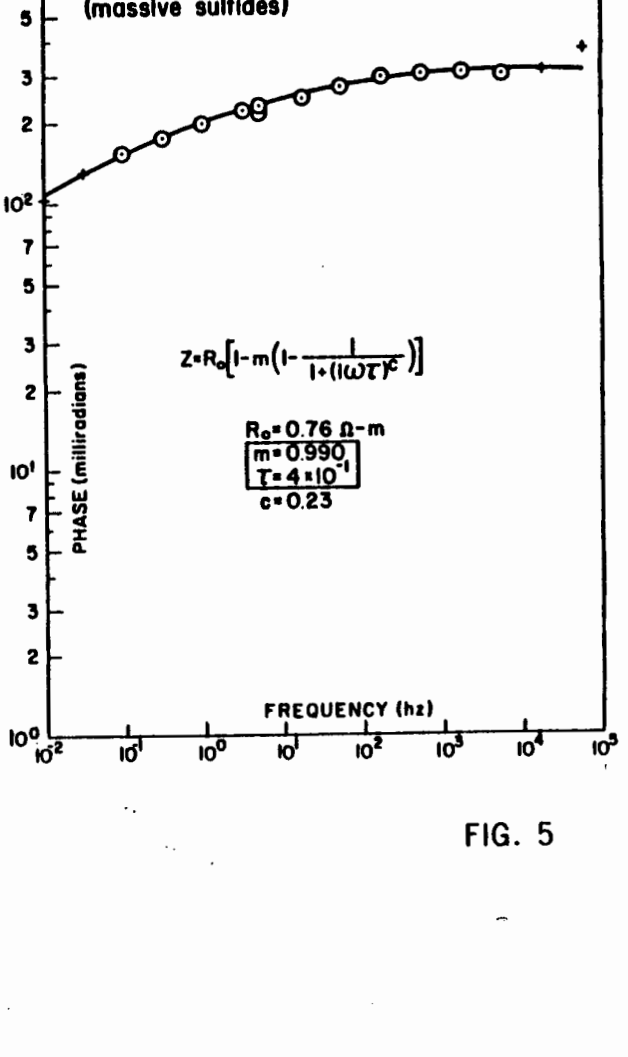


FIG. 5

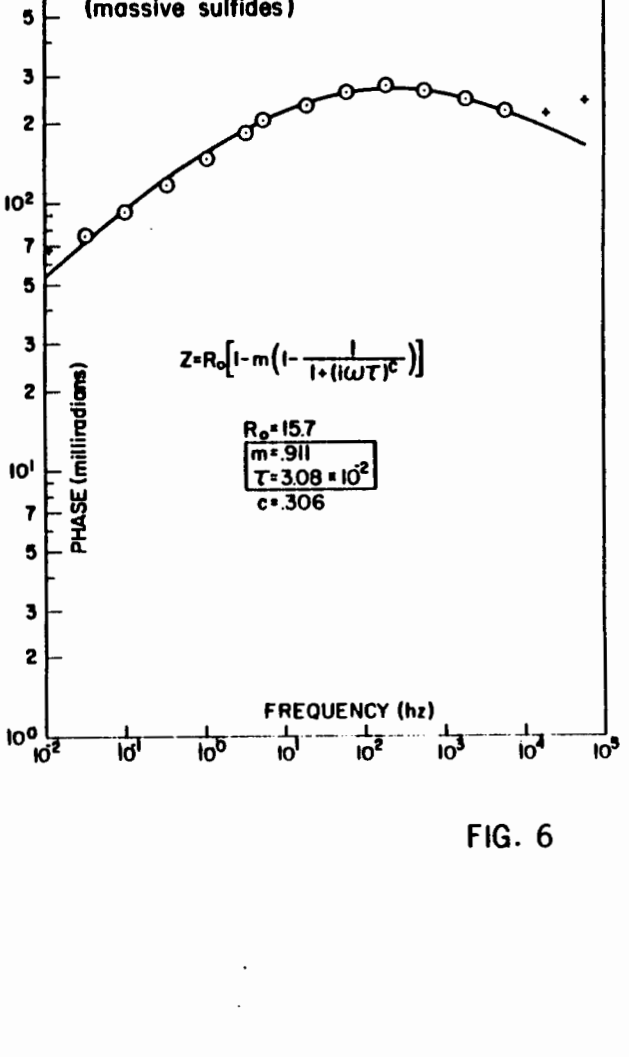
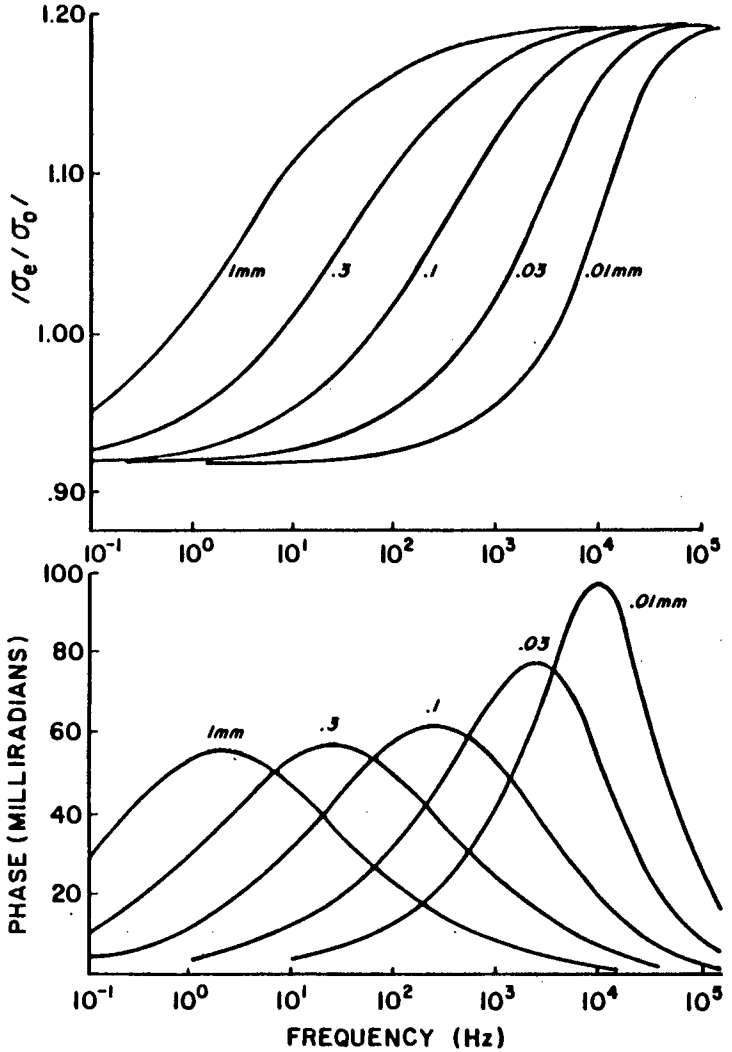


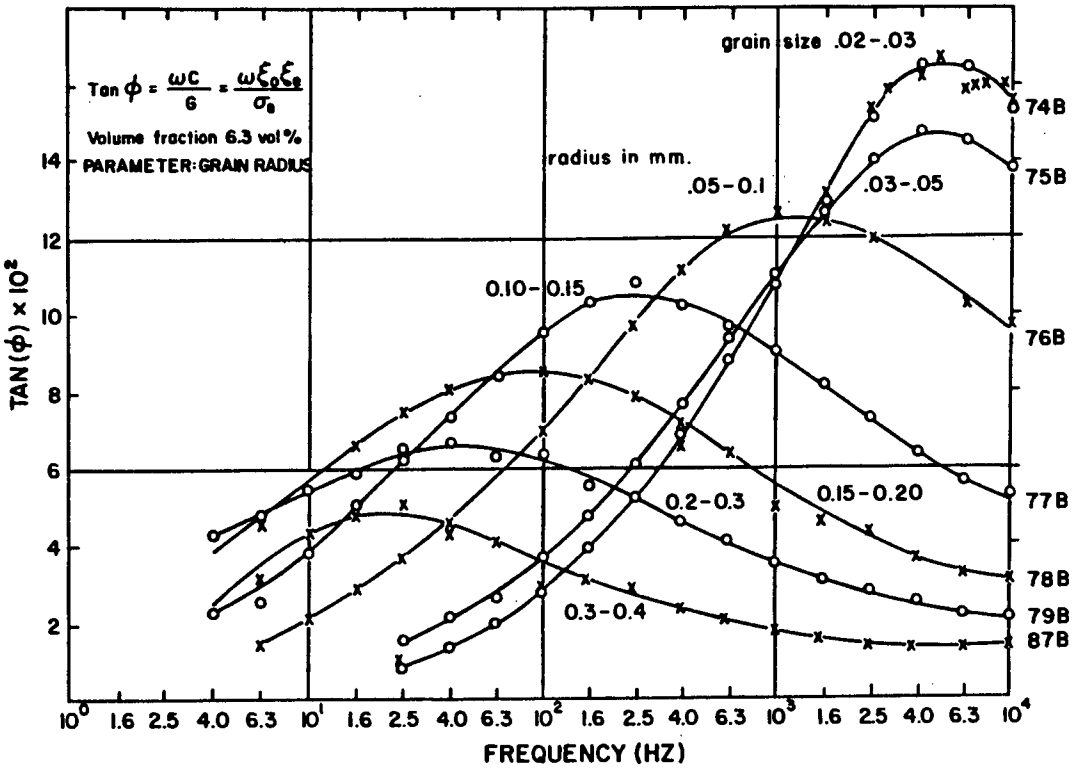
FIG. 6

THEORETICAL RESULTS FOR VARIATION IN GRAIN SIZE OF POLARIZABLE PARTICLE



from Wong

FIG. 7



from Wong
data by Grissemann

FIG. 8

our research has shown. The time-constant (τ) of a spectral IP dispersion curve is directly related to the physical size of the metallic particles that are the source of the IP effect. The critical (Fc) is therefore inversely related to the grain-size. Thus, for all of the massive sulphide deposits for which we have spectral measurements, the effective grain-size of the polarizable particles is appreciably smaller than that for graphite sources.

There is one additional test we have devised to confirm the validity of the electrochemical model we have developed to describe the detailed nature of the IP phenomenon. The spectral IP results for a single mineral electrode (pyrite, chalcopyrite, bornite, galena, etc.) immersed in distilled water can be measured, and then inverted using the computer. This inversion determines the various electrical parameters that describe the electrical transfer function for that particular mineral. These electrical parameters, and the analytically determined concentrations of the metal cation in the solution after steady-state current flow has been achieved, can be used to calculate the reaction valence (total number of electrons involved) of the chemical reaction at the interface. This measured value of the reaction valence can be compared to the various values that would be possible from various chemical reactions.

In past research, these measured numbers have not agreed within an order of magnitude with those predicted by the commonly accepted dissolution reaction equations for the various sulphide minerals. The results we have achieved for galena (Figure 10) and chalcopyrite (Figure 9) are typical of the work that has been done recently. The measured values of the reaction valence give much closer agreement to the predicted valence than was previously the case. For chalcopyrite, the predicted reaction varies with the copper ion concentration, and the agreement is still quite acceptable.

With the success of the above described research, has come the implication that we may now understand the IP phenomenon well enough to use some of our knowledge in a predictive way. The resistivity and phase-shift data plotted in the pseudo-section format on Figure 11 are from the Kennedy Property near Winnemucca, Nevada. The results suggest a broad, weak IP anomaly that might be due to a "porphyry copper" type source containing a small concentration of metallic mineralization. However, one notices immediately that the phase-shifts measured at 9.0 Hz are the same magnitude as those measured at 0.11 Hz (a factor of 3^{-4} lower in frequency). This is the same Spectral IP characteristic that was previously measured at the Brenda Mine in British Columbia.

This unusual circumstance is confirmed by the spectral plots for two typical dipole pairs, shown in Figure 12 and Figure 13. With the inductive coupling effects removed by computer inversion, the phase-shift vs. frequency curve is very flat over a frequency range of 3^{8}Hz. This requires a very low (c_1) value of 0.125 (see Figure 3); more importantly, a value of IP effect (m) in excess of 0.500 is necessary. Therefore, although the measured phase-shifts are low in magnitude, the true IP effect within the source material must be large. This should not be considered to be a weak anomaly.

CHALCOPYRITE

$[CuSO_4]$ 0	10^{-5}	10^{-4}	10^{-3}	Reaction Valence
4.6				
3.5	1.5	.95	.53	Measured
3.6				
4.0	1.33	1.33		Actual

$$CuFeS_2 \longleftrightarrow Cu^{2+} + Fe^{2+} + 2S + 4e^-$$

$$\frac{2}{3}\,CuFeS_2 + Cu^{2+} + \frac{4}{3}e^- \longleftrightarrow \frac{1}{3}\,Cu_5FeS_4 + \frac{1}{3}\,Fe^{2+}$$

(Wadsworth, 1980)

FIG. 9

GALENA

[NaCl] 0.10	Reaction Valence
1.6	
1.6	Measured
2.0	Actual

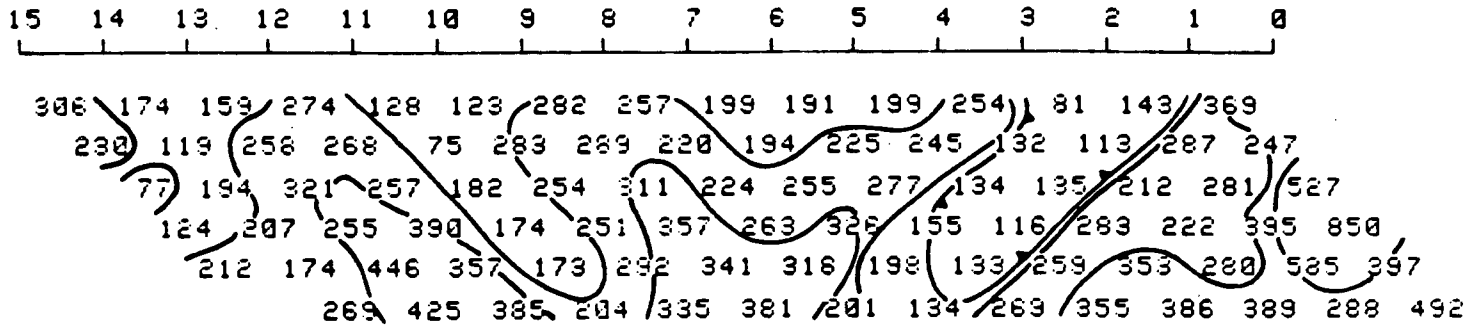
$$PbS \longleftrightarrow Pb^{2+} + S^0 + 2e^-$$

(Sato, 1960)

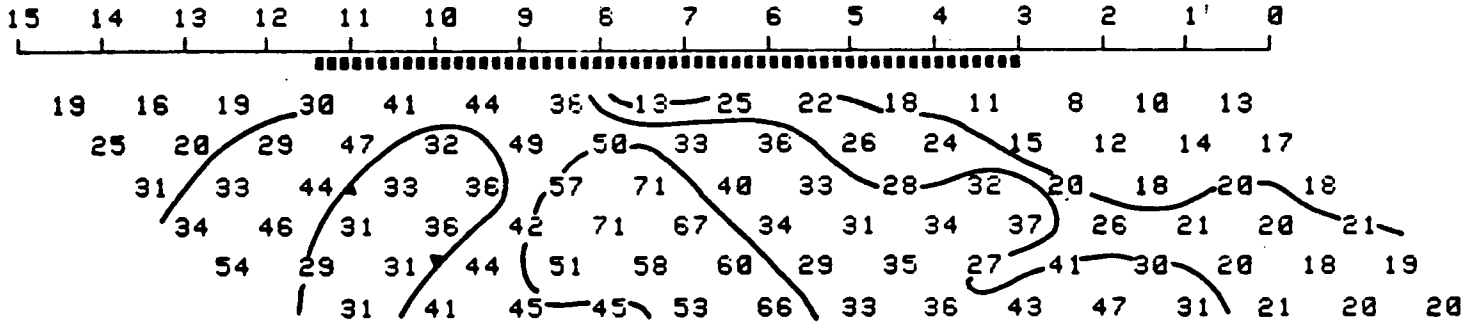
FIG. 10

W A BOWES KENNEDY AREA WINNEMUCCA NEVADA X=200 JUNE 1979

Apparent Resistivity(ohm-m)



Decoupled Phase(mrad) 9 Hz



Decoupled Phase(mrad) .1111 Hz

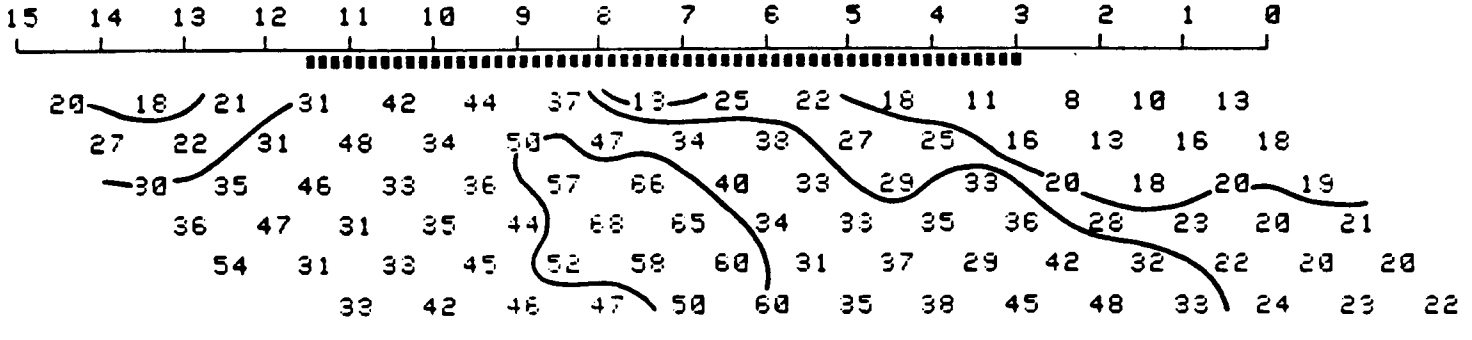
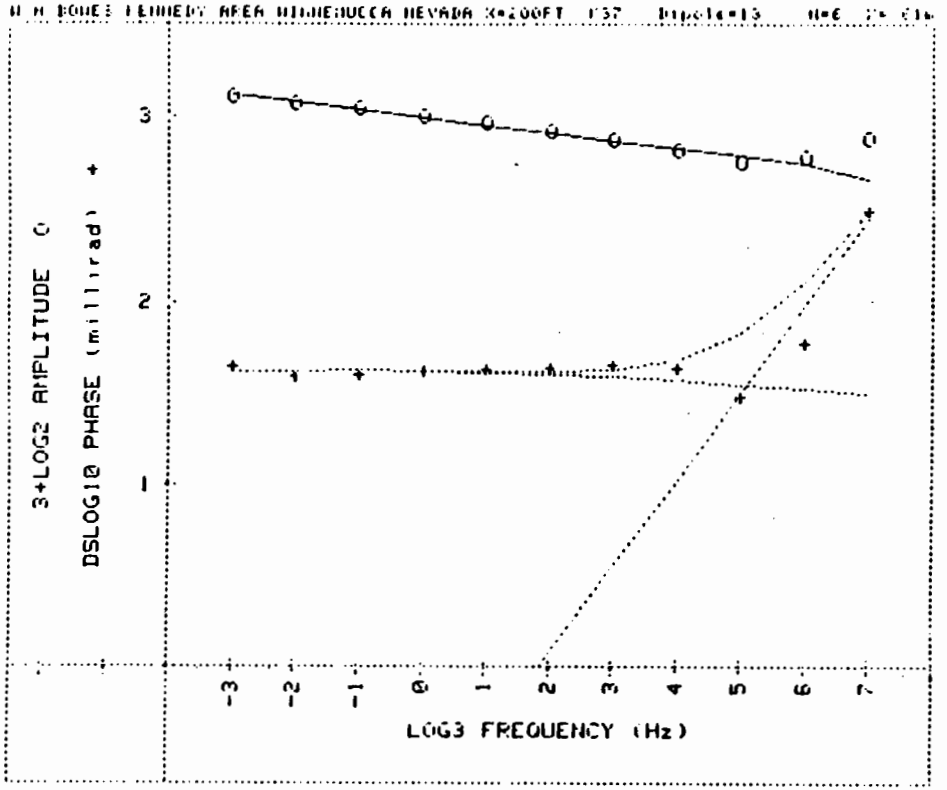


FIG. 11



Iter	Lambda	Rchsq	P0	M1	T1	C1	M2	T2	C2
0	1.E-02	.00068	1.599	.587	2.0E+01	.125	1.000	2.0E-05	.992
1	1.E-01	.00064	1.599	.586	2.0E+01	.125	1.000	2.1E-05	1.000
2	1.E+00	.00063	1.596	.584	2.0E+01	.125	1.000	2.1E-05	1.000
3	1.E+00	.00063	1.595	[.583]	2.0E+01	[.125]	1.000	2.1E-05	1.000
Pct Std Deviations			5.4	1.6	499.4	0.0	0.0	10.5	9.6

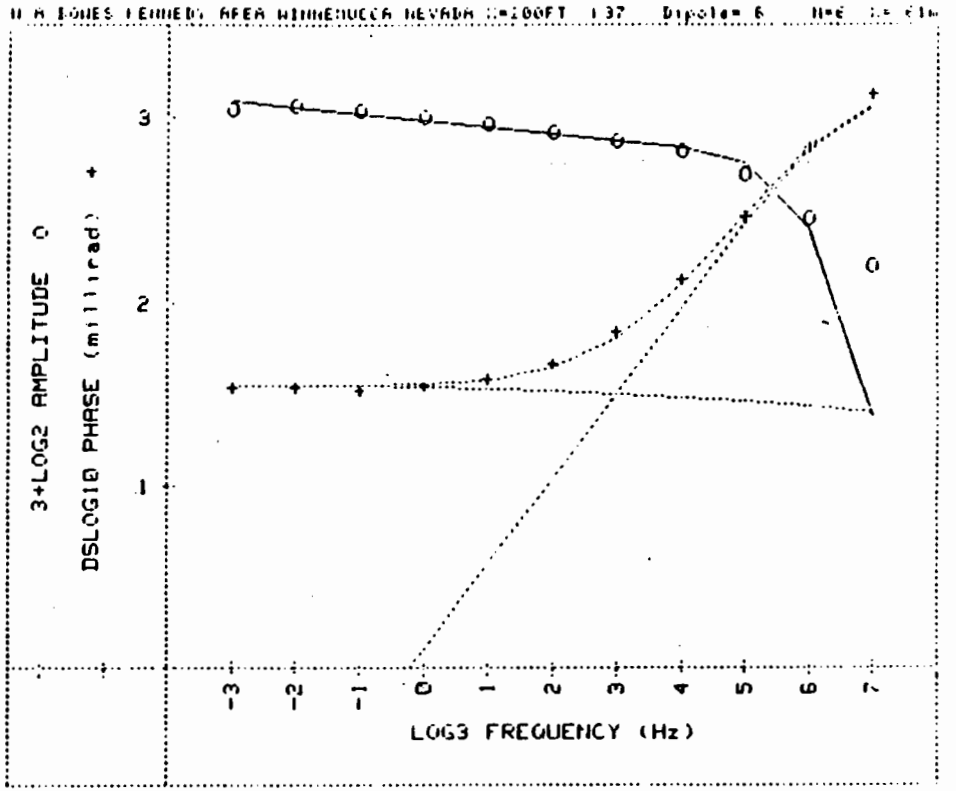
Correlation Matrix

1.0000						
.5235	1.0000					
.9782	.3667	1.0000				
0.0000	0.0000	0.0000	0.0000			
0.0000	0.0000	0.0000	0.0000	0.0000		
-.3604	.0864	-.3990	0.0000	0.0000	1.0000	
-.6447	.0924	-.7125	0.0000	0.0000	.7305	1.0000

Apparent Resistivity Measured at 1 Hz is 425

Apparent Resistivity Calculated from Inductive Coupling is 2117

FIG. 12



Iter	Lambda	Rchsq	P0	M1	T1	C1	M2	T2	C2
0	1.E-02	.00102	1.482	.517	2.0E+01	.125	1.000	1.8E-04	.977
1	1.E-02	.00102	1.481	[.518]	1.9E+01	[.125]	1.000	1.8E-04	.978
Pct Std Deviations			6.7	2.6	1243.0	0.0	0.0	5.4	2.0

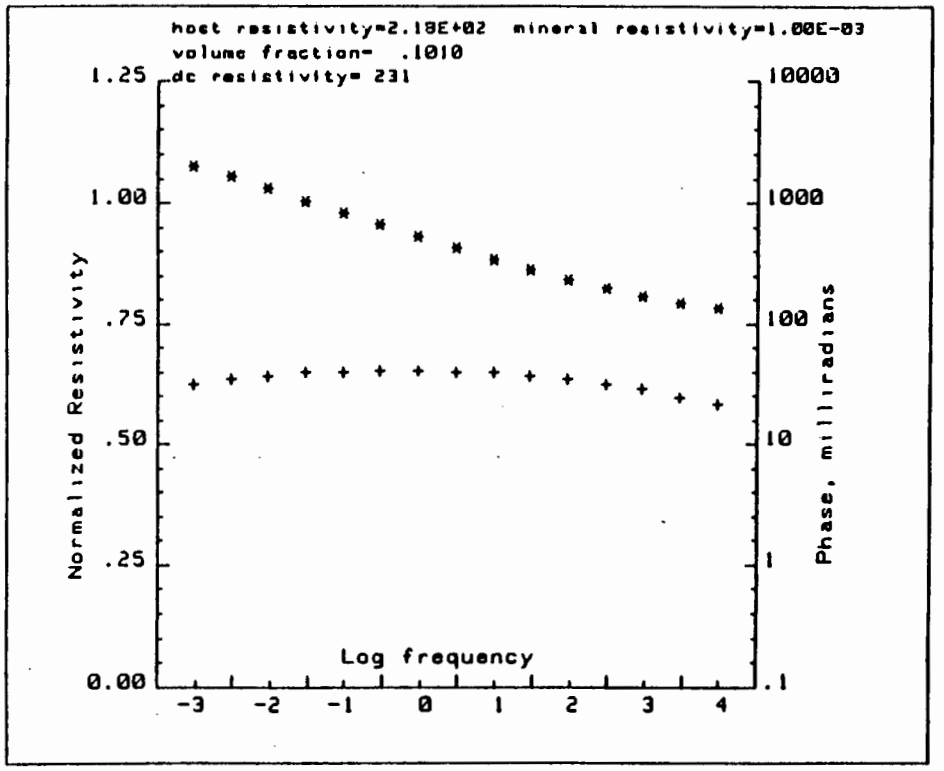
Correlation Matrix

1.0000						
.6234	1.0000					
.9760	.4857	1.0000				
0.0000	0.0000	0.0000	0.0000			
0.0000	0.0000	0.0000	0.0000	0.0000		
.1989	.0726	.2067	0.0000	0.0000	1.0000	
-.4224	.0478	-.4506	0.0000	0.0000	.4189	1.0000

Apparent Resistivity Measured at 1 Hz is 201

Apparent Resistivity Calculated from Inductive Coupling is 235

FIG. 13


host resistivity=2.18E+02 mineral resistivity=1.00E-03
volume fraction= .1010
dc resistivity= 231
Normalized Resistivity
Phase, milliradians
Log frequency
1.25
1.00
.75
.50
.25
0.00
10000
1000
100
10
1
.1
-3 -2 -1 0 1 2 3 4

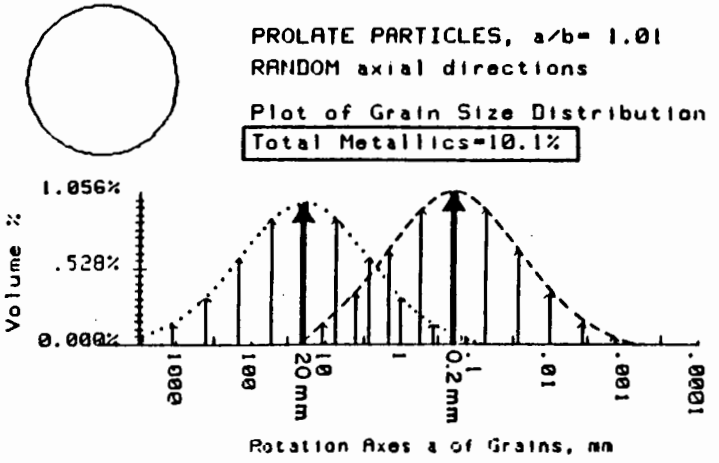
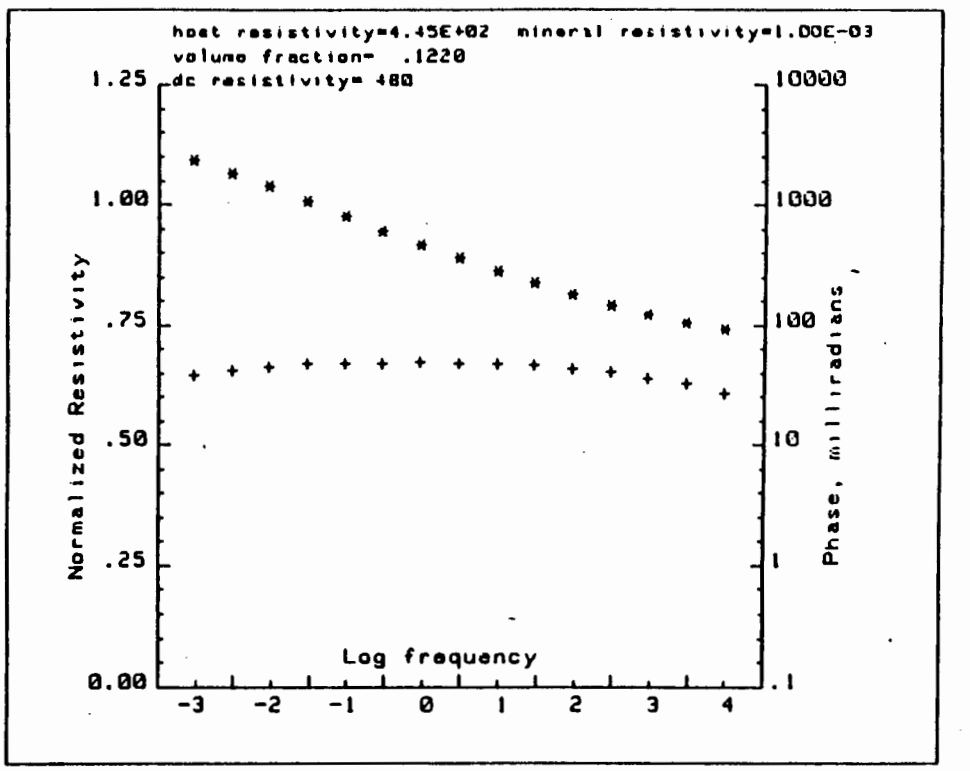

PROLATE PARTICLES, a/b= 1.01
RANDOM axial directions
Plot of Grain Size Distribution
Total Metallics=10.1%
Volume %
1.056%
.528%
0.000%
1000
100
20mm
10
1
0.2mm
.1
.01
.001
.0001
Rotation Axes a of Grains, mm

FIG. 14


host resistivity=4.45E+02 mineral resistivity=1.00E-03
volume fraction= .1220
dc resistivity= 480
Normalized Resistivity
Phase, milliradians
Log frequency
1.25
1.00
.75
.50
.25
0.00
10000
1000
100
10
1
.1
-3 -2 -1 0 1 2 3 4

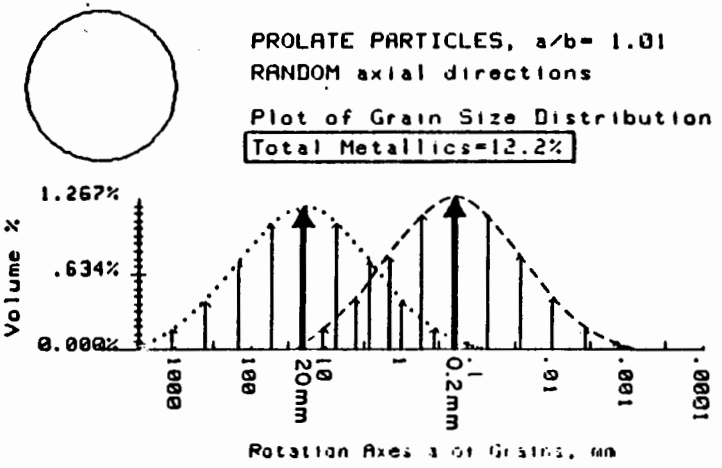

PROLATE PARTICLES, a/b= 1.01
RANDOM axial directions
Plot of Grain Size Distribution
Total Metallics=12.2%
Volume %
1.267%
.634%
0.000%
1000
100
20mm
10
1
0.2mm
.1
.01
.001
.0001

FIG. 15

We used these results in our first attempt to predict the nature of the mineralization that is the source of the "weak" anomaly shown in Figure 11. The mathematical formula used to predict the spectra shown in Figure 7 has been expanded to include prolate and oblate spheroids, as well as spheres, of metallic material. By a trial and error process, the spectra shown in Figure 14 and Figure 15 were generated as being a "good fit" to the measured data.

The chosen parameters for the sources are probably not unique; however, some valid points can be drawn from the calculation presented.

i) the flat spectrum (small c value) cannot be obtained from a single grain-size (time-constant) population. There must be at least two different grain-size populations present.

ii) Although the two grain-size distributions, with mean values of 20mm and 0.2mm, are probably not exactly correct, a difference of at least two orders of magnitude is necessary to produce the value c = 0.125.

iii) Despite the low magnitude for the IP field anomaly, the true IP effect within the source is large ($m_1 > 0.500$) and this results in a fairly high concentration of metallic mineralization predicted for the source (10 - 12% total metallic mineralization).

The first drill hole at the Kennedy Project is now nearing completion; it was collared at approximately station No. 5 along the line of data shown in Figure 11. There was metallic mineralization throughout the drill hole, with an increase below about 75-80 meters of depth.

Throughout the entire length of the drill hole (in excess of 250 meters), there were two different types of mineralization present. There were veinlets (large grain-size) that might, or might not, contain quartz. All of the veinlets contained chalcopyrite or molybdenite or chalcopyrite with molybdenite; some pyrite was also present. There was also fine-grained disseminated metallic magnetite throughout the hole (the small grain-sized source). The magnetite contains appreciable gold value; there is enough gold present to give detectable assays throughout the length of the hole.

We do not have enough information to determine if the total concentration of metallic mineralization approaches 10 to 12 percent. However, in other respects the source of the IP anomaly does seem to approximate that predicted by the spectral IP analysis.

IMPROVED MEASUREMENT TECHNIQUES AND INSTRUMENTATION

The much publicized "explosion" in solid-state, semi-conductor

electronic components has produced as many changes in the geophysical instrumentation industry as it has in other phases of modern life. Beginning with diodes and transistors and now including complex microprocessor chips, there has been a bewildering number of improvements in this industry. They have resulted in a major reduction in the size of, and the power requirements of (smaller battery packs), geophysical field instruments; at the same time the reliability, digital data storage capability and analysis capability have been almost infinitely increased.

The Phoenix IPV-2, Prospecting Phase IP system is an example of one of the least complicated units that can be engineered with modern electronics. The types of features that can now be made available are:

i) Microprocessor-controlled signal stacking of each measurement to give almost infinite noise rejection through coherent detection.

ii) Matched, heated crystal clocks give phase stability between current source and voltmeter without connecting cable.

iii) Dual-channel electronics permits two separate voltages to be measured simultaneously.

iv) Digital readout of magnitude and phase-shift of measured voltage at either channel.

v) Five frequency capability (0.11, 0.33, 1.0, 3.0, 9.0 Hz) permits limited analysis of spectral character of any anomaly.

vi) Appreciable increase in survey speed over either frequency-domain or time-domain IP systems.

By completing a reconnaissance survey with a single frequency (typically 0.33 Hz or 1.0 Hz) it is possible to achieve the lowest cost possible for IP field surveys. However, once an anomaly is detected, the IPV-2 can be used to make detailed measurements that give some feeling for the character of the spectral response of the source.

If detailed measurements are made at only two frequencies, it is possible to make some statement about the critical frequency (Fc) of the IP spectrum from the source. On Figure 17 and Figure 18 are shown the detailed phase-IP measurements made using X = 100' and 0.33 Hz over two anomalies previously located by a reconnaissance IP survey using larger electrode intervals. On both Line 18E and Line 15E the anomalous pattern indicates a relatively narrow source, with some depth to the top.

During the detailed survey with X = 100', several of the anomalous values in each anomalous pattern were measured at both 0.33 Hz and 3.0 Hz.

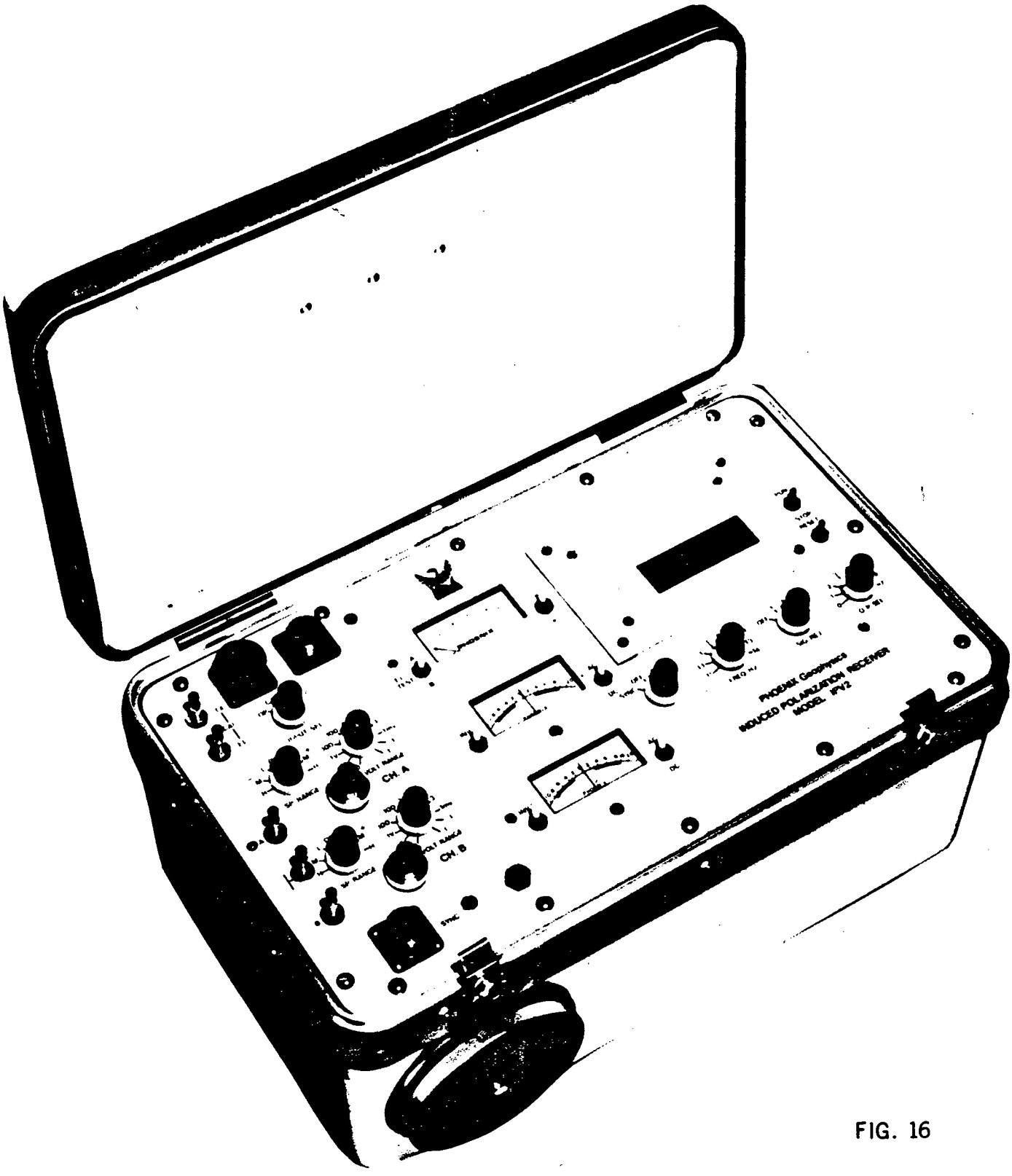

PHOENIX Geophysics
INDUCED POLARIZATION RECEIVER
MODEL IPV2
CH. A
CH. B

FIG. 16

PRICE COMPANY BLOCK NO.8 PROPERTY
IPV-2 PHASE IP TEST

LINE-18E

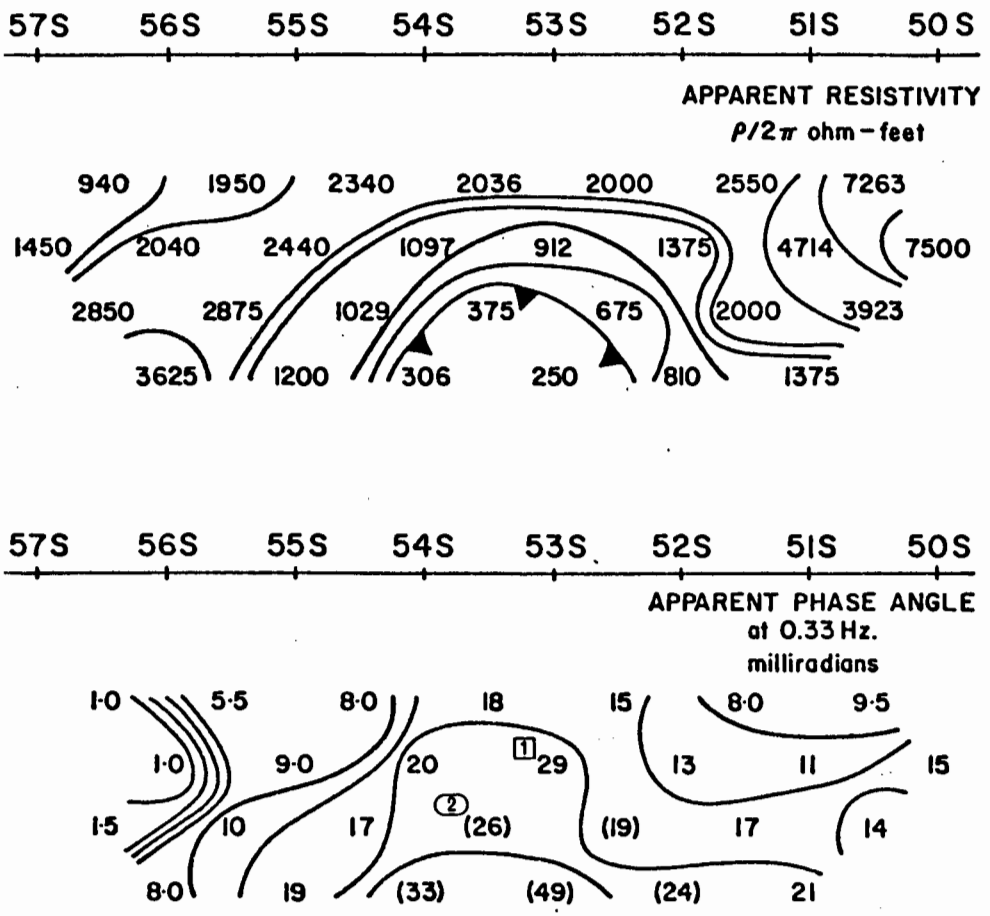


FIG. 17

PRICE COMPANY BLOCK NO.8 PROPERTY
IPV-2 PHASE IP TEST

LINE-15E

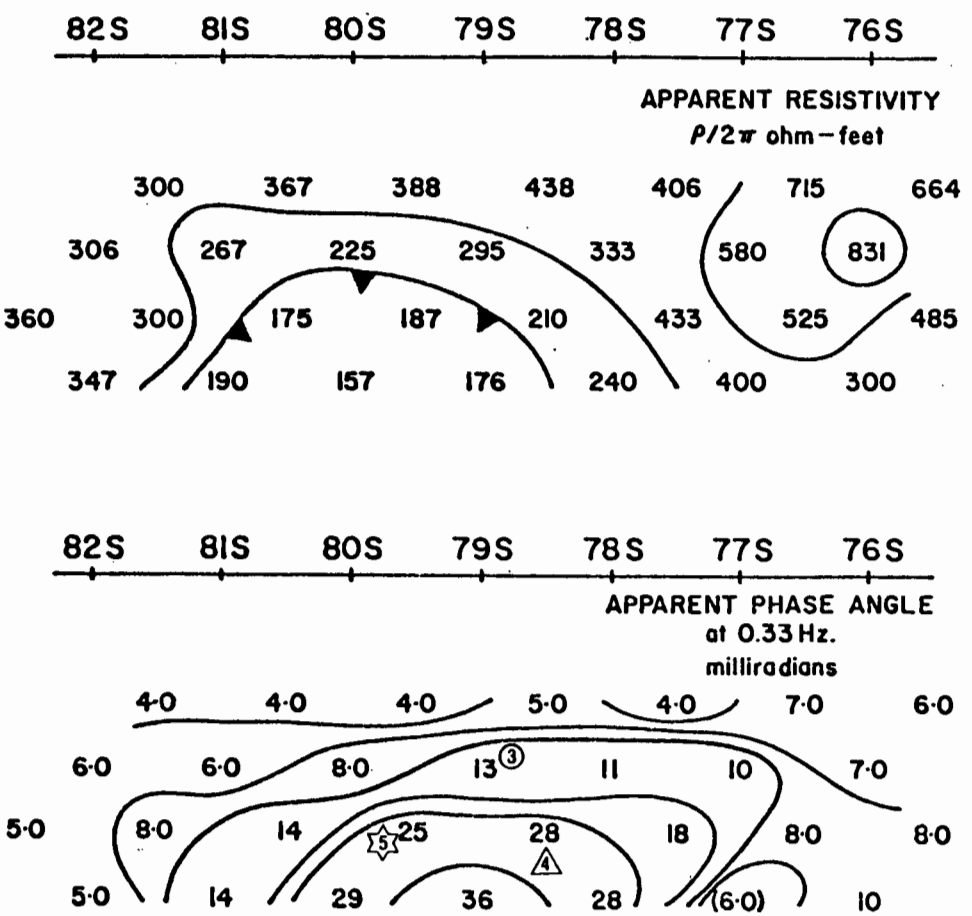


FIG. 18

The results are shown on Figure 19 and Figure 20. On Line 18E, the apparent phase values measured increase with frequency, indicating a value for Fc above 3.0 Hz. On Line 15E the apparent phase values were decreasing with frequency, indicating a value for Fc that is below 0.33 Hz.

The relationship we have established between the critical frequency (Fc) - the time constant (τ) - and the grain-size of the polarizable particles, coupled with our experience over known zones suggests that the grain-size of the source of the anomaly on Line 18E is appreciably smaller than the grain-size of the source of the anomaly on Line 15E.

Our expectation that the large grain-size source is more likely to be graphite is confirmed by the drilling of the two anomalies. The anomaly on Line 18E was found to be due to massive sulphide mineralization; the source of the anomaly located on Line 15E was a graphitic tuff zone, with small concentrations of pyrite.

If field time is taken to make measurements at all five frequencies, it is possible to make a more formal presentation of the spectral characteristics of two anomalies. On Figure 21, is shown a computer-plotted pseudo-section of a single line of phase IP data. The plot shows the apparent resistivity value and the apparent phase value (1.0 Hz) measured for each dipole pair. At the lower part of the data plot is shown the short (five frequency) spectrum (normalized to the value at 1.0 Hz) for each dipole pair.

In this case, the two anomalous zones had a considerable strike length, in an area where the surface was largely covered. The electrical parameters of the two sources were much the same; however, as shown on Figure 21, the source of Zone I is clearly different from the source of Zone II. From drilling, it is known that Zone I is due to a broad, irregular zone of pyrite and sphalerite (with appreciable silver) in a tuffaceous rock unit. The source of Zone II is pyrrhotite in an adjoining andesite rock unit.

Another example of a difference in spectral character is shown in Figure 22. In this location, the source of Zone A had been traced for a considerable distance along strike. Zone B was detected only on two adjacent lines. The difference in spectral character strongly suggests that Zone B is not merely a greater width to the mineralized zone that is the source of Zone A.

The Phoenix IPV-3, Spectral IP Receiver is the most advanced induced polarization receiver ever put into field operation (Figure 23). It completely replaces a truck-mounted system that was assembled largely from off-the-shelf computers, voltmeters, oscilloscopes, etc. The entire system is controlled by the Phoenix CP-1, geophysical computer, that was designed especially for this function. Through an FM-modulated link, the CP-1 also controls the spectral IP current source. Some of the more important features of the IPV-3 are:

i) Six simultaneous voltage channels plus current monitor.

LINE-18E $R\Phi_{0.3-3.0}$ TEST

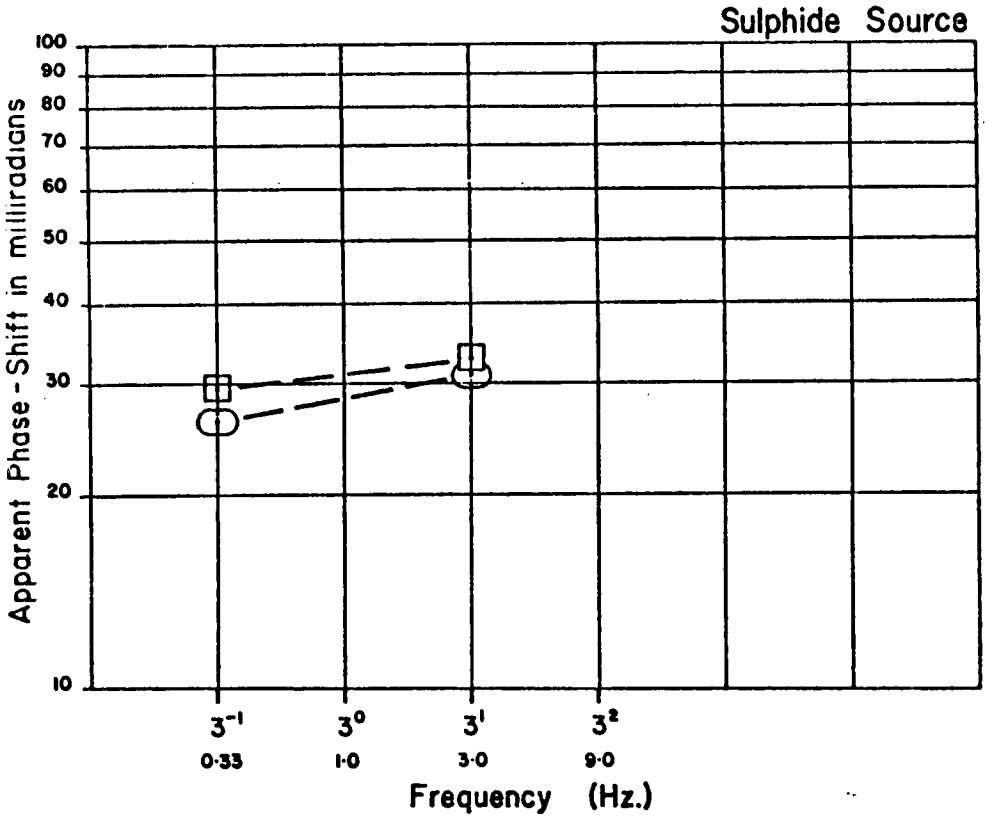


FIG. 19

LINE-15E $R\Phi_{0.3-3.0}$ TEST

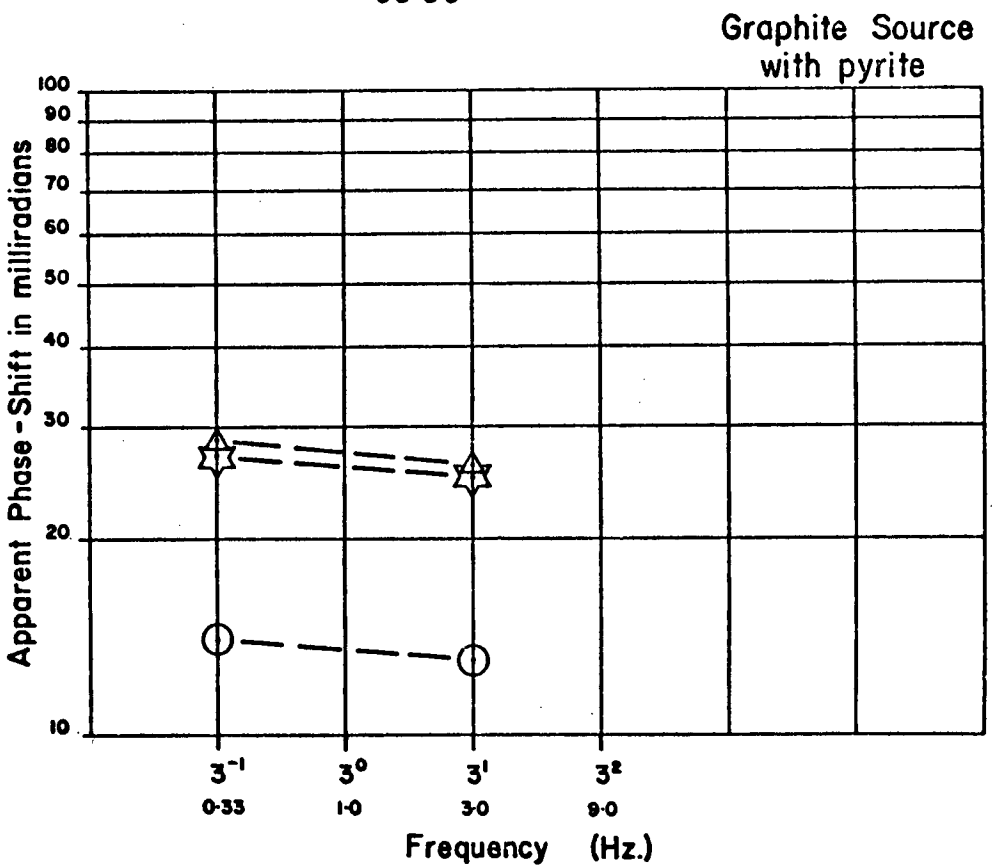


FIG. 20

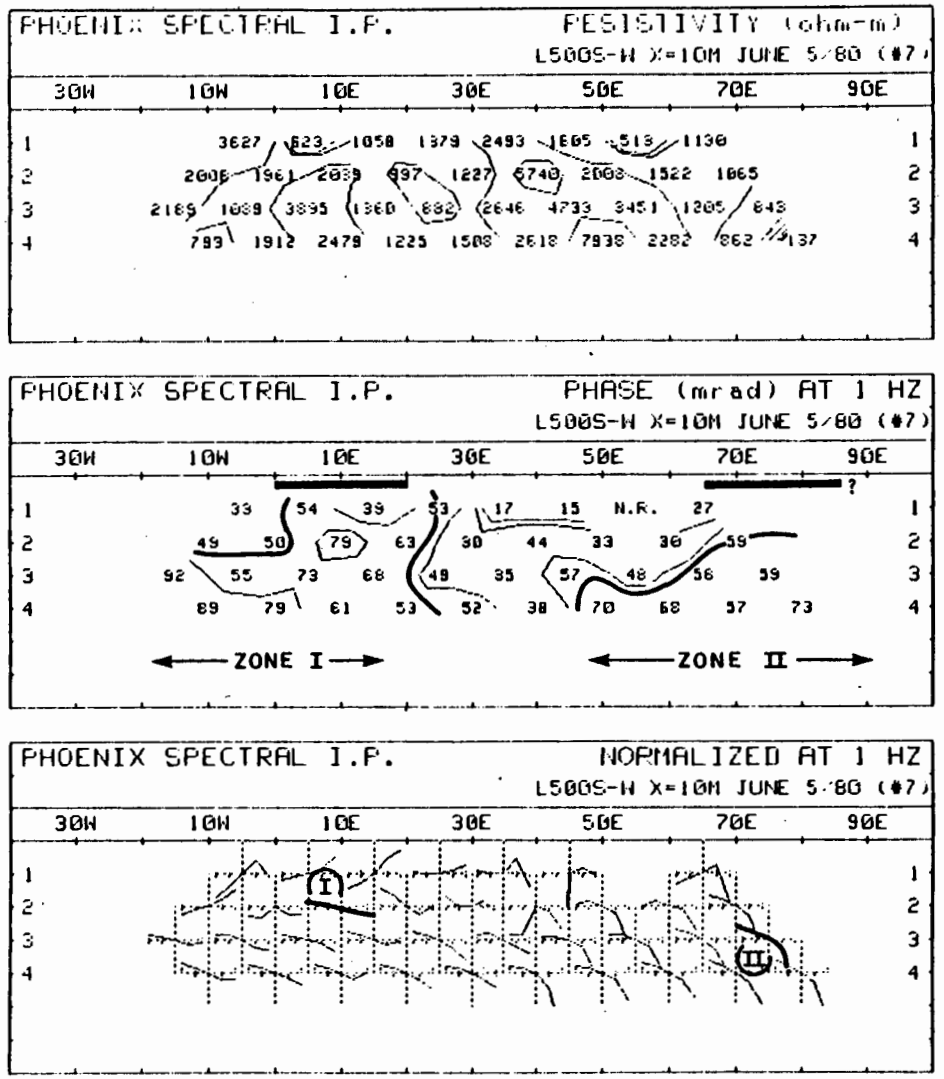

PHOENIX SPECTRAL I.P.
RESISTIVITY (ohm-m)
L500S-W X=10M JUNE 5/80 (#7)
30W 10W 10E 30E 50E 70E 90E
1 3627 823 1058 1379 2493 1805 513 1130
2 2008 1961 2039 697 1227 6740 2008 1522 1865
3 2185 1089 3895 1360 882 2646 4733 3451 1205 843
4 793 1912 2479 1225 1508 2618 7938 2282 862 137
PHOENIX SPECTRAL I.P.
PHASE (mrad) AT 1 HZ
L500S-W X=10M JUNE 5/80 (#7)
30W 10W 10E 30E 50E 70E 90E
1 33 54 39 53 17 15 N.R. 27
2 49 50 79 63 30 44 33 36 59
3 92 55 73 68 48 35 57 48 56 59
4 89 79 61 53 52 38 70 68 57 73
ZONE I
ZONE II
PHOENIX SPECTRAL I.P.
NORMALIZED AT 1 HZ
L500S-W X=10M JUNE 5/80 (#7)
30W 10W 10E 30E 50E 70E 90E
I
II

FIG. 21

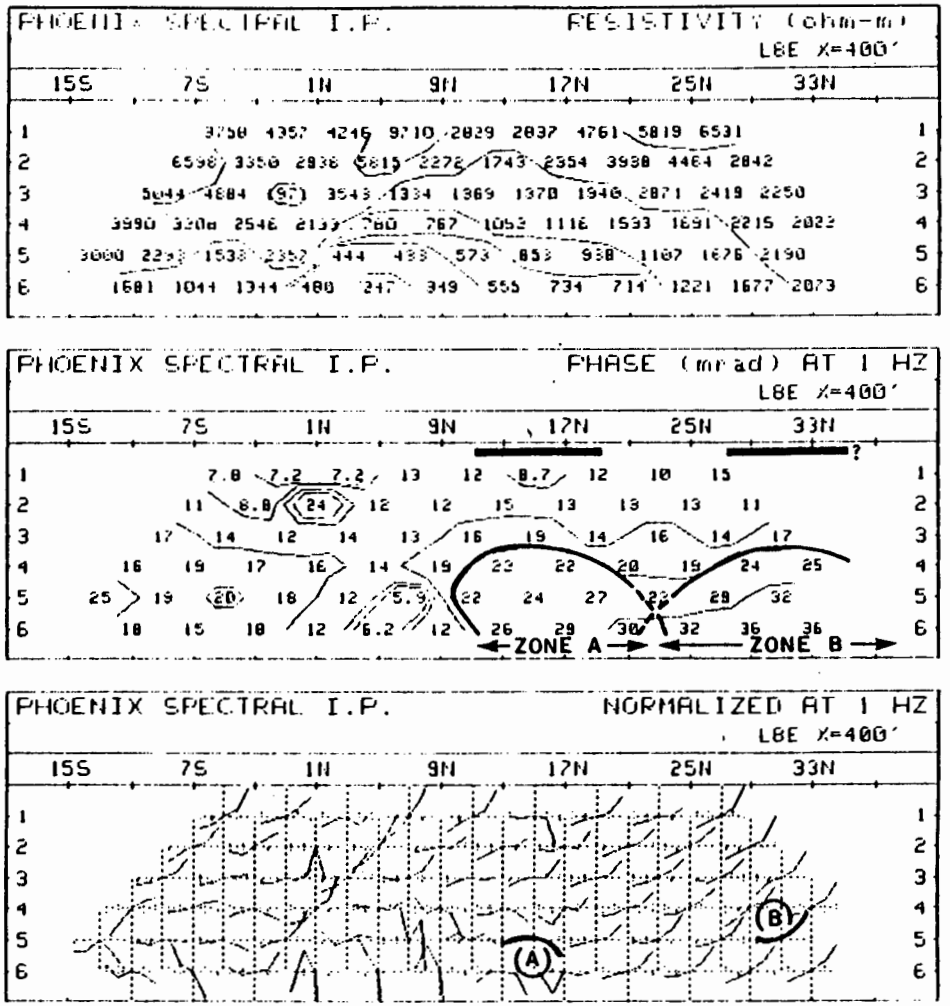

PHOENIX SPECTRAL I.P.
RESISTIVITY (ohm-m)
L8E X=400'
15S 7S 1N 9N 17N 25N 33N
1 3750 4357 4246 9710 2829 2837 4761 5819 6531
2 6598 3350 2838 5815 2278 1743 2354 3938 4484 2842
3 5044 4884 3543 1334 1369 1378 1940 2871 2419 2250
4 3990 3208 2548 2139 780 767 1052 1116 1593 1891 2215 2022
5 3000 2293 1538 2352 444 433 573 853 938 1107 1676 2190
6 1681 1044 1344 480 247 349 555 734 714 1221 1677 2073
PHOENIX SPECTRAL I.P.
PHASE (mrad) AT 1 HZ
L8E X=400'
15S 7S 1N 9N 17N 25N 33N
1 7.8 7.2 7.2 13 12 8.7 12 10 15
2 11 8.8 24 12 12 15 13 13 13 11
3 17 14 12 14 13 16 19 14 16 14 17
4 16 19 17 16 14 19 22 22 20 19 24 25
5 25 19 20 18 12 5.9 22 24 27 28 32
6 18 15 10 12 6.2 12 26 29 30 32 36 36
ZONE A
ZONE B
PHOENIX SPECTRAL I.P.
NORMALIZED AT 1 HZ
L8E X=400'
15S 7S 1N 9N 17N 25N 33N
A
B

FIG. 22

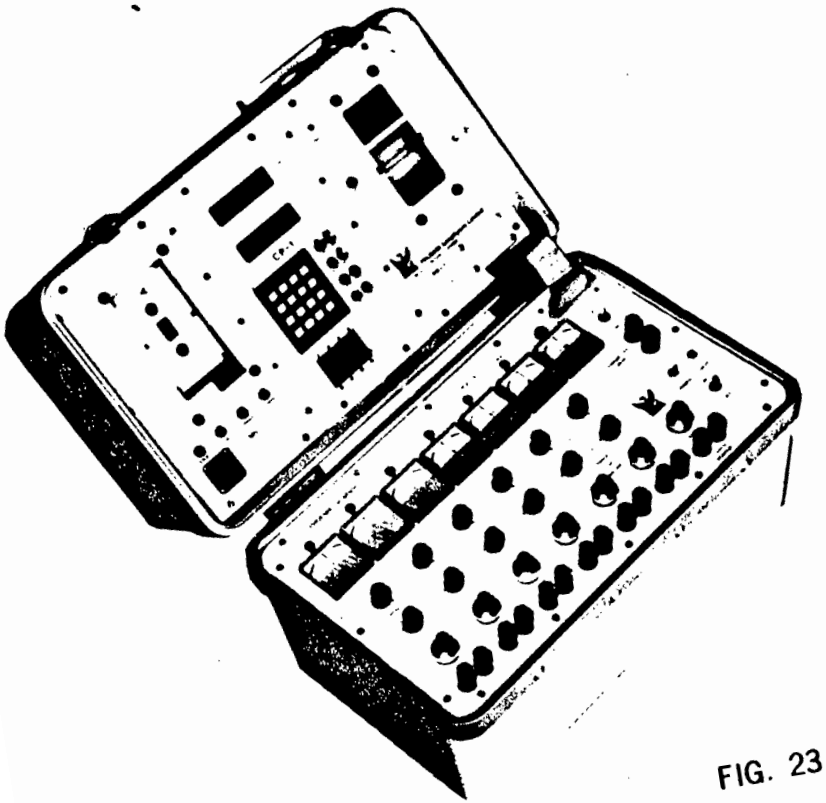


FIG. 23

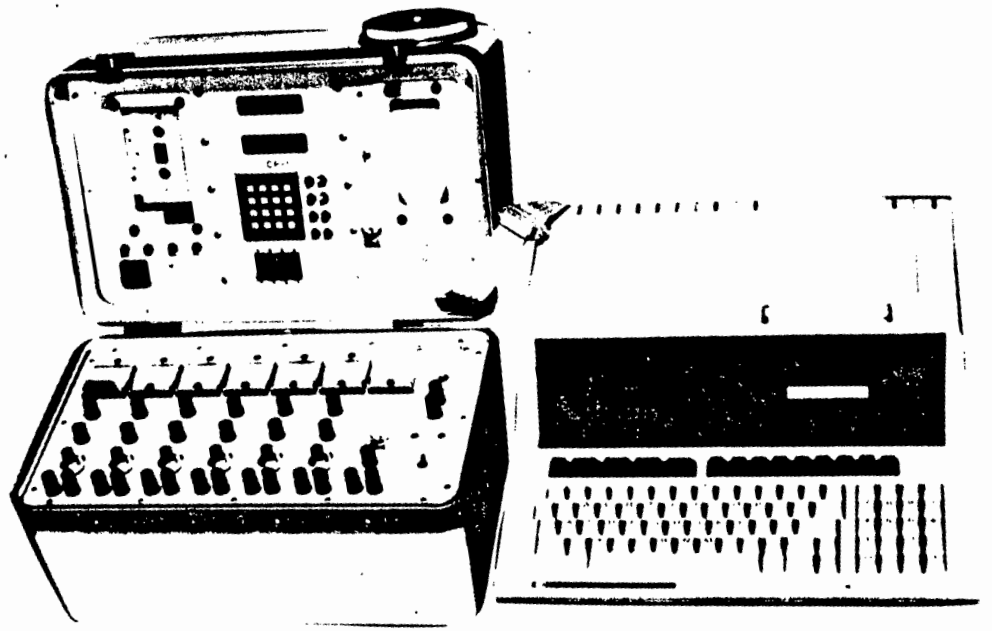


FIG. 24

ii) Frequency range from 2^{-14} Hz (0.00006 Hz) to 2^{+16} Hz (65,536 Hz) with automatic scanning programmable through CP-1.

iii) Real time de-convolution and coherent filtering via use of CP-1.

iv) Field Data available through digital read-out and recorded on paper tape and tape cassette.

v) Field results directly transferrable from tape cassette through CP-1 and interface to computer for analysis and interpretation. (Figure 24).

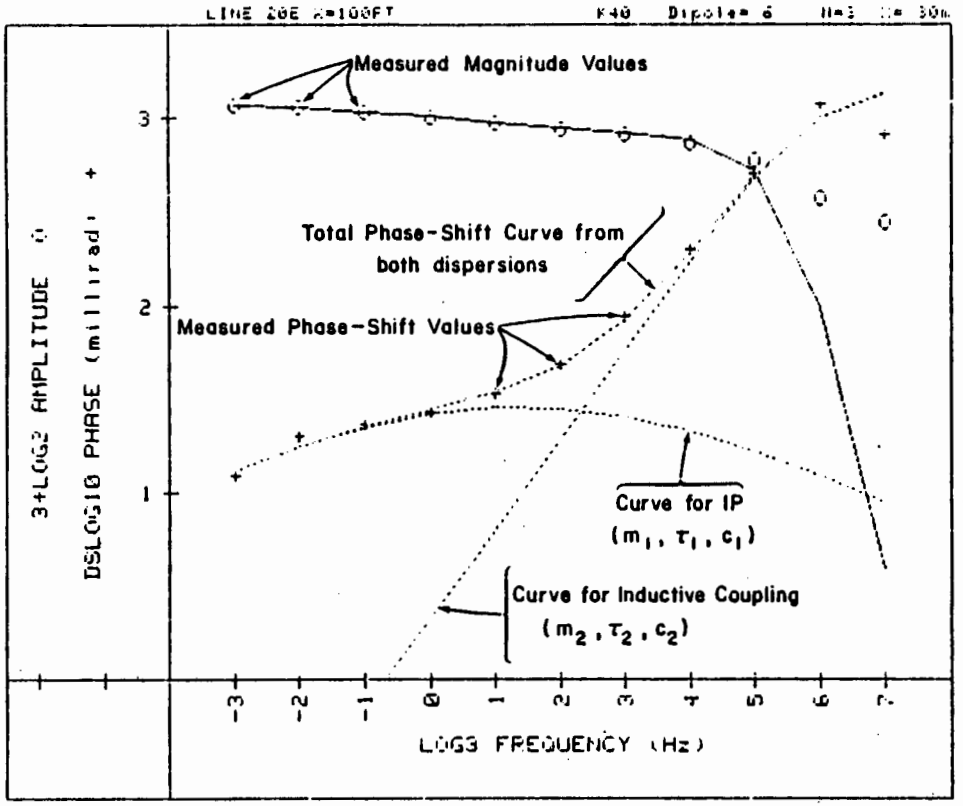
By using the IPV-3 and the HP=85 computer in the field, the geophysicist has at his disposal all of the interpretational power of the spectral IP method. As shown on Figure 25 it is possible to remove the inductive coupling effects from the broad-band spectral IP results. When this information is removed, it is possible to invert the remaining, decoupled IP spectra and determine the apparent values of Ro, m, τ, c for that particular dipole-pair measurement.

For the spectra shown in Figure 25, the values are m = 0.172; c = 0.376; τ = 0.044 sec.; these parameters suggest a small grain-size, and in fact the source is a massive sulphide zone in New Brunswick. The parameter values obtained by inverting the spectral curve from all of the anomalous dipole pairs were essentially the same; we have found this to be universally true if the anomaly is due to a single, more-or-less uniform source.

For the spectral curve shown in Figure 26, the parameter values of the source are m = 0.509; c = 0.180; τ = 540 seconds. The large time-constant confirms the large grain-size for the graphite zone that is the source of the anomaly.

For IP measurements with large electrode intervals in areas of low resistivity (high conductivity) inductive coupling effects will completely distort IP field data. This can happen even for low frequency measurements (in the variable frequency method) or long time delay measurements (in the time domain technique). When the inductive coupling effects are removed from the spectral curve for each dipole pair (as in Figure 12 and Figure 25) the pseudo-section can be reconstructed using the decoupled data.

The data pseudo-section shown in Figure 27 is from the Elura Deposit near Cobar, New South Wales. The resistivity results show a deep, variable high conductivity surface layer. The phase IP measurements at 3.0 Hz with X = 100 meters are completely dominated by inductive coupling effects that essentially depend only upon the electrode separation (n). However, when the inductive effects are removed from the data for each dipole pair, the pseudo-section clearly shows the presence of the massive sulphide zone, at depth, at approximately station 2500E.



				IP EFFECT			INDUCTIVE COUPLING EFFECT		
Iter	Lambda	Rchsq	R0	M1	T1	C1	M2	T2	C2
0	1.E-02	.03405	1.089	.221	4.0E-02	.329	1.000	1.1E-04	1.000
1	1.E-01	.00168	1.063	.196	2.5E-02	.373	1.000	3.6E-04	1.000
2	1.E-03	.00063	1.072	.186	3.1E-02	.355	1.000	3.3E-04	1.000
3	1.E-04	.00067	1.071	.174	4.3E-02	.373	1.000	3.4E-04	1.000
4	1.E-05	.00066	1.071	.172	4.4E-02	.376	1.000	3.4E-04	1.000
Pct Std Deviations			.8	16.4	84.2	13.5	0.0	5.5	0.0

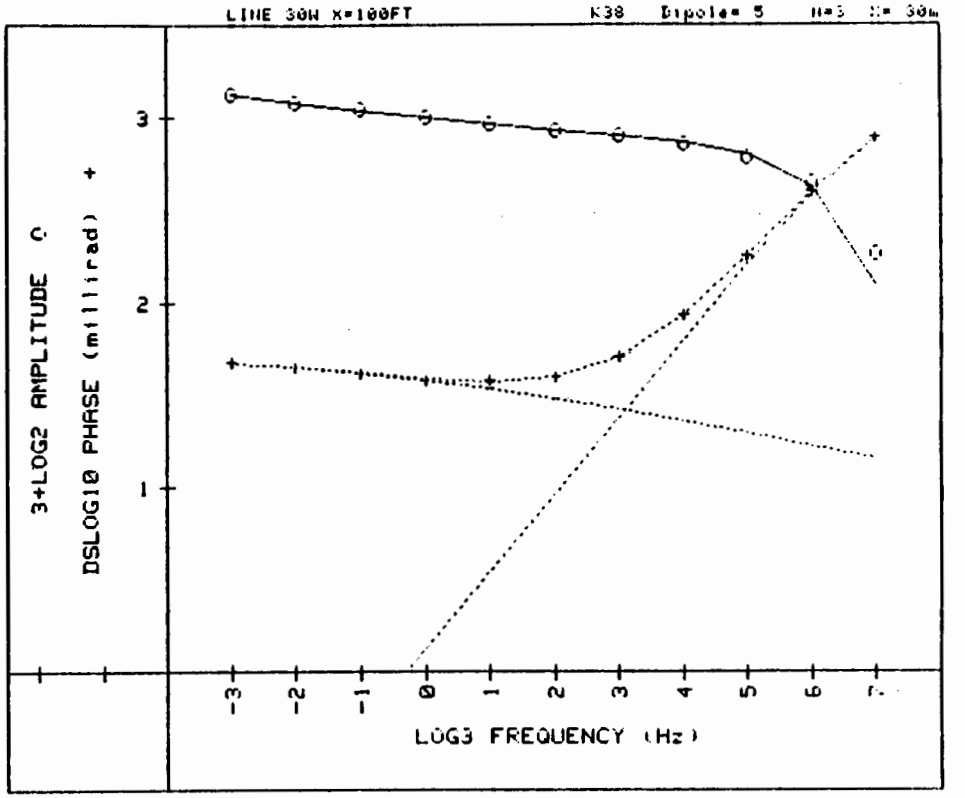
Correlation Matrix

1.0000							
.5173	1.0000						
-.4289	-.9715	1.0000					
-.5302	-.9438	.8971	1.0000				
0.0000	0.0000	0.0000	0.0000	0.0000			
-.2093	-.6596	.6657	.5343	0.0000	1.0000		
0.0000	0.0000	0.0000	0.0000	0.0000	0.0000	0.0000	

Apparent Resistivity Measured at 1 Hz is 78

Apparent Resistivity Calculated from Inductive Coupling is 10

FIG. 25



Iter	Lambda	Rchsq	R0	M1	T1	C1	M2	T2	C2
0	1.E-02	.01496	1.776	.571	1.2E+02	.180	1.000	1.5E-04	.970
1	1.E-02	.00083	1.569	.483	1.3E+02	.180	1.000	9.3E-05	.883
2	1.E-03	.00008	1.616	.487	1.9E+02	.180	1.000	8.8E-05	.891
3	1.E-04	.00006	1.677	.502	4.0E+02	.180	1.000	8.7E-05	.882
4	1.E-05	.00005	1.704	.508	5.3E+02	.180	1.000	8.7E-05	.879
5	1.E-06	.00005	1.707	.509	5.4E+02	.180	1.000	8.7E-05	.879
Pct Std Deviations			2.4	2.0	53.1	0.0	0.0	2.0	1.6

Correlation Matrix

1.0000						
.9916	1.0000					
.5885	.9710	1.0000				
0.0000	0.0000	0.0000	0.0000			
0.0000	0.0000	0.0000	0.0000	0.0000		
-.1166	-.0389	-.1282	0.0000	0.0000	1.0000	
-.4909	-.4268	-.5273	0.0000	0.0000	.7128	1.0000

Apparent Resistivity Measured at 1 Hz is 231

Apparent Resistivity Calculated from Inductive Coupling is 26

FIG. 26

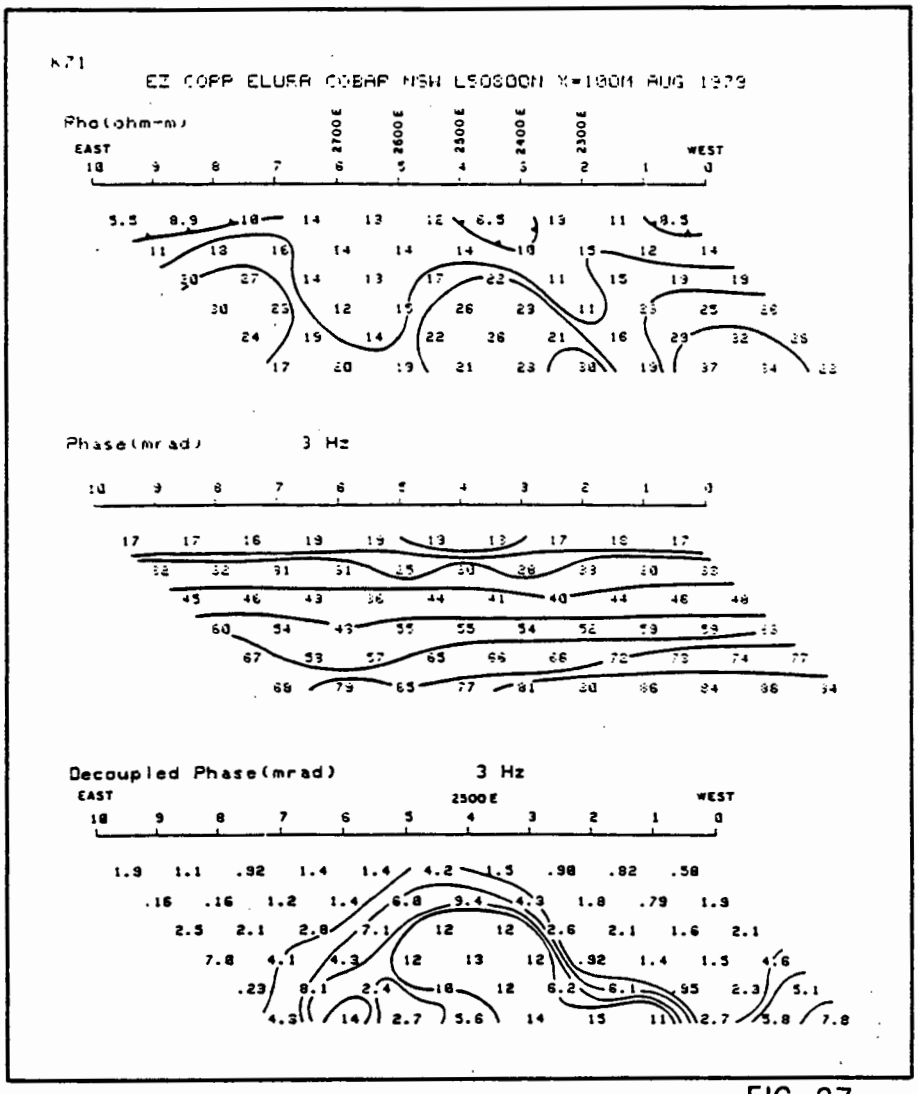


FIG. 27

COMPUTER ASSISTED INTERPRETATION OF IP DATA

The increased size, storage capability and speed of the modern digital computer has been a big boon to the exploration geophysicist. Forward problem solutions for potential methods (gravity, magnetics, etc.) have been available for some time. Recently, numerical modelling methods and large, very fast computers have made similar forward problem solutions available for applied field geophysics such as resistivity and induced polarization.

The forward problem solution shown in Figure 28 is for a fairly normal, dipping source. (The geometry is Two-Dimensional). The patterns of the induced polarization and resistivity pseudo-sections are similar to those we have previously seen from field data over dipping sources.

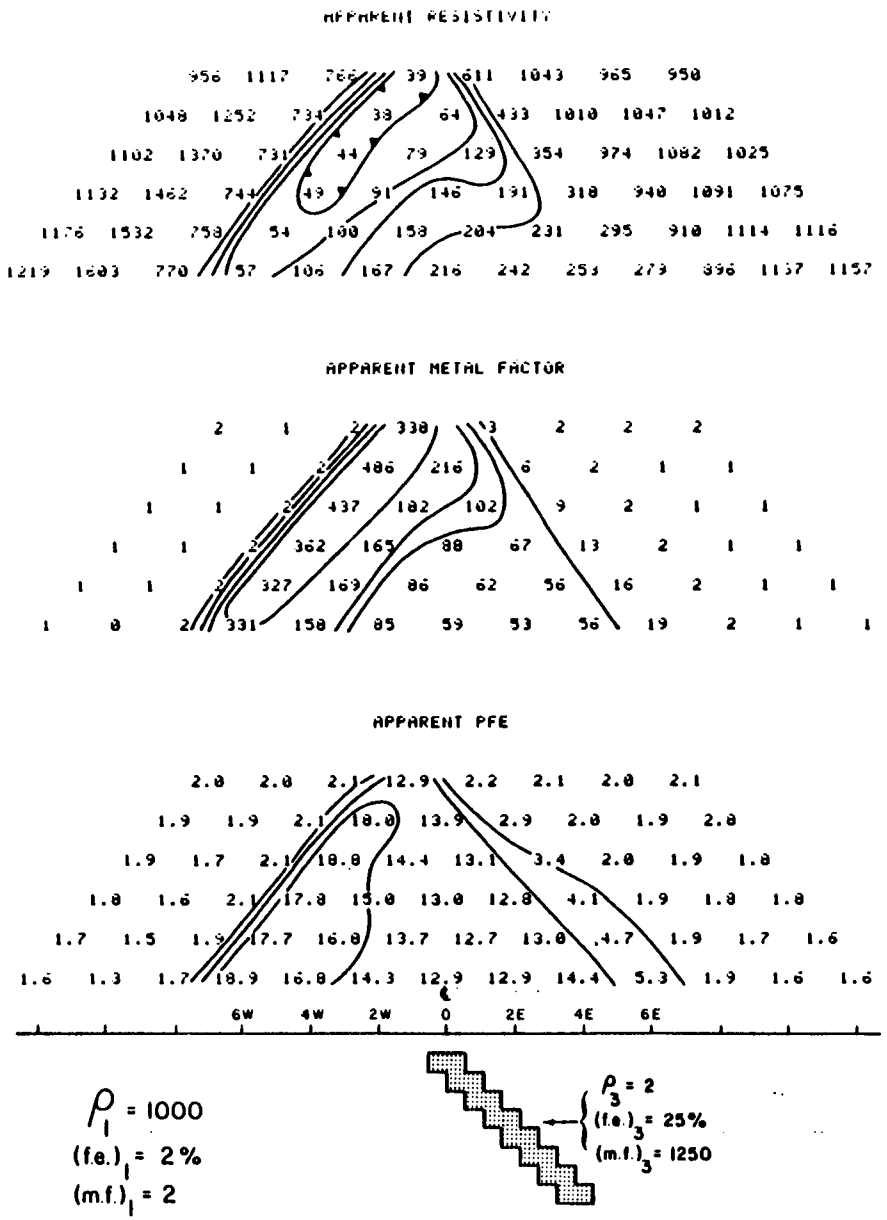

APPARENT RESISTIVITY
APPARENT METAL FACTOR
APPARENT PFE
6W 4W 2W 0 2E 4E 6E
ρ_1 = 1000
(f.e.)$_1$ = 2%
(m.f.)$_1$ = 2
ρ_3 = 2
(f.e.)$_3$ = 25%
(m.f.)$_3$ = 1250

FIG. 28

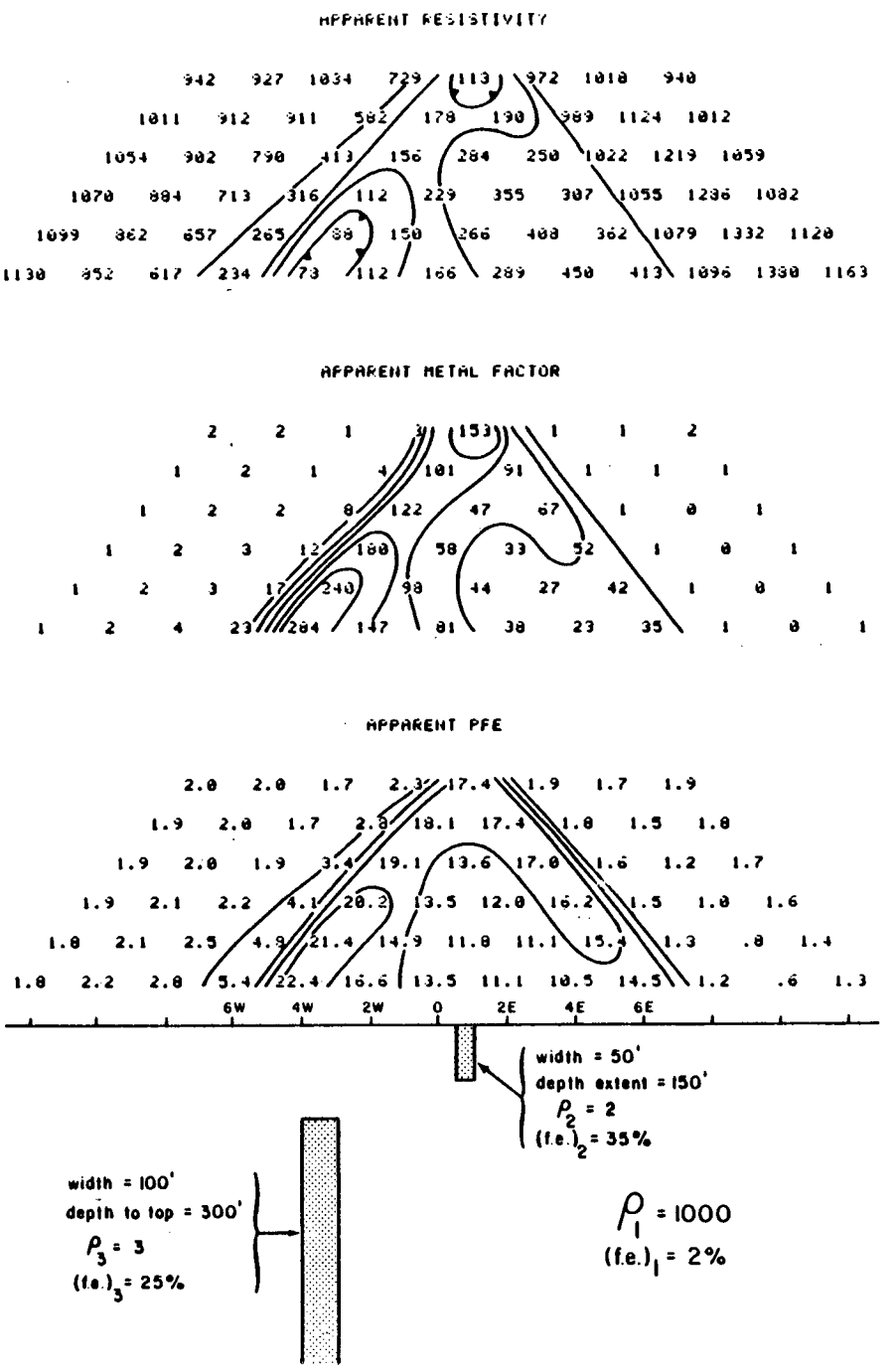

APPARENT RESISTIVITY
APPARENT METAL FACTOR
APPARENT PFE
6W 4W 2W 0 2E 4E 6E
width = 50'
depth extent = 150'
ρ_2 = 2
(f.e.)$_2$ = 35%
width = 100'
depth to top = 300'
ρ_3 = 3
(f.e.)$_3$ = 25%
ρ_1 = 1000
(f.e.)$_1$ = 2%

FIG. 29

Recently however, we had occasion to try to interpret a field anomaly that was very similar to that shown in Figure 29. The presence of the shallow, limited depth extent source was known from previous drilling. By the trial and error method, we were able to show that the pattern (which is very similar to that in Figure 28) need not have originated from a dipping source.

By limiting the solutions somewhat, it is possible to create computer programs to do the inverse problem. That is, the computer accepts the field data as input and as output gives the vertical, tabular source that gives the best "least square fit" to that data. For comparison, the computer also outputs the pseudo-section data that would be measured for the source it has chosen.

The simplest problem is for resistivity data alone. The results shown in Figure 30 are from a geothermal exploration program in which the resistivity survey was completed using X = 250 meters. The large, deep resistivity low was measured on the side of an extinct volcano, under recent lava flows. The computer inversion gives a major, poorly determined, conductor (with a high conductivity times width product) at a depth of 350 to 400 meters. This data was used to show the geologist that the source of the resistivity anomaly could be a good geothermal target.

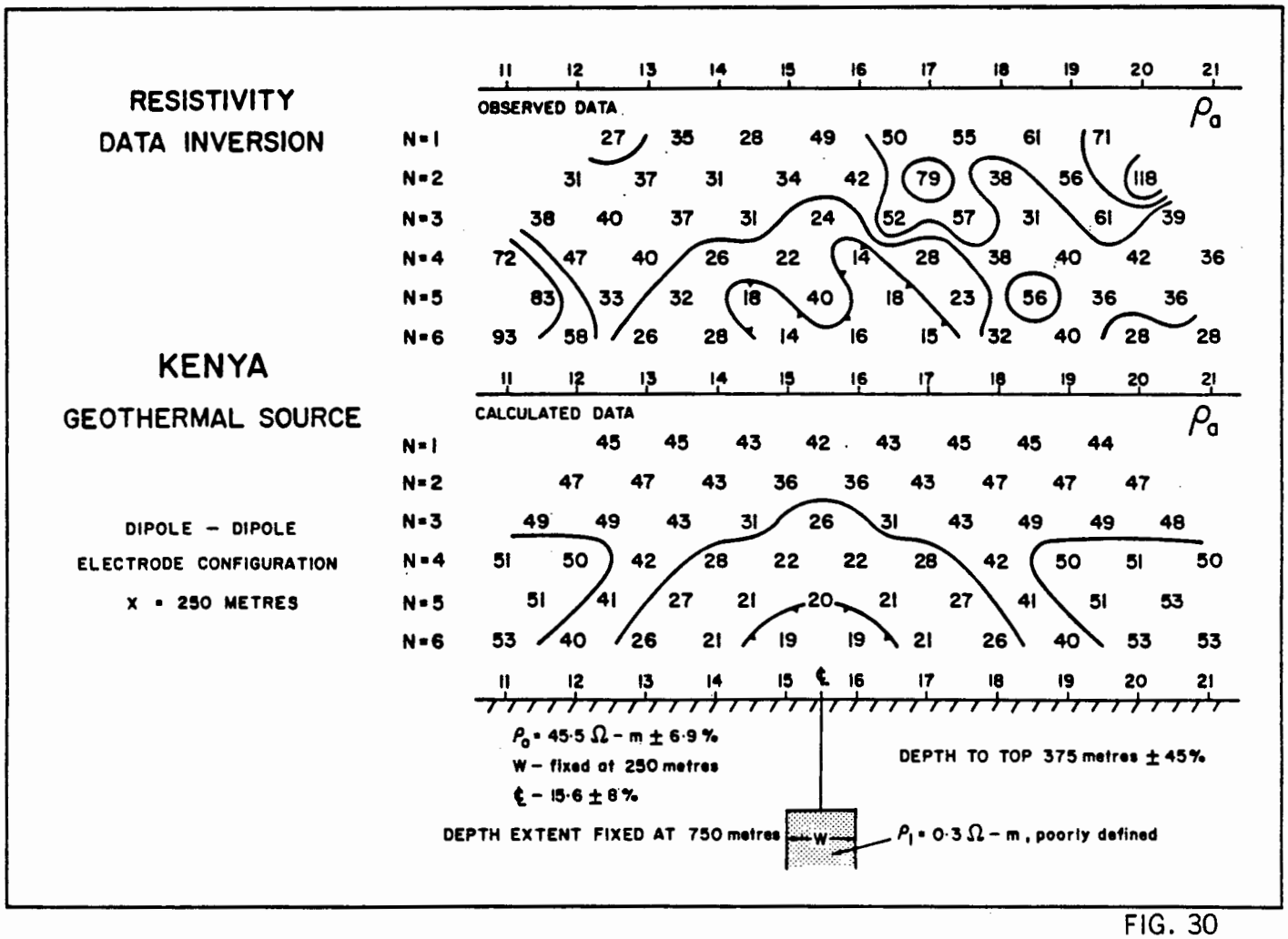


FIG. 30

The example shown in Figure 31 and Figure 32 is from the Pine Point Area. The computer inversion shows that in this case the source has a poor resistivity contrast with the surrounding limestones. However, the IP effect is quite anomalous.

If there is conductive overburden present, and the source itself is conductive, the inversions will be more complex. The data shown on Figure 33 and Figure 34 were measured with X = 100 feet, in an area where the depth of overburden was determined to be about fifty feet. The calculated results give a "good fit" to the measured data, and the source described by this inversion is a typical Canadian Shield, massive sulphide deposit.

The inversion program can also be used to show that two dissimilar anomalies can in fact be due to the same type of source. The inversions of the IP data shown in Figure 35 and Figure 36 are those for the field data previously shown in Figure 17 and Figure 18. The background resistivities are very different, and the depths to the top of the sources are different by a factor of three. However, the indicated source parameters are much the same. As we saw previously, the spectral characteristics of the IP anomaly from the two sources are quite different.

The use of the computer inversion techniques make it possible to obtain an estimate of the source parameters, even in situations in which an unusual geologic environment would make it difficult to interpret the data. The field results shown in Figure 37 are from a deeply buried source in a highly conductive environment. The rocks in which the survey was completed were porous, and filled with saline water. However, the inversion output on Figure 38 shows the source is not unlike that determined in Figure 34.

WHAT OF THE FUTURE?

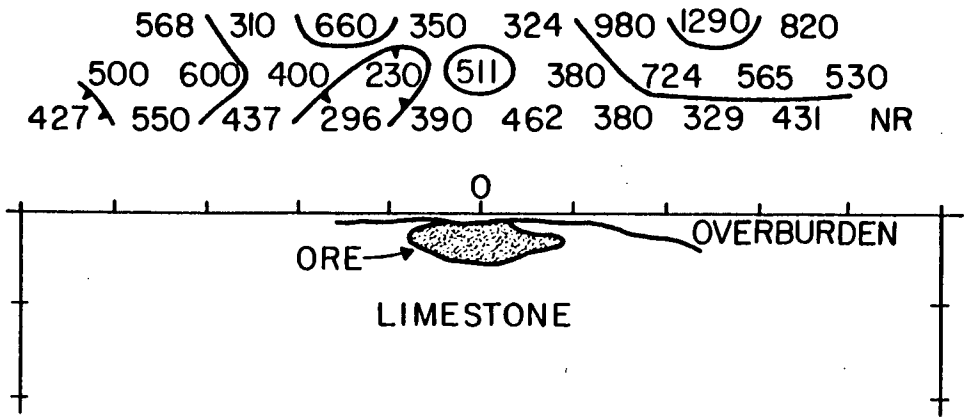
There seems to be almost no limit to the future development of the induced polarization method. As the orebodies for which we search become deeper, and more difficult to detect, we will need all of the help we can get.

A simple extension of what we are now doing should lead to the following examples in the next twelve to twenty-four months.

a) The computer can be used to store parameters obtained by the computer inversions of spectral IP data. Therefore, it will be possible to correlate the electrical parameters (m, τ, c) of all sources known in a given geographical area or a certain geologic environment. For a new, unknown source, the computer could be asked to output the probability that the unknown source will be due to metallic mineralization of a certain type.

The data shown in Figure 39 was a first attempt at such a correlation. On the plot are shown the IP effect vs. Time-Constant (m, vs.τ) coordinates for a few massive sulphide

PINE POINT, N-38A, X=200FT



RESISTIVITY MODEL

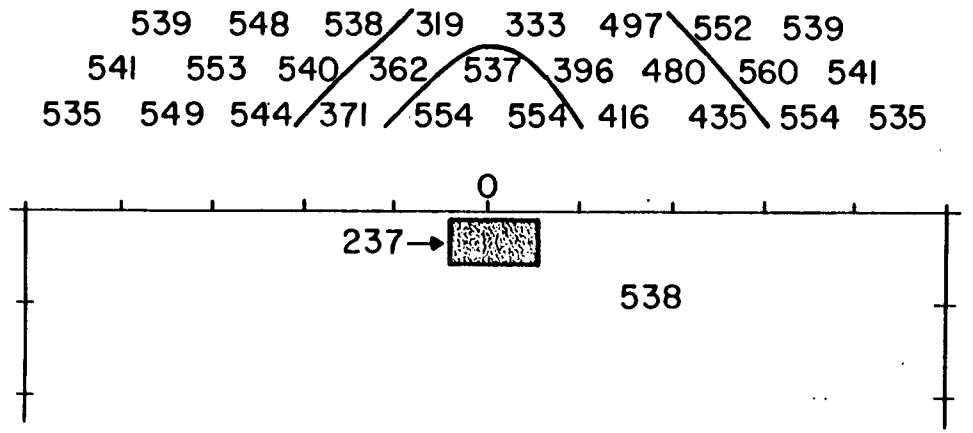
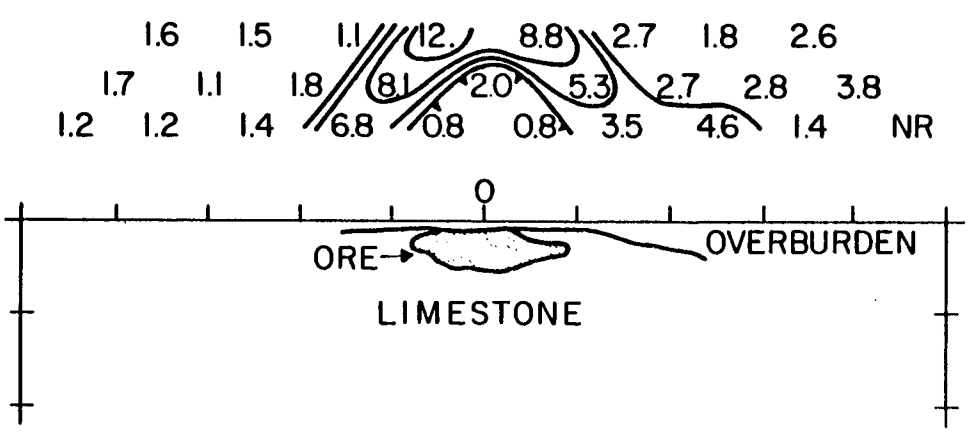


FIG. 31

PINE POINT, N-38A, X=200 FT



IP MODEL

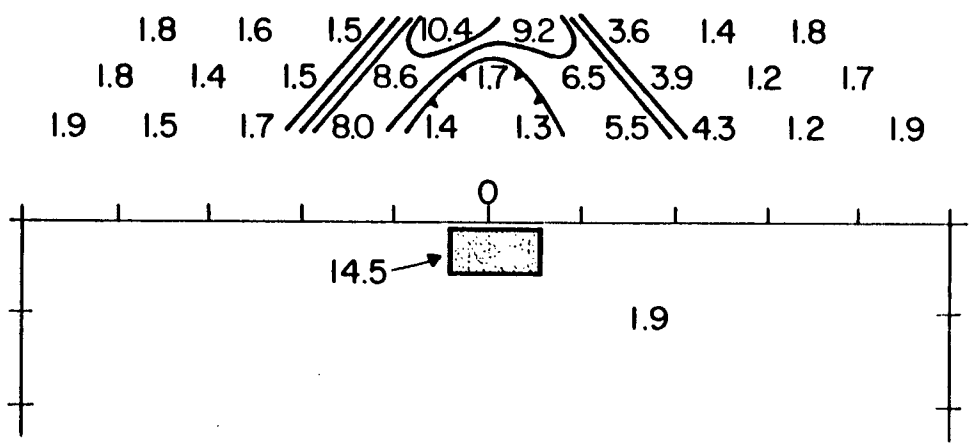


FIG. 32

COMPUTER INTERPRETATION

OF GEOPHYSICAL DATA

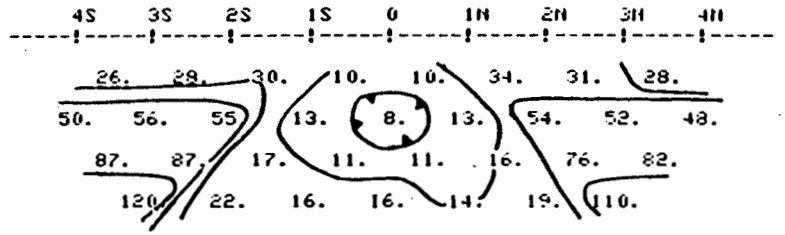
INDUCED POLARIZATION AND RESISTIVITY

CANADIAN SHIELD MASSIVE SULPHIDE DEPOSIT, OVERLAIN BY CONDUCTIVE OVERBURDEN
ISO - COPPERFIELDS LINE 0+00

DETERMINE: HORIZONTAL POSITION
DEPTH TO TOP
WIDTH
RES OF SOURCE
RES OF OVERBURDEN
IP OF SOURCE

DIPOLE-DIPOLE ARRAY X = 100 FEET 100FT

RESISTIVITY DATA - OBSERVED (OHM-METERS)



INDUCED POLARIZATION DATA - OBSERVED (PFE)

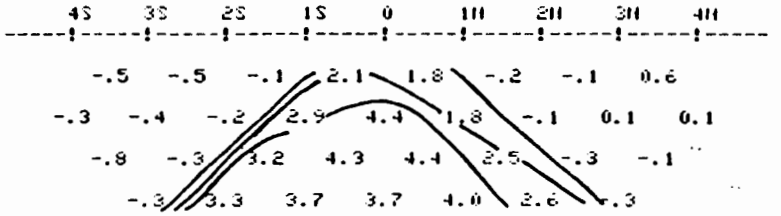
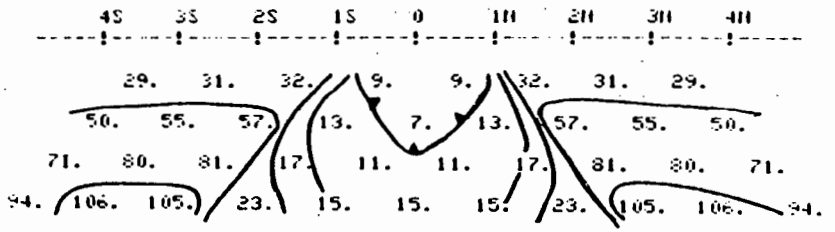
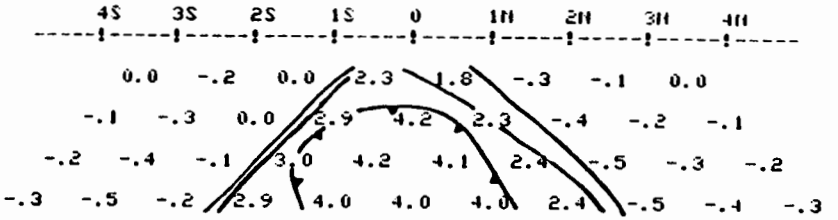


FIG. 33

RESISTIVITY DATA - CALCULATED (OHM-METERS)



INDUCED POLARIZATION DATA - CALCULATED (PFE)



PARAMETERS OF THE CALCULATED SOURCE

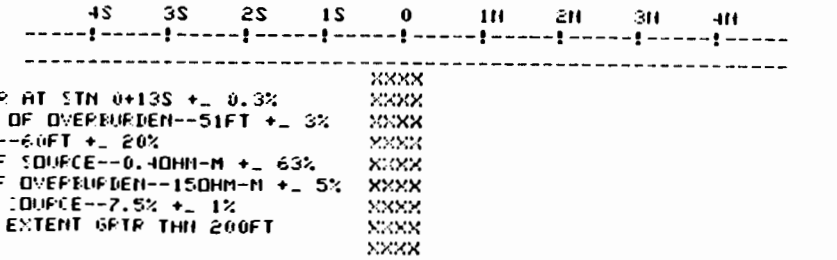


FIG. 34

LINE-18E

FINAL MODEL FOR DATA SET 1

OBSERVED DATA

1.5 1.5 8.0 18.0 15.0 8.0 1.5 1.5
1.5 1.0 9.0 20.0 29.0 13.0 11.0 1.5 1.5
1.5 1.5 10.0 17.0 26.0 19.0 17.0 14.0 1.5 1.5
1.5 1.5 8.0 19.0 33.0 49.0 24.0 21.0 17.0 1.5 1.5

100*DIAGONAL OF INFORMATION DENSITY MATRIX

0. 0. 2. 12. 12. 1. 0. 0.
0. 0. 4. 27. 16. 24. 1. 0. 0.
0. 1. 7. 21. 17. 17. 22. 2. 0. 0.
0. 1. 8. 20. 18. 21. 18. 22. 3. 1. 0.

CALCULATED DATA

1.2 .7 .6 13.1 11.5 -.5 1.1 1.1
1.1 .2 .1 18.0 32.0 14.6 -1.4 .0 1.0
.9 -.3 -.4 19.4 29.2 28.8 16.4 -2.3 .3 .0
.6 -.9 -1.0 20.3 27.4 25.9 27.5 17.2 -3.1 -.1 .5

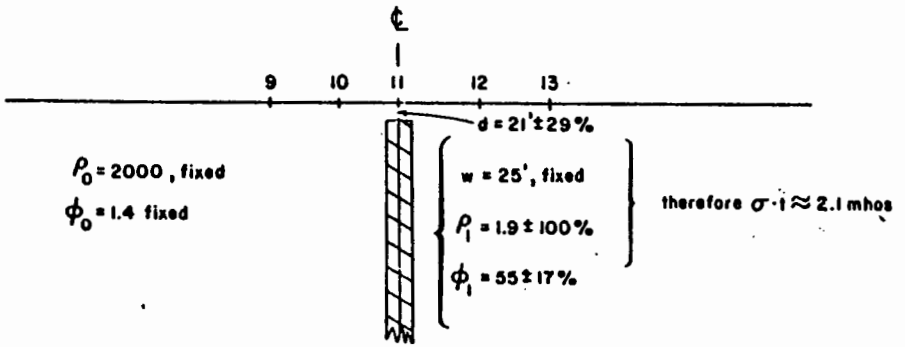


FIG. 35

LINE-15E

graphite source, with some pyrite

LINE-15E

phase at 0.3 Hz.

FINAL MODEL FOR DATA SET 1

OBSERVED DATA

4.0 4.0 4.0 4.0 5.0 4.0 4.0 4.0
4.0 4.0 6.0 8.0 14.0 11.0 10.0 4.0 4.0
4.0 4.0 8.0 14.0 27.0 28.0 18.0 8.0 4.0 4.0
4.0 4.0 5.0 14.0 29.0 36.0 28.0 16.0 10.0 4.0 4.0

100*DIAGONAL OF INFORMATION DENSITY MATRIX

0. 0. 0. 1. 0. 0. 0. 0.
0. 0. 0. 7. 42. 7. 1. 0. 0.
0. 1. 1. 13. 24. 23. 15. 1. 1. 0.
1. 2. 2. 19. 28. 52. 28. 21. 2. 2. 1.

CALCULATED DATA

2.7 2.5 2.1 4.2 4.7 2.1 2.4 2.7
2.4 1.0 1.6 8.8 18.4 8.9 1.6 1.8 2.4
2.0 1.2 .9 11.0 25.7 25.8 11.2 1.0 1.2 2.0
1.6 .5 .3 12.2 28.3 31.2 28.4 12.4 .3 .5 1.6

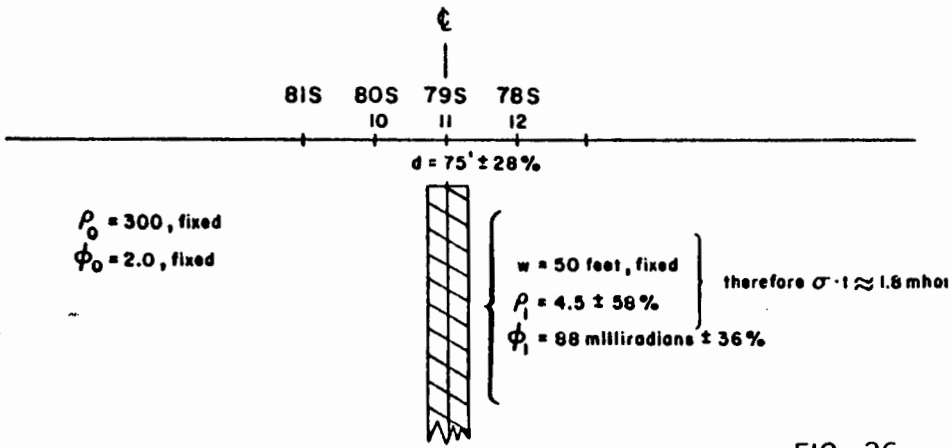


FIG. 36

COMPUTER INTERPRETATION

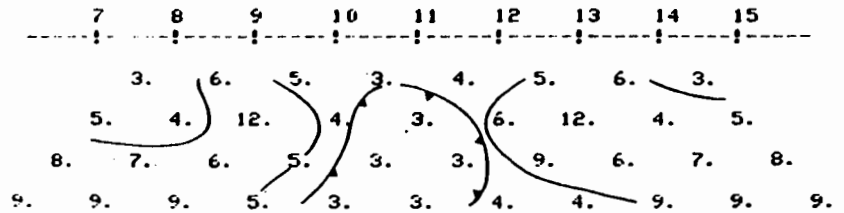
OF GEOPHYSICAL DATA

INDUCED POLARIZATION AND RESISTIVITY

DEEPLY BURIED SOURCE IN VERY CONDUCTIVE ENVIRONMENT - DETERMINE POSITION, DEPTH, AND PHYSICAL PROPERTIES OF SOURCE

DIPOLE-DIPOLE ARRAY X = 25 METERS 25M

RESISTIVITY DATA - OBSERVED (OHM-METERS)



INDUCED POLARIZATION DATA - OBSERVED (PFE)

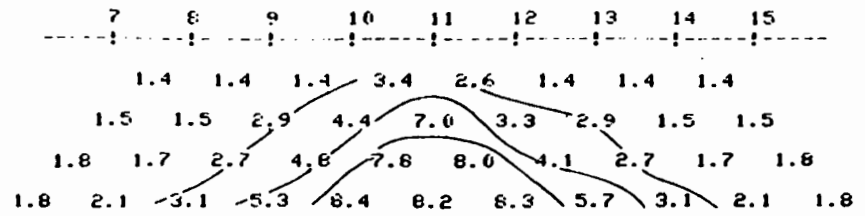
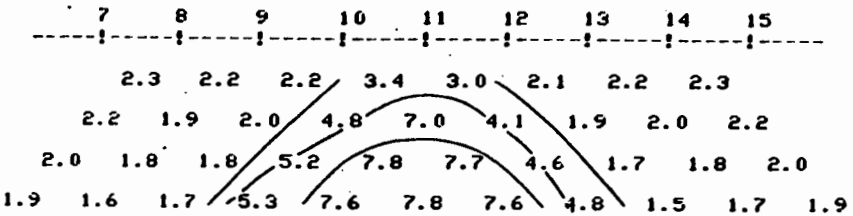


FIG. 37

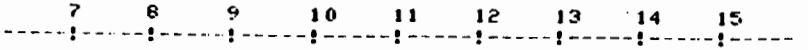
RESISTIVITY DATA - CALCULATED (OHM-METERS)



INDUCED POLARIZATION DATA - CALCULATED (PFE)



PARAMETERS OF THE CALCULATED SOURCE



DEPTH TO TOP--23M +_ 11%
RES OF SOURCE--0.30HM-M +_ 45%
RES OF HOST--6.50HM-M +_ 5%
IP OF SOURCE--23 +_ 16%
IP OF HOST--2.3 +_ 11%
CENTER AT STN 10+90 +_ 1%

+++++
+++++
+++++
+++++
+++++
+++++
+++++

DEPTH EXTENT FIXED AT >50M
WIDTH FIXED AT 25M

FIG. 38

sources and massive graphite sources in Canada. More recent determinations have not been added to the plot, although additional field work in North America and Australia has shown the same grouping.

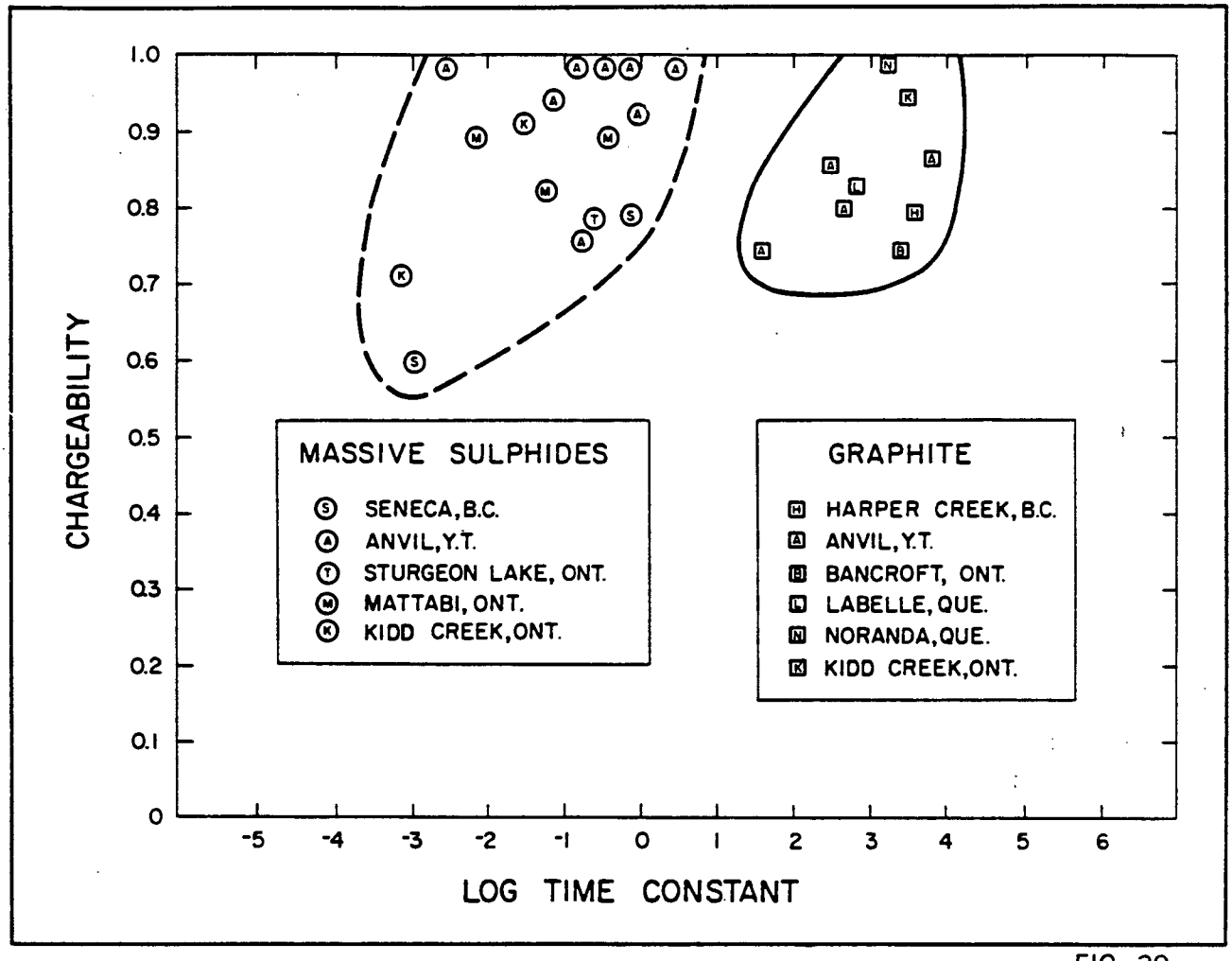


FIG. 39

b) The frequency range of spectral IP measurements with the IPV-3 System extends well up into the range that is normally used for electromagnetic prospecting. Indeed, as we have shown previously, the inductive coupling (EM) effects must be removed from the spectral IP plot before the electrical parameters of the source can be determined. In the near future, it should be possible to use this electromagnetic coupling information to gain further insight about the source.

The induced polarization and resistivity results in Figure 40 are from an area in South Australia. There is a known

pyrrhotite zone at Station 4 to Station 3, and a narrow Pb-Zn-Ag zone at about Station 0. The resistivity data shows a low over the conductive pyrrhotite zone. The raw phase data at 9.0 Hz and 0.11 Hz shows that IP effects are present, but the measurements (particularly at 9.0 Hz) are distorted by inductive coupling (EM) effects. When the inductive effects are removed, there is a definite IP anomaly from the pyrrhotite zone and a weak IP anomaly from the Pb-Zn-Ag zone. (see Figure 41).

The pseudo-sections shown in Figure 42 are a first attempt to use the inductive effects that have been removed from the dipole-dipole IP data. The M3 parameter is the electromagnetic component that has been removed from the measurement with each dipole pair.

The source centered at Station 4 to Station 3 gives a resistivity low, an IP high, and also a very large electromagnetic component. The source centered at Station 0 gives a weak, but definite IP anomaly. This source is not large enough to give a resistivity low using X = 25 meters. However, the electromagnetic coupling between the IP survey wires and the source is different from the resistive coupling between the electrodes and the source. There definitely is an electromagnetic component due to the Pb-Zn-Ag source.

c) With small desk-top computers, the calculation of a single forward IP problem can require five to ten hours. However, recent advances in small computers and new, interaction interfaces between CRT Displays and light-stylus hardware, will soon give the exploration geophysicist almost instantaneous interpretation capability.

For instance, the geometry shown on Figure 43 could be the first guess at the source of an IP anomaly. The geometry would be drawn upon the CRT Display by the geophysicist using an active light-stylus. At the push of a key, the computer would almost instantly display the pseudo-section shown. The computer would then print a "hard copy" of the field data, the calculated data and the geometry and parameters of the source.

The geophysicist could then use the light-stylus to alter the geometry to that shown in Figure 44. A push of the "operate" key would produce the pseudo-section shown in Figure 44. The pattern is only slightly different, but if it has greater similarity to the field data pattern, the geophysicist knows that he is on the right track.

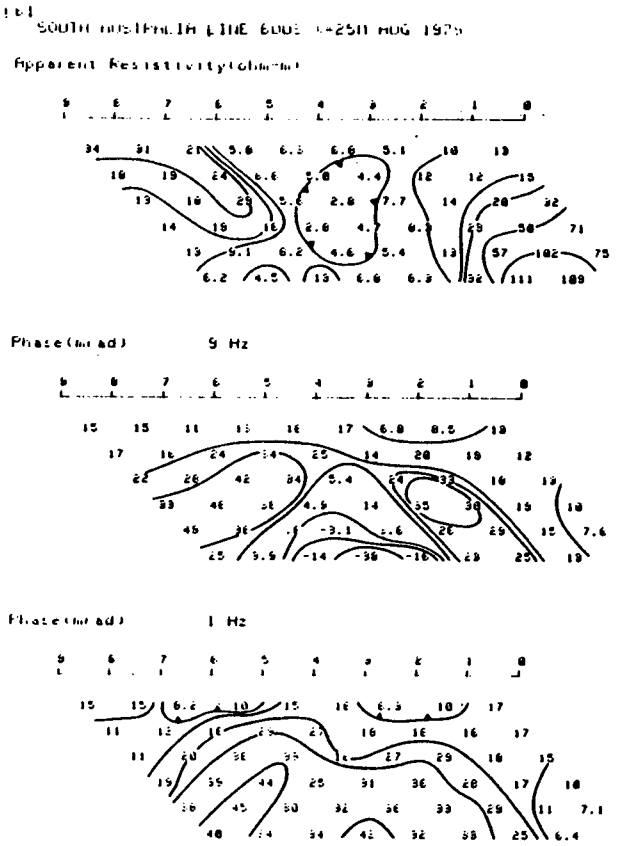


FIG. 40

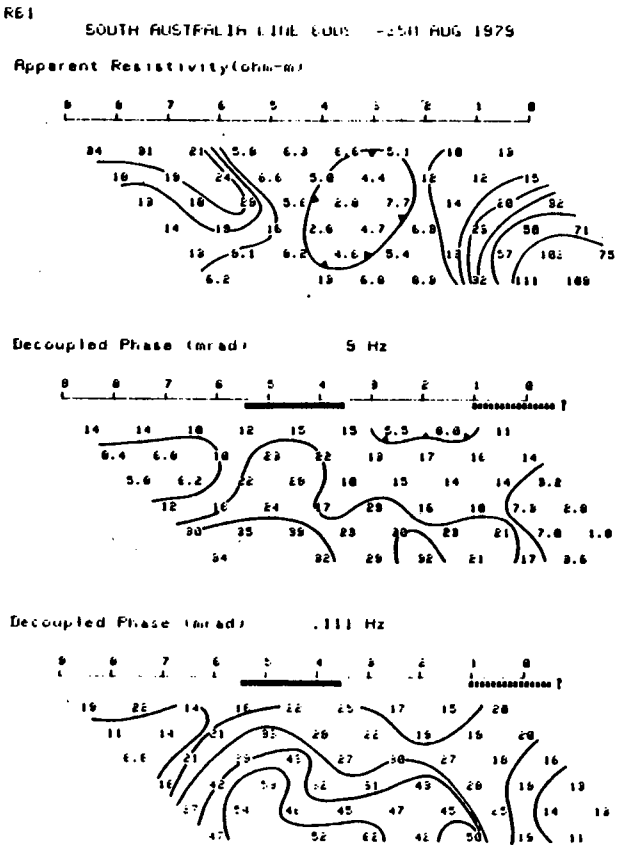


FIG. 41

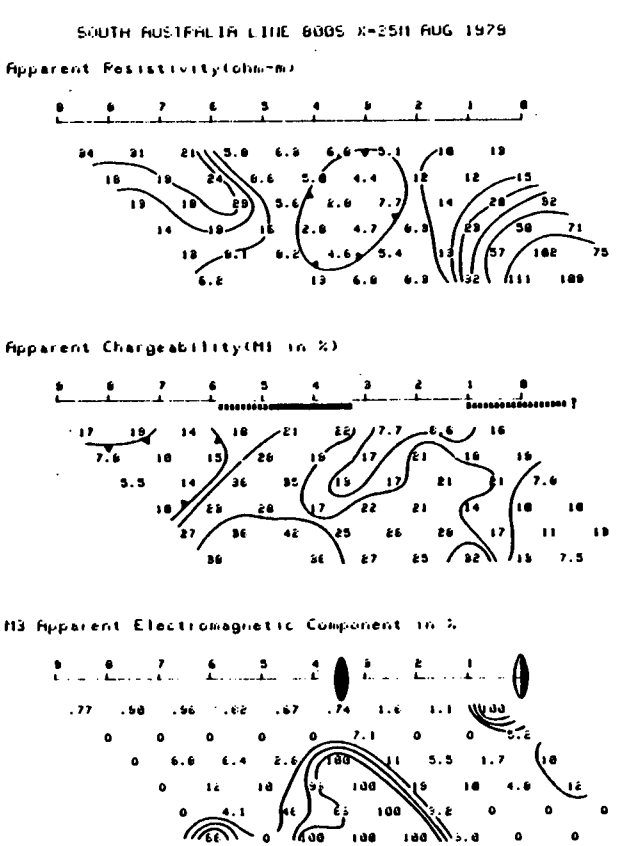


FIG. 42

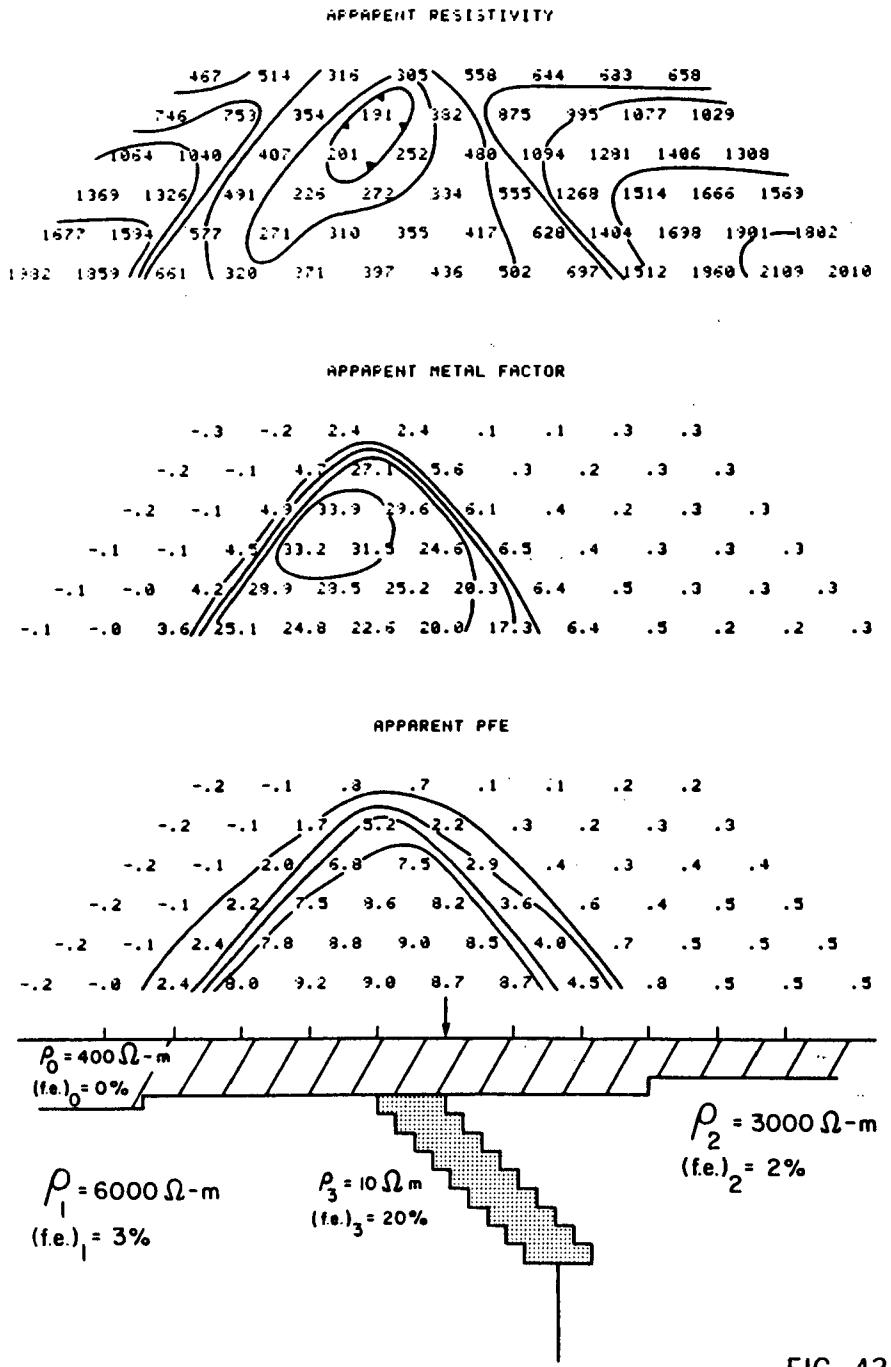

APPARENT RESISTIVITY
467 514 316 305 558 644 683 658
746 753 354 191 382 875 995 1077 1029
1064 1040 407 201 252 480 1094 1291 1406 1308
1369 1326 491 226 272 334 555 1268 1514 1666 1569
1677 1594 577 271 310 355 417 628 1404 1698 1901 1802
1882 1859 661 320 371 397 436 502 697 1512 1960 2109 2010
APPARENT METAL FACTOR
-.3 -.2 2.4 2.4 .1 .1 .3 .3
-.2 -.1 4.1 27.1 5.6 .3 .2 .3 .3
-.2 -.1 4.3 33.9 29.6 6.1 .4 .2 .3 .3
-.1 -.1 4.5 33.2 31.3 24.6 6.5 .4 .3 .3 .3
-.1 -.0 4.2 29.9 29.5 25.2 20.3 6.4 .5 .3 .3 .3
-.1 -.0 3.6 25.1 24.8 22.6 20.0 17.3 6.4 .5 .2 .2 .3
APPARENT PFE
-.2 -.1 .8 .7 .1 .1 .2 .2
-.2 -.1 1.7 5.2 2.2 .3 .2 .3 .3
-.2 -.1 2.0 6.8 7.5 2.9 .4 .3 .4 .4
-.2 -.1 2.2 7.5 8.6 8.2 3.6 .6 .4 .5 .5
-.2 -.1 2.4 7.8 8.8 9.0 8.5 4.0 .7 .5 .5 .5
-.2 -.0 2.4 8.0 9.2 9.0 8.7 8.7 4.5 .8 .5 .5 .5
$\rho_0 = 400\ \Omega$-m
$(f.e.)_0 = 0\%$
$\rho_1 = 6000\ \Omega$-m
$(f.e.)_1 = 3\%$
$\rho_3 = 10\ \Omega$m
$(f.e.)_3 = 20\%$
$\rho_2 = 3000\ \Omega$-m
$(f.e.)_2 = 2\%$

FIG. 43

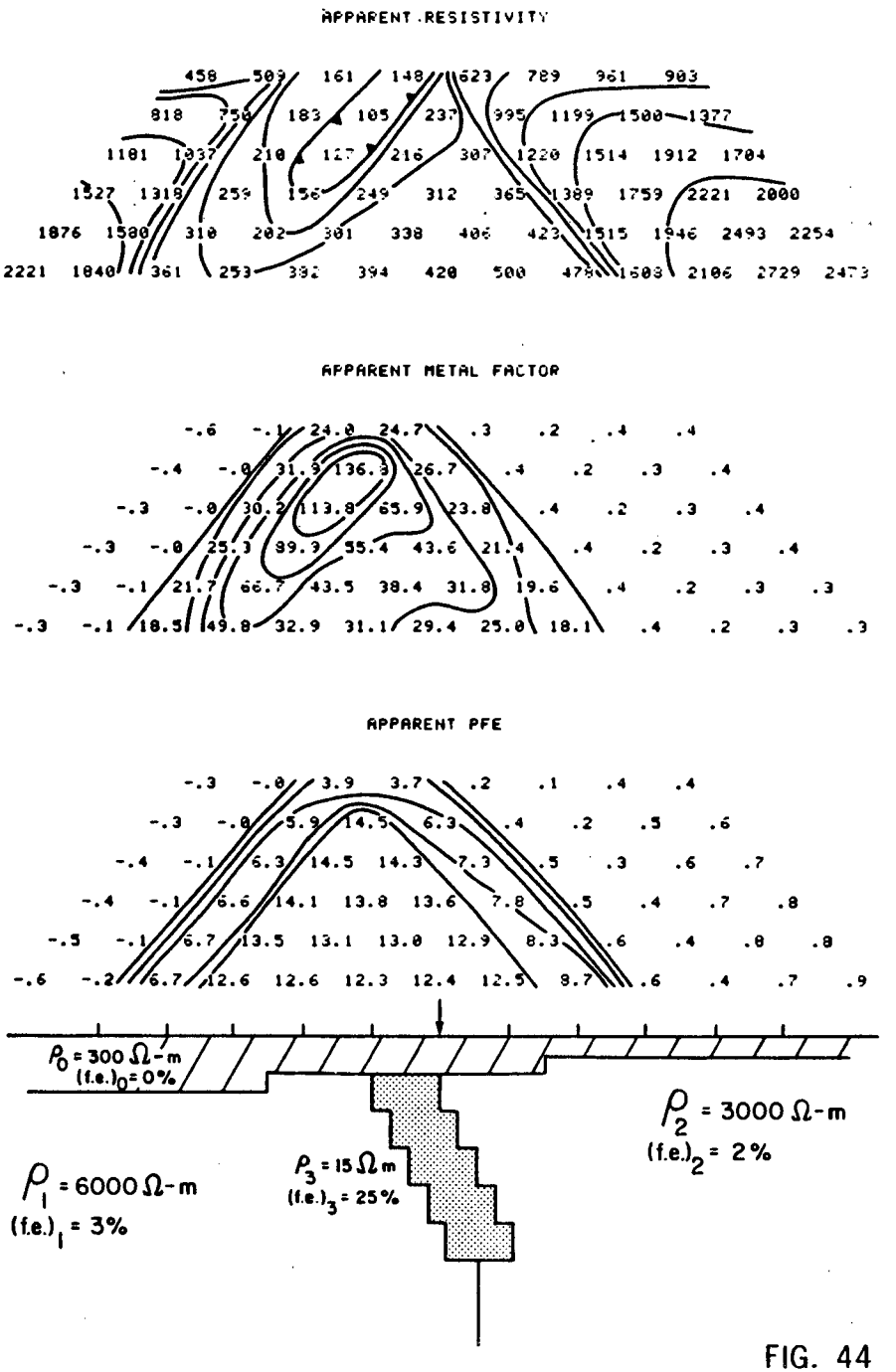

APPARENT RESISTIVITY
458 509 161 148 623 789 961 903
818 758 183 105 237 995 1199 1500 1377
1181 1037 210 127 216 307 1220 1514 1912 1704
1527 1318 259 156 249 312 365 1389 1759 2221 2000
1876 1500 310 202 301 338 406 423 1515 1946 2493 2254
2221 1840 361 253 382 394 420 500 478 1603 2106 2729 2473
APPARENT METAL FACTOR
-.6 -.1 24.0 24.7 .3 .2 .4 .4
-.4 -.0 31.9 136.3 26.7 .4 .2 .3 .4
-.3 -.0 30.2 113.8 65.9 23.8 .4 .2 .3 .4
-.3 -.0 25.3 89.3 55.4 43.6 21.4 .4 .2 .3 .4
-.3 -.1 21.7 66.7 43.5 38.4 31.8 19.6 .4 .2 .3 .3
-.3 -.1 18.5 49.8 32.9 31.1 29.4 25.0 18.1 .4 .2 .3 .3
APPARENT PFE
-.3 -.0 3.9 3.7 .2 .1 .4 .4
-.3 -.0 5.9 14.5 6.3 .4 .2 .5 .6
-.4 -.1 6.3 14.5 14.3 7.3 .5 .3 .6 .7
-.4 -.1 6.6 14.1 13.8 13.6 7.8 .5 .4 .7 .8
-.5 -.1 6.7 13.5 13.1 13.0 12.9 8.3 .6 .4 .8 .8
-.6 -.2 6.7 12.6 12.6 12.3 12.4 12.5 8.7 .6 .4 .7 .9
$\rho_0 = 300\ \Omega$-m
$(f.e.)_0 = 0\%$
$\rho_1 = 6000\ \Omega$-m
$(f.e.)_1 = 3\%$
$\rho_3 = 15\ \Omega$m
$(f.e.)_3 = 25\%$
$\rho_2 = 3000\ \Omega$-m
$(f.e.)_2 = 2\%$

FIG. 44



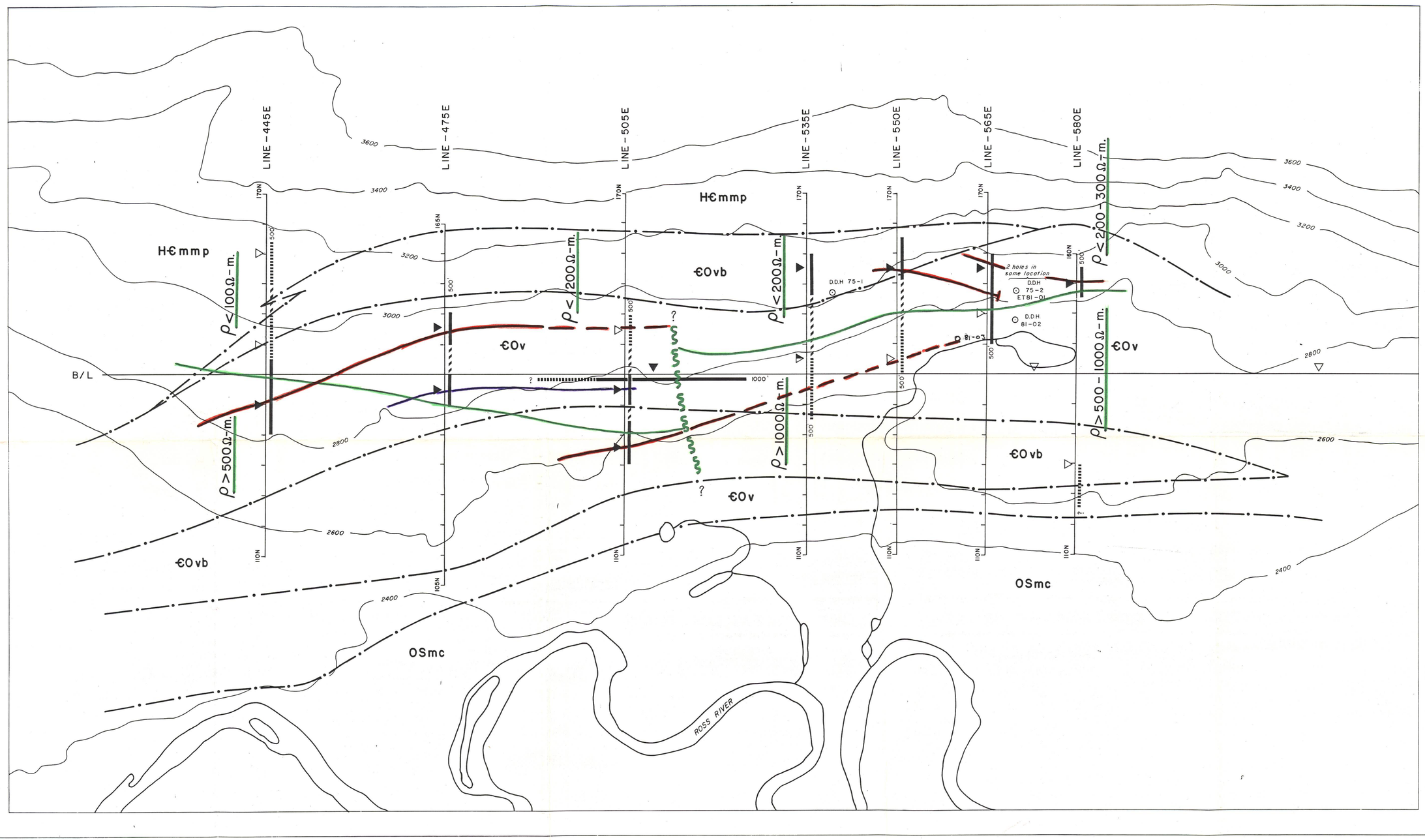
Toronto Office: 200 Yorkland Blvd., Willowdale, Ont. M2J 1R5
Vancouver Office: 310 - 885 Dunsmuir St., British Columbia, V6C 1N5
Denver Office: 4690 Ironton St., Colorado, 80239, U.S.A.

DWG. NO. - S.I.P.P. - 3109

PHOENIX GEOPHYSICS LIMITED

RECONNAISSANCE SPECTRAL INDUCED POLARIZATION SURVEY

PLAN MAP



SURFACE PROJECTION OF ANOMALOUS ZONE

DEFINITE ▼
PROBABLE ▽
POSSIBLE ▽
} NARROW SOURCE

NUMBER AT END OF ANOMALIES INDICATES SPREAD USED.

– APPROXIMATE POSITION OF RESISTIVITY CONTACT

– GEOLOGICAL CONTACT

– AXIS OF DEEP IP ANOMALOUS ZONE

– AXIS OF SHALLOW IP ANOMALOUS ZONE

CYPRUS ANVIL MINING CORPORATION

TENAS PROJECT, WHITEHORSE M.D.

YUKON TERRITORY

SCALE

500 0 1000 2000 3000 FEET

100 0 200 400 600 800 METRES

1:10000

inches 0 1 2

centimetres 0 1 2 3 4 5

YUKON GEOLOGICAL SURVEY

This reference scale bar has been added to the original map. It will scale at the same rate as the image, therefore it can be used as a reference for the original size.

DRAWN: R.J.P

DATE: JAN. 1982

APPROVED:

DATE: 1/21/82

Expires February 25, 1982

DWG. NO. - S.I.P.P. - 3109

Dwg. S.I.P.P.3109

APPENDIX II

SUMMARY DRILL LOGS FOR

ET81-01

ET81-02

ET81-03

SUMMARY LOG

DDH ET81-01

METERS

From	To	Code	Description
0.0	4.4		Triconed - no core.
4.4	48.2	€Ovn	Non-calcareous, variably chloritic phyllite, including minor bull quartz; lower Vangorda - Upper Mr. Mye.
48.2	56.0	€Ovcp	Siliceous, banded, garnet bearing, chloritic phyllite.
56.0	62.6	€Ovp	Variably carbonaceous, calcareous chloritic phyllite with minor intervals of €Ovcp .
62.6	67.8	€Ovcp	Laminarly banded chloritic phyllite with inor sericite alteration, pyrite and pyrrhotite as blebs and veinlets; minor graphitic phyllite.
67.8	77.7	€Ovgp	Variably calcareous graphitic phyllite, pyrite < pyrrhotite as blebs and foliaform seams within silica ribbons, less than 1%.
77.7	85.8	€Ovcp	Laminarly banded chloritic phyllite with minor pyrrhotite.
85.8	120.8	€Ovgp	Variably calcareous, graphitic phyllite; pyrrhotite (<1%) as blebs and discontinuous thread like seams foliaform to S_2.
120.8	127.7	€Ovb	Metabasite with minor bull quartz veining.
127.7	146.2	€Ovgp	Graphitic phyllite, chlorite bearing, minor pyrrhotite.
146.2	157.5	€Ovcp	Laminarly banded, variably siliceous chloritic phyllite.
157.5	158.2	€Ovgp	Siliceous graphitic phyllite; silica "beads", minor pyrrhotite.
158.2	165.9	€Ovb	Metabasite, minor €Ovcs and €Ovcp.

From	To	Code	Description
165.9	173.0	€Ovgp	Siliceous graphitic phyllite with trace of red-brown sphalerite at 166.3 m within siliceous horizons. Lithology is similar to unmineralized graphitic quartzites.
173.0	196.2	€Ovp	Variably calcareous chloritic phyllite; interval is characteried by quartz-chlorite (pyrrhotite)-carbonate alterationveinlets. Similar to the margins of the alteration envelope associated with the Vangorda deposit.
196.2	197.8	€Ovgp	Graphitic phyllite.
197.8	198.1	€Ovgp	Siliceous graphitic phyllite. 1-2% sphalerite as blebs and crosscutting (S2) veinlets This interval is similar to mineralized graphitic quartzites present in the Anvil deposits.
198.1	200.5	€Ovgp	Siliceous graphitic phyllite.
200.5	201.4	€Ovgp	Siliceous graphitic phyllite, as in interval 197.8 - 198.1; sphalerite appears stratiform.
201.4	212.4	€Ovgp	Variably siliceous graphitic phyllite; pyrrhotite (1%) common as blebs and veinlets.
212.4	215.5	€Ovcs	Calc-silicate phyllite/schist, with 30% EOvpm.
215.5	220.0	€Ovp	Calcareous muscovite-sericite-chlorite biotite phyllite.
220.0	221.0	€Ovcs	Calc-silicate phyllite/schist.
221.0	338.3	H€mmp	Non-calcareous biotite-muscovite phyllite /schist.
338.3	345.2	H€mmb	Metabasite with laminarly banded intervals.
345.2	396.0	H€mmb	Andabesite bearing, non-calcareous biotite-muscovite phyllite/schist.
396.0	408.6	Kgd	Quartz monzonite.
408.6	421.8	H€mmp	Andalusite bearing, non-calcareous biotite-muscovite phyllite/schist.

From	To	Code	Description
421.8	428.9	Kgd	Quartz monzonite.
428.9	461.8	HЄmmp	Andalusite bearing non-calcareous biotite-muscovite phyllite/schist.

END OF HOLE

SUMMARY LOG

DDH ET81-02

METERS

From	To	Code	Description
0.0	6.1		Triconed - no core.
6.1	46.8	€Ovp	Calcareous muscovite-chlorite ± biotite phyllite.
46.8	49.4	€Ovcp	Laminarly banded chloritic phyllite with quartz carbonate pods.
49.4	62.4	€Ovgp	Variably calcareous and siliceous, graphitic phyllite. Minor pyrrhotite common.
62.4	77.4	€Ovb	Calcareous metabasite.
77.4	81.4	€Ovgp	Calcareous muscovite-chlorite ± biotite phyllite; pyrrhotite common in quartz-carbonate interlaminated seams.
81.4	86.0	€Ovb	Metabasite
86.0	93.5	€Ovgp	Variably calcareous graphitic phyllite, bleby pyrrhotite 1% overall.
93.5	124.3	€Ovb	Metabasite
124.3	129.5	€Ovcp	Laminarly banded chloritic phyllite.
129.5	153.7	€Ovgp	Variably siliceous and calcareous graphitic phyllite, minor pyrrhotite and pyrite in siliceous bands, no base metals.
153.7	163.9	€Ovp	Variably carbonaceous, calcareous phyllite.
163.9	166.0	€Ovcp	Laminarly banded chloritic phyllite.
166.0	171.1	€Ovgp	Non-calcareous, locally silica rich graphitic phyllite.
171.0	194.6	€Ovb	Calcareous metabasite
194.6	203.7	€Ovcp	Siliceous, laminarly banded chloritic phyllite.

DDH ET81-02 (cont'd)

From	To	Code	Description
203.7	206.8	€Ovgp	Siliceous graphitic phyllite, pyrrhotite (1-2%) as blebs in quartz stringers, trace sphalerite.
206.8	210.8	€Ovb	Metabasite
210.8	229.9	€Ovgp	Non-calcareous graphitic phyllite, variably siliceous.
229.9	266.5	€Ovp	Carbonaceous, variably calcareous, chlorite, muscovite, biotite phyllite, locally has alteration appearance due to interlaminated €Ovcp.
266.5	286.9	€Ovgp	Variably siliceous, calcareous graphitic phyllite, locally pyrite and pyrrhotite bearing in quartz carbonate pods; minor and interlaminated; trace sphalerite at 267.8, 269.3 and 271.8; similar in form to ET8101 as foliaform and blebs.
286.9	288.3	€Ovp	Carbonaceous and calcareous phyllite.
288.3	292.2	€Ovpm	Phyllite marble and silicated marble.
292.2	405.2	H€mmp	Non-calcareous muscovite-chlorite ± biotite phyllite, pyrrhotite common in blebs.
405.2	410.6	H€mmb	Metabasite
410.6	458.4	H€mmp	Non-calcareous phyllite, variably siliceous.

END OF HOLE

SUMMARY LOG

DDH ET8103

METERS

From	To	Code	Description
0.0	6.0		Triconed
6.0	261.8	€Ovp	Calcareous, grey, muscovite-chlorite ± biotite phyllite minor pyrite and pyrrhotite.
261.8	276.0	€Ovb	Dark green, variably calcareous massive to banded metabasite.
276.0	279.4	€Ovp	Calcareous and siliceous muscovite, chlorite phyllite.
279.4	282.3	€Ovgp	Siliceous, variably calcareous graphitic phyllite.
282.3	292.0	€Ovcp	Laminarly banded variably calcareous chloritic phyllite.
292.0	305.6	€Ovb	Metabasite
305.6	309.0	€Ovgp	Calcareous graphitic phyllite.
309.0	313.0	€Ovcp	Laminarly banded calcareous chloritic phyllite.
313.0	323.6	€Ovgp	Calcareous graphitic phyllite.
323.6	327.2	€Ovb	Metabasite
327.2	356.2	€Ovgp	Siliceous variably calcareous graphitic phyllite, locally interval is ribbon banded graphitic quartzite; pyrite is very finely disseminated; trace of sphalerite occurs at the following depths 332.8, 348.6, 352.6, 353.0, 353.4; occurs in S_2 foliation in silica rich zones, locally ribbon chert.
356.2	359.4	€Ovb	Metabasite
359.4	373.5	€Ovgp	Variably calcareous graphitic phyllite, locally siliceous to graphitic quartzite; trace of galena and sphalerite within silica cemenent and breccia at 373.5.

DDH ET81-03 (cont'd)

From	To	Code	Description
373.5	374.7	€Ovpm	Carbonaceous phyllitic marble and silicated marble.
374.7	377.0	€Ovgp	Graphitic phyllite.
377.0	464.3	H€mmp	Non-calcareous muscovite-chlorite ± biotite phyllite.
464.3	497.4	H€mmb	Metabasite

END OF HOLE